A Study of Methods to Achieve Somatic Cell Reprogramming

Thesis submitted for the degree of

Doctor of Engineering
In
Biochemical Engineering

Jordan Robert Plews

The Advanced Centre for Biochemical Engineering
Department of Biochemical Engineering
University College London

2010

Declaration

I, Jordan Robert Plews, confirm that the work presented in this thesis is my own. Where information has been derived from other sources, I confirm that this has been indicated in the thesis.

Acknowledgments

I would like to thank my supervisors, Professor Peter Andrews and Professor Chris Mason, for their advice, encouragement, and patience during the past four years. Professor Mason got me involved in this project and has helped shape this project as it has evolved. Professor Peter Andrews has been an excellent at providing key insights and suggestions, and always looking out for the welfare of those in his lab, myself included. Thanks are also due to all members of the Centre for Stem Cell Biology (CSCB) and my colleagues at UCL, both past and present, particularly Paul Gokhale, Jack Li, Christian Unger, Neil Harrison, Ivana Barbaric, Jamie Jackson, Dean Owen, Mark Jones, Meg Gillett and Farlan Veraitch. There are also many others at the CSCB and UCL that deserve thanks, without which this project would not have been possible including Christine Pigott, Derrick Abraham, Professor Mike Hoare, Professor Nigel Titchner-Hooker and Professor Peter Dunnill. However, special thanks are reserved for Dr Jie Na, for both experimental and intellectual assistance, but also for helping me to keep things in perspective. She has taught me more in the past four years than anyone else I have had the pleasure of working with and I will always be grateful to her for her assistance with this project.

I would also like to thank my friends and family, particularly my father, for providing the mental, physical, and financial support that has enabled me to complete this project.

Finally, I would like to thank the Engineering and Physical Sciences Research Council (EPSRC), Axordia, and ESTOOLS for supporting this research.

Abstract

While the potential of pluripotent cells and their role in the future of regenerative medicine has rapidly evolved since the derivation of human embryonic stem cells in 1998, ethical issues surrounding the derivation and clinical use of pluripotent cells still remain. Somatic cell reprogramming offers an ethically preferred, potentially patient specific method for deriving pluripotent cells, but this technology is based on integration of genes that have been linked to oncogenesis and therefore limit clinical usefulness.

This project, started in late 2005, has explored new methods towards achieving somatic cell reprogramming with the specific goal of reprogramming human somatic cells without altering genomic DNA. Through the use of cytoplasm from pluripotent cells, total RNA from pluripotent cells, and specific mRNAs coding for known reprogramming factors, attempts to reprogram somatic cells were made, along with the goal to better understand the process of reprogramming and the associated gene expression changes that catalyse it.

To gauge reactivation of the embryonic genome, an Oct4-GFP fibroblast reporter line was successfully established. A protocol for the isolation of membrane encapsulated, nuclear DNA free pluripotent cell cytoplasm, or cytoplasts, was developed. Following fusion of cytoplasts to somatic reporter cells resulted in temporary OCT4 activation, but no pluripotent cells were isolated. Subsequently, an electroporation protocol was developed and optimised to transfect total RNA and total mRNA from pluripotent cells into somatic cells, in place of cytoplasts. This method successfully showed temporary upregulation of key pluripotency genes, but not full reversion to a pluripotent state.

In 2006, it was shown that only four factors (OCT4, SOX2, cMYC, and KLF4) are required for somatic cell reprogramming, but the issue of DNA manipulation remained. Synthetically produced mRNA coding for the key reprogramming factors was then made and transfected into human fibroblast cells. It was found that transfected mRNA can successfully upregulate specific genes of interest, including pluripotency factors, in a more controlled and predictable manner than DNA. Although mRNA only causes upregulation for 3-4 days, in some cases lasting changes on endogenous expression of pluripotency genes were detected, including OCT4. This work shows that mRNA transfection can be a useful tool for temporary upregulation of specific gene expression and, with further optimisation, may provide a method for catalysing somatic cell reprogramming without genetic alteration. Additionally, mRNA has potential as an important tool for differentiation, transdifferentiation, and pluripotency studies.

Table of Contents

List of Figures

Chapter 1 Figures:

Chapter 2 Figures:

Chapter 3 Figures:

Chapter 4 Figures:

Chapter 5 Figures:

Chapter 6 Figures:
None

Chapter 7 Figures:
None

Chapter 8 Figures:

Appendix Figures:

List of Tables

Abbreviations

bp	Base Pair
BSA	Bovine Serum Albumin
cDNA	Complementary DNA
CM	Conditioned Media
CSCB	Centre for Stem Cell Biology (University of Sheffield)
ddH_2O	Deionised 0.2 µm filtered Water
DMEM	Dulbeccos Modified Eagle's Medium
DMSO	Dimethyl Sulfoxide
DNA	Deoxyribonucleic Acid
dNTP's	Deoxyribonucleoside triphosphates
DTT	Dithiothreitol
EB	Embryoid Body
EC	Embryonal Carcinoma
EG	Embryonic Germ
ES	Embryonic Stem
EDTA	Ethylenediaminetetra-acetic acid
EtBr	Ethidium Bromide
FACS	Fluorescence Activated Cell Sorting
FBS	Foetal Bovine Serum
FITC	Fluorescein Isothiocyanate
FS	Forward Scatter (event size)
g	Acceleration due to gravity
GFP	Green fluorescent protein
bFGF	Basic Fibroblast Growth Factor
KO-DMEM	Knockout Dulbeccos Modified Eagle's Medium
KO-SR	Knockout Serum Replacement
LB Medium	Luria-Bertani bacterial medium

m	Milli
M	Molar
mL	Millilitre
MEF	Mouse Embryonic Fibroblasts
mRNA	Messenger RNA
n	nano
neo	Neomycin phosphotransferase
NT2	NTERA2 clone D1 Embryonal Carcinoma cell line
OD	Optical density
OSKM	OCT4 + SOX2 + KLF4 + cMYC
OSKMT	OCT4 + SOX2 + KLF4 + cMYC + SV40 Large T
P	Passage
PBS	Phosphate Buffered Saline
PCR	Polymerase Chain Reaction
PFA	Paraformaldehyde
Q-PCR	Quantitative Real Time Polymerase Chain Reaction
rpm	Revolutions per minute
RPMI 1640	Roswell Park Memorial Institute Medium 1640
RNA	Ribonucleic Acid
RT	Reverse Transcription
SDS	Sodium dodecyl sulphate
SS	Side Scatter (granularity)
SSEA	Stage specific embryonic antigen
TE	Tris/EDTA
µg	Micro-grams
µL	Micro-litres
µm	Micro-metres
µM	Micro-molar
UV	Ultra-Violet

Chapter 1 – General Introduction

1.1 Importance of Autologous Pluripotent Cells

Human embryonic stem (ES) cells are pluripotent (capable of differentiating into nearly any cell type in the body), self-renew (divide endlessly in culture), and appear to have the ability to differentiate into all cell types of the body (Thomson et al. 1998). Human ES cells may, therefore, provide an essentially unlimited source of specific human cells for basic biology, drug screening, and transplantation medicine. We already know that human ES cells have the potential to be used to treat a wide array of degenerative diseases and conditions, everything from neurodegenerative disorders such as Alzheimer's (Carpenter et al. 2001; Reubinoff et al. 2001; Schuldiner et al. 2001) and Parkinson's (Odorico et al. 2001), to diabetes (Assady et al. 2001) and heart failure (Odorico et al. 2001). However, human ES cells are limited in their ability to be used clinically; despite other safety concerns, this is due to the fact that current human ES cell lines, like any other foreign tissue, would not be histocompatible with a patient's immune system and would likely be rejected upon transplantation. If autologous human ES cell equivalents could be derived, this would surely bring human ES cell therapies closer to widespread clinical application while also potentially resolving questions about the nature of pluripotency.

The underlying concept behind the derivation of autologous lines is reprogramming. Reprogramming, in this context, refers to starting with a given patient's cell(s) and deriving cells with a human ES cell phenotype *without* affecting the genotype. What this presupposes is that the genes responsible for displaying an embryonic phenotype can be reactivated and that the genes expressed at the embryonic stage in development are still present in the nucleus of every cell in our bodies, but that they have been silenced. The first evidence that this might be possible came from Gurdon's work in the early 1960's using frog embryos which showed that the developmental capacity of somatic cells could be altered from a unipotent to a pluripotent state

(Gurdon 1962c; Gurdon 1962d; Gurdon 1962a; Gurdon 1962b). Following Gurdon's work, however, the work was not carried over in mammals for over 30 years. Until the successful cloning of Dolly the sheep (Wilmut et al. 1997), it was questionable as to whether these dormant genes could be reactivated in mammals, let alone be reactivated in the correct manner to recreate an embryonic phenotype capable of directing embryonal development. Now that it is known that reprogramming and reactivation of embryonic genes is indeed possible, the next step is to understand the mechanism, and from there it should be possible to design a process to derive clinical grade autologous and disease-specific human ES cell equivalent lines for therapeutic use.

1.2 Epigenetics and Reprogramming

Although one might infer that reprogramming requires rearranging or adding to a cell's genetic code, in fact, it is actually the epigenetic code that is most important. Epigenetic code refers to the complex arrangement of molecules that are bound to and intertwine the chromatin, effecting the way the DNA is read. Since all the genes needed for human development are stored on our chromosomes, the same chromosomes found in every cell of our bodies, if the way in which those genes are read is altered, then a cells 'programming' would theoretically be altered. Such changes in gene transcription can result in phenotypic changes, thus resulting in transdifferentiation or, under the right circumstances, reprogramming to a pluripotent state.

The pattern in which our chromosomes are deciphered, the way the DNA is read, is dependent on more than just the nucleotide sequence that makes up our DNA. There is a secondary level of code (or programming) 'on the surface' of our DNA code that dictates what sections of the DNA are to be read and when, as well as how to read them; this coding is referred to as epigenetic coding. While the chromatin in the nucleus of every cell has the instructions for every gene for every cell type that makes up an organism, epigenetic code selectively blocks or allows transcription of genes,

making sure a cell only expresses the genes it is supposed to; it is responsible for designating a skin cell as a skin cell, a brain cell as a brain cell, and so on and so forth.

The epigenetic code present on a cell's DNA is unique to that cell phenotype; epigenetic differences are what make different cell types unique despite the fact that they all carry identical chromosomal DNA (when from the same individual). When stem cells differentiate, genes are instructed to turn on or off in a specific pattern, these genes cause a cascade of proteins and factors to be coded for that eventually results in a cell that has a final, specific designation, such as a cardiac muscle cell or reproductive spermatozoa cell. Although the mechanisms involved are not yet fully understood, it stands to reason that if one could control epigenetics, the state of a cell could be controlled, pushing it towards a specific differentiated state, or potentially back, towards a pluripotent state, enabling the creation of autologous pluripotent cell lines.

Epigenetics are controlled in the cell by alterations in the methylation, phosphorylation, and/or acetylation patterns on the DNA and the histones which package the DNA into chromatin (Jenuwein et al. 2001). Changes in these patterns affect the way the DNA is read by altering which regions of the chromosomal DNA are open or 'unlocked' for translation. The 'unlocked' genes then lead to changes in the proteome and subsequently the intracellular environment, these changes can eventually catalyse changes in cell state or phenotype. Specifically, there is evidence that chromatin patterns related to maintenance of ES cell pluripotency selectively block transcription factors that are thought to be linked to developmental differentiation lineages (Kimura et al. 2004; Szutorisz et al. 2005; Surani et al. 2007; Hochedlinger et al. 2009). In essence, differentiation, both towards and away from pluripotency, is managed by epigenetics and epigenetics are key in controlling a cell's phenotype and fate.

1.3 Methods of Reprogramming

1.3.1 Cell Fusion

Cell fusion is a well-established phenomenon that happens both naturally (Barski et al. 1960; Barski et al. 1962; Loutit et al. 1982; Huppertz et al. 1998; Taylor 2000; Vignery 2000; Huppertz et al. 2001) and can also be provoked in vitro (Harris et al. 1965; Norwood et al. 1976). Combinations of various cell types have been known to form hybrids (or heterokaryons) (Harris et al. 1965; Cowan et al. 2005). Furthermore, some hybrids display distinct characteristics of one of the two fusion partners (Darlington et al. 1982; Flasza et al. 2003; Cowan et al. 2005; Yu et al. 2006), even when cells from different species have been mixed (Harris et al. 1965; Darlington et al. 1974; Darlington et al. 1982; Flasza et al. 2003). Through fusion, the genetics and epigenetics of both cell types can be affected; altered in such a way that a new phenotype is observed (Harris et al. 1965; Poste et al. 1971; Darlington et al. 1982).

Upon successful cloning of Dolly, the mindset of scientists was dramatically altered as it clearly showed that the differentiated state of mammalian cells is, at least in some cases, reversible (Wilmut et al. 1997). Given this change of mindset, it seems no coincidence that following the success of Dolly, there was a proliferation of publications suggesting that adult cells were much more plastic than previously thought (Poulsom et al. 2002; Horb et al. 2003; Chen et al. 2004; Grove et al. 2004; Jang et al. 2004; Song et al. 2004). Although the extent of plasticity amongst populations of adult cells remains controversial, it has been shown that at least some of the reported “transdifferentiation” events were actually a consequence of cell fusion (Terada et al. 2002; Alvarez-Dolado et al. 2003; Vassilopoulos et al. 2003; Wang et al. 2003). For instance, studies in the mouse have shown that myeloid cells derived from bone marrow can spontaneously fuse with host hepatocytes, resulting in their functional recovery (Vassilopoulos et al. 2003; Wang et al. 2003). Although this does not offer definitive proof against transdifferentiation, such examples simply highlight cell fusion as one mechanism by which transdifferentiation can occur.

The idea of reprogramming using cell fusion is nothing new. In fact, Miller and Ruddle, in publications released in 1976 and 1977, showed that, fusion between embryonal carcinoma (EC) cells and thymic cells or friend-erythroleukemia cells resulted in hybrids which displayed an altered, EC-like phenotype (Miller et al. 1976; Miller et al. 1977b; Miller et al. 1977a). Similar results in which the pluripotent fusion partner demonstrated phenotypic dominance have also been reported by other groups as well (McBurney 1977b; McBurney et al. 1978; McBurney et al. 1979; Baron et al. 1986). Further proving the reprogramming potential of EC cells and its conservation across species, Flasza *et al* showed that endogenous expression of key embryonic genes Oct-4 and Sox-2 in combination with simultaneous down-regulation of the lymphocytic cell marker CD45 was achieved in human T-lymphoma cells when fused with the pluripotent P19 murine EC cell line (Flasza et al. 2003). This is compounded by other intra-species fusion reports where hybrid cells expressed markers associated with pluripotency, such as the transcriptional regulator, Oct-4 (Scholer et al. 1989), tissue non-specific alkaline phosphatase (Berstine et al. 1973), and high levels of telomerase (Bestilny et al. 1996). Fusions were even shown to contribute to developing embryonic structures when implanted into blastocysts (McBurney 1977a). Similarly, embryonic germ (EG) cells and embryonic stem (ES) cells have also been shown to confer elements of pluripotency upon other cell types through fusion/hybridisation. Mouse EG cells, after fusion with thymic lymphocytes, are capable of demethylating both imprinted and non-imprinted genes in lymphocyte derived nuclei (Tada et al. 1997). Similarly, mouse ES cells, when fused with thymocytes, can result in reactivation of an *OCT4*–enhanced green fluorescent protein (*EGFP*) transgene, as well as the silenced X chromosome (Tada et al. 2001). Hybrids created from ES cells also exhibited hyperacetylation at histone H3 and H4, while lysine 4 (K4) of H3 became globally hyper di- and tri- methylated, similar to the epigenetic patterns seen in the ES cell genome (Kimura et al. 2004). These studies infer that EC, EG, and ES cells all share the ability to mimic, at least to an extent, the reprogramming activity present in unfertilized

oocytes, although the common element(s) of these cell types that plays a role in conferring pluripotency remains poorly understood.

Following in the footsteps of previous groups, in 2005, hybrids from human ES cells and human fibroblasts were created which displayed the markers, growth characteristics and, to some extent, the differentiation capacity of the parental human ES cells. However, the resulting hybrid cells contained the nuclei of both somatic and human ES cells (Cowan et al. 2005). Although, through cell fusion, the mechanisms underlying nuclear reprogramming can be observed by studying the epigenetic changes that occur in somatic-pluripotent cell hybrids, the fact remains that cell fusion results in hybrid formation, creating near tetraploid (4n) cells (or often polyploid cells), which, in a clinical sense are not very useful. However, two strategies have been reported that address this issue and may lead to a solution; 1) selective elimination of tetraploid nuclei and 2) selective insertion and removal of specific ES cell chromosomes after reprogramming. While these strategies might prove effective in some situations, neither is very efficient.

A novel approach for producing normal, diploid reprogrammed cells through cell fusion was suggested in a report from the Verma laboratory (Pralong et al. 2005). They proposed that it may be possible to generate tetraploid ES cells through cell fusion, then subsequently fuse the tetraploid ES cells with normal diploid somatic cells and, after enough time to reprogram has passed, the “heavy” tetraploid ES cell nucleus could, in theory, be centrifuged out of the heterokaryon as a karyoplast, leaving a normal diploid cell behind. However, the hybrid cell must exist as a heterokaryon (i.e., a cell with two distinct nuclei) and the tetraploid nucleus must be eliminated prior to mitosis, where mixing of both genomes occurs.

As of yet, this experiment has not been reported. However, Pralong *et al.* (2005) do provide evidence that mouse tetraploid ES cells can be successfully fused to diploid ES

cells, and that the tetraploid nucleus can indeed be eliminated from the heterokaryon under specific centrifugation conditions, resulting in mouse ES cells that are expectedly diploid and retain ES cell properties. Successful application of this approach has not yet been reported using somatic cells, but selective extrusion of a tetraploid nucleus by centrifugation may be an option for eliminating the pluripotent cell genome from a heterokaryon once its contribution to reprogramming has been made.

A potentially more efficient alternative to centrifugal elimination of the pluripotent genome is targeted chromosome elimination. A Cre-*loxP*-mediated chromosome rearrangement strategy has been reported which selectively eliminates ES cell chromosomes from hybrid cells (Matsumura et al. 2007). This could mean that specific ES chromosomes that code for pluripotency genes could be integrated into hybrid cells, then once reprogramming of the somatic genome has completed, these chromosomes could be selectively eliminated using Cre recombinase. Matsumura *et al* (2007) demonstrated that, following the introduction of a chromosome elimination cassette (CEC) which integrates into specific desired regions of the mouse genome, mouse chromosomes 11, 12, and both copies of 6 could be eliminated upon induction of a CEC-mediated sister chromatid recombination by transient Cre expression (Matsumura et al. 2007). In principle, it should be possible to selectively eliminate entire sets of undesired chromosomes using this method. Also, this approach might be more powerful as it would not require maintaining the hybrid cells as heterokaryons, plus it would allow for a longer exposure of the ES cell reprogramming factors in the somatic target cell, potentially enhancing reprogramming efficiency.

Targeted chromosome elimination may also be relevant to the derivation of patient-specific major histocompatibility complex (MHC) matched stem cells for regenerative medicine applications. In the same study, Matsumura *et al.* (2007) proposed that MHC class I and class II genes, clustered on chromosome 6 in humans, could be selectively eliminated from somatic cell-ES cell hybrids, then a microcell mediated chromosome

transfer could be used subsequently to replace the copies of chromosome 6 with a patient matched, somatic cell derived pair which would theoretically result in MHC matched pluripotent cells (Matsumura et al. 2007). Although these cells would not be truly autologous, if production could be made efficient, they might have a viable role in regenerative medicine therapies, at least until fully autologous, safe pluripotent cells can be derived reproducibly.

However, despite these various methods and publications, the question remains, is the cytoplasm, the nucleus, or both in combination responsible for catalyzing the somatic cell reprogramming process that leads to pluripotency? It is known that reprogramming is reflected by changes in the nucleus and alterations in transcription at the genetic level, which would infer that the nucleus is key in reprogramming, but the advent of somatic cell nuclear transfer and the birth of Dolly seems to indicate otherwise.

1.3.2 Somatic Cell Nuclear Transfer (SCNT)

Adult somatic cells can be reprogrammed after fusion with a matured oocyte, a process commonly known as somatic cell nuclear transfer (SCNT). SCNT offers potential for deriving autologous stem cells, albeit in the case of humans, the availability of donated human eggs is a major limiting factor and the use of human eggs can be ethically challenging. Also, although the technique is relatively well understood in animals, demonstrated first by the production of live animals (Gurdon 1962a; Wilmut et al. 1997; Wakayama et al. 1998a) and secondly by the derivation of embryonic stem cells from the inner cell mass cells of SCNT embryos (Wakayama et al. 2001), the rate of success is very low. This has been further shown most recently in SCNT derivation studies with Rhesus monkeys, a close genetic relative to humans, however, only 2 of the 304 oocytes (0.7%) collected resulted in stable ES lines from SCNT (Byrne et al. 2007). In an attempt to address the issue of human oocyte availability and further test the conservation of reprogramming factors across species, Chen *et al.* reported that human fibroblasts can be reprogrammed into an ES cell state by SCNT into rabbit

oocytes (Chen et al. 2003). Despite its obvious drawbacks, SCNT remains a potentially viable method for production of autologous stem cell lines and these studies provide proof that somatic nuclei can be reprogrammed to a pluripotent state by factors present in the oocyte cytoplasm, and furthermore, that reprogrammed nuclei are capable of directing embryonic development to term.

Although Wilmut and his team were the first to reprogram a mammalian somatic nucleus to full, undisputed pluripotency, the use of cytoplasm as a reprogramming medium (albeit not from an oocyte) has its roots in work done over 20 years prior to the birth of Dolly. Following the work of Gurdon et al. (Gurdon 1962d; Gurdon 1962a), a technique similar to SCNT was achieved in 1971 through the fusion of cytoplasts and karyoplasts, products of enucleation (Poste et al. 1971). After treatment with cytochalasin, an actin depolymerization agent, centrifugal force can be used to segregate a cell into two membrane encapsulated components, one composed primarily of cytoplasm (the cytoplast) and one containing primarily the nucleus surrounded by a thin membrane (the karyoplast or nucleoplast). Veomett *et al.* showed that cytoplasts and karyoplasts isolated from two different parental cell lines, when fused, resulted in cells with a unique phenotype as compared to either parental cell, so-called 'reconstituted cells' (Veomett et al. 1974). Wallace and Bunn showed one year later that enucleation of one of the parental cells could be omitted and that cytoplasts alone could transfer chloramphenicol resistance upon fusion, giving proof of cytoplasmic inheritance in humans (Wallace et al. 1975). The resulting cell type from this procedure was termed a cytoplasm hybrid or 'cybrid' (Wallace et al. 1975). Bunn and Eisenstadt then went further, finding that the greater the ratio of cytoplasts to whole cells, the greater the number of viable cybrids produced (Bunn et al. 1977). Cytoplasmic 'inheritance' was also evidenced by the immortalisation of cybrids after fusion of human lymphocytes with cytoplasts from the mouse L929 fibrosarcoma cell line, a key feature shared by cancer and embryonic stem cells (Abken et al. 1986). These studies show that varying levels of partial reprogramming and/or

transdifferentiation can be achieved through the addition of cytoplasm (through cytoplasts) to a given cell and also that increased levels of cytoplasm seem to be more effective in producing reprogramming effects. Although the pluripotent partner's phenotype often dominates, as evidenced by the studies above, pluripotent teratocarcinoma cells have been shown to differentiate after fusion with rat myoblasts, demonstrating the capability of somatic cell cytoplasm to induce differentiation of pluripotent cells (Iwakura et al. 1985). The evidence suggests that both the cell types involved are important, as well as the relative amount of cytoplasm contributed by each cell type involved in making the given cybrid or reconstituted cell. This hypothesis is supported by the work of Wakayama and Yanagimachi, who showed that mouse oocytes, which we know are capable of catalysing reprogramming, were capable of supporting development (which involves reprogramming the pronuclei) with up to half of their cytoplasm removed, but failed to reach even the two cell stage with any less than half (Wakayama et al. 1998b). While, prior to the inception of this work, SCNT was currently the method of choice for creating autologous (donor matched) ES cells, technical hurdles, ethical guidelines, and government regulations have prevented the successful use of this technology on human somatic cells and have subsequently triggered the development of alternative strategies for reprogramming somatic cells to pluripotency.

1.3.3 Whole Cell Extracts

While the literature has clearly shown that oocytes and pluripotent cells are capable of catalysing reprogramming, the exact elements of oocytes and pluripotent cells that make this possible are not well defined. It is known that oocytes are comprised primarily of proteins and RNA, which raises the question, are non-nuclear (or non-genomic DNA) elements capable of catalysing reprogramming? Work done with pluripotent cell extracts has attempted to answer this question.

Treating somatic cells with cell extracts involves reversible permeabilization of the somatic cells' membranes, followed by exposure to the reprogramming extract, then resealing of the cells. In some cases, cell extracts have been shown to elicit phenotypic changes that result in differentiation, transdifferentiation or show signs of dedifferentiation (Hakelien et al. 2002; Gaustad et al. 2004; Hakelien et al. 2005; Qin et al. 2005). Gaustad et al. (2004) showed that extracts from rat cardiomyocytes can trigger cardiomyocyte function from human adipose stem cells (Gaustad et al. 2004), while Qin et al. was able to more effectively induce differentiation of mouse ES cells into pneumocytes using extracts of murine type II pneumocytes (Qin et al. 2005). These findings lead to the hypothesis that an extract from a pluripotent cell would provide the regulatory components required to direct a nuclear 'program' characteristic of the pluripotent cell phentoype, potentially resulting in somatic cell reprogramming.

To test this idea, Xenopus egg extracts were shown to induce the formation of ES cell-like colonies along with expression of pluripotency genes in human epithelial cells and leukocytes (Hansis et al. 2004). Unfortunately, the leukocytes only had a limited lifespan and cells did not express surface markers characteristic of ES cells, so that under these conditions, only partial reprogramming occurred. However, perhaps the most convincing evidence of the potential of cell extracts was published by Taranger et al. (2005) where they demonstrated that human fibroblast cells can be induced to express a panel of ES cell markers following exposure to pluripotent embryonal carcinoma cell extracts or mouse ES cell extracts, while also providing a strong argument that the expression is endogenous, not detected from the extracts (Taranger et al. 2005). In spite of this, the authors refrain from claiming that these altered fibroblasts are truly pluripotent, fully reprogrammed ES cell equivalents; which may be due to the inability of these cells to maintain expression of all the fundamental ES cell markers long term.

In a review of reprogramming, Collas and Gammelsaeter, reasoned that the lack of full, long-term reprogramming through cellular extracts might be due to “variations in the extent of transcriptional reprogramming that may reflect incomplete reprogramming or progressive deregulation of the new program” (Collas et al. 2007). They also hypothesized that the procedure could be improved by “repeated extract exposure, destabilization of the epigenome with chromatin modifying agents, or induction of a dedifferentiation step before triggering a new target cell–specific program” (Collas et al. 2007). From the cell extract work referenced above, it seems clear that while the extracts are clearly having an effect, dosage, cell state, and culture conditions play a role in switching a cell’s ‘programming’ effectively and permanently.

Despite the remarkable successes in relation to reprogramming achieved by cellular extracts, it seems nearly impossible to eliminate the possibility of contamination by nuclear DNA from the pluripotent donor cells. In such a scenario, DNA from a pluripotent cell could end up mixing and recombining with somatic cell DNA, driving the partial pluripotent phenotype observed. In a clinical sense, any extraneous DNA would cause reason for concern and would make the resulting cells a heterogenous, indefinable population and as such, difficult to characterize and derive reproducibly. For the purposes of this work, we aimed to achieve the same successes, without the possibility of DNA contamination.

1.3.4 Viral Induction of Pluripotency

In 2006, approximately one year after the start of this project, Takahashi and Yamanaka published the remarkable finding that mouse embryonic and adult fibroblasts could be dedifferentiated to a state of induced pluripotency using viruses which over express the key pluripotency factors OCT4, SOX2, cMYC, and KLF4 (Takahashi et al. 2006). This initial publication was discounted by some as incomplete reprogramming, and many researchers remained sceptical about the possibility of

success using the same process on human somatic cells. However, doubts about the process subsided in 2007 when Yamanaka and Jaenisch's groups independently showed that under slightly different conditions, they could create induced pluripotent stem (iPS) cells that pass the most stringent test of pluripotency, germ line competence (Okita et al. 2007; Wernig et al. 2007). Furthermore, only a few months later, work done independently in Yamanaka and Thomson's labs was published demonstrating that pluripotency could also be induced using a similar protocol in human somatic cells; not only by OCT4, SOX2, cMYC, and KLF4, but also by OCT4, SOX2, LIN28, and NANOG (Takahashi et al. 2007; Yu et al. 2007).

The studies outlined above set in motion a furious proliferation in reprogramming publications and research such that within only two years of these landmark studies over 200 publications and scientific review articles on the subject of "induced pluripotent stem cells" have appeared. It should be noted that at the inception of this work, many researchers in the stem cell community remained understandably sceptical and felt that reprogramming or complete dedifferentiation to a state of pluripotency was nothing sort of impossible; it is therefore all the more remarkable that within such a short time span that the scientific community has reversed this line of thinking and speedily accepted induced pluripotency as an important part of stem cell research and development. An article published in Nature (April 2009) entitled "Stem Cells: Fast and Furious" embodies the research environment experienced by scientists working on reprogramming and this project was no different and has been a constantly evolving process with efforts made to incorporate the rapid advances published on the subject (Baker 2009).

Beyond the initial fascination with reprogramming and its implications, deeper questions began to arise about what was happening during the transition from the base, somatic cell state to pluripotency. In an attempt to better understand the timing, Jaenisch's group, followed by others, used inducible viral vectors coding for the

reprogramming factors (Brambrink et al. 2008; Hockemeyer et al. 2008; Maherali et al. 2008a; Woltjen et al. 2009). Using a doxycycline inducible system, it was reported that, in mice, alkaline phosphatase and SSEA1 were early indicators of dedifferentiation, detectable at day 3 and day 9. OCT4 and NANOG, however, were not detectable until at least 15 days post transduction (Brambrink et al. 2008). Similarly, Jaenisch's group also showed in 2008 that inducible vectors could be used to make human iPS cells and that, using their system, a minimum of eight days transgene expression was required (Hockemeyer et al. 2008). Understanding the timing and gene expression patterns that arise over the transition or 'reprogramming' period from somatic to pluripotent cell states could lead to a safer, more efficient method for iPS cell generation.

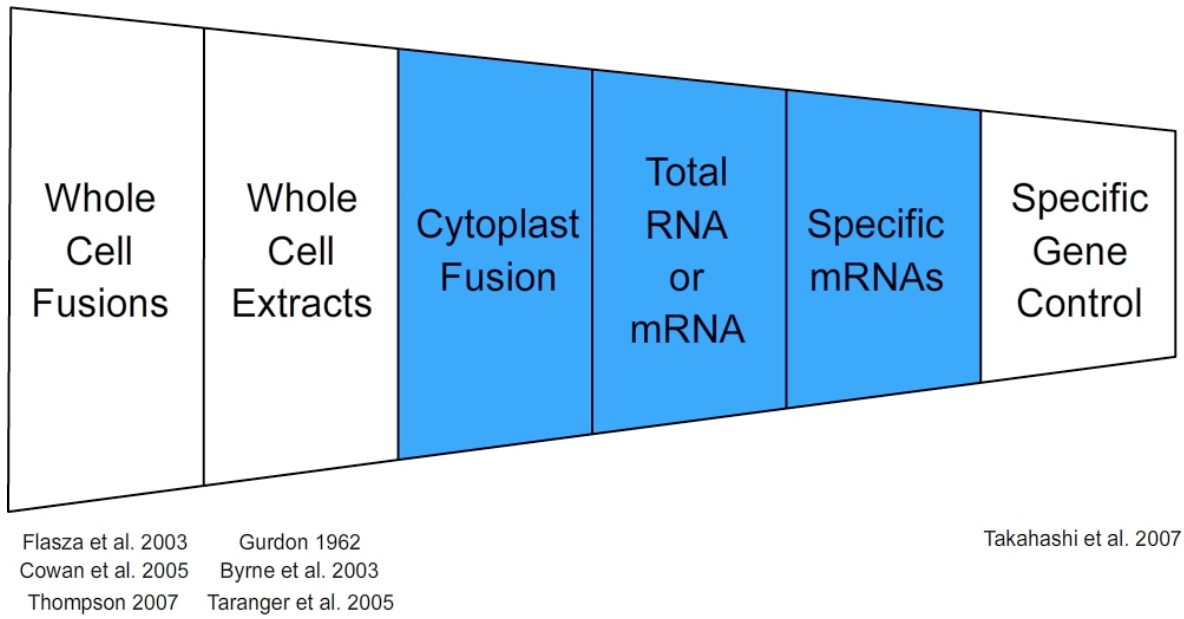

Figure 1.1: Reprogramming 'Focal Spectrum'

Of the many known methods of reprogramming, prior to the use of specific reprogramming factors, most involve the use of cellular and/or genetic material. This spectrum depicts the range of potential reprogramming options, from the use of whole cells (through fusion) down to specific gene manipulation/control. A few key references are cited below the relevant portions of the spectrum. This work has chosen to focus on the highlighted region in blue; using cytoplasts from pluripotent cells, Total RNA, Total mRNA, and specific upregulation of reprogramming genes by mRNA in an effort to catalyse a 'state change' towards the pluripotent phenotype, including expression of key markers and pluripotency genes. The methods explored evolved with the literature as, at the inception of this project, 4-factor reprogramming had not yet been developed.

1.4 A Brief History of Pluripotency

Arguably, the field of stem cell research originates from the work of Ernest A. McCulloch and James E. Till that began with research on mice in Canada in the 1960's (Till et al. 1963; Till et al. 1964; Till et al. 1967). Their work began to elucidate the natural regenerative processes within mammals. Over the 40 years to follow, stem cell research slowly progressed through the use of mice and other animal models (Till et al. 1964; Friedrich et al. 1991; Moreadith et al. 1992; Graves et al. 1993; Sukoyan et al. 1993; Labosky et al. 1994). Notably, in the 1970's Papaioannou did embryonal carcinoma (EC) work with Gardner, McBurney, and Evans (Papaioannou et al. 1975; Papaioannou et al. 1978; Papaioannou et al. 1979). They found that the tumours formed from these cells shared similarities to embryonic development and their work eventually lead up to Evans' discovery of mouse embryonic stem cell derivation techniques in 1981 (Evans et al. 1981). Evans and Kaufman in the UK (Evans et al. 1981) and Martin in the US (Martin 1981) are jointly credited with the discovery of embryonic stem cell derivation. From their earlier work on mouse EC cells, they deciphered the conditions and methods under which derivation of embryonic stem cells was possible, such as the use of feeder cells, enabling researchers to begin to understand regeneration and pluripotency in terms of embryonic development. In 1995, stem cells moved closer to applicability to humans through the derivation of primate ES cells (Thomson et al. 1995). Then, in 1998, stem cell research made another leap forward when the first *human* embryonic lines were derived (Gearhart 1998; Thomson et al. 1998).

Stem cells, by their very nature, are undifferentiated (or unspecialised) cells that renew themselves for long periods of time through cell division and yet retain their ability to become specialized cells. By altering physiological or environmental conditions, human ES cells derived from the inner cell mass (ICM) of a blastocyst stage embryo

(see Figure 1.5) can be directed down a specific cell lineage resulting in almost any cell type found in the body; this ability is referred to as pluripotency.

1.5 Human ES Cells: The Standard for Pluripotency

1.5.1 Defining Characteristics of a Stem Cell

Despite slightly varying 'standard' definitions of what a stem cell is, the fact remains that the definition is ever changing. While projects like the International Stem Cell Initiative are helping to standardise and define stem cells (Andrews et al. 2005a), at this time, there is still a lot of controversy and the line is yet to be drawn between what is and what is not a true stem cell. But it has been agreed that all stem cells, regardless of their source, have three general properties:

1. They are capable of dividing and renewing themselves for long period of time
2. They are unspecialised (some having more plasticity than others)
3. They can give rise to specialised cell types.

Beyond this general definition for all stem cells, it should be noted that there is a clear difference between embryonic stem (ES) cells, which can only technically be derived from cells at the earliest stages of development, and other stem cell populations found within the human body, which are often referred to as mesenchymal or adult stem cells.

Unlike most cells in the body, such as blood cells, muscle cells, or nerve cells, which do not normally replicate themselves, stem cells may replicate many times. An initial population of stem cells that is allowed to proliferate for many months in the laboratory can yield millions of cells. If the resulting cells continue to be unspecialized, like the parental stem cells, then the cells are considered to be capable of 'long-term self-renewal.' Embryonic stem cells are an example of stem cells with long-term self-renewal capabilities, they can potentially divide endlessly; whereas, adult stem cells tend to divide more than somatic cells, but they have a limited number of divisions before reaching senescence. It should be noted that self-renewal capacity alone is not

enough to define a stem cell, but merely characteristic of stem cells, both mesenchymal (or adult) and embryonic.

Stem cells are unspecialised. While a heart muscle cell can work with its neighbours to pump blood through the body, a red blood cell can transport oxygen through the bloodstream, and a nerve cell can send electrochemical signals to other cells that allow the body to move; a stem cell can do none of these things. However, unspecialised stem cells can differentiate into specialised cells, including neurons, heart muscle cells, blood cells, and many others (Thomson et al. 1998; Assady et al. 2001; Carpenter et al. 2001; Odorico et al. 2001; Reubinoff et al. 2001; Schuldiner et al. 2001). Mesenchymal stem cells and ES cells, while both being classed as unspecialised, differ in their range of differentiation abilities.

Stem cells can give rise to specialised cells. When unspecialised stem cells give rise to specialised cells, the process is called differentiation. The ability to differentiate, or change epigenetically and/or phenotypically, is a fundamental property of stem cells. Although the signals that trigger stem cell differentiation have not yet been fully elucidated, we know that stem cells are affected by a number of internal and external factors. A cell's genes and epigenetic state control the internal signals, which affect the instructions for all the functions of a cell. The external signals for cell differentiation include: compounds secreted by other cells (also known as paracrine factors), physical contact with neighbouring cells, environmental effects (such as gases and temperature), and a variety of molecules in the microenvironment and other still unknown factors. While ES cells are pluripotent, meaning they can differentiate into any cell type found in the body, mesenchymal stem cells are only capable of differentiating into a limited subset (such as bone, fat, muscle, and blood) and are therefore classed as multipotent.

Although we know that the telomere repairing enzyme telomerase is responsible for the seemingly endless proliferation of human ES cells, the mechanism is still under

investigation (Bayne et al. 2005; Krtolica 2005). Through embryonic stem cells, it may be possible to understand how cell proliferation is regulated during normal embryonic development or during the abnormal cell division that leads to cancer. Understanding the mechanisms involved in pluripotency and self-renewal is key to understanding reprogramming.

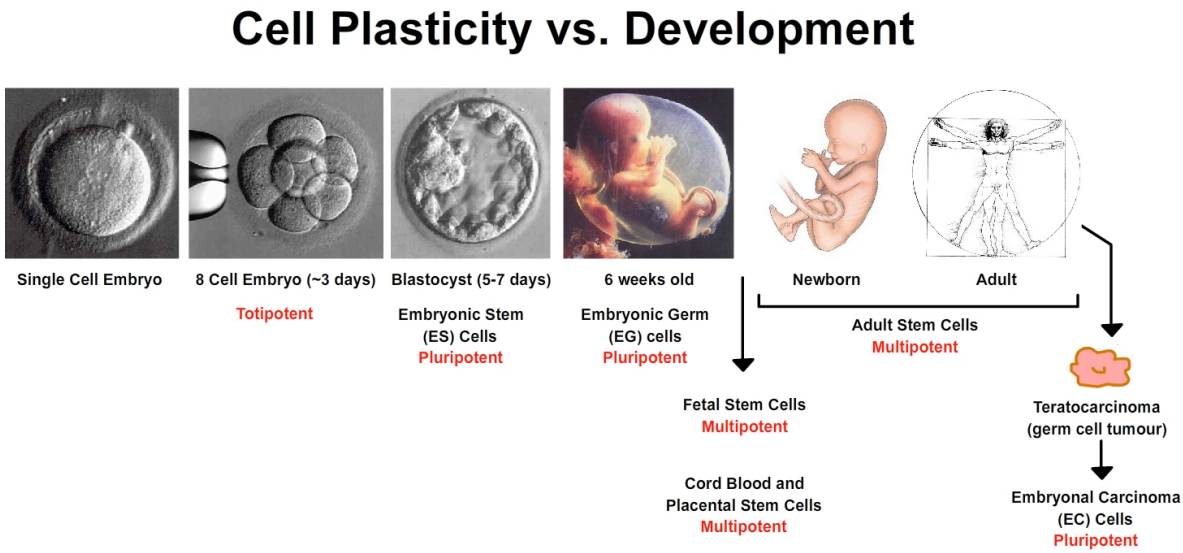

Figure 1.2: Stem Cells and Development
This figure gives an overview of the origins of stem cells throughout development, with stem cell plasticity typically decreasing as cells mature and differentiation into adult tissues occurs. As shown above, human embryonic stem cells are derived from day 5-7 embryos. The process starts with a fertilised IVF egg, which is nurtured in vitro until the embryo reaches the blastocyst stage. Once a blastocyst has formed, the inner cell mass (ICM) is plated out onto a tissue culture dish with a layer of feeder cells. Using a combination of feeder cells, specially formulated media, and a relatively controlled environment the ICM derived human ES cells will proliferate, in colonies, remaining pluripotent until pushed to differentiate.

1.6 Pluripotent NTERA2 Cells

1.6.1 Origins of NTERA2 Embryonal Carcinoma Cells

NTERA2 (NT2) embryonal carcinoma (EC) cells are a very useful tool since they act very much like embryonic stem cells, and can, like ES cells, differentiate into components from each of the three germ layers. However, NTERA2 cells are not embryonic stem cells as they are derived from a teratoma, not embryos (Andrews et al. 1985). Teratoma describes a type of tumour that derives from pluripotent germ cells and typically arises from cells in the ovaries in women, the testes in men, and the sacrum in children. A teratoma is a complex tumour that has various cellular or organoid components, these components normally consist of derivatives from more than one germ layer.

The widely used and highly characterised NTERA2 cell line was originally derived from the TERA-2 cell line. The cell line 'TERA-2' was derived by J. Fogh from a lung metastasis of a 22-year-old Caucasian man with a primary testicular germ cell tumour. According to Andrews et al (1980), the pathologist's report described the primary tumour as embryonal carcinoma of the testis and the explanted metastasis as embryonal adenocarcinoma and teratoma. Preliminary morphologic examination of a subline transferred to The Wistar Institute in 1976 suggested that it was not composed of human EC cells, and tumour formation in nude mice was not then observed (Jewett 1978; Andrews et al. 1980a). However, in a subsequent experiment, a tumour that had a component of EC cells in combination with more differentiated cell types, was obtained from a nude mouse. After growth in a nude mouse, the 'TERA-2' line was thereafter designated NTERA-2 (also known as NTERA2 or simply NT2). From this line Andrews et al. separately seeded 86 cells onto irradiated STO feeder cells and 40 clones were obtained (Andrews et al. 1980a). Three of these clones (NT2/B9, NT2/D1, and NT2/D3) were selected at random for further study and adapted to growth without feeder cells (Andrews et al. 1984b). The original clones of NT2 from the mid 1970's

still survive today and the feeder free lines are commonly used, both for comparative studies and for fundamental cancer and differentiation studies (Duran et al. 2001; Schwartz et al. 2005; Skotheim et al. 2005; Park et al. 2007b). Typically, NTERA2 is known for its propensity toward neuronal lineages (Andrews 1984), but it does have some plasticity and has been known to differentiate into a number of cell types (Wertkin et al. 1993; Moasser et al. 1995; Schwartz et al. 2005; Skotheim et al. 2005). The NTERA2 cell line is possibly the most widely studied human EC line; its clones are used by research groups around the world (Skowronski et al. 1985; Andrews et al. 1994; Gokhale et al. 2000; Garbuzova-Davis et al. 2002; Borghi et al. 2003; Bahrami et al. 2005; Schwartz et al. 2005; Liu et al. 2006; Park et al. 2007a).

NTERA2 has been an important tool for comparative studies with human ES cells due to its striking similarities despite being derived from a cancer (Andrews et al. 1985; Andrews 1998; Andrews 2002; Schwartz et al. 2005; Liu et al. 2006). Like human ES cells, undifferentiated NTERA2 cells are not only OCT4 positive, but also display many of the same surface markers including the glycolipid antigens stage specific embryonic antigen (SSEA)-3 and SSEA-4, but not SSEA-1, the proteoglycan antigens TRA-1-60 and TRA-1-81, the liver/bone/kidney associated alkaline phosphatase (ALP) antigens, and TRA-2-49 and TRA-2-54 (Andrews et al. 1982; Andrews et al. 1984a; Andrews et al. 1984b; Andrews et al. 1984c; Andrews et al. 1996; Thomson et al. 1998; Reubinoff et al. 2000; Draper et al. 2002). NTERA2 cells, while being similar to human ES cells, are much more robust in terms of culturing and maintenance. They grow in monolayer, they do not require a feeder layer for growth, and they are partial to proliferation, rather than differentiation, despite their ability to differentiate into a wide variety of cell types under set conditions (Andrews 1988; Andrews et al. 1994; Andrews 1998; Schwartz et al. 2005; Skotheim et al. 2005). If human ES cells could be made to adopt the beneficial qualities of EC cells without drastic karyotypic change or becoming carcinogenic, this would make growth and quantification of human ES cells much

easier, but until that is accomplished, NTERA2 cells are able to serve as a good preliminary model.

1.6.2 EC vs ES – Opposite Ends of the Spectrum?

While ES cells are programmed to eventually develop into specifically differentiated cell types in accordance with embryo development, EC cells are adapted to survive and proliferate. They are like stem cells, except with a higher propensity for survival, but *will* differentiate if pushed. ES cells, on the other hand prefer to differentiate, but can be made to survive long term if cultured properly (Andrews 1998; Andrews 2002). It is as if the two cell types are on opposite ends of a spectrum, or "opposite sides of the same coin" (Andrews et al. 2005b).

Perhaps EC cells resemble an adapted version of ES cells, an accumulation of mutations that has managed to survive and proliferate because its ability to gain helpful genetic additions, giving them an advantage over other surrounding cell types. The implications for this are exciting and worrisome at the same time, as this suggests that regenerative cells that are able to help us could also be potentially carcinogenic.

1.6.3 What affects the 'spectrum'?

Stem cell scientists in many labs have observed mutations within a variety of human ES cell lines, grown under a variety of conditions (Draper et al. 2004b; Hanson et al. 2005; Maitra et al. 2005; Forsyth et al. 2006). If stem cells have an inherent propensity toward mutations that could lead toward cancer, then their use in a clinical setting would be severely limited. But many scientists are optimistic that this is a problem that can be solved with proper culturing techniques, better understanding of stem cell biology, and through proper (irreversible) differentiation protocols. EC cells may well

be the key to understanding the natural progression of human ES cell mutations and through this model we might be able to control such mutations.

1.6.4 EC Cells - A Good Model for Human ES Cells

Publications have inferred that NTERA2 cells and embryonic stem cells are closely related (Draper et al. 2004a; Baker et al. 2007; Harrison et al. 2007). Studies have also shown that ES cells have a tendency towards mutation and that these mutations often bring them karyotypically closer to EC lines, such as NTERA2 (Draper et al. 2004b; Andrews et al. 2005b; Schwartz et al. 2005). This research suggests that EC cells may well be like ES cells that have undergone multiple rounds of selection, resulting in a more robust, albeit carcinogenic, cell line. This of course ties in with an array of medical advancement possibilities, most poignantly cancer and the way it develops *in vivo*. EC cells could very well be representative of the natural endpoint (through selective pressures) for embryonic stem cells cultured *in vitro.*

Whereas human ES cell lines tend to grow in colonies on feeder cell layers and differentiate spontaneously, NTERA2 cells can be grown stably in monolayer without feeders. EC cells are well characterised and have already been successfully used in cell fusion reprogramming applications (Flasza et al. 2003; Wu et al. 2004). It is for all these reasons and more that we believe that the NTERA2 line suffices as a good model for human ES cells. Also, for this work, we plan to use NTERA2 cells to serve as donors for pluripotency factors, and as a platform for initial experimentation until human ES cells can be implemented into the same experimental framework.

1.7 Project Evolution

The goals of this project at its inception were based around using NTERA2 EC cells, human ES cells and existing publications pertaining to cell fusion, reprogramming and transdifferentiation to gain a better understanding of what is required to catalyze

phenotypic change from a unipotent somatic cell toward a pluripotent cell state. From this initial standpoint, experiments were based primarily around fusion studies, the work of Gurdon et al., and various publications involving the derivation and use of cytoplasts (Gurdon 1962b; Gurdon 1962a; Gurdon 1962d; Gurdon 1962c; Veomett et al. 1974; Bunn et al. 1977; McBurney et al. 1979; Abken et al. 1986) (see Chapter 3 for related results). However, as outlined briefly in this chapter, primarily during the last half of this project, a number of landmark studies reshaped the way we think about pluripotency and reprogramming, including how to induce pluripotency, the efficiency of reprogramming, and the timing and gene expression changes involved in the derivation of induced pluripotent stem cells. As such, this project has attempted to evolve with the current literature in order to establish data in unexplored areas of somatic cell reprogramming research.

Arguably the most significant publication to affect the course of induced pluripotency and reprogramming research was by Yamanka's group in 2006 with the announcement that they had been able to use a creative process of elimination technique to find that the gene expression profile linked to pluripotency could be reactivated in mammalian cells with just four key genes (Takahashi et al. 2006). These genes (OCT4, SOX2, KLF4, and cMYC) were specifically upregulated through the use of retroviral constructs and allowed for relatively easy mass transfection of somatic mouse fibroblasts. Publications in this area of research increased at an exponential rate ever since, however, to this day, there is still limited work pertaining to the clinical safety associated with adapting this technology to the derivation of human iPS cells. It was our goal to develop a new method of upregulating the specific genes shown to be responsible for induced pluripotency, to study how these genes affect somatic human cells individually and in combination, and to attempt to reprogram human somatic cells without the need for altering the DNA (as viral methods do) with the ultimate goal of developing a protocol for deriving iPS cells that are free from contaminating, foreign DNA.

The process of reprogramming human fibroblasts, as it was published in 2007 by Yamanaka's group, and also by Thomson's group (Takahashi et al. 2007; Yu et al. 2007) was carefully examined. Starting with four viruses, one for each reprogramming factor used, the published protocols involve transduction of viruses into human somatic cells (typically human fetal fibroblasts), where they then integrate into the genome. Then, in a small percentage of treated cells, the viruses code for the mRNA associated with each factor, which is then translated into protein. The proteins go to work within the cell, catalyzing a poorly understood chain of gene expression changes that result in iPS cells. However, there are risks associated with altering the DNA as the viral methods do; a publication by Yamanaka's group reported that at least one of the key factors, cMYC, was directly linked to carcinogenesis in approximately 20% of offspring derived from iPS cells (Okita et al. 2007).

Based on the process, there appeared to be two main options for eliminating the need for viral constructs and the negative effects associated with integrated reprogramming gene constructs: 1) make mRNA in vitro coding for the key factors necessary for reprogramming and transfect human somatic cells with this mRNA cocktail, or 2) produce reprogramming factor proteins in vitro and administer them to the cells. Due to limited available experience in making properly folded proteins in vitro and the issue of transferring the proteins into cells, we decided to attempt to transcribe the mRNA in vitro and use electroporation as our method of transfection. The inspiration for the protocols developed for this work stemmed from total RNA transfection papers used in cancer research studies which showed that dendritic cells can be phenotypically altered to display specific anti-cancer antigens using electroporated RNA and mRNA from the specific cancer cells used (Ponsaerts et al. 2002a; Ponsaerts et al. 2002b; Saeboe-Larssen et al. 2002; Minami et al. 2005).

As shown in chapter 5, by combining the constantly growing pool of information and

protocols from the reprogramming literature available with RNA electroporation protocols and our own work, we kept to our original aims by using mRNA coding for the specific reprogramming factors to more specifically induce upregulation of the essential reprogramming proteins and study their effects. We also chose this system because we felt that the ability to titrate mRNA concentration of each factor, and control when it was administered to the cells, would add an additional level of insight into the reprogramming process as compared to methods involving homologous recombination.

Chapter 2 – Materials and Methods

2.1 Tissue Culture

Table 2.1: Cell lines used in this study

Cell Line	Description
NTERA2.D1	Embryonal Carcinoma (EC)
NTERA2-GFP	EC with ubiquitous GFP & Puro resistance expression
NTERA2-TG11	EC line with sensitivity to aminopterin (HAT medium) and resistance to neomycin [universal fuser]
Hep 2.5	HeLa derived, cervical cancer line
K562	Human Caucasian Leukemia cell line (suspension)
HuF1b	Human foetal fibroblast cell line
HuF1b+pOCT4-GFP	HuF1b fibroblast line containing GFP driven by the OCT4 promoter with ubiquitous neomycin resistance
MRC5	Human fetal lung fibroblasts
Shef4	Karyotypically normal male human ES cell line derived in Sheffield.
H7S6+pOCT4-GFP	Abnormal hESC line containing GFP driven by the OCT4 promoter with ubiquitous neomycin resistance
Hues1	Karyotypically normal female human embryonic stem cell line obtained from Harvard University

2.1.1 General Culture Conditions

All tissue culture was carried out under sterile conditions in a Class II laminar flow safety cabinet unless otherwise noted. Prior to culture, the cabinet was sterilised using a 70% methylated spirit [Fisher, M/4440/17] vapour spray, as was all equipment prior to placement within the cabinet. Waste products were aspirated into a conical flask containing trigene [Fisher, HYG-700-040T] using a vacuum pump. Following completion of tissue culture, the cabinet was sterilised again.

All cells were grown in 25cm^2 (T25) or 75cm^2 (T75) tissue culture flasks [Nunc], or well plates [Nunc] and maintained at 37^{o}C in a humidified atmosphere of 5% CO_2 for human embryonic lines and 10% CO_2 for all other lines [Galaxy], unless otherwise noted. Also, growth mediums for each cell type were always pre-warmed to 37^{o}C in a water bath prior to use.

Where necessary, cells were enzymatically removed from culture flasks using 0.05% trypsin [Gibco, 15090-046] in PBS containing 0.5 mM EDTA [Sigma, E-5134], herein this formulation will simply be referred to as 'trypsin.'

2.1.2 Cancer Cell Lines

2.1.2.1 NTERA2.D1 Embryonal Carcinoma Cell

NTERA2 clone D1 (NT2) cells were grown in Dulbecco's modified Eagle's medium (DMEM) with 200 mM L-glutamine and 4.5 g/L glucose [Gibco] with no pyruvate, to this 10% v/v fetal bovine serum (FBS) [Gibco, 16000-044] was added. This media formulation will herein be referred to as "DMEM +10% FBS" in the text. Cells were kept in a humidified incubator with 10% CO_2 and ambient O_2 (~21%). NT2 cells were typically passaged at a ratio of 1:3 approximately every 4 days. Cells were routinely passaged upon reaching confluency by means of mechanical detachment using glass beads [Ballotini, 136-022]. The glass beads were HCL treated, autoclaved, and dried prior to use. Upon passage, growth medium was aspirated, leaving only a small volume (~2 mL) for the cells to be suspended into as they were removed, then the glass beads were drawn back and forth across the base of the flask by shaking the flask side to side. NT2 cells were then resuspended in pre-warmed 37^{o}C growth medium and split according to their confluency.

2.1.2.2 NT2-TG11 Embryonal Carcinoma Cells

NT2-TG11 cells were grown using the same medium as NT2 cells and passaged in the same way (see section 2.1.2.1). NT2-TG11 cells were typically passaged 1:3 approximately every 4 days. These cells are identical to NT2 cells, but due to a genetic mutation, these cells do not have an active amino acid salvage pathway and, similarly to antibiotic selection, cannot survive in the presence of medium containing aminopterin. By adding 1x hypoxantine/aminopterin/thymidine (HAT) [Fisher] (containing 400 nM aminopterin) to the culture medium, NT2-TG11 cells tend to die off within 5 days.

2.1.2.3 NT2-GFP Embryonal Carcinoma Cells

NT2-GFP cells were grown using the same medium as NT2 cells and passaged in the same way (see section 2.1.2.1). NT2-GFP cells were typically passaged 1:3 approximately every 4 days. These cells are identical to NT2 cells, but glow green under UV light due to ubiquitous GFP expression.

2.1.2.4 Hep 2.5 (HeLa) Cervical Cancer Cells

Hep 2.5 cells were grown using the same medium as NT2 cells (see section 2.1.2.1). Hep 2.5 cells were typically passaged at a ratio of 1:20 approximately every 5 days. Hep 2.5 cells were passaged using trypsin (0.25% trypsin (w/v) + 0.5 mM EDTA in PBS), diluted 1:5 from stock [Sigma]. Approximately 3 mL of trypsin was allowed to coat the cells growing on the base of a T75 (1 mL for a T25) for 3 minutes while kept in an incubator at 37^{o}C. Then, the flask was knocked with an open palm until the cells were released from the base of the flask and 7 mL fresh 37^{o}C growth medium was added; trypsin is quenched by serum in the medium. Loose cells were spun down in 15 mL centrifuge tubes at 250 g. Hep 2.5 cells were then resuspended in fresh growth medium and plated accordingly to confluency.

2.1.2.5 K562 Human Caucasian Leukemia Cells

K562 cells are suspension cells and were grown in Roswell Park Memorial Institute Medium 1640 [RPMI-1640; Sigma] supplemented with 10% (v/v) FBS [Gibco], 2mM L-glutamine, and 500 µg/mL Gentamycin [Invitrogen] in upright T25 flasks [Nunc] containing 20 mL of media. K562 cells were typically passaged at a ratio of 1:100 every 7 days. Since K562 cells grow in suspension, passaging simply involved mixing the cells in suspension by pipetting up and down several times, followed by a transferring ~0.2 mL (out of 20 mL) to a fresh T25 flask containing 20 mL of growth medium.

2.1.3 Human Embryonic Stem Cell Culture & Cryopreservation

All human embryonic stem (ES) cell lines were grown on irradiated mouse embryonic feeder cells in human ES media in a humidified incubator with 5% CO_2. Alternatively,

where noted, human ES cells were grown in feeder free culture on Matrigel with conditioned medium according to the protocol below.

2.1.3.1 Preparation of human ES medium (all hES lines except Hues1)

For 200 mL hES medium (Amit et al. 2000):

1. Add 10 mL PBS (w/o Ca^{++}, Mg^{++}) to 0.146g L-glutamine in a 15 mL tube.
2. Add 7 µL of β-mercaptoethanol to the L-glutamine/PBS mix well.
3. Into a 225 mL 0.2 micron cellulose acetate filtering unit add:
    - 160 mL knockout DMEM
    - 40 mL Knockout SR.
    - 2 mL L-Glutamine/ β-mercaptoethanol solution
    - 2 mL 100X non-essential amino acid solution
    - 400 µL of 2 µg/mL bFGF stock.
    - Antibiotics (optional, e.g. 120 µM Gentamicin)
4. Filter.
5. Store at 4°C and use within two weeks.

Table 2.2: Standard human embryonic stem cell medium composition

Final Concentration	Stock Concentration	Cat #
80% Knockout DMEM		Gibco 10829-018
20% GIBCO knockout SR		Gibco 10828-028
1% Non-essential amino acid solution	100X MEM non-essential amino acid solution	Gibco 11140-035
1mM L-glutamine	0.146g in 10 mL PBS	Gibco 21051-016
0.1mM β-mercaptoethanol	14.3M b-mercaptoethanol	Sigma M-7154
4ng/mL human bFGF	2µg/mL in PBS (w/o Ca^{+}, Mg^{++}) with 0.1% BSA	Gibco 13256-029

2.1.3.2 Preparation of HUES1 medium (650 mL)

1. Add the following into a 0.2 micron cellulose acetate filtering unit:
    - 500 mL Knockout D-MEM [Gibco, 10829-018]
    - 65 mL Knockout Serum replacement [Gibco, 10829-028]
    - 65 mL Plasmanate [Bayer, 613-25]

- 7.7 ng/mL FGF-2 [Peprotech, 500-P18]
- 6.5 mL non-essential amino acids [Gibco, 11140-035]
- 7µL 0.1 mM β-mercaptoethanol [Sigma, M-7154]
- 6.5 mL 100x Glutamax [Gibco, 35050-038]

2. Filter.
3. Store at 4°C and use within two weeks.

2.1.3.3 Preparation of MEF Medium (500 mL)

1. Add the following into a 0.2 micron cellulose acetate filtering unit:
   - 450 mL D-MEM (with 4.5 g/L glucose) [Gibco, 41965-039]
   - 50 mL Heat-inactivated U.S. origin Fetal calf serum [Gibco, 16000-044]
   - 2 mM L-glutamine [Gibco, 21051-016]
2. Filter.
3. Store at 4°C and use within two weeks.

2.1.3.4 Preparation of Mouse Embryonic Fibroblast (MEF) feeder layers

MEF stocks were prepared from mouse embryos by eviscerating and finely dicing the embryos. Following this, the fibroblast stocks were expanded by growing in a gelatin-coated 75 cm^2 tissue culture flask with MEF medium in a 10% CO_2 incubator. At confluence, upon which 90% of the flask was covered in a MEF monolayer, MEF medium would be removed and cells were treated with 1 mL 0.05% trypsin + 0.5 mM EDTA in PBS and placed in a 10% CO_2 incubator at 37°C for five minutes. The T75 was then removed from the incubator and the trypsin inactivated by adding 9 mL MEF medium. The cells were resuspended by triturating 5 to 10 times and the suspension removed from the flask and placed in a sterile 15 mL tube. The suspension was subsequently centrifuged at 1000 rpm (123 g) for three minutes at 4°C.

Following centrifugation, the tube was returned to the laminar flow hood, the supernatant aspirated and the pellet resuspended in 12 mL MEF medium. For every T75 harvested, 3 T75s coated in gelatin were prepared and 6 mL MEF medium added. The cell suspension was then added in a 1:3 ratio (4 mL) to each T75. Upon reaching passage 5, cells were mitotically inactivated by removing MEF medium, adding mitomycin C solution [Acros organics, BPE2531-2] to the feeders and placing in a 10% CO_2 incubator at 37°C for 2.5 hours. Following incubation, the mitomycin C solution was removed and treated with bleach for 2 hours in a closed container prior to discard. The MEFs were washed three times with 8 mL PBS prior to harvesting as normal. Instead of passaging into T75s, the cells were split 1:3 and frozen at -80°C (see 2.1.3.6). Upon thawing, the cells in one vial were counted (see 2.2) and seeded out as appropriate into MEF medium in T25s for use in human ES cell culture. NOTE: in the case of MEFs, around 36 hours are required for cells to attach and extend processes post-thaw prior to supporting human ES cells.

2.1.3.5 Passage of Human ES cells

1. Aspirate medium from flask.
2. Add 2 mL of collagenase per T25 and incubate at 37°C in CO_2 for 8-10 min. – until the edges of the hES colonies start to curl up.
3. Gently scrape with glass beads (or, if using plates, the tip of a glass Pasteur pipette rounded off with a flame).
4. Add a 5 mL of hES medium and gently aspirate. Transfer to a 10 mL centrifuge tube.
5. Spin at 50 g for 3 min at 4°C.
6. Whilst the cells are spinning, remove the medium from the fresh flasks of MEF feeders and wash once with PBS.
7. Aspirate supernatant, leaving hES cell pellet.
8. Remove PBS from MEFs.
9. Gently flick tube to disperse hES pellet.

10. Gently re-suspend hES cell pellet in an appropriate volume of hES medium (e.g. 4 mL for a 1:4 split into 4 x T25s (at 1 mL per T25)) and distribute between flasks of feeders. Add 4 mL hES medium per T25.
11. Carefully place in CO_2 incubator, maintaining an even distribution of cells across the flask.

Notes:

- Human ES cells require feeding every day with fresh hES medium.
- Areas of spontaneous differentiation can be removed from cultures by picking with a sterile pipette. Alternatively, undifferentiated hES colonies can be picked, either by: (1) picking colonies with a pipette and transferring to fresh feeder layers, or (2) performing a longer collagenase treatment, which should preferentially loosen/detach the undifferentiated hES colonies. These can then be removed by gently drizzling medium over the surface of the culture followed by transferral to fresh feeder layers. It may be necessary to mechanically break up the colonies by pipetting.
- Collagenase IV solution is made by adding 1mg/mL collagenase type IV [Gibco, 17104-019] in DMEM/F12 and sterilised with a 0.2 micron cellulose acetate filter. Store at 4°C. Use with a 2 weeks.

2.1.3.6 Cryopreservation of human ES cells

1. Aspirate medium from flask
2. Add 2 mL of Collagenase per T25 and incubate at 37°C for 8-10min. – until the edges of the hES colonies start to curl.
3. Gently scrape with glass beads (or, if using plates, the tip of a glass Pasteur pipette rounded off with a flame)
4. Add a 5 mL of hES medium and very gently aspirate – larger clumps survive the freezing process better than smaller clumps. Transfer to a 15 mL centrifuge tube.
5. Spin down at 50 g for 3 minutes.

6. Aspirate medium and very gently flick tube to disperse pellet. Wash the pellet by re-suspending pellet in 5 mL hES medium.
7. Spin down at 50 g for 3 minutes.
8. Carefully re-suspend the pellet in 600 µl ice-cold Freezing Medium and transfer 200 µl per cryovial. We typically freeze one T25 into 3 cryovials. Keep cryovials on ice and when ready place in a freezing container and transfer to a -70°C freezer.
9. The next day transfer cryovials from -70°C to liquid nitrogen for long-term storage.

Notes:

- It should be noted that the freezing and subsequent thawing of hES cells typically results in substantial cell death. Indeed, no satisfactory method has yet been published for the efficient freezing of whole cultures of hES cells.
- A controlled-rate Nalgene Cryo 1°C Freezing Container was used [Nalgene, 5100-0001] to freeze hES cells.
- Appropriate precautions should be taken when handing liquid nitrogen**!**

2.1.3.7 Thawing human ES cells.

1. Remove vial from liquid nitrogen and slightly loosen cap to allow trapped nitrogen to escape.
2. Thaw by immersing the bottom half only of the cryovial in a 37°C water bath and swirl the tube around. Do not immerse the whole tube in the water bath - this can lead to contamination problems.
3. Gently transfer the contents of the cryovial to a 15 mL centrifuge tube.
4. Gradually add 10 mL of hES medium to the tube drop by drop.
5. Spin down at 50 g for 3 minutes.
6. Aspirate medium and very gently flick tube to disperse pellet.
7. Re-suspend hESC cell pellet in an appropriate volume of hES medium (5 mL) and transfer in the flask with feeders.

8. Carefully place in C02 incubator, maintaining an even distribution of cells across the flask.

Notes: The best results are achieved when defrosted cultures are re-grown onto an area equivalent or, preferably, less than that originally frozen (e.g. a cryovial containing 1 well of a 6 well plate would be defrosted into 1 well of a 6 well plate or 2 wells of a 12 well plate).

2.1.4 HUES1 human ES Cell Culture and Passaging

Cell-lines derived using trypsin rather than collagenase, such as Hues1, require slightly different maintenance and sub-culturing than other human ES lines. Feeder layers of higher density ($5x10^5$ cells/cm^2) and medium with a different formulation (HUES1 medium – see section 2.1.3.2) were used for routine growth.

Upon reaching confluence, medium was aspirated from the flask and 1 mL 0.05% trypsin [Gibco, 15090-046] in EDTA [Sigma, E-5134] added. After 3-5 minutes, colonies began to disaggregate and detach around the edges and 80% of mouse feeders detached or retracted. 9 mL HUES medium was added to each T25 and pipetted until cells were washed off of the flask and were in suspension. The cells were then harvested and seeded out as described in 2.1.5.4.

2.1.5 Culture of hES cells on Matrigel with Conditioned Medium

MEF Medium

DMEM
10% Fetal Calf Serum (Hyclone)
2 mM Glutamate

Human ES Media

KO DMEM
20% Serum Replacement
1X Non-Essential Amino Acids
1 mM Glutamate
0.1 mM β-Mercaptoethanol

2.1.5.1 Preparation of Conditioned Medium (CM)

1. Plate irradiated MEFs on 0.1% Gelatin, at 56,000 cells/cm^2 in MEF medium. The final volumes should be 3 mL/well plate, 10 mL/T75, and 50 mL/T225.

2. To condition medium, replace MEF medium with human ES medium (0.5 mL/cm^2) supplemented with 4 ng/mL human bFGF (0.4 mL/cm^2) one day before use.

3. Collect CM from feeder flasks or plates after overnight incubation. Filter through a 0.2 μM filter, and add and additional 8 ng/mL human bFGF.

4. Add fresh human ES serum replacement medium containing 4 ng/mL human bFGF (0.4 mL/cm^2) to the feeders.

5. The MEFs can be used for 1 week, with CM collection once everyday.

2.1.5.2 Preparation of Matrigel

1. Either growth factor-reduced Matrigel or regular Matrigel can be used for coating plates/flasks.

2. To prepare Matrigel aliquots, slowly thaw Matrigel at 4˚C overnight to avoid the formation of a gel.

3. Add 10 mL of cold Knockout DMEM to the bottle containing 10 mL Matrigel. Keeping the mixture on ice, mix well with pipette.

4. Aliquot 1-2 mL into each pre-chilled tube; store at -20˚C.

2.1.5.3 Preparation of Matrigel-coated plates

1. Slowly thaw Matrigel aliquots at 4°C for at least 2 hours to avoid formation of a gel.

2. Dilute Matrigel aliquots 1:15 in cold Knockout DMEM (for a final dilution of 1:30).

3. Add 1 mL of Matrigel solution to coat each well of a 6-well plate.

4. Incubate the plates for 1-2 h at RT or at least overnight at 4°C. The plates with Matrigel solution can be stored at 4°C for one week.

5. Remove Matrigel solution immediately before use.

2.1.5.4 Passage of human ES cells on Matrigel

1. Aspirate medium from human ES cells, and add 1 mL of 200 units/mL collagenase IV per well of 6-well plate.

2. Incubate 5-10 minutes at 37°C in incubator. Incubation time will vary among different batches of collagenase; therefore, determine appropriate the appropriate incubation time by examining the colonies. Stop incubation when the edges of the colonies start to pull away from the plate.

3. Aspirate the collagenase, and gently wash once with 2 mL PBS.

4. Add 2 mL of CM into each well.

5. Gently scrape cells with a cell scraper or a 10 mL pipette to collect most of the cells from the well, and transfer cells into a 15 mL tube.

6. Gently dissociate cells into small clusters (100-500 cells) by gently pipetting. Do not aspirate cells to a single cell suspension.

7. Remove Matrigel-containing solution from the plates.

8. Seed the cells into each well of Matrigel-coated plates. The final volume of medium should be 4 mL per well. In this system, the human ES cells are maintained at high density. At confluence (usually one week in culture) the cells will be at 300,000-500,000 cells/cm^2. We find that optimal split ratio is 1:3 to 1:6. Using these ratios, the seeding density is approx 50,000-150,000 cells/cm^2.

9. Return the plate to the incubator. Be sure to gently shake the plate left to right and back to front to obtain even distribution of cells (do not swirl the dish as the cells will concentrate in the middle of the dish).

10. The day after seeding, undifferentiated cells are visible as small colonies. Single cells in between the colonies will begin to differentiate. As the cells proliferate, the colonies will become large and compact, representing the majority of surface area of the culture dish.

2.1.5.5 Daily maintenance of feeder-free culture

1. Collect CM from feeders, filter using a 0.2μm filter, and add human bFGF to a final concentration of 8ng/mL.

2. Feed human ES cells daily with 4 mL of CM supplemented with human bFGF for each well of a 6-well plates every day.

3. Passage when cells are 100% confluent. At this time, the undifferentiated cells should represent at least 80% of the surface area. The cells in between the colonies of undifferentiated cells appear to be stroma-like cells. The colonies (but not the stroma-like cells) show positive immunoreactivity for SSEA-4, Tra-1-60, Tra-1-81 and alkaline phosphatase.

2.1.5.6 H7S6+pOCT4-GFP (abnormal) human ES cell line

The H7S6 human ES cell line was transfected with a plasmid containing GFP linked to an OCT4 minimal promoter and neomycin resistance to make a reporter line. A stable clone from this transfection was isolated and glows green when cells are expressing OCT4. This cell line was grown according to the standards and practices of normal hES cell lines (see section 2.1.3), but tended to proliferate at a higher rate than non-culture adapted, karyotypically normal ES cells.

2.1.6 Human Fibroblast Cell Lines

2.1.6.1 HuF1 Human Fetal Fibroblast cell line

This human fetal fibroblast cell line was grown in DMEM [Gibco] +10% FBS [Gibco, 16000-044] (also referred to in the text as 'fibroblast medium') and passaged using 3-5 minutes exposure to 0.05% trypsin [Gibco, 15090-046] in 0.5 mM EDTA [Sigma] at 37^{o}C. HuF1b cells were typically passaged at a ratio of 1:5 about every 5 days.

2.1.6.2 MRC5 Human Fetal Lung Fibroblast cell line

This human fetal lung fibroblast cell line was grown in DMEM +10% FBS and passaged using 3-5 minutes exposure to 0.05% trypsin in 0.5 mM EDTA at 37^{o}C. MRC5 cells were typically passaged at a ratio of 1:3 about every 4 days.

2.1.7 Cryopreservation and Retrieval of Non-ES Cells

Cells were detached from their culture flasks, resuspended in growth medium, and then the cell suspension was centrifuged at ~150 g in sterile 15 mL tubes for 3 min. Then, medium was aspirated and the cell pellet was resuspended in freezing medium consisting of 90% FBS [Gibco] and 10% DMSO [Fisher]. The cell suspension was then

aliquoted into 1 mL cryovials [Nunc] and frozen gradually within a Nalgene Cryo-freezing container [Nalgene] for a minimum of 24 hrs. Following this, vials were submerged in liquid nitrogen storage tanks. All cells stored in the tanks were recorded in a logbook for future retrieval.

After retrieval of frozen stocks from liquid nitrogen storage, cells were thawed rapidly in a 37^{o}C water bath. Once thawed, growth medium was carefully reintroduced to cells drop wise over the course of 3-5 minutes to limit osmotic shock. Then cells were washed in 10 mL of fresh growth medium and centrifuged for 3 minutes at ~150g to remove traces of DMSO, due to cytotoxicity. Cells were then typically resuspended in 8 mL of growth medium and seeded into a T25 flask.

2.2 Calculation of Cell Number

To calculate cell number, in the case of attachment cells, cell media was aspirated and the cells were incubated at 37^{o}C for approximately 3 minutes in trypsin (0.05% trypsin (w/v) and 0.5 mM EDTA in PBS w/o Mg or Ca). Typically, 3 mL of trypsin per T75 and 1 mL per T25 unless otherwise noted. Normal growth medium was then added to produce a single cell suspension in 10 mL. Cells were counted using a Neubauer counting chamber. Cell number was determined for each of the four 4x4 1 mm^2 fields after addition of approximately 10-20 uL of mixed cell suspension using a long glass Pasteur pipette and then the mean multiplied by 1x10^4 to give a value of cells/mL suspension (see Figure 2.1).

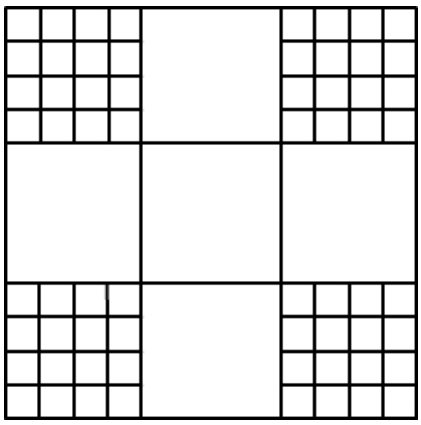

Figure 2.1: Representation of Haemocytometer field

After adding 10-20 µL of medium containing cells in single cell suspension to the haemocytometer, cells in the four 4x4 corner sections were counted, averaged, then multipled by $1x10^4$ to obtain an estimate of the number of cells/mL.

2.3 Solutions and Buffers

2.3.1 General Solutions and Buffers

2.3.1.1 Water

There are many grades or types of water with varying levels of purity. In this study, unless otherwise stated, 0.2um filtered water herein referred to as ddH_2O was used. However, in the case of resuspension and storage of DNA or RNA, microbiology grade, DNAse and RNAse free water was used [Gibco].

2.3.1.2 Phosphate Buffered Saline (PBS) Solution

Stock PBS is made up in large quantities on-site for lab use and is aliquoted into 500 mL clean clear glass bottles, then autoclaved. The formulation of "PBS", as it will herein be referred to, is: 0.16 M NaCl, 0.003 M KCl, 0.008 M disodium hydrogen phosphate and 0.001 M potassium dihydrogen phosphate in distilled water, supplied in concentrated liquid form [Invitrogen, AM9625]. Diluted to 1x in distilled water (ddH_2O), filter sterilised and autoclaved prior to use.

2.3.1.3 Trypsin Solution (in PBS)

Trypsin [Gibco, 15090-046] was mixed in PBS containing 0.5 mM EDTA [Sigma, E-5134] to a final concentration of 0.05%.

2.3.2 Cell Culture Solutions and Buffers

2.3.2.1 Collagenase type IV (10 mL)

10 mL DMEM/F12	[Gibco, 21331-020]
10 mg Collagenase IV powder	[Gibco, 17104-019]

2.3.2.2 Gelatin – 0.1%

1x Phosphate Buffered Saline	[Gibco, 14190-094]
Gelatin	[Sigma, G1890]

2.3.2.3 Freezing medium

90% U.S. origin Fetal calf serum	[Gibco, 16000-044]
10% DMSO	[Sigma, D2650-100ML]

2.3.2.4 Dispase

1x Phosphate Buffered Saline	[Gibco, 14190-094]

1:4000 dispase [BD Bioscience, 354235]

2.3.2.5 G418 (Geneticin)

Stock solution made by dissolving G418 Sulphate (PAA Lab, GmbH Austria) in distilled water to 100 mg/mL. Filter sterilised through a 0.2µm syringe filter and stored at –20^{o}C.

2.3.2.6 Cell Growth Medium

See section 2.1 for composition of cell culture mediums used.

2.3.3 Agarose Gel Electrophoresis Buffers

2.3.3.1 10X TBE Buffer

0.89 M Tris-HCl pH 8.0, 0.89 M borate and 0.02 M EDTA.

Recipe: 108 g Tris Base, 55 g Boric acid, 40 mL 0.5 M EDTA (pH 8).

2.3.3.2 Type III DNA Loading dye (6X)

0.25% bromophenol blue, 0.25% xylene cyanol and 30% glycerol

2.3.3.3 Gel Purification Elution Buffer (Qiagen)

10mM Tris-HCl, pH 8.5

2.4 Reverse Transcription PCR Analysis

2.4.1 RNA Extraction Protocol

2.4.1.1 Cell Preparation

Cells for reverse transcription polymerase chain reaction (RT-PCR) analysis were removed from the culture flask using standard methods for passaging dependent on cell type. Detached cells were then transferred to a sterile 15 mL centrifuge tube and centrifuged at 250 g for 3 min. Medium was then aspirated and the pellet was resuspended in PBS. Samples were then transfered to 1.5 mL vials [Eppendorf].

2.4.1.2 Protocol

Gently centrifuge vials at 800 rpm (~100 g) in Eppendorf 5417R Centrifuge [Eppendorf] for 3 min. Aspirate off PBS and tap vials gently to resuspend cells. Add 1 mL of TRIZOL reagent [Invitrogen, 15596-018] per 1.5 mL vial. Pipette up and down to lyse cells until no visible cell pellet remained. NOTE: 1 mL TRIZOL reagent lyses

approximately 10^7 cells, make sure not to saturate the TRIZOL by using more cells than this.

Leave samples on ice for 2-3 min. Then, centrifuge vials in an Eppendorf 5417R centrifuge at 4°C at 12,000 g for 10 min. Transfer all supernatant to a new vial, leaving the pellet. Add 200 µL of chloroform [Sigma] to each tube. Shake samples vigorously, vortex briefly using a Fisions Whirlimixer, then put on ice for 3-5 min. Centrifuge at 4°C at 12,000 g for 15 minutes. Transfer the upper, clear aqueous phase, which contains all the RNA (~600 µL), into a new vial. NOTE: Avoid taking ANY protein from the interphase.

Add 500 µL of isopropanol. Invert vials several times to mix and leave on ice for 30 min. NOTE: At this point, if pressed for time, the vials can be left overnight at -20°C and the rest can be done the following day.

Next, centrifuge samples at 4°C at 12,000 g for 15 minutes. A white RNA pellet should then be visible at the bottom of the vial. Discard the supernatant. Then, add 1 mL of 75% EtOH and vortex samples to dislocate the pellet. To wash the pellet, centrifuge at 4°C, 12,000 g for 10 min. Decant EtOH, add another 1 mL of 75% EtOH. At this point, RNA pellet can be stored like this in EtOH at -20°C for several months.

2.4.1.3 Nucleic Acid Quantification

Remove samples stored at -20°C in EtOH and centrifuge at 12,000 g at 4°C for 10 minutes. Then, decant Ethanol into waste and leave vial upside down on paper towel to dry out briefly. NOTE: There should be no droplets on the vial walls and when the pellet is dry, it should appear transparent.

On ice, add 50 µL of tissue culture grade, ultra-pure, DNase and RNase free water. Vortex all samples and put back on ice. Since degradation is more likely to occur at room temperature, always keep samples on ice.

The UV lamp on a Beckman DU-650 Spectrophotometer was switched on for at least 15 minutes prior to usage in order to warm up the bulb and achieve accurate results. A blank should be set up using 99 µL ultra pure DNase and RNase free molecular biology grade water [Sigma, W4502] in a cuvette. Following the blank, add 1 µL of sample to 99 µL molecular biology water and read absorbance. Absorbance at 260nm and 280nm should be recorded and an average taken of 3 readings. Repeat this process for each sample, washing the cuvette thoroughly between readings. Blanks need to be re-run as necessary or typically once per 10 samples.

2.4.1.4 Calculation for RNA concentration

$$\text{RNA concentration (µg/µL)} = \frac{40 \times A_{260} \text{ (reading)} \times 100 \text{ (dilution factor)}}{1000}$$

$$\text{DNA concentration (µg/µL)} = \frac{50 \times A_{260} \text{ (reading)} \times 100 \text{ (dilution factor)}}{1000}$$

A_{260} = Absorbance at 260nm

A_{260} = RNA/DNA and A_{280} = contaminating protein, therefore the ratio of A_{260} / A_{280} should be about 1.8-2.0 for high purity RNA.

NOTE: There is ~10-15 pg RNA/cell. So, 1 x 10^6 cells should have approximately 10 µg of total RNA.

2.4.1.5 DNase treatment

Using an Ambion Turbo DNA-free kit, [Ambion, AM1907] 5 µL 10x DNase buffer and 1 µL DNase1 were added to the 50 µL sample tube. The tube was incubated at 37°C for 30 minutes, prior to 5 µL DNase inactivation reagent being added and a further incubation at room temperature for 2 minutes. The tube was then centrifuged at 10,000 g for 1 min and the supernatant removed (avoiding the inactivation beads) to a fresh Eppendorf tube.

2.4.1.6 cDNA Production Using Reverse Transcription

The following reagents were added to a fresh Eppendorf tube: 0.5µg RNA (calculated from quantification); 1 µL oligo-dT primer; 0.5 µL dN6 primer; ∞µL DEPC water (to make 10 µL total volume). Sample tubes were spun briefly in a Beckman Microfuge E, before being placed on a Biometra T-gradient thermal cycler (with preheated lid to 105°C) set to run at: 70°C for 5 minutes, 50°C for 30 seconds, 40°C for 30 seconds, and then 4°C for 30 minutes. After the primer extension step, each 10 µL sample had the following added: 6 µL 5x buffer; 0.5 µL dNTP mix; 1 µL RT enzyme; 1 µL RNase inhibitor; 11.5 µL molecular biology water (to make 30 µL total). Sample tubes were spun briefly in a microfuge, then placed on a PCR thermal cycler (with preheated lid to 105°C) set to run at: 42°C for 60 minutes, 70°C for 5 minutes, and then held at 4°C. Samples could then be stored at -20°C. NOTE: Typically SuperScript III Reverse Transcriptase [Invitrogen] was used, consult manufacturer's instructions for additional details.

2.4.1.7 Polymerase Chain Reaction

The following reagents were placed into a PCR tube: 27 µL PCR master mix; 1 µL forward primer; 1 µL reverse primer; 1 µL cDNA (from 30 µL total). The PCR tubes were placed on a PCR thermal cycler for appropriate time and cycles (See Table 2.3) Tubes were stored at -20°C.

2.4.1.8 Gel Electrophoresis

A 1% agarose gel was made by adding 1 g agarose to 100 mL 1X Tris/Borate/EDTA (TBE). The solution was heated for 2-3 minutes in a microwave on full power until fully dissolved and allowed to cool to 37°C in a 37°C incubator. 5µl of ethidium bromide was added to the solution and thoroughly mixed. The solution was poured in a gel tray with end and combs in place before being left to set on a level surface for a minimum of 30 minutes. When set, the ends and combs were removed and the tray placed in a gel tank. TBE was then added to the tank so as to cover the gel. 3µl loading buffer was

added to each sample tube (33 µl total) and 16µl loaded into each well. 12µl of an appropriate sized DNA ladder was also added to at least one well on each row to determine fragment size. The gel was run at approximately 100V for 45mins. Following this, the gel was removed and imaged on a Syngene INGenius transilluminator before being discarded.

Table 2.3: Reverse Transcription PCR Primers Used

Gene	T_A(°C)	cycles	length	Oligo
Actin NM_001101	60	20	838	F: atctggcaccacaccttctacaatgagctgcg R: cgtcatactcctgcttgctgatccacatctgc
GAPDH NM_002046	60	23	240	F: tgatgacatcaagaaggtggtgaag R: tccttggaggccatgtgggccat
OCT4 NM_002701	60	22	577	F: cgaccatctgccgctttgag R: ccccctgtcccccattccta
NANOG NM_024865	60	25-27	401	F: gcctcagcacctacctaccc R: ggttgcatgttcatggagtag
SOX2 NM_003106	59	25-27	488	F: cccccggcggcaatagca R: tcggcgccggggagatacat
Rex1 NM_174900	60	25-27	298	F: gctgaccaccagcacactaggc R: tttctggtgtcttgtctttgcccg

*NOTE: Sometimes different numbers of cycles were used, depending on the experiment or conditions being tested.

2.5 Real Time Quantitative PCR

Q-PCRs were carried out with SYBR Green JumpStart Kit on a Bio-Rad iCycler according to manufacturer's instructions. The sequences of the primers used are listed in Table 2.4.

Table 2.4: Q-PCR Primers Used

Gene	Accession	Forward	Reverse	T_A(°C)
CD1	NM_053056	gggggcgtagcatcatagta	tgtgagctggcttcattgag	60
CMYC	NM_002467	cttcccctaccctctcaacg	agtgggctgtgaggaggttt	59
DNMT3b	NM_006892	caggagacctaccctccaca	tgtctgaattcccgttctcc	60
GAPDH	NM_002046	tgatgacatcaagaaggtggtgaag	tccttggaggccatgtgggccat	60
KLF4	NM_004235	cccacacaggtgagaaacct	ttctggcagtgtgggtcata	60
LIN28	NM_024674	acacagtgaaaccccgtctc	gctctgtaaccaggctggag	59
MDM2	NM_002392	gtgatcttggctcactgcaa	acgaggtcaggagatcgaga	60
NANOG	NM_024865	ggatggtctcgatctcctga	cctcccaatcccaaacaata	60
NeuroD1	NM_002500	aagccatgaacgcagaggaggact	agctgtccatggtaccgtaa	60
OCT-4	NM_002701	cgaccatctgccgctttgag	ccccctgtcccccattccta	60
p21	NM_000389	ttagcagcggaacaaggagt	gccgagagaaaacagtccag	60
PAX6	NM_000280	gccagcaacacacctagtca	ggggaaatgagtcctgttga	60
REX1	NM_174900	gctgaccaccagcacactaggc	tttctggtgtcttgtctttgcccg	60
SALL4	NM_020436	gccgtgaagaccaatgagat	ctccttccacgcaagttctc	60
SOX1	NM_005986	catgcaccgctacgacat	cgggcaagtacatgctgat	59
SOX2	NM_003106	catgtcccagcactaccaga	gtcatttgctgtgggtgatg	60
XenUTR*	N/A		actccattcgggtgttcttg	60

*Primer used for ectopic gene detection as it is homologous to the xenopus derived polyA tail that was synthetically added to our mRNA through in vitro transcription. Overlapping primers from the end of the gene of interest into the Xenopus UTR were used to selectively target ectopic mRNA by Q-PCR.

2.5.1 PCR Quantification

While traditional Reverse Transcription PCR was used to detect gene expression in circumstances where it was important to simply gauge whether a gene of interest was being expressed or not, generally Q-PCR was used when quantification was desired. Q-PCR was preferred due to the fact that it is much more sensitive and accurate in terms of detection of small gene expression fold changes. The BioRad software provided by the manufacturer was used to convert ΔC_t values into normalised bar graphs in Microsoft Excel using a proprietary macro or the data was exported into GraphPad Prism for analysis. Data was always normalised against a GAPDH control, as this was decided to be a better point of reference than ACTIN when comparing somatic and embryonic stem cells. Also, non-treated or human ES cells were used as controls, depending on the experiment.

2.6 Fluorescence Activated Cell Sorter (FACS)

2.6.1 General FACS Principles

FACS graphs are constructed by argon lasers measuring “events” within a 1024 x 1024 channel “field of view”, this grid, along with the lasers themselves, needs to be regularly calibrated to ensure that the results are reproducible and accurate. Also, beads of a given size should be used to calibrate the size of events and standard flurophore markers can be used to attest to the purity and intensity of fluorescently labelled samples. FACS plots can have a variety of axes depending on the information of interest, this section outlines some of the set up parameters used in this study and how they should be interpreted.

2.6.1.1 Isolation of events based on size and granularity

A FACS is capable of producing graphs in many formats. For the purposes of determining the size and granularity of events within a sample a graph can be created

such that the x-axis of the graph depicts forward scatter and the y-axis gives side scatter. Forward scatter is depicted in either of two formats, linear (FS lin) or log (FS log). Forward scatter gives the operator a relative measure of the size of the individual events. Similarly, the y-axis gives side scatter in either of two formats, linear (SS lin) or log (SS log). Side scatter is a measure of granularity, the lower the granularity, the more transparent an event is, the higher the granularity, the more light is reflected off of it or does not pass through it. For example, the solid sizing beads used to calibrate the forward scatter (x-axis) show up at the top end of the granularity scale, as light does not pass through them (see Figure 2.3).

2.6.1.2 Isolation of events based on fluorescence

FACS also produces graphs based on the reflected light from UV laser induced fluorescence. In this instance, the FACS plot x-axis is replaced with 'fluorescence intensity' at a particular wavelength, again, in either linear (lin) or logarithmic (log) form. Depending on the fluorophore of interest, the events will show up in varying specific ranges of the colour spectrum, a particular wavelength of interest can be chosen and its intensity monitored. Depending on the concentration or intensity of the fluorescence, a variety of factors can be tested for, including uptake of a fluorescently labelled compound, transcription of a construct with a fluorescence gene, or DNA or protein quantification by fluorescent labelling.

2.6.1.3 Cell Sorting

By electrically charging droplets containing the sample of cells of interest, the FACS uses user controlled parameters and magnets to selectively sort events. In terms of the FACS, an "event" is anything that registers as a particle by distorting or reflecting the laser light. In a relatively pure sample containing cells, most events will be cells, while very small events will be debris.

2.6.1.4 FACS Sorting Preparation

Confluent flasks of cells were treated with trypsin until in single cell suspension. FACS wash buffer (5% FBS [Gibco, 16000-044] in 1x PBS [Gibco,14190-094]) was added to the cell suspension and pipetted to break up any small cell aggregates. The suspension was transferred to a sterile 15 mL centrifuge tube and a small sample removed with a sterile glass pipette to count the cells on a haemocytometer. Following a cell count, the suspension was centrifuged at 250 g for 3 minutes at 4°C. The supernatant was aspirated from the tube and the cells resuspended in wash buffer to a concentration of 10^7 cells/mL. Samples to be sorted using FACS were done so using a Dakocytomation MoFlo. Where sorting was not necessary, such as simple quantification of a fluorescent label, flow cytometry was performed with a Dakocytomation CyAN.

2.6.1.5 Quantitative analysis of FACS data

Analysis of FACS plots was dependent upon the experiment, but typically involved the retrieval of graphs from the Summit software provided by the manufacturer and readings of size, fluorescence intensity, and proportion of cells in a given subsection were transferred to Excel [Microsoft] for simple graphs or Graphpad [Prism] software for statistical analysis using ANOVA.

2.6.2 Interpreting FACS Plots

This section outlines how events are read by the FACS and how the resulting graphs should be interpreted through a series of figures and accompanying explanations.

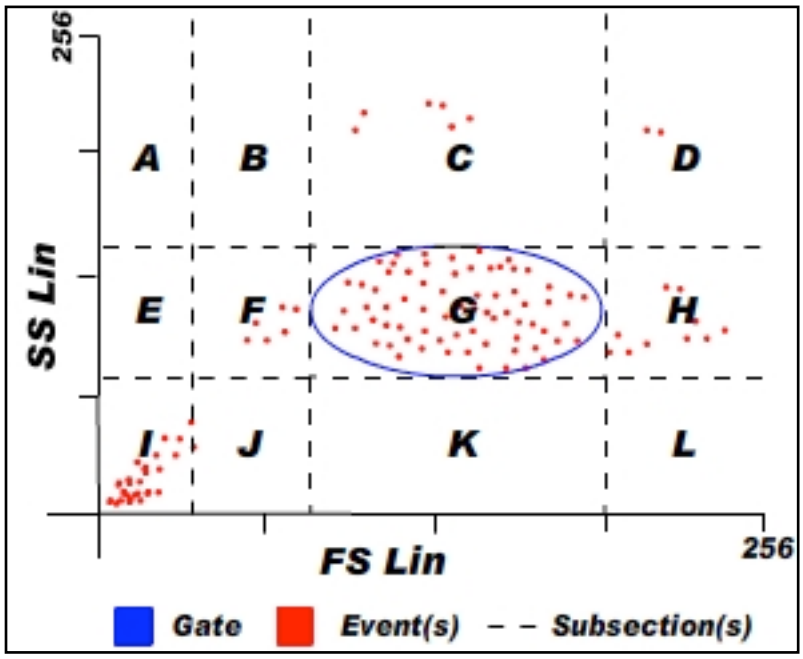

Figure 2.2: FACS Gating

Figure 2.2 depicts an annotated mock FACS plot. The plot has been divided into subsections "A" through "L" to denote significant regions in reference to gating. Technically, a gate is any subsection of the graph region that has been isolated by the FACS operator; however, there is always a preliminary gating procedure that sets the control for future samples and is typically based on a sample from the parental population, or population of cells that have not undergone experimental treatment. In this figure, subsection G contains the gate. This gate is based on many factors. First, the density of the population in this region is very high, in other words, many if not most of the events detected lie in this region, and therefore it is most likely that this region contains the "average" parental cell population which we are trying to capture, to set as a control for future samples (Note: a minimum of 1000 events is used to set the gate, typically ~10,000 events are used depending on total cell number and sample variation). Second, based on the forward scatter (FS Lin), the events lie in the typical size range for a cell. Of course, this will vary depending on cell type, the health of the cells in the sample, and the orientation of the cell event as it passes through the laser. Also, sizing beads should be used prior to gating where event size is important to the results (see Figure 2.3). Third, the side scatter (SS Lin) shows that the events are in the typical range for the cells of interest. Side scatter is a relative measure, based on

the amount of light that passes through the sample, as opposed to how much is reflected back. The more transparent an event, the lower its side scatter reading, likewise, a dense, non-reflective event will show up as having a high side scatter or 'granularity' value. Both axes of the graph are labelled from zero to 256. These numbers are representative of channels. There are actually 1024 channels for forward scatter (x-axis) and 1024 for side scatter (y-axis), these form a 1024x1024 grid where an event can be classified as being a member of one of the grid squares. These channels are then condensed into 4x4 channel 'blocks', making a 256x256 grid where events have a forward scatter (x) and side scatter (y) component.

Description of Figure 2.2 Subsections (A-L)

A) This section represents highly granular (dense & non-reflective) events of very small size. Events are not expected to occur in this region, mainly because normal cells are not that small, nor that granular.

B) Again, highly granular, but slightly larger in size. This subsection is typically empty, unless sizing beads are being used, which are highly granular.

C) This subsection represents events that are in the typical size range for cells, but appear highly granular. These are typically apoptotic cells, cells shift upwards, out of the gate, then down to the left on the plot during apoptosis.

D) Events in this region are both large in size and highly granular. It is likely that these events are doublets, triplets, etc. that are highly granular. Events in this region are rare.

E) Region E is for very small particles that have a medium granularity, similar to cells, just a lot smaller. High granularity cell debris is sometimes recorded in this section of the plot.

F) This subsection would contain events that have equal granularity to cells, but are of a slightly smaller size, as compared to the parental cells and the sizing beads. A karyoplast or cytoplast containing organelles might fall within this region.

G) This region, primarily based on the parental sample, holds the 'average' cell population based on a control group of cells.

H) Although these events register within the normal range of granularity, they appear too large to be single cells and are likely doublets, triplets, etc. Sometimes bloated/oversized cells can end up in this region.

I) This subsection typically contains debris. Since debris is very small, it will register on the low end of the forward scatter (size) scale and since debris typically does not typically reflect much light, it will tend to be on the low end of the side scatter (granularity) scale.

J) Anything bigger than debris, but smaller than a typical cell with a low granularity reading will end up in this region. Cytoplasts without organelles would be expected to appear in this region.

K) Events in this subsection would be roughly the size of a parental cell, but with lower granularity, or in other words, more transparent than a typical cell.

L) No events are normally detected in this region. This region represents events that are very large, but with low granularity.

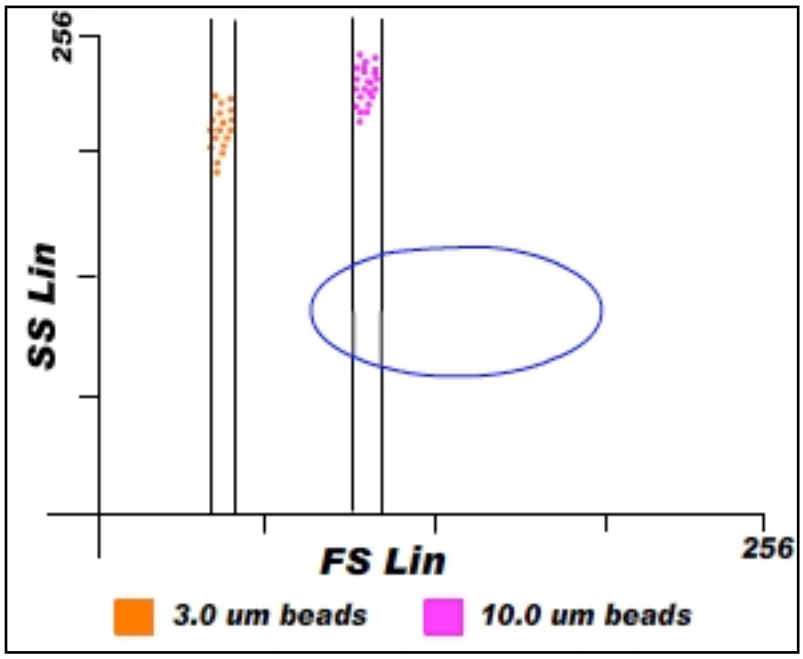

Figure 2.3: FACS Sizing Beads

Before setting the gate, to calibrate the FACS lasers and output graphs, a number of controls are needed. Since the FACS plots display events on a relative scale, sizing beads are run through the machine to calibrate the FACS, enabling the user to look for cells in the right size region. The beads typically show up as highly granular events (in comparison to cells) in distinct regions and correlate size to on the forward scatter axis (x-axis). The side scatter (y-axis) values registered by the beads do not tell us anything in particular about our sample; their side scatter values are representative of the fact that, as we already know, the beads are solid, dense particles of a predetermined size (i.e. the FACS shows 100% granularity when detecting a solid, non-translucent event, cells show up as semi-translucent and therefore give a lower granularity readout). The sizes given by the beads are recorded by selected regions, as shown, to give an approximation of the size of future events. These regions also help to determine the gate by giving the operator a good idea as to what can be classified as debris and what can be classified as the low end of the size spectrum for a particular cell type. Although sizing beads are not explicitly needed for gating, they can serve to further validate the data recorded by the FACS.

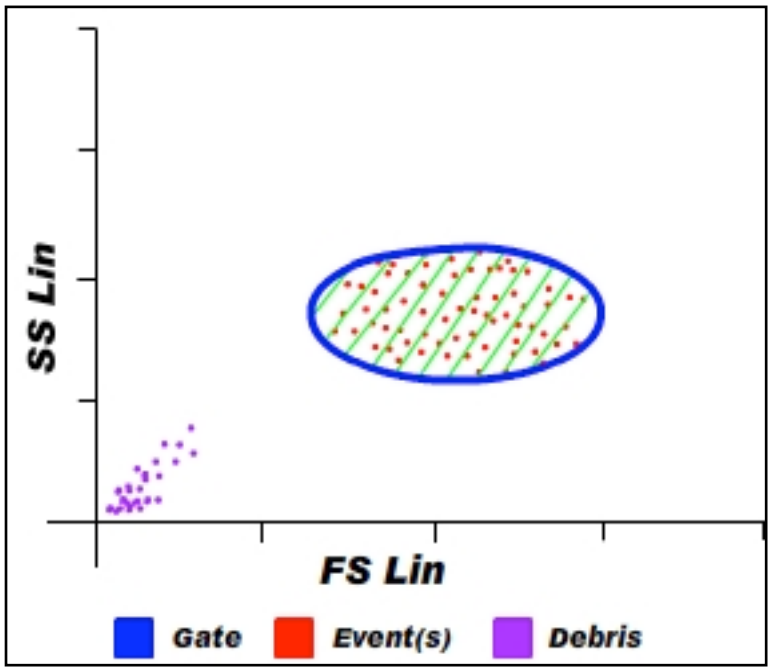

Figure 2.4: Gating cell populations

The figure above shows a gated parental population. Each 'event' is depicted by a red dot, the gate, in blue, is stationary. We can safely assume that the population at the bottom left is debris, it is smaller in size than a typical cell and very low in granularity, properties of small cellular debris. When cells are subjected to experimentation, such as enucleation over a Ficoll gradient, their changes in size and granularity can be detected by comparing samples against the gate, set using the parental population. Additionally, fluorescent markers can be used; positive and negative events being differentiated by their colour.

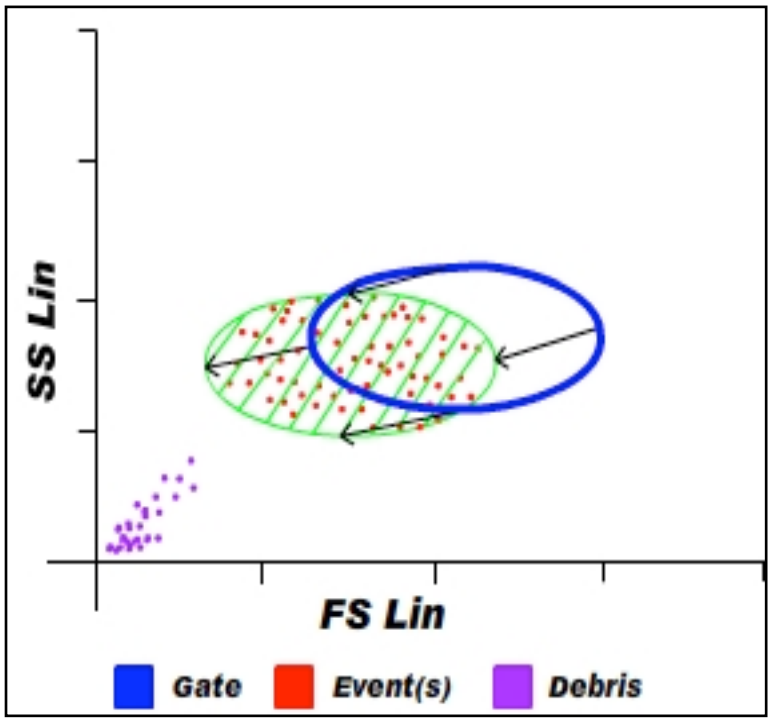

Figure 2.5: Detecting population shifts

As depicted by the green shaded area and the arrows, the population of events (red dots) has shifted in this figure. The shift is down and to the left, indicating that the general population has lost size and some granularity. This is the kind of shift one might expect to see from enucleation, as the overall cell size will decrease upon losing its nucleus. Accompanying the loss of size would likely be a significant loss in granularity as the nucleus accounts for a large proportion of a cell's granularity as it tends to block a lot of the light shown through single cells by the FACS lasers, therefore leading to a lower side scatter (y-axis) value.

In addition to detecting the size and granularity, the FACS can also show similar shifts in fluorescence intensity. In most cases it is also useful to treat cells with Propidium Iodide (PI) prior to FACS analysis so that dead or dying cells can be gated out of the sample. PI turns apoptotic cells, cells with holes in their membrane, red, which can be easily detected by FACS.

2.7 Immunocytochemistry

2.7.1 Immunostaining Preparation

2.7.1.1 40% Paraformaldehyde (PFA) stock solution

Mix PFA in ddH_2O to a final concentration of 40% PFA, pH=7.0. Aliquoted stock solution can be stored in -20^{o}C for years. PFA is difficult to dissolve, heat up to 50-60 degrees and add 10M NaOH to help dissolving. After dissolving, adjust pH to 7.0 with HCl. Check pH with pH test paper. NOTE: Do not try to read pH of PFA solution on a pH meter.

2.7.1.2 Fixative Solutions (make fresh)

For cell surface protein, 4% PFA in 1x PBS [Gibco, 14190-094] pH=7-7.4.

For intracellular and nuclear protein, 4% PFA in PBS pH=7-7.4, 0.1% TritonX-100 [Sigma, T9284].

2.7.1.3 Permeabilisation buffer (make fresh)

Cytoplasmic and membrane bound protein, PBS with 0.20% Triton X-100. Leave at room temperature for 20 minutes.

2.7.1.4 Blocking buffer

3% BSA or 5% serum (either sheep, donkey, goat, FBS depending on the 1st Ab) in PBST (PBS with 0.1% Tween 20).

2.7.1.5 Other Solutions and Stocks

1x PBS

Triton X-100 in ddH2O	10%
Tween 20 in ddH2O	10%

PBST (PBS with 0.1% Tween 20)

2.7.2 Immunostaining Cell Surface Proteins

1. Remove medium and wash cells gently with PBS 2-3 times

2. Fix cells with 4% PFA in PBS for 20 minutes at room temperature.

3. Wash 3 times with PBST

4. Block with PBS+5% serum for 30 min at RT or at least 1 hour at 4^{o} C.

NOTE: Other serums can be used depending on the source of antibodies being used. Efficient blocking is particularly important when using polyclonal antibodies, extended blocking times with species matched serum is recommended.

5. Wash 3 times with PBST

6. Add primary antibody and leave overnight at 4^{o} C

7. Wash 3 times with PBST

8. Add secondary antibody and incubate in the dark for ~1hr at room temperature.

9. Wash 2x with PBS for 15+ min

10. Image cells

2.7.3 Immunostaining Intracellular and Nuclear Proteins

1. Remove medium and wash cells gently with PBS 2-3 times

2. Fix cells with 4% PFA in PBS with 0.2% Triton X-100 for 20 minutes at room temperature, so cells are permeabilised and fixed at the same time.

NOTE: For nuclear proteins, it is typically more effective to fix with 4% PFA for 20 min at room temperature, then permeabilise with 0.1% Triton X-100 for 45-60 min at room temperature.

3. Wash 3 times with PBS + 0.1% Tween 20.

4. Block with PBS+5% FBS for 30 min at RT or at least 1 hour at 4^{o} C.

NOTE: Other serums can be used depending on the source/type of antibodies being used. Efficient blocking is particularly important when using polyclonal antibodies, extended blocking times with species matched serum is recommended.

5. Wash 3 times with PBS + 0.1% Tween 20.

6. Add primary antibody (Typically 1:1000 dilution in PBS) and leave overnight at 4^{o} C

7. Wash 3 times with PBS + 0.1% Tween 20.

8. Add secondary antibody and incubate in the dark for ~1hr at RT

9. Wash 2x with PBS for 15+ min

10. Image cells

2.7.3.1 Hoechst 33342

Hoechst 33342 [Invitrogen, H3570] comes as a 10mg/mL (16.2 mM) solution in water. Hoechst 33342 is a live cell stain for nuclear DNA and should be used at a concentration of 5 µg/mL in ddH_2O. NOTE: Hoechst 33342 is degraded by light and should therefore always be kept away from light until ready for use.

2.7.4 Alkaline Phosphatase Staining

Alkaline phosphatase (AP) staining was performed using the Sigma Alkaline Phosphatase Red Microwell kit [Sigma, AR0400-1KT]. Cells were fixed for 1.5 minutes in 4% PFA then incubated for 15 min in AP Red, a 1:1 mix of components A and B provided by the manufacturer. Cells positive for AP turn red.

2.8 Protein Analysis by Western Blot

Cells were trypsinised, washed with PBS three times, counted, and lysed in SDS loading buffer. For each sample, lysate from 2x10^5 cells was loaded per lane.

2.8.1 Western Blotting Solutions

2.8.1.1 2X SDS loading buffer

0.125M Tris-HCl, pH=6.8, 4% SDS, 20% Glycerol, 0.2% Bromophenol Blue in distilled water.

2.8.1.2 Lysis Buffer

5 mM Tris-HCl, pH 7.4, 2mM EDTA, 10 µl Protease Inhibitor Cocktail (1000 x stock), 10 mg/mL benzamidine, 5 mg/mL leupeptin, 5 mg/mL trypsin inhibitor

2.8.1.3 10X SDS PAGE Running Buffer

250 mM Tris-HCl, 2.5 M glycine and 1% SDS pH adjusted to 8.3 with concentrated hydrochloric acid (HCl) in distilled water. Recipe: Tris Base 60.55 g, Glycine 288.27 g, SDS 20 g, ddH2O – complete up to 2 litres.

2.8.1.4 Western Transfer Buffer

0.5 M Tris-HCl, 3.84 M glycine pH adjusted to 8.3 with concentrated HCl in distilled water, 20% methanol added to 1x buffer prior to use. Recipe: Trisbase 12.11 g, Glycine 57.65 g, Methanol – 100 mL, ddH_2O – complete up to 4 litres

2.8.1.5 TBS Buffer

Tris-HCl 12.11 g, NaCl 116.8 g, ddH_2O – complete up to 4 litres, set to pH 7.5 with Tris Base.

2.8.1.6 TBST Buffer

Dissolve the following in 800 mL of ddH_2O: 8.8 g of NaCl, 0.2g of KCl, 3g of Tris base, add 500ul of Tween-20. Adjust the pH to 7.5. Add ddH_2O to 1 L. Sterilise by filtration.

2.8.1.7 Immunoblotting Blocking solution

5% (w/v) skimmed milk powder [Marvel] with 1% (v/v) FBS, 1% (v/v) BSA and 0.1% (v/v) Tween-20 in PBS.

2.8.1.8 Immunoblotting Wash Solution

0.1% Tween-20 in PBS. Recipe: dissolve 0.1 mL Tween-20 with 100 mL PBS.

2.8.1.9 Stripping Buffer

Make stock solution of 62.5 mM Tris (pH 6.7) with 2% SDS. When ready to use, make a working solution by adding 0.6 mL β-mercaptaethanol (2-ME) to 100 mL of stock solution.

2.8.2 Gel Preparation

2.8.2.1 Resolving Gel

Resolving gels should be made based on the size of the protein(s) of interest. Typically a 10% resolving gel was suitable for our purposes and was made using the following recipe: 4 mL ddH_2O, 5 mL 30% Acrylamide mix, 5.7 mL 1.0 M Tris (pH 8.8),

0.15 mL 10% SDS, 0.15 mL APS, 6 µL TEMED, which should give a total volume of 15 mL. This recipe should make 2-4 gels, depending on the thickness of the spacers used. Add ddH_2O on top of the resolving gel to level the top of the gel and reduce bubbles. Should take ~1 hr to set. NOTE: TEMED polymerises the gel, make sure to add it last and load the gel solution soon after it is mixed in. Also, be sure to check carefully for leaks once solution is loaded.

2.8.2.2 Stacking Gel

Carefully decant the water from the top of the resolving gel and remove excess with a pipette. Once free from water, add stacking gel. To make 6 mL stacking gel, mix: 4.1 mL ddH_2O, 1 mL 30% Acrylamide mix, 750 µL 1.0 M Tris (pH 6.8), 60 µL 10% SDS, 60 µL 10% APS, and 6 µL TEMED. Make sure to fill the stacking gel to the top of the gel housing, then insert the comb carefully, avoiding bubbles. Then leave to set. NOTE: Be careful when removing comb, so as not to damage the lane barriers. Also, make sure to rinse lanes with fresh 1x electrophoresis buffer before loading samples.

2.8.3 Sample Preparation

Normally, for a fair standard of comparison, a standard curve should be made using the Bradford Assay. However, for the purposes of comparing the amounts of protein between human fibroblast cells and human embryonic stem cells, cells which vary greatly on the amount of protein per cell, lysate from equal numbers of cells was used to make a fair comparison. Lysate from 200,000 cells was taken for each sample and equal volumes loaded in each lane. NOTE: when using a 10 lane mini gel, no more than 50 µL should be loaded per lane.

Following isolation of 200,000 cells from each sample to be tested, cells should be centrifuged, medium aspirated, and then resuspended in no more than 50 µL lysis buffer containing bromethyl blue. Pipette up and down to lyse cells and then heat in a tube @ 70^{o}C for 2 min. Place samples on ice.

2.8.4 Electrophoretic Separation

Place gels in holder assembly, then fill the inner and outer compartments with 1x SDS-PAGE Running Buffer (see 2.8.1.3). Make sure that the level of running buffer in the inner compartment is above the wells, coating and filling the wells. Then, carefully load samples with a fine-tipped pipette with at least one lane containing a marker ladder. NOTE: Wells/lanes should be facing the center of the assembly. Make sure to boil samples for ~2 min with loading dye (bromethyl blue) @ 70^{o}C, then put on ice just before loading.

2.8.5 Running Conditions

Refer to manufacturer's instructions. For our purposes, using our equipment, gels were run under the following conditions:

2.8.5.1 Stacking Gel

Run at 20-30 mA (constant mA) for ~30 minutes. If running 2 gels in 1 tank, 30-40 mA (constant mA).

2.8.5.2 Resolving Gel

Run at 50-60 mA (constant mA) for ~1 hour. If running 2 gels in 1 tank, 60 mA (constant mA). NOTE: watch gels carefully, do not allow samples to run off the gel.

2.8.6 Transfer to Nitrocellulose Membrane

Cut nitrocellulose membranes into rectangles slightly larger than the gel (6 cm x 9 cm). Just prior to use, soak the membrane you want to use for transfer in ice cold transfer buffer. Transfer buffer should be kept as cold as possible; put it in -20^{o}C freezer for ~20 minutes prior to filling the transfer tank. Make sure to place the gel closest to the negative (black) side of the transfer 'cage' with the nitrocellulose membrane on the positive (red) side, 'shiny' side against the gel, as the proteins will be driven away from the negative side towards the positively charged side. Typically, ladder markers contain a pink band that can be easily seen (check with manufacturer). Depending on the size of proteins of interest, usually when the pink band is near the bottom of the gel it should be about finished. NOTE: for best results, use this arrangement: negative side

(black), foam sponge, 3x filter paper, western gel, nitrocellulose, 3x filter paper, foam sponge, positive side (red).

Once assembled, place sandwiched gel/membrane in transfer buffer tank and fill it with ice cold transfer buffer. Then, fill in the space around the tank with ice in a foam box to keep it as cold as possible. Using the BioRad Power Pac 300, set to 140-180 mA/gel or 300 mA for 2 gels simultaneously. Run for 1.5-2 hours. NOTE: Running for too long can result in proteins going through the nitrocellulose onto the filter paper.

After protein transfer, carefully remove the nitrocellulose membrane, rinse with ddH_2O, then add Ponseau S (red), just enough to coat the membrane. Allow it to sit on the membrane for about 1 minute. Then, rinse 3x in ddH_2O, photograph, then rinse in TBST. Place membrane in a shallow box with blocking buffer and leave on a shaker overnight. After blocking, rinse well with TBST and ddH_2O, then apply primary antibody.

2.8.7 Antibody Staining

Typically 1^o antibodies are at a stock concentration that needs to be diluted 1:1000 (check with manu.). Primary should be left on the membrane in TBST for at least 2 hours while on a shaker. Then, rinse membrane 3x for 15 minutes in TBST (45 min total) before applying the 2^o antibody. Secondary should typically be diluted 1:5000 in TBST and left on the membrane for 1+ hours at room temperature. Again, rinse 3x for 15 minutes with fresh TBST. When ready to develop the membrane, wash once with PBS prior to the ECL reaction.

2.8.8 Developing

During the final wash of the 2^o antibody, turn on the developing machine to warm up for ~15 minutes prior to use and have pre-cut film ready. For ECL reaction, follow manufacturer's instructions. Typically, ECL reagents should be mixed 1:1 and left on the membrane for about 3 minutes. Reaction should remain active for up to 4-5 hours.

After ECL reaction, place the membrane carefully between two sheets of clear acetate and squeeze away excess ECL solution.

Two developments should be performed, one that is short (~1 minute) and a longer one (10-30 minutes). Exposure times can be extremely variable and care should be taken to determine the optimal exposure parameters. NOTE: After developing, the nitrocellulose should be saved for stripping and reblotting and can be used multiple times as long as it is stripped properly and kept in fresh PBS at 4^{o}C.

2.8.9 Stripping and Reblotting

To strip, put membrane in small plastic dish with 50 mL working solution at 50^{o}C in water bath for 30 minutes. Then, rinse stripping buffer down sink in a fume hood and gently wash membrane with H_2O multiple times. Do 3x 15 minute washes with TBST, using plenty of TBST and make sure all 2-ME is gone before applying blocking buffer. Block with blocking buffer for 1+ hours at room temperature, then reblot.

Table 2.5: Antibodies used for Western Blotting

Antibody Target	Company	Cat. No.
CMYC	Santa Cruz	SC-764
KLF4	Santa Cruz	SC-20691
LIN28	R&D systems	AF3757
OCT4	Santa Cruz	SC-5279
NANOG	R&D systems	AF1997
SOX2	Chemicon	AB5603

2.9 Karyotype analysis

Karyotype analysis was performed on live cells by the Cytogenetics Department at the Sheffield Children's Hospital, Western Bank, Sheffield using G-banding techniques. Cells were cultured in a T25 flask, then treated with 0.1µg/mL Colcemid [Invitrogen] for 4 hours. Then, cells were dissociated with trypsin/versene and pelleted via centrifugation before being re-suspended in pre-warmed 0.0375 M KCl hypotonic

solution and incubated at 37°C for 10 minutes. Following centrifugation the cells were re-suspended in a methanol and acetic acid fixative (3:1).

Metaphase spreads were prepared on glass microscope slides and G-banded by brief exposure to trypsin and stained with Gurr's/Leishmann's stains (4:1). At least 20 cells were analysed per flask, with a minimum of 3 spreads analysed and 17 counted in order to determine how representative the sample assay was of the entire culture. NOTE: It has been observed on occasion that multiple karyotypes can be present in cultures undergoing adaptive change.

2.10 Chapter 3 Materials & Methods

2.10.1 Cytochalasin D

Cytochalasin D [Sigma, C8273] comes as a powder in a vial and must be dissolved in DMSO prior to use. Cytochalasin D is most stable at -20^{o}C when stored at relatively high concentrations (2 mg/mL or higher is recommended by the manufacturer). Typically, 5 mL of sterile DMSO was added to 10 mg of Cytochalasin D powder and mixed well until powder was completely dissolved. Then, 1 mL aliquots were stored in cryovials, labelled with the date and concentration (2 mg/mL), and stored at -20^{o}C for use within 6 months.

2.10.2 Ficoll Solution Preparation

Ficoll-400 [Sigma], in powder form, was added to ddH_2O and the percentage Ficoll determined by weight (w/v). A stock solution of 30% Ficoll (or greater) was used to make lower concentrations by serial dilution.

Example:

30% Ficoll solution:

15g Ficoll-400 powder was measured into a beaker on a balance. Double distilled water or better was then added until the total weight, Ficoll-400 + water, reached 50g

(for a ~50 mL solution). Other desired percentages were made in a similar way with varying amounts of Ficoll-400 and water.

Ficoll-400 does not readily dissolve in water and must be stirred for many hours. Higher Ficoll concentrations take longer to dissolve. Ficoll solutions were left to stir in a beaker overnight with parafilm sealing the beaker to decrease water loss due to evaporation.

Preparations of water and Ficoll-400 were weighed prior to stirring and again after the Ficoll dissolved. Discrepancies in weight were corrected by the addition of additional ddH_2O. After the Ficoll solution contained no visible traces of powder and had been weighed, it was autoclaved (30 min. at 121^oC) in an attempt to eliminate contamination/infection.

After autoclaving, since Ficoll-400 is a sucrose polymer, the sucrose content (% Ficoll) of the stock solution was checked by refractometer [Bellingham+Stanley] (see Figure 2.6). If evaporation has resulted in a significant change in Ficoll concentration, sterile water was used to correct the discrepancy.

Next, the other components were added. Cytochalasin D should be added aseptically from the 2 mg/mL stock to a final concentration of 10 µg/mL cytochalasin within the Ficoll solution. Throughout development of this protocol, further additions were altered and optimized, but all solutions used contained Ficoll-400 and cytochalasin. Further additions or changes were made as noted in the results chapters. Below is a recipe table to make the standard, optimised Ficoll solution. All solutions were made aseptically in a Class II safety cabinet and mixed in sealed 50 mL centrifuge tubes [Corning] after all components had been added. Table 2.6 was used as a recipe for various concentration of Ficoll solution after optimisation of all components.

Table 2.6: Ficoll Solution Make-up

	30% Ficoll (mL)	ddH_2O (mL)	Cyto-chalasin (µL)	10x HBSS (mL)	Total Volume (mL)
5.0%	6.67	29.33	200uL	4.00	40.00
6.0%	8.00	28	200uL	4.00	40.00
6.5%	8.67	27.33	200uL	4.00	40.00
7.0%	9.33	26.67	200uL	4.00	40.00
8.0%	10.67	25.33	200uL	4.00	40.00
9.0%	12.00	24	200uL	4.00	40.00
10.0%	13.33	22.67	200uL	4.00	40.00
11.0%	14.67	21.33	200uL	4.00	40.00
12.0%	16.00	20	200uL	4.00	40.00
12.5%	16.67	19.33	200uL	4.00	40.00
13.0%	17.33	18.67	200uL	4.00	40.00
14.0%	18.67	17.33	200uL	4.00	40.00
15.0%	20.00	16	200uL	4.00	40.00
16.0%	21.33	14.67	200uL	4.00	40.00
17.0%	22.67	13.33	200uL	4.00	40.00
18.0%	24.00	12	200uL	4.00	40.00
19.0%	25.33	10.67	200uL	4.00	40.00
20.0%	26.67	9.33	200uL	4.00	40.00
21.0%	28.00	8	200uL	4.00	40.00
22.0%	29.33	6.67	200uL	4.00	40.00
23.0%	30.67	5.33	200uL	4.00	40.00
24.0%	32.00	4	200uL	4.00	40.00
25.0%	33.33	2.7	200uL	4.00	40.00

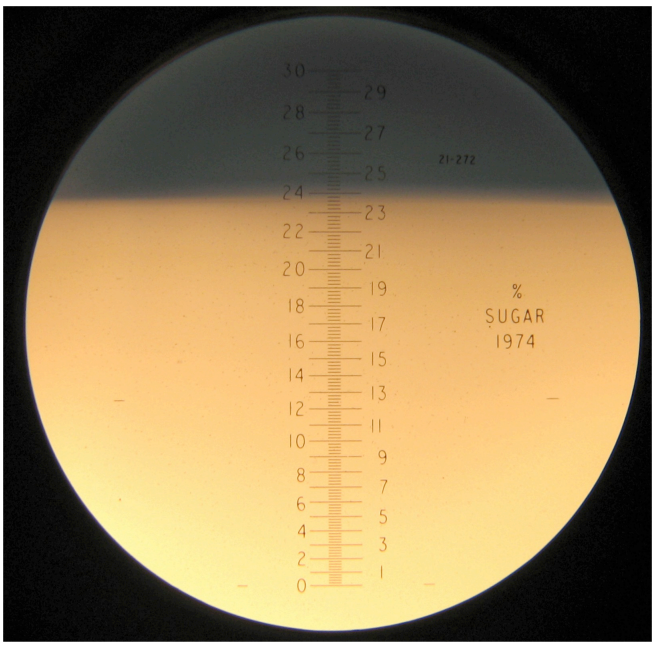

Figure 2.6: Refractometer for checking Ficoll concentration
The figure shows a refractometer reading of 24%, equivalent to 24% sucrose content. Since Ficoll is a sucrose polymer, the refractometer directly quantifies the purity of each aliquot of Ficoll solution. Readings were taken from each aliquot of Ficoll solution used before layering the gradients.

2.10.3 Gradient Preparation

Ficoll step gradients were prepared by layering solutions containing Ficoll-400 [Fluka, 46324] (a sucrose polymer) into clear 50 mL polycarbonate, screw-cap centrifuge tubes [Nalgene, 05-529C]. These tubes were chosen on the basis of their strength and clarity. Most standard tubes buckle under the high g-force required for enucleation.

Gradients were layered with the highest Ficoll concentration at the base of the tube (Ficoll/sucrose concentration determined by refractometer), with progressively lower densities of Ficoll (in layers) 'stacked' on top. The layers of ficoll solution were carefully added, sequentially by sucrose density, using a Pipetboy Acu mechanical pipette [Integra Biosciences, Switzerland]. All Ficoll solution volumes were predetermined to result in a specific layer arrangement as per the experiment.

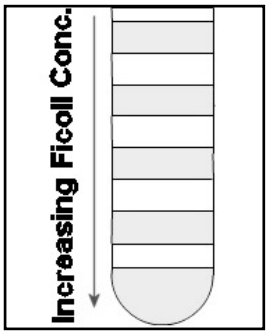

2.10.4 Gradient Storage

Since making gradients must be done very carefully, taking a significant amount of time in the lab, it seemed sensible to store gradients prior to use. However, through storing gradients for different lengths of time, it was found that gradient stability varied according to time, storage temperature, and gradient composition. Therefore, gradients were made fresh and used as soon as possible.

2.10.5 Preparing Cells for Enucleation

A confluent T75 of cells was treated with 10 mL of media supplemented with 10 µg/mL cytochalasin D for 15 minutes. After cytochalasin exposure, the media was aspirated and 3 mL 0.05% trypsin + 0.5 mM EDTA (in PBS) was added and left on the cells in an incubator at 37^{o}C for 3 min. Then, the cells were detached from the T75 flask by knocking the side with an open palm until all cells appeared to be in solution, this was verified visually under the microscope. The trypsin was then quenched by addition of 7 mL fresh growth medium containing 10% serum. The cell suspension was then pipetted up and down many times and the base of the flask was rinsed thoroughly,

making sure to obtain all cells, while also dissociating cell clumps. Then, cells were pipetted into a 50 mL plastic, screw cap centrifuge tube [Sarstedt] and centrifuged at 1000 rpm (150 g) for 3 minutes in a Megafuge 1.0 [Heraeus] lab top centrifuge. Then, media was aspirated and cells were resuspended in pre-warmed, 37^{o}C Ficoll solution.

2.10.6 Gradient Loading

Gradients were 'loaded' with cells just prior to the centrifugal enucleation step. The concentration of the Ficoll solution that the cells were resuspended in varied with experiment and gradients were typically warmed in an incubator for at least 1 hour prior to centrifugal enucleation on the Beckman J2-MC centrifuge. Following resuspension in Ficoll, the cell-Ficoll suspension was carefully layered on top of a pre-made gradient using a pipetteboy [Integra-Biosciences].

Then, the tube containing the loaded gradient was balanced with another tube that was filled with water and ran on the Beckman J2-MC centrifuge (Figure 2.7) under the conditions specified.

2.10.7 Centrifugation Conditions

Each enucleation run was performed under set centrifugation parameters including: temperature (^{o}C), speed (rpm), time (min), accel setting (0, 1, 2), and decel setting (0, 1, 2). These parameters are outlined in the study for each run/experiment and were optimized depending on cell type and separation needs.

Figure 2.7: J2-MC Centrifuge
This centrifuge was used for all centrifugal enucleations discussed in Chapter 3.

2.10.7.1 Rotor

The Beckman J2-MC Centrifuge was used to perform all enucleations for this study and is capable of using a variety of rotor heads. It was chosen due to the fact that it is the largest, most powerful centrifuge available in the CSCB. Two rotors were used for the purposes of this study, the JA-20 and the JS-13.1. Rotors should always be properly counterbalanced prior to use.

1.1.1.1.1 JA-20 Rotor

The JA-20 rotor is an angled head rotor designed to take up to six 50 mL tubes and operates at a maximum of 20,000 rpm (48,400 rcf). This was the most powerful rotor head that took 50 mL tubes.

Figure 2.8: JA-20 Angled Head Rotor

1.1.1.1.2 JS-13.1 Rotor

The JS-13.1 rotor is a swing-out rotor that operates in the range of 13,000 rpm (26,500 rcf). The JS-13.1 is designed to take 50 mL tubes and allows cells to travel perpendicular to the gradient layers along a straight path, giving cells approximately the same exposure to the layers and the sheer forces created by them. This rotor was obtained, on loan, from Dr. Debbie Sutton of the University of Sheffield, Dept. of Molecular Biology and Biotechnology, following experiments with the JA-20 angled head rotor.

Figure 2.9: JS-13.1 Swing-out Rotor

2.10.8 Centrifugal Enucleation

The rotor was pre-warmed, either by running for 3 hours at the desired temperature or by leaving the rotor in an incubator overnight. Once the gradient was loaded and balanced, the balanced tubes were placed into the Beckman J2-MC centrifuge in diametrically opposed slots. Next, the desired conditions for the rotor, temperature, speed (rpm), accel, decel, and time (min) were set and the run started.

2.10.9 Post-enucleation Protocol

At the end of the centrifugal enucleation step, the gradient was removed as soon as possible and the layer locations recorded. Samples were then taken from relevant layers, washed 3x in PBS, and resuspended in fresh medium to remove Ficoll solution. Hoechst 33342 was used at 5 µg/mL to check for nuclear DNA. Further testing differed depending on experiment (see results section for more information).

2.10.10 PEG Fusion Protocol

2.10.10.1 PEG Fusion Solution

PEG fusion solution is made with 41% polyethylene glycol (PEG) in DMEM (without serum) containing 10% DMSO. This recipe is based on "Dimethyl sulfoxide enhances polyethylene glycol-mediated somatic cell fusion" (Norwood et al. 1976). After trialing a small range of PEG and DMSO percentages, this concentration was found to be the best balance between of fusion efficiency and cell death.

Example:

7g polyethylene glycol (solid) + 9 mL DMEM + 1 mL DMSO = 41% PEG Fusion Soln.

This recipe was scaled in accordance to necessity. Fusion solution was made from fresh components, stored at 4^{o}C and used within 1 month.

2.10.10.2 Fusion Protocol

For suspension fusion, wash cells at least 2x with PBS, then resuspend cells at 2 x 10^{6} cells/mL in PEG fusion solution for one minute. Two minutes can be used if more fusion is desired, but increased PEG exposure quickly leads to more cell death. For monolayer fusion, carefully wash cell at least 2x with PBS, then use just enough PEG fusion solution to coat the cells and leave in the incubator for five minutes.

2.10.11 Cell Tracker Dye Protocol

Cell tracker green and red dyes [Invitrogen, C2925 & C34552] were used as per manufacturer's instructions at a concentration of 5 uM in serum-free medium. Cells were exposed to DMEM containing dye for 45 minutes at 37^{o}C, then the medium was replaced with fresh medium without dye. We found that cells would readily take up the dyes, staining all live cells tested (K562, NTERA2, and HuF1) equally for up to 3-5 days. Dyes should be stored at -20^{o}C when not in use. For this study, the dyes were used to track fusions between different cell types stained opposing colours.

2.11 Chapter 4 Materials & Methods

2.11.1 Total RNA Isolation for Transfection

See section 2.4.1 for RNA extraction protocol. Make sure Total RNA is quantified by spectrophotometer and solubilised in ddH_2O prior to transfection.

2.11.2 Total mRNA Isolation for Transfection

Total mRNA was extracted from total RNA samples as per manufacturer's instructions using Oligotex [Qiagen]. See section 2.4.1 for extraction protocol. Total RNA was solubilised in ddH_2O and quantified by spectrophotometer prior to starting the oligotex protocol. For the full protocol refer to page 23 of the Oligotex Handbook (May 2002), which can be found on the Qiagen website.

Oligotex beads are coated in dT30, 30 base strands of thymine that match with the poly A+ tails of mRNA sequences. By running total RNA through the beads with the proper binding buffers, mRNA attaches to the beads. After a few wash steps, highly purified mRNA can then be easily eluted with the manufacturer's elution buffer. Purified mRNA was resuspended in ddH_2O and checked by spectrophotometer for concentration. mRNA samples were then aliquoted and stored at -80^{o}C until needed for transfection. NOTE: Since mRNA is highly sensitive and breaks down easily, make sure to always keep it on ice once thawed and avoid multiple freeze/thaw cycles.

2.11.3 Electroporation Protocol

2.11.3.1 General Electroporation Principles

Electroporation uses electrical current, in pulses of specific voltage and pulse length (in milliseconds), to open 'pores' in the cell membranes of live cells. Osmotic force and force driven by electrical charge then allows for molecules to be transferred from the surrounding environment, consisting of electroporation buffer plus any additives, into the cells. The size of the molecules, the electroporation settings, and the buffered microenvironment all play a key role in the efficiency of electroporation.

2.11.3.2 Electroporation Preparation

Electroporations were carried out using a BTX ECM 830 Square Wave electroporator [Harvard Apparatus]. Cells should be 80% confluent on the day of electroporation. Remove cells from the flask and disperse into a single cell suspension using trypsin. NOTE: Our experience also shows that passaging confluent fibroblasts 1:2 a day before electroporation tended to result in higher transfection efficiencies.

Before electroporation, prepare a flask or well plate with fresh medium. Leave it at 37^{o}C in an incubator with 10% CO_2 for 30-60 min prior to electroporation. Then, count cells, wash them in PBS, then resuspend them in Electrobuffer [Cell Projects, EP-110] at 10^6 cells/200 µL. Then transfer cell suspension into 4 mm electroporation cuvettes [Cell Projects, EP-104] and add desired compound for transfection (i.e. DNA plasmid, RNA, mRNA). NOTE: All steps should be performed aseptically where possible.

2.11.3.3 Electroporation Parameters

Place the sealed cuvette containing the cell suspension into the electroporation chamber and make sure it is firmly seated. Take care to make sure the metal electrodes of the cuvette are against the anode and cathode. Set the desired pulse voltage (V), pulse length (ms), number of pulses, and pulse interval (ms). When ready, close the electroporation chamber and press the “start” button. For fibroblasts, 250-300V 3x 5ms, with 100 ms pulse interval was found to be best.

Use a fine tipped pipette to transfer a small volume of warm medium into the cuvette, washing the sides, before transferring the whole contents of each cuvette into a separate well or flask with warm medium. Place flask or well plate back into the incubator and let cells recover overnight before testing for DNA/RNA uptake.

2.11.3.4 Electroporation Quantification

Electroporation was typically quantified by cell count and fluorescence. Cells were counted before and 24 hours after electroporation in parallel with an analysis of the

intensity of a transfected fluorescent marker, such as GFP. Cell counts allow quantification of how many cells survived electroporation and the fluorescent marker (which can be quantified quickly by FACS) gives an indication of how efficiently cells can take up a compound of interest under the given conditions. Propidium Iodide should also be used in combination with fluorescence markers of other colours to assess cell viability where possible, giving values for dead cells, live or 'viable' cells, and fluorescently labelled positive cells.

2.12 Chapter 5 Materials & Methods

2.12.1 Ligation Protocol

This protocol was used for the ligation of coding region DNA fragments into RN3P.

Mix the following for a 5 µL Ligation:

2.5 µL 2x Ligation Buffer

0.5 µL Vector (pre-cut RN3P plasmid)

1.5 µL PCR fragment to be inserted

0.5 µL Ligase

Let the ligation reaction occur over 2-4 hours at room temperature or 4^{o}C overnight.

2.12.2 Bacterial Transformation for Plasmid Expansion

After ligation of genes into appropriate plasmid vector backbone (RN3P), competent bacteria was used to expand the plasmid into a large master stock.

Transformation Protocol:

1. Thaw competent bacteria on ice.
2. Mix 50-100 µL competent bacteria and 1-10 µL ligation reaction product and leave on ice for 10 minutes.
3. Heat shock bacteria by placing vial in 42^{o}C water bath for 1 minute.
4. Place vial back on ice for 10 minutes.
5. Add 200-300 µL of LB or 2YT broth [Invitrogen] to each sample vial.
6. Attach samples to a shaker and shake at 37^{o}C for 40-60 minutes.

7. Plate out the contents of each sample on LB plates containing the appropriate antibiotic selection (i.e. 100 µg/mL Ampicillin, Kanamycin, etc.). Spread samples across the plates using a ethanol/flame sterilized glass rod or similar.
8. Place plates upside down in a 37^{o}C incubator overnight.
9. Pick colonies and grow them out in broth containing 50 µg/mL Ampicillin or relevant antibiotic.

   NOTE: For plasmids with lactase/x-gal selection system, add 2 µL of 40 mg/mL xGAL to the sample vial just prior to plating.

2.12.3 In vitro mRNA Synthesis protocol

For mRNA in vitro transcription, RN3P plasmids containing the genes of interest (OCT4, SOX2, cMYC, KLF4, LIN28, NANOG, SV40 Large T) were linearised with Sfi I enzyme, and capped mRNAs were synthesised using the AmpliCap-Max T3 High Yield Message Maker kit [Epicentre]. mRNA was then purified as described below and stored in ddH_2O at -80^{o}C until needed for transfection.

2.12.4 Linearisation of RN3P with Sfi 1

RN3P plasmid must be linearised prior to in vitro synthesis in order to attain maximum efficiency. A strategically placed Sfi1 restriction site after the recombinant polyA tail sequence allows the full mRNA sequence to be effectively copied many times during a single in vitro synthesis reaction. 10ug of RN3P plasmid was digested with Sfi1 enzyme (New England Biolabs, NEB) as follows.

Mix the following components in the order listed (100 µL reaction volume):

ddH_2O	to 100 µL
RN3P plasmid containing gene to be synthesised into mRNA	10 µg
10x Buffer 2 (NEB)	10 µL
100x BSA (NEB)	1 µL
Sfi1 enzyme (20,000 units/mL) (NEB)	10 µL

Place the vial containing the mixture in a water bath at 50°C for 2-3 hours to allow digestion. Following digestion, enzyme cut DNA was isolated by phenyl:chloroform extraction to remove left over enzyme, BSA, and other contaminants.

2.12.5 Phenol:chloroform Extraction

The following steps were carried out on ice where possible with all centrifugation steps done at 4°C using an Eppendorf 5417R centrifuge. For RNA, use phenol:chloroform at pH 4, for DNA use pH 7.

1. Add 1 volume phenol:chlorofom [Sigma, P3803] to each sample, vortex using a Fisions Whirlimixer, then centrifuge at 14,000 rpm (20,000 g) for 5 minutes.
2. Transfer supernatant to a new vial and add 1 volume of chloroform, vortex, and centrifuge at 14,000 rpm (20,000 g) for 5 minutes.
3. Transfer the supernatant to a new vial and add 0.1 volume of NaAcetate (3 M, pH 5.2) and 2.5 volumes 80% ethanol, then briefly mix samples by inversion.
4. Incubate samples for a minimum of 3 hours at -20°C to allow DNA/RNA to precipitate. Then, centrifuge at 14,000 rpm for 10 minutes. *NOTE: this step can be sped up by placing samples in a -80°C freezer for 30-60 minutes.
5. Discard supernatant, being careful not to dislodge the white pellet. Then add 80% ethanol and vortex to dislodge and wash the pellet. Centrifuge at 14,000 rpm for 5 minutes. Do a second 80% ethanol wash, centrifuge, then discard ethanol. Be careful not to decant the pellet.
6. Allow samples to dry at room temperature until the pellet starts to become translucent and all ethanol had evaporated.
7. Once dry, add ddH_2O to desired concentration.

2.12.6 In vitro mRNA synthesis

The AmpliCap-Max T3 High Yield Message Maker kit protocol was scaled up from 10 µL to 50 µL of concentrated mRNA product.

The components were mixed as follows:

RN3P pDNA Template		2.5 µg	
ddH_2O		up to 50 µL	
10x T3 Buffer		5 µL	
Cap/NTP mix		20 µL	
100 mM DTT		5 µL	
T3 Enzyme mix		5 µL	*Make sure to add Enzyme mix last
Total volume	=	50 µL	

2.12.7 Post synthesis mRNA Purification Protocol

After in vitro transcription, mRNA products were treated with DNAse (0.5 units/10 µL) for 15 minutes at 37^{o}C to degrade the template; DNAse was then heat inactivated. To remove salts, left over dNTPs, and other synthesis contaminants, the mRNA was purified using Illustra S-200 HR Microspin columns [GE Healthcare, 27-5120-01]. Afterwards, Phenol:chloroform extraction was used to isolate and further purify the mRNA (see section 2.12.5). mRNA was then resuspended in ddH_2O. To test for contaminants, 1 µL from each sample of mRNA was checked on a 1% agarose gel. mRNA concentration was quantified by spectrophotometer (see section 2.4.1.3), mRNA stocks were typically stored at 1-5 ug/mL and aliquots were made as needed.

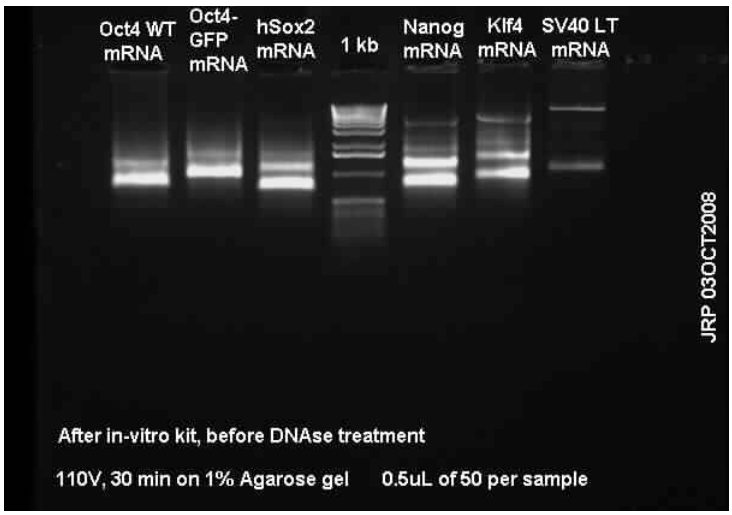

Figure 2.10: 1% Agarose gel following in vitro mRNA synthesis

From our stock of RN3P plasmids, we were able to produce a large stock of mRNA for each of the genes of interest. This stock tended to be replenished about every three to

six months from the same plasmid stock, ensuring reproducibility between mRNA batches.

2.12.8 mRNA Quantification

mRNA was quantified in the same way as total RNA, see section 2.4.1.3.

NOTE: There is ~10-15 pg RNA/cell. mRNA = 1-5% of total RNA. So, 7 x 10^6 cells should have approximately 70 µg of RNA and therefore about 0.7 µg mRNA.

2.12.9 Microporation

Human fibroblast cells cells were electroporated using a MP100 Microporator [Invitrogen], using two 20 ms pulses of 1400V, 100 ms apart. These parameters came from optimisation experiments (see section 5.2.13.4). Following microporation, cells were transferred into pre-warmed fibroblast medium, DMEM with 10% FCS.

2.12.9.1 Standard Microporation Protocol

All steps should be carried out aseptically where possible. If using mRNA, make sure to always keep it on ice and prevent freeze/thaw cycles as much as possible to prevent break down.

1. Trypsinise cells to get them into a single cell suspension.
2. Wash cells 2x with PBS, then resuspend them in proprietary microporation buffer R [Invitrogen] at 10^6 cells/100 µL.
3. Add desired mRNA or other desired transfection molecule/nucleic acid. Mix by pipetting slowly up and down. Be careful not to dilute the Buffer R too much with mRNA or DNA, etc. as it will decrease microporation efficiency in high amounts.
4. Draw cell suspension containing mRNA (or other molecules) into the microporation pipette. NOTE: This needs to be done very slowly and carefully, so as to avoid getting any air bubbles into the pipette tip. Air bubbles will cause the microporation tip to spark upon shocking and result in significantly lower transfection efficiency. To avoid this it is usually appropriate to making 120% the volume you would like to transfect.

5. Place the microporation pipette firmly into the microporation chamber, making sure that there is 3 mL of buffer in it (as per manufacturer's instructions).
6. Enter the microporation parameters (voltage, pulse length, pulse number, pulse width) and press the start button. NOTE: Fibroblasts were found to reach highest transfection efficiency using 1400V, with two 20 ms pulses and a pulse width of 100 ms.
7. Following microporation, cells should be immediately transferred into fresh, prewarmed medium and placed in the incubator. NOTE: For some cell types gelatin coating or 10 μM γ-27632 can help improve cell survival and attachment post shock.

2.13 Small Molecules

2.13.1 Trichostatin A (TSA)

TSA [Sigma, T8552] was aliquoted at 1 mM and stored at -20^{o}C.

2.13.2 5-aza-2'-deoxycytidine (5Aza)

5Aza [Sigma, A3656] was aliquoted at 2 mM and stored at -20^{o}C. 5Aza was typical used at 0.5 μM.

2.13.3 Valproic Acid (VPA)

VPA [Sigma, P4543] was aliquoted at 2 M and stored at -20^{o}C. VPA was typically used at 0.2 μM, but varied by experiment.

2.13.4 BIX01294 (BIX)

BIX [Sigma, B9311] was aliquoted at 2 mM and stored at -20^{o}C. BIX was typically used 1 μM.

2.13.5 γ-27632 (ROCKi)

ROCKi [Sigma, Y0503] was aliquoted at 10 mM and stored at -20^{o}C. To use, ROCKi was added directly into the medium and gently mixed, making a final concentration of 10 μM.

2.14 Polymersome Encapsulation Protocol

1. Measure out $PMPC_{25}PDPA_{70}$ (raw chemical form of polymersomes)
2. Dilute into ethanol:chloroform in a glass vial, then dehydrate in an oven.
3. Glass containers should have a film of dehydrated $PMPC_{25}PDPA_{70}$ which can then be solubilised in PBS with HCl added to bring pH down to 2.0. NOTE: lower pH causes faster, more complete solubilisation of polymersomes.
4. Sonicate for ~15 min. Polymersomes are sonicated to remove 'onion-like' structures, or capsules within capsules and this will increase the free polymersomes. Also, it helps create smaller, more uniform polymersomes.
5. After sonication, NaOH is added to bring pH up to 6.0.
6. Add mRNA (or DNA, siRNA, or live cell dye). Then adject pH to 7.0 with NaOH, which catalyses the formation of polymersomes. NOTE: up to 200 µg of mRNA per mL of polymersome solution was tested. Individual applications require optimisation of the ratio of desired transfection material and polymersomes.
7. Sonicate for 15 min.
8. Apply sample(s) to sephadex 4B sepharose column [GE Healthcare].
9. Start collecting sample when eluant becomes cloudy, discard pre/post flowthrough (which should be relatively clear).
10. Seed cells you wish to treat with polymersomes in a well plate ahead of time.
11. Apply polymersomes to cells in 1:10 ratio (e.g. 50 µL polymersomes per 500 µL medium. NOTE: Lower volumes of media are best for polymersome transfection. Also, FBS does not affect the transfection efficiency of polymersomes.
12. Give at least 4 hours for cells to ingest/take-up polymersomes before changing the medium.

Chapter 3 – Cytoplasm Isolation for Reprogramming

3.1 Introduction

This chapter is based on the hypothesis that the uncharacterized factors (including proteins, mRNAs, microRNAs, etc.) needed to catalyse the reprogramming of a somatic cell to a pluripotent cell state reside in the cytoplasm of pluripotent cells. Also, that these factors, if isolated and administered to somatic cells in appropriate amounts, can reprogram somatic cells. This work is based upon nuclear transfer, cell fusion and transdifferentiation work, from the 1950s until today.

Somatic cell nuclear transfer (SCNT) experiments in amphibians carried out in the 1950s and 60s (Briggs et al. 1952; Gurdon 1962c; Gurdon 1962d; Gurdon 1962a) and later in mammals (Wilmut et al. 1997; Hochedlinger et al. 2002a; Eggan et al. 2004; Inoue et al. 2005) demonstrated that the genomes of individual, adult cells are able to generate viable cloned animals. These studies indicate that the oocyte contains factors capable of mediating the reprogramming of adult cells into an embryonic state and that the developmental restrictions imposed on the genome during differentiation are likely due to reversible epigenetic changes, as opposed to permanent genetic modifications (Hochedlinger et al. 2002b).

The reprogramming mechanism was further elucidated through the study of pluripotent cell types. The isolation of pluripotent embryonal carcinoma cell lines from teratocarcinomas (Kleinsmith et al. 1964; Finch et al. 1967; Kahan et al. 1970; Andrews et al. 1980a; Bronson et al. 1980; Andrews et al. 1984b), the subsequent derivation of mouse ES cells from blastocysts (Evans et al. 1981; Martin 1981), and of embryonic germ (EG) cells from primordial germ cells (Matsui et al. 1992; Resnick et al. 1992) led to a greater understanding concerning the nature of pluripotency. Despite their differences in source, all three cell types were found to remain undifferentiated in culture, able to undergo differentiation into all cell types when introduced into

blastocysts (Brinster 1974; Mintz et al. 1975; Bradley et al. 1984; Matsui et al. 1992) and have demonstrated the ability to reprogram somatic cells when fused with them, generating pluripotent tetraploid hybrids (Miller et al. 1976; Tada et al. 1997; Tada et al. 2001; Cowan et al. 2005). Interestingly, these fusion experiments also demonstrate that the pluripotent state can be dominant over the differentiated state. However, others have reported that similar circumstances have only resulted in partial dedifferentiation or loss of multipotentiality, implying that the process is more complicated than the simple administration of factors, that there are additional variables that need to be resolved in order for the pluripotent state to override the somatic phenotype (Finch et al. 1967; McBurney et al. 1978; Andrews et al. 1980b).

Although the kinetics of cloning are not yet fully understood, it is clear that the oocyte, comprised primarily of lipids, proteins, and various forms of RNA, can alter the nucleus of a somatic cell to a primitive, embryonic state capable of directing embryonic development. Similarly, cell fusion work has indicated that pluripotent cells are, under the right conditions, capable of causing reprogramming (McBurney 1977b; McBurney et al. 1978; McBurney et al. 1979; Baron et al. 1986; Tada et al. 2001; Cowan et al. 2005). Given these findings, we hypothesized that the cytoplasm from pluripotent cells, not unlike the cytoplasm of an oocyte, may also be capable of effectively reprogramming somatic cells.

While fusing two cells has been shown to result in successful reprogramming, or at least partial reprogramming, the resulting fused cell always has two sets of chromosomes. Often the two nuclei hybridise through mitosis, which can result in a totally new cell type with a mixture of phenotypic characteristics taken from both cells. While the characteristics of this hybrid cell may, in some cases, be advantageous, the issue remains that the reprogrammed, dual nuclei cell is no longer compatible with either parental cell type and would be relatively useless in terms of clinical application. Although some groups claim to have developed methods for selectively removing the

unwanted extra nucleus post-fusion (Pralong et al. 2005; Matsumura et al. 2007), at present, reproducible methods for producing mononuclear cells with the benefits of cell fusion mediated reprogramming, but without the potential for genetic recombination or hybridization, remain an unsolved problem. However, cytoplasm mediated reprogramming attempts to solve this issue by taking the benefits of cell fusion, while preventing nuclear hybridisation. See Figure 3.1 for an overview of the discussed reprogramming methods.

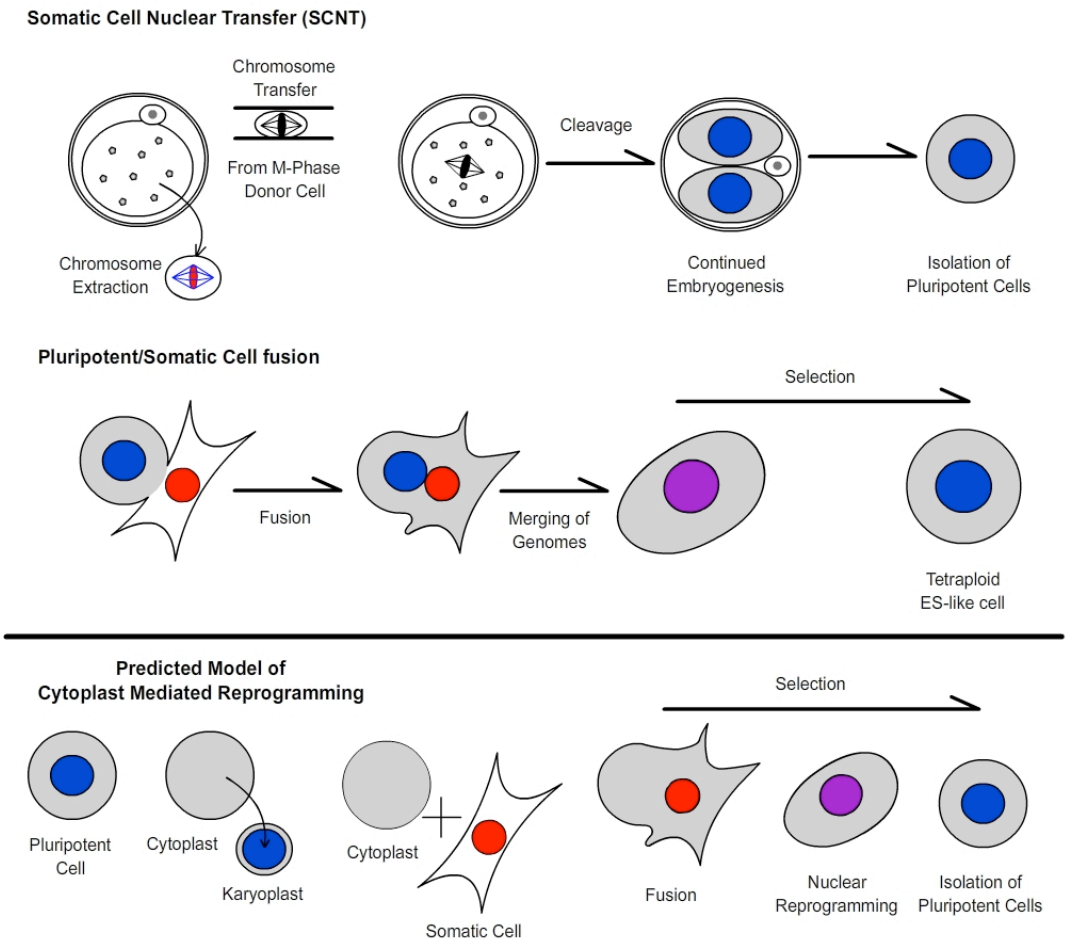

Figure 3.1: Methods of Reprogramming
Somatic cell nuclear transfer (SCNT) and pluripotent/somatic cell fusions have previously been shown to successfully reprogram somatic cells to a pluripotent state. The cytoplast mediated reprogramming process, as depicted, is based upon the hypothesis that cytoplasm isolated from pluripotent cells can catalyse somatic cell reprogramming, similarly to oocyte cytoplasm. **Note:** at the time this work was carried out, viral transduction based reprogramming had not yet been published.

3.1.1 Cytoplast Mediated Reprogramming

Cytoplast mediated reprogramming is a concept that stems from the 1971 publication by Poste and Reeve (Poste et al. 1971) who concluded that cytoplasmic factors were important in regulating gene expression and that this could be tested by combining enucleated and nucleated cells. Many adaptations have since been published, many of which have been taken into consideration throughout the development of this method (Prescott et al. 1973; Ber et al. 1978; Shay 1987). Wigler and Weinstein's (W&W) method, which utilises a discontinuous Ficoll step gradient, was chosen over other enucleation methods due to the fact that it boasted high enucleation efficiency, even when using high cell numbers (e.g. >1 million cells per enucleation) and it could easily be adapted to multiple cell types (Wigler et al. 1975). Other published methods involve cutting a disc of tissue culture plastic (or similar growth surface) from a flask coated in a monolayer of cells, then treating those cells with cytochalasin followed by inversion and centrifugation to 'pull' the nuclei away from the cytoplasm encapsulated by cell membrane, which remains attached to the disc (see Figure 3.2)(Prescott et al. 1973; Ber et al. 1978). These methods were "limited by the total surface area which can be conveniently centrifuged" (Wigler et al. 1975).

Wigler and Weinstein's "A Preparative Method for Obtaining Enucleated Mammalian Cells" (Wigler et al. 1975) was used as a starting point for the enucleation protocol developed in this work with additions and variations being made primarily through testing individual parameters. Not a lot has changed with this process technology since the 1970's, however the ways in which cells (and cell components) can be isolated and sorted has, which is part of the reason this methodology was revisited. See Figure 3.2 for a comparison between previously published enucleation methods.

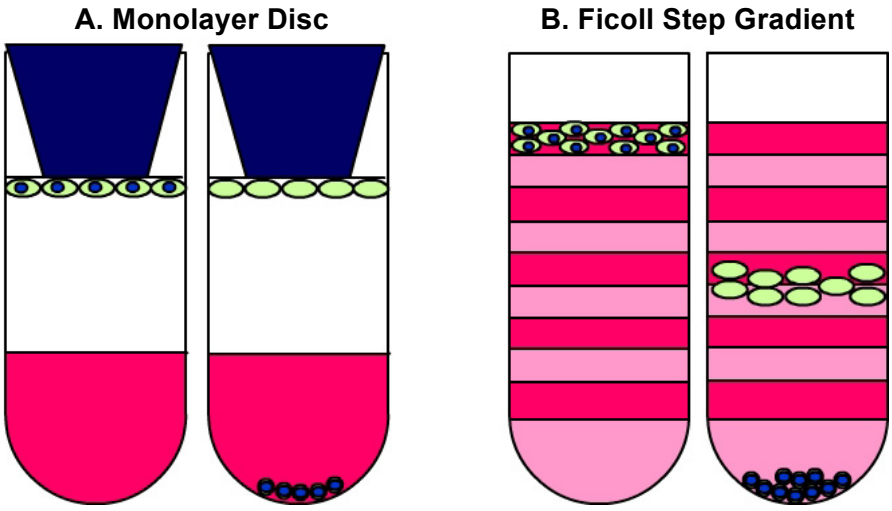

Figure 3.2: Monolayer vs. Suspension Enucleation
The two enucleation methods shown represent to two popular published methods shown to result in reproducible enucleation. The Ficoll step gradient was chosen as the basis for the enucleation protocol used in this work because it is capable of enucleating attachment or suspension cells in high numbers and can be done aseptically. The two methods work as follows: A) A circular disc of cells grown in monolayer are treated with cytochalasin and attached to a rubber stopper with adhesive, then centrifuged to 'pull' the nuclei away from the cytoplasm, based on the increased density of the nucleus, to the bottom of the tube; B) Cells in suspension are treated with cytochalasin, then centrifuged through a discontinuous step gradient. The differing densities between the nuclei and the cytoplasm should result in separation based on density.

3.1.2 Ficoll Gradient Enucleation

Although the Wigler and Weinstein method was taken as a starting point for the enucleation protocol, there are a couple fundamental differences between the parameters they used and those available in our lab. Improvements and changes made are discussed briefly below.

3.1.1.1 Cytochalasin D

Older enucleation publications, including Wigler and Weinstein, used cytochalasin B (cytoB) (Low et al. 1975; Low et al. 1976; Dancker et al. 1979), but more recent publications indicate that cytochalasin D (cytoD) is up to 10x more effective at depolymerising the actin cytoskeleton (Cooper 1987). To assess the effectiveness of cytoD, separate flasks of NTERA2 clone D1 (NT2) cells were incubated in medium with 10 µg/mL cytoD and 10 µg/mL cytoB then carefully monitored under a microscope. After treatment with cytochalasin, cells appeared to round up and blebs formed on the surface of the cells. The term blebbing is used to describe bubble-like protrusions where the cell membrane has lost stability due to the depolymerisation of the actin cytoskeleton. Blebbing, to some extent, is normal, but blebs are typically quickly retracted as the cell repairs the depolymerised areas of the cytoskeleton (Charras et al. 2006). However, as expected, the blebs seen in both flasks remained on the cell surface in the presence of cytochalasin as it hinders the natural cytoskeleton repair process.

Although both cytoB and cytoD appeared to effectively depolymerise the cell membranes of NT2 cells, those treated with cytoD not only appeared to form blebs at a higher rate, but also to a greater extent. While some cells in the cytoB treated flask did not appear to be affected at all, nearly 100% of cells treated with cytoD appeared to round up and bleb as expected. Cells were exposed and monitored for 30 minutes, however, exposure beyond 10 minutes did not appear to strengthen the effect on the cells' morphology, therefore 15 minutes was deemed to be an appropriate amount of

exposure time in order to be certain that all cells' cytoskeletons were properly depolymerised prior to centrifugation.

3.1.1.2 Cell Types Enucleated

Wigler and Weinstein used mouse L fibroblast cells in their 1975 publication (Wigler et al. 1975), but in a correspondence to C.L. Bunn, they also mentioned success with this protocol when enucleating Normal Rat Kidney (NRK), Vero (African Green Monkey fibroblasts), and rat liver cells. Compared to the various cell lines used by Wigler and Weinstein, NT2 cells used in this work are generally smaller than most mammalian cells types and are noted for their large nucleus to cytoplasm ratio and prominent nucleoli, similar to embryonic stem cells.

3.1.1.3 Centrifuge and Centrifuge Rotor

The original paper by W&W used a SW41 swinging bucket rotor in an L 3-50 ultracentrifuge at 25,000 rpm (r_{min} = 47,200 rcf, r_{max} = 107,000 rcf), however, that centrifuge was not available and the best available approximation to that was used instead, a Beckman J2-MC with the JA-20 angled rotor at 20,000 rpm (max speed) (r_{min} = 14,300 rcf, r_{max}= 48,400 rcf). Although the power of the J2-MC is less than the L 3-50, Pralong *et al.* showed that mouse embryonic stem cells (which much more closely resemble NT2 embryonal carcinoma cells as compared to those used by Wigler and Weinstein) could be enucleated at rates of up to 95% at 14,500 rcf (Pralong et al. 2005), which is well within the capability of the Beckman J2-MC centrifuge.

3.1.1.4 Fusion Protocol

After isolation of cytoplasts, the next step is to fuse the cytoplasts with somatic cells, creating cybrids, cytoplast and nuclear or whole cell fusions between different cell types (Poste et al. 1971; Veomett et al. 1974), and then select for surviving fusions. For this, a number of previously published fusion strategies were found and researched: 1) inactivated sendhai virus induced fusion, 2) polyethylene glycol (PEG_{6000}) induced fusion (Hui et al. 1985; Flasza et al. 2003), and 3) lysolecithin (Hui et al. 1985). After further evaluation, PEG_{6000} induced fusion was chosen as it is the most straightforward,

high efficiency protocol, and the reagents are easily obtainable. As a starting point, the publication "Dimethyl Sulfoxide Enhances Polyethylene Glycol-Mediated Somatic Cell Fusion" (Norwood et al. 1976) was used as it presents a semi-optimised technique using mammalian somatic cells that boasts higher efficiency than other similar publications and has been referenced by many subsequent papers for its fusion protocol.

According to Norwood *et al.* (1976), the efficiency of PEG_{6000} mediated fusion is improved, by increasing the levels of PEG_{6000} (up to 50%) and adding DMSO (10-15%) to the formulation of fusion medium. For our purposes, fusion conditions were tested using the best conditions found by Norwood *et al.* as a starting point and basis of comparison.

3.1.3 Overview

The methods and experiments outlined in this chapter are based on the assumption that cytoplasm, specifically cytoplasm from pluripotent cells, contains all the necessary factors involved in reprogramming a cell. The hypothesis being that, given the right ratio of cytoplasm (and hence reprogramming factors), reprogramming from a somatic to ES cell-like state is possible. In order to obtain just the cytoplasm, the nucleus will be separated from the rest of the cell leaving behind a cytoplast, which is comprised primarily of cytoplasm encapsulated by the cell membrane.

3.1.4 Chapter Aims

I. Development of a protocol to isolate cytoplasts from pluripotent cells (hypothesized to contain reprogramming factors)
II. Development of a method for quantification of isolated cytoplasts.
III. Optimisation of the cytoplast isolation protocol, taking into consideration scale-up and reproducibility.

IV. Establish a method of administering the cytoplasts to somatic cells without transferring genomic DNA.

V. Development of a qualitative assay to determine the effectiveness of isolated reprogramming factors on altering the phenotype of somatic cells.

3.2 Results

3.2.1 Optimisation of Wigler & Weinstein Protocol

After approximating Wigler and Weinstein's conditions as best as possible, a few initial runs showed that the adapted protocol needed further alterations, in addition to those previously discussed, in order to achieve efficient enucleation.

3.2.1.1 JA-20 Angled Head Rotor Replaced by JS-13.1 Swing Out Rotor

The JA-20 angled head rotor (run in the J2-MC Beckman Centrifuge) resulted in cells being forced into the wall at high velocity, circumventing the intended shearing forces of the layered Ficoll solution and instead being sheared on the wall of the tube, creating a 'smear' of cells along the wall of the centrifuge tube. As shown in Figure 3.3, the separation of the cells into distinct layers was very poor. It was concluded that a swing-out rotor was necessary to achieve the desired separation by forcing the cells down through the tube on a perpendicular path to the layers of Ficoll.

Dr. Debbie Sutton of the University of Sheffield, Dept of Molecular Biology and Biotechnology, graciously supplied a Beckman JS-13.1 swing-out rotor, to use with the Beckman J2-MC centrifuge. The J2-MC is compatible with the JS-13.1 rotor for speeds up to 13,000 rpm (26,500 rcf); still adequate enough for this work based on Pralong *et al.* (2005). This rotor was used in place of the JA-20 from this point onwards. See Materials & Methods section 2.10.7.1 for information on rotors used.

3.2.1.2 Centrifugation Temperature

Temperature is very important for enucleation. Higher temperatures promote fluidisation of the cellular membrane and allow for increased enucleation efficiency (Amatruda et al. 1979). The temperatures used were based on Wigler & Weinstein's enucleation experiments, which were done at 31^{o}C (Wigler et al. 1975). Further testing showed that temperatures below about 30^{o}C (according to the J2-MC temperature sensor) resulted in relatively low levels of enucleation. The rotors used were always prewarmed to at least 31^{o}C prior to use.

A B C

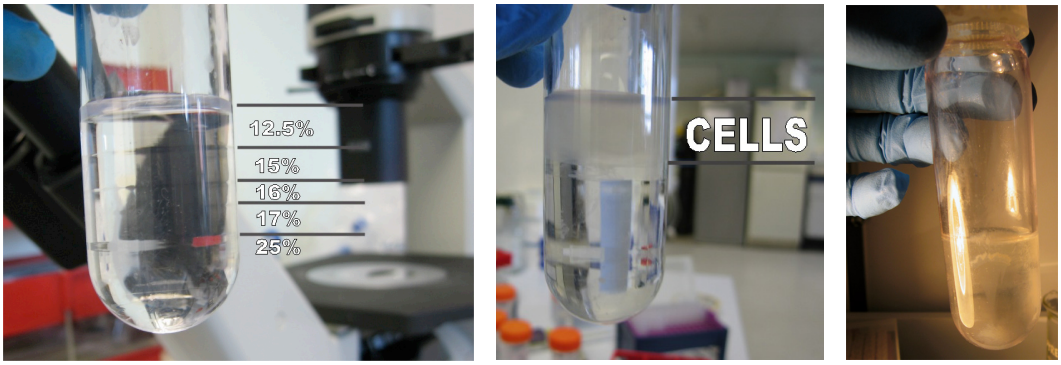

Figure 3.3: Initial Ficoll Gradient

A) Freshly made 12.5-25% Ficoll gradient, you can roughly see the layer divisions by eye here. B) Cells resuspended in Ficoll and loaded on top of the Ficoll gradient as shown. C) This post-centrifugation photo shows the 'smearing' effect of the JA-20 angled head rotor. Cells loaded on the top of the gradient were pulled down and outwards into the tube wall resulting in the pattern shown.

3.2.2 Ficoll Gradient Stability

Since making gradients must be done very carefully and takes a significant amount of time in the lab, it seemed sensible to store gradients prior to use. However, after using gradients that had been stored for different lengths of time, it was found that gradient stability varied according to time, storage temperature, and gradient composition.

3.2.2.1 Effect of Temperature on Ficoll Gradient

Immediately after layering a Ficoll gradient, crisp lines form, indicating the layers of differing percentages of Ficoll. However, it was noticed that these crisp lines faded at different rates, depending primarily on temperature.

Table 3.1: Initial Gradient Composition (as per Wigler & Weinstein)

Layer Location	Layer Composition
1st (Top) Layer	2 mL 12.5% Ficoll
2nd Layer	0.5 mL 15% Ficoll
3rd Layer	0.5 mL 16% Ficoll
4th Layer	2 mL 17% Ficoll
5th Layer	5 mL 25% Ficoll

Room Temperature (~20°C)

The gradient, left untouched, was sealed in a 50 mL polycarbonate tube for approximately 48 hours at room temperature (~20°C). Subsequent examination found that the gradient had lost distinct meniscuses at layer interfaces. 100 µL samples were carefully removed by pipette and tested by refractometer [Bellingham-Stanley, UK]. After taking samples from each layer at points where the original layers should have resided, the following readings were obtained:

Table 3.2: Gradient Stability at 20°C

Layer Location	Original Layer %	% After 48 hours @ ~20°C
1st (Top) Layer	12.5%	15%
2nd Layer	15%	16%
3rd Layer	16%	21%
4th Layer	17%	21%
5th Layer	25%	25%

Refrigerated Gradient (4°C)

Two gradients, left untouched, sealed in a 50 mL polycarbonate tube for 48 hours and seven days at 4°C were examined and found to have maintained distinct, visible layer interfaces, however, the layer boundaries appeared blurred. After taking five 100 µL

samples, using a pipette [Gilman], at points where the original layers should have resided, the following readings were obtained:

Table 3.3: Gradient Stability at 4°C

Layer Location	Original Layer %	% After 48 hrs @ 4°C	% After 7 days @ 4°C
1st Layer (Top)	12.5%	12.5%	12.5%
2nd Layer	15%	15%	15%
3rd Layer	16%	16%	16%
4th Layer	17%	17%	17%
5th Layer (Base)	25%	25%	25%

Results showed that the gradients are more stable at 4°C. Although the gradients appeared unaffected at 4°C after seven days, there is a temperature related effect on gradient stability and for this reason, gradients were subsequently used fresh on the day they were made to reduce variability.

3.2.3 Adapted W&W Protocol Using Swing-out Rotor

After the optimisations discussed, the JS-13.1 swing-out rotor was used, matching the remaining conditions as closely as possible to those used by Wigler and Weinstein. Ficoll solution was made by diluting a 30% stock solution with PBS and adding cytochalasin to a final concentration of 10 µg/mL (See Table 3.4 for recipe used). Below, the composition of the gradient and the conditions of centrifugation used are shown.

Initial Run Centrifugal Enucleation Conditions

Layer Location	Layer Composition
1st (Top) Layer	2 mL 12.5% Ficoll + Cytochalasin D
2nd Layer	0.5 mL 15% Ficoll + Cytochalasin D
3rd Layer	0.5 mL 16% Ficoll + Cytochalasin D
4th Layer	2 mL 17% Ficoll + Cytochalasin D
5th Layer	5 mL 25% Ficoll + Cytochalasin D

Parameter	Setting
Speed	13,000 rpm (26,500 rcf)
Run Time	60 minutes
Temp	31°C
Accel	1
Decel	1
Cells	2 x 10^7 NT2 cells P38

Table 3.4: Initial Ficoll Recipe

	30% Ficoll (mL)	PBS (mL)	Cyto-chalasin (µL) [2 µg/µL]	Total Volume (mL)
5.0%	6.67	33.33	200	40.00
6.0%	8.00	32	200	40.00
6.5%	8.67	31.33	200	40.00
7.0%	9.33	30.67	200	40.00
8.0%	10.67	29.33	200	40.00
9.0%	12.00	28	200	40.00
10.0%	13.33	26.67	200	40.00
11.0%	14.67	25.33	200	40.00
12.0%	16.00	24	200	40.00
12.5%	16.67	23.33	200	40.00
13.0%	17.33	22.67	200	40.00
14.0%	18.67	21.33	200	40.00
15.0%	20.00	20	200	40.00
16.0%	21.33	18.67	200	40.00
17.0%	22.67	17.33	200	40.00
18.0%	24.00	16	200	40.00
19.0%	25.33	14.67	200	40.00
20.0%	26.67	13.33	200	40.00
21.0%	28.00	12	200	40.00
22.0%	29.33	10.67	200	40.00
23.0%	30.67	9.33	200	40.00
24.0%	32.00	8	200	40.00
25.0%	33.33	6.7	200	40.00

After centrifugation using the JS-13.1 spin out rotor, there was a visible pellet and some faint layers from the cells (or cell debris) spread between the 12.5% to 20% region of the gradient with no distinct layers at Ficoll interfaces. In order to determine whether enucleation had occurred, three 2mL samples were extracted from the top (~12.5%), middle (~15-17%), and bottom (~25%) of the gradient. Samples were diluted in fresh 37^{o}C DMEM +10% FBS and placed in wells of a 6 well plate at 37^{o}C with 10 µg/mL Hoechst 33342 for 15 min prior to imaging. See Figure 3.4 for images of the enucleation products.

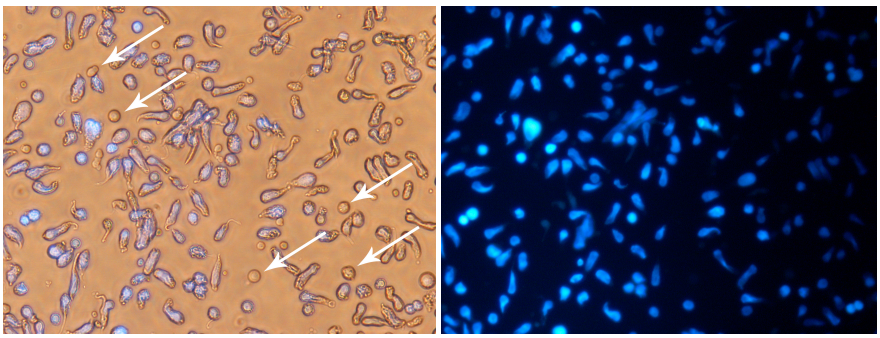

A: Top Region - Phase and UV

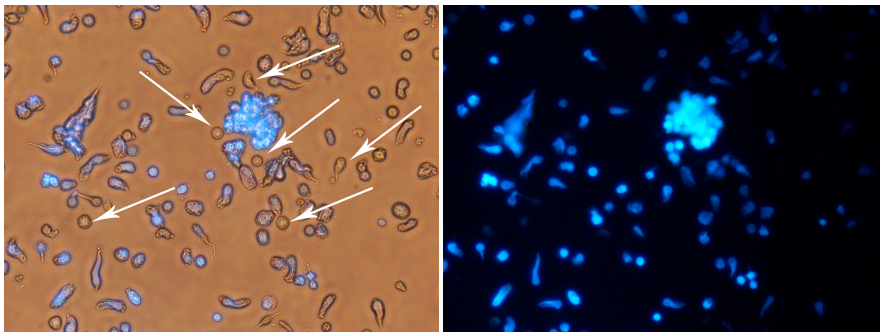

B: Middle Region – Phase and UV

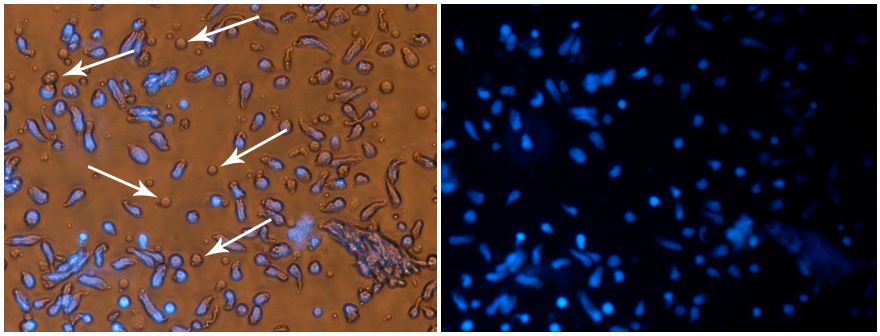

C: Bottom Region – Phase and UV

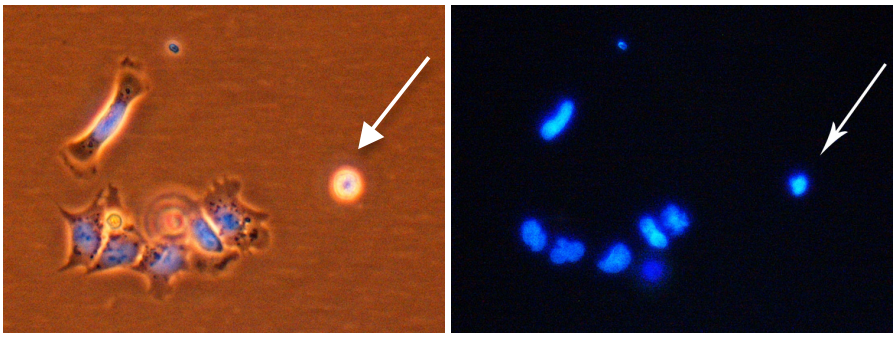

D: Magnified Karyoplast vs Whole Cells

Figure 3.4: Enucleation Products using Swing Out Rotor
The photos shown were taken after carefully removing sections from the top (A), middle (B), and bottom (C) of the gradient described in section 3.2.3 after enucleation. Notice that the overall brightness of events in B and C is less than that in A and also the number of events that are Hoechst negative is higher in B and C. The Hoechst negative events are cytoplasts, some have been marked by arrows for clarity. (D) This set of images shows a single karyoplast marked by the white arrow next to a group of whole cells for comparison.

3.2.3.1 Conclusions

As shown in Figure 3.4, the Ficoll gradient did enucleate cells, but overall, separation was poor as there were still nuclei throughout the gradient and no single area seemed to be primarily karyoplasts or cytoplasts. After five with similar results, the process was reviewed and a number of possible explanations were reviewed: 1) the number of cells loaded on the gradient was too high (or the loading volume was too low) and cell clumping (as seen in Figure 3.4 B) affected the enucleation efficiency negatively; 2) the high nucleus to cytoplasm ratio of NT2 cells makes separation of the cytoplasm more difficult as compared to other mammalian cell types; 3) the gradient itself needs further optimisation; 4) the nuclei of the cells were in different phases of the cell cycle, thus had different sized nuclei, and were affected differently despite undergoing similar shear forces; 5) the shear forces experienced by the cells were not consistent, resulting in a variety of enucleation products in terms of size and composition, ultimately leading to enucleation products separating out in different areas of the gradient instead of into distinct layers consisting primarily of just karyoplasts, cytoplasts, or whole cells, as hypothesised. Theoretically, the cells could be overwhelming the gradient's layer interfaces as they simultaneously pass through layer boundaries, diminishing the shearing effect at the interface for subsequent cells as they move through the gradient and resulting in lower overall enucleation efficiency. Also, the loaded cells surely cause mixing of the Ficoll layers on the micro scale as they pass through the gradient, again, generally decreasing the effective sheer at layer interfaces and ultimately lowering enucleation efficiency.

At this point, it was concluded that any or all of these reasons could be playing a role in the lower than anticipated efficiency. Therefore, one by one, variables were tested with the goal of discovering the limiting factors and bottlenecks of the enucleation process.

3.2.4 Expanded Ficoll % Gradient

After limited success with the Wigler and Weinstein gradient configuration, a new gradient with a wider range of layers with varying Ficoll percentages was designed. This 'wider' gradient with more layers across a greater set of Ficoll densities was conceived after reviewing the enucleation microenvironment and the engineering variables involved. Between Ficoll layers there is an interface and at each interface a surface tension exists. Based on the Navier-Stokes equation, the greater the difference in layer densities at these interfaces, the greater the shear force a small spherical particle (in this case a cell) will endure in crossing the interface between one density to another.

After consulting the Beckman website (www.beckman.com) and obtaining all the information about the JS-13.1 rotor, the relative centrifugal force (rcf or g) values across our 50 mL tube were calculated. By using the rcf equation below for the JS-13.1 rotor at varying speeds (1,000 – 13,000 rpm), a table giving an approximation of the g-force across the tube at various speeds was compiled (Note: *r* at max is 140mm)

$$\mathrm{RCF} = 1.118 \times 10^{-6} \times r \text{ (in mm)} \times (\mathrm{rpm})^2$$

As shown in Table 3.5, the location of the cells within the gradient relates to the amount of g-force they initially and ultimately experience. Therefore, the total volume affects the height of loading, which affects the initial rcf and potentially enucleation efficiency. Cells loaded onto a lower volume gradient will see higher g-force levels sooner than similarly designed gradients with lower volume layers. Also, according to stokes law, the viscosity of the fluid, Ficoll in this instance, affects the rate at which cells move through the gradient, ultimately effecting enucleation efficiency.

Recognizing from past runs that very few cells surpass the 20% mark within the Ficoll gradients previously tested, this new gradient was designed with layers from 3% Ficoll

down to 20% Ficoll. Layers within the gradient were spaced 1-2% apart across the whole of the gradient, with the 20% base layer to collect everything except the fastest moving, most dense particles, assumed to primarily be karyoplasts, which should reside in the pellet. With more interfaces and a wider range of Ficoll densities, the goal was to tweeze out the specific Ficoll densities in which cytoplasts, karyoplasts, and whole cells preferred to reside, with the assumption that the varying densities between these three different types of events or entities are different enough to separate on density alone.

In addition to changes in the gradient, the number of NT2 cells loaded was lowered from 20 million to 10 million per gradient in an effort to increase the efficiency by decreasing cell clumping, as observed in previous runs. Lower cell numbers should result in better stability of the layers as fewer cells break the layer interfaces as they move through the gradient, potentially providing more uniform levels of shear to all cells.

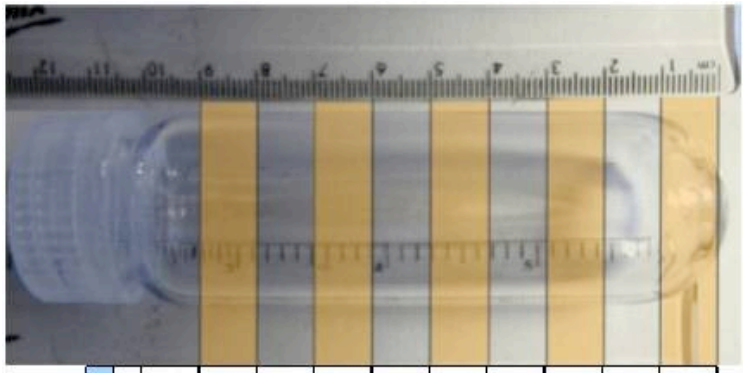

POWER GRADIENT

G-FORCE	RPM												
1000	2000	3000	4000	5000	6000	7000	8000	9000	10000	11000	12000	13000
73	294	663	1179	1841	2651	3609	4713	5965	7364	8911	10605	12445
82	331	746	1326	2072	2984	4062	5304	6713	8288	10029	11935	14007
92	368	829	1474	2303	3316	4514	5896	7462	9212	11147	13266	15568
101	405	912	1622	2534	3649	4967	6487	8210	10136	12265	14596	17130
110	442	995	1770	2765	3982	5420	7078	8959	11060	13383	15927	18692
120	479	1078	1918	2996	4314	5872	7670	9707	11984	14501	17257	20253
129	516	1162	2066	3227	4647	6325	8261	10456	12908	15619	18588	21815
138	553	1245	2213	3458	4980	6778	8852	11204	13832	16737	19918	23377
148	590	1328	2361	3689	5312	7230	9444	11953	14756	17855	21249	24938
157	627	1411	2509	3920	5645	7683	10035	12701	15680	18973	22579	26500

Table 3.5: Power Gradient
This table shows the approximate rcf (g) that cells are subjected to at various gradient depths and centrifugation speeds (rpm).

3.2.5 Effect of Speed on Enucleation Efficiency

After implementing the changes discussed in the previous section, a range of centrifuge speeds was tested with the goal of optimising for the best enucleation conditions. Five conditions were tested in triplicate at 5,000, 7,000, 9,000, 11,000, and 13,000 rpm.

5 Runs on 3-20% Gradient (5,000 rpm – 13,000 rpm)

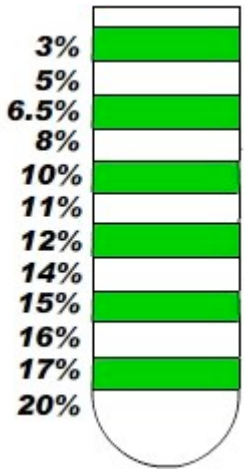

Layer Composition
3 mL 3% Ficoll in PBS + Cyto D + Cells
2 mL 5% Ficoll in PBS + Cyto D
2 mL 7% Ficoll in PBS + Cyto D
2 mL 8% Ficoll in PBS + Cyto D
2 mL 10% Ficoll in PBS + Cyto D
2 mL 11% Ficoll in PBS + Cyto D
2 mL 12% Ficoll in PBS + Cyto D
2 mL 14% Ficoll in PBS + Cyto D
2 mL 15% Ficoll in PBS + Cyto D
2 mL 16% Ficoll in PBS + Cyto D
2 mL 17% Ficoll in PBS + Cyto D
5 mL 20% Ficoll in PBS + Cyto D

Parameter	Setting
Speed	5,000 rpm (3,913 g) to 13,000 rpm (26,500 g)
Run Time	60 minutes
Temp	31^{o}C
Accel	1
Decel	1
Cells	1x10^{7} NT2 cells P42

It was discovered from this set of runs that speeds between 7,000 rpm (9,587 g) and 13,000 rpm (26,500 g) resulted in distinct, visible layers of enucleation products while 5,000 rpm (4891 g) was not enough to move the cells through the gradient. Reliable quantification of enucleation efficiency is very difficult without Fluorescent Activated Cell Sorter (FACS) analysis after every enucleation run. However, due to limitations on the availability of the FACS, these initial development runs were quantified by eye. This was done by diluting the total gradient contents in PBS (-Mg, -Ca), then centrifuging the enucleation products down at 250 g and resuspending them in 5 mL fresh prewarmed medium, then counting the number of total events versus Hoechst 33342 positive events within four or more 1 mm x 1 mm haemocytometer fields (see

Materials and Methods, Figure 2.1 for an illustration) at 10x to get an idea of the efficiency of enucleation. An event was counted as any cell like or spherical entity that was at least half the diameter of a typical trypsinised NT2 cell, anything that was smaller or highly irregular was considered to be debris and was not included in the count. Most events could clearly be distinguished as a whole cell, a cytoplast (an enucleated cell consisting primarily of cytoplasm encapsulated by cell membrane), or a karyoplast (the nuclear by product of enucleation consisting primarily of a nucleus encapsulated by cell membrane).

It was found that 9,000 rpm was the best of the conditions tested. Also, by eye, cytoplasts visually appeared to get smaller with increased centrifugation speed. Interestingly, 9,000 rpm is equivalent to a RCF_{max} of ~12,700 g, the closest of the conditions tested to 14,500 g, the force determined to be best by Pralong *et al.* for the enucleation of mouse ES cells, the cells most similar to NT2 cells of cell types reported in enucleation publications (Pralong et al. 2005). See Figure 3.5 for quantification of cytoplasts detected following varied centrifuge speed.

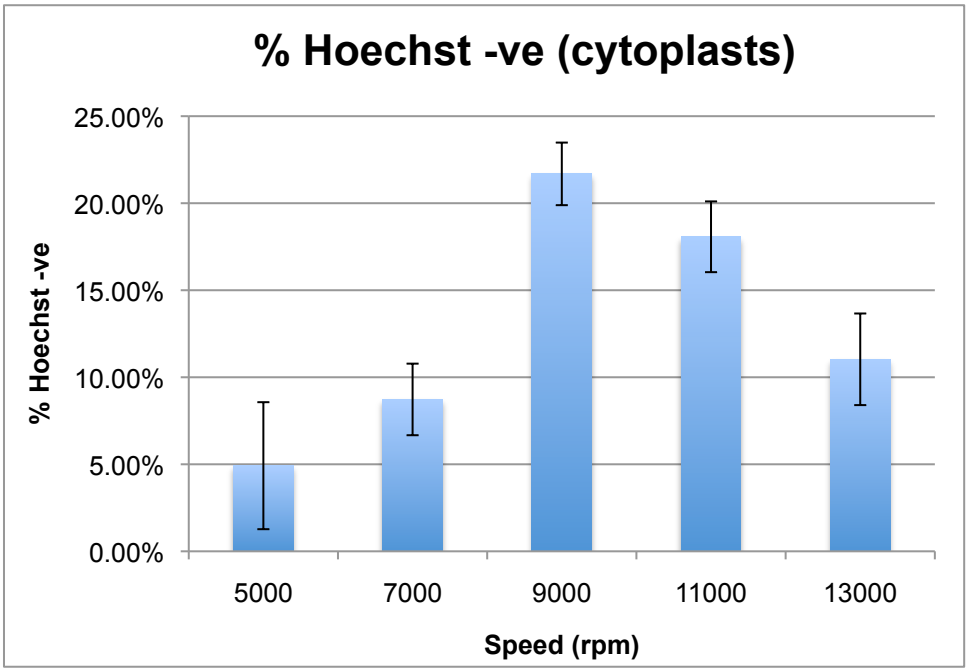

Figure 3.5: Percent of Hoechst negative events at varying centrifugation speed Using Hoechst 33342 staining and a Haemocytometer, estimations of the percentage of 'events' that appeared to by cytoplasts (roughly half the size of a whole cell with no detectable nuclear DNA) were made. As shown, 9,000 rpm (12,700 g) resulted in the highest percentage of cytoplasts detected by eye and correlated most closely to the forces reported by Pralong et al (2005) to successfully enucleate mouse ES cells. **Note:** Error bars represent the range from the 3 runs tested at each condtion (n = 3).

3.2.6 Effect of Centrifugation Time on Efficiency

After narrowing down the speed and therefore the level of g-force required to efficiently enucleate NT2 cells, we wanted to determine how much centrifugation time factored into the efficiency. Knowing that Ficoll is not the best medium for cells to be in for extended length of time, we aimed to reduce the time that the cells and enucleation products remained in the Ficoll. With this in mind, in addition to the 60 minute time suggested in previous enucleation publications, 15, 30, and 45 minute runs were also performed and then six samples were taken from each gradient.

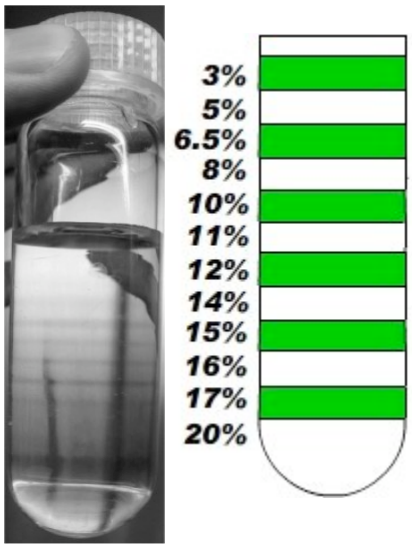

Layer Composition		
3 mL	3%	Ficoll in PBS + Cyto D + Cells
2 mL	5%	Ficoll in PBS + Cyto D
2 mL	6.5%	Ficoll in PBS + Cyto D
2 mL	8%	Ficoll in PBS + Cyto D
2 mL	10%	Ficoll in PBS + Cyto D
2 mL	11%	Ficoll in PBS + Cyto D
2 mL	12%	Ficoll in PBS + Cyto D
2 mL	14%	Ficoll in PBS + Cyto D
2 mL	15%	Ficoll in PBS + Cyto D
2 mL	16%	Ficoll in PBS + Cyto D
2 mL	17%	Ficoll in PBS + Cyto D
5 mL	20%	Ficoll in PBS + Cyto D

Parameter	Setting
Speed	9,000 rpm (12,700 g)
Run Time	15 - 60 minutes
Temp	31^{o}C
Accel	1
Decel	1
Cells	1x10^{7} NT2 cells P50

Six 1 mL samples were carefully taken at the following regions from top to bottom: 3-5%, 6.5-8%, 10-11%, 12-14%, 15-16%, and 17-20%. These six samples were then individually diluted and washed in PBS (-Mg, -Ca), as done previously, and then resuspended in fresh, pre-warmed medium containing 10 µg/mL Hoechst 33342 and left for 15 minutes. After 15 minutes incubation in Hoechst 33342, the layers were examined using a haemocytometer. Four 1 mm x 1 mm fields were counted under phase contrast and UV fluorescence and the number of Hoechst positive and negative events were tabulated, these results are shown in Figure 3.6. The number of cytoplasts

by location was estimated by counting the number of Hoechst negative events in four fields, dividing by four, multiplying by 10,000, and multiplying by the volume (in millilitres) sampled. From these estimates, an approximate efficiency of enucleation was calculated based on 100% enucleation being 10 million cytoplasts as each group consisted of a starting population of 10 million NT2 cells, this assumes that one cell is capable of producing, at most, one karyoplast and one cytoplast, although we cannot be certain that this is always true. However, events smaller than roughly half the size of a whole cell were not included as part of the count and were instead considered to be debris. It was clear from the results that a minimum centrifugation time of 30 minutes is needed. It appears that between 15 and 30 minutes of centrifugation, the majority of cytoplasts are generated and settle into the 12-16% region of the gradient. Contrary to the hypothesis, instead of clear separation of events into three uniform layers: whole cells, karyoplasts and cytoplasts, it appears that karyoplasts and cytoplasts of every size are produced and each different sized event settles into a different region of the gradient with only a few common regions enriched primarily with cytoplasts or karyoplasts (See Figure 3.6 and 3.7). It is unclear to what degree this variability can be effectively reduced, but even in the event that cytoplasts could be better isolated, the issue remains, if even <1% of the events collected for reprogramming include nuclei, this would potentially provide unwanted DNA and led to false positives following fusion. For this reason, it was decided that this semi-optimised protocol would be used to make cytoplasts, followed by sorting by fluorescence activated cell sorter (FACS) to stringently sort out cytoplasts based on size and Hoechst 33342 staining with the aim of eliminating contaminating whole cells and karyoplasts from the cytoplast enriched regions of isolated from the gradient.

From this analysis, 9,000 rpm for 30 minutes was settled upon as the best conditions for enucleation as this proved to be the shortest effective centrifugation time, subsequent experiments were performed using this set of process conditions as a baseline for further improvements.

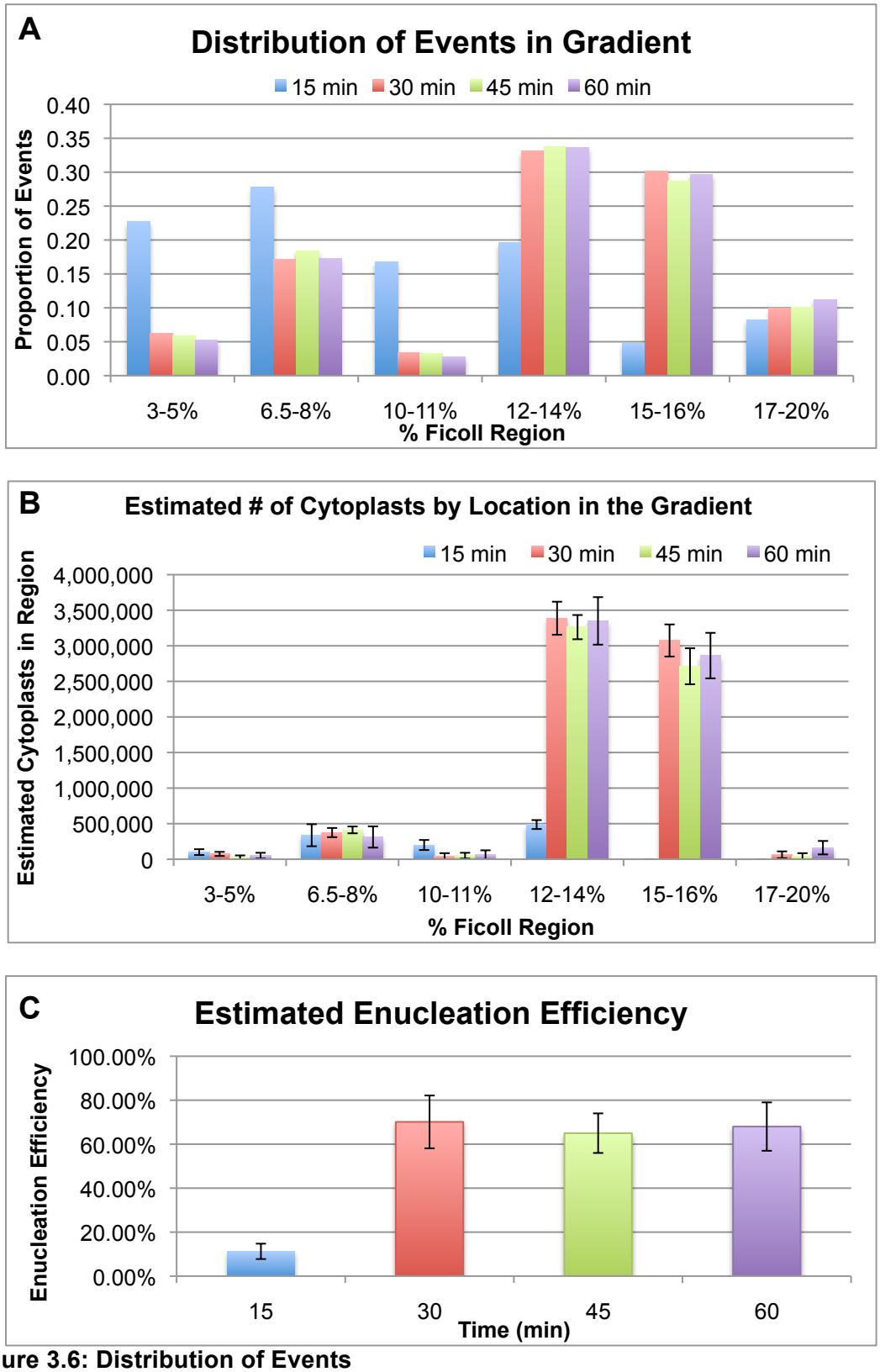

Figure 3.6: Distribution of Events
A) Mean distribution of events within the Ficoll gradient (sorted by Ficoll concentration) following enucleation at 9,000 rpm with varying centrifugation times; B) Estimated number of cytoplasts by gradient region as judged by Hoechst 33342 negative events in haemocytometer counts; C) Estimated enucleation efficiency at 9,000 rpm with varying centrifugation time. Based on these results, a minimum of 30 minutes is needed to achieve enucleation of 10^7 NT2 cells with most cytoplasts residing between 12 and 16% Ficoll. **Note:** n=4 and error bars represent standard deviation.

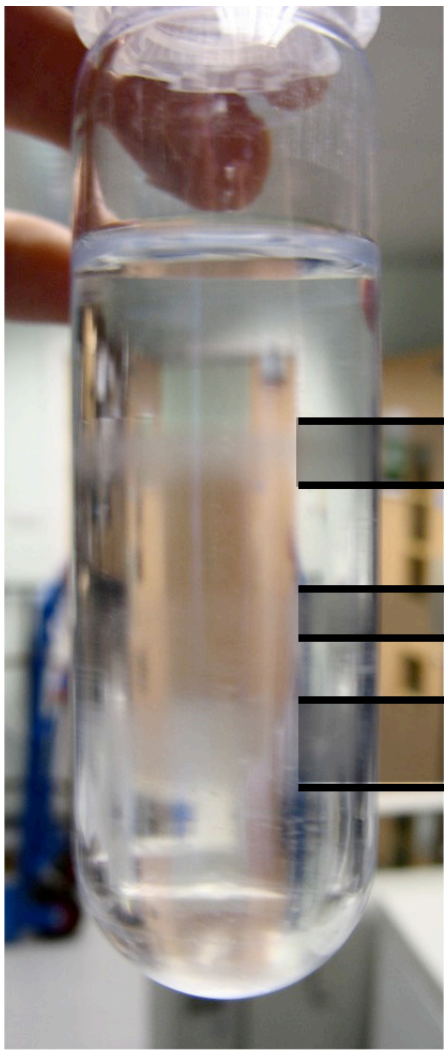

Figure 3.7: Post-Enucleation Photo of Layers
This is a photo of the 3-20% gradient just after the centrifugation step (9,000 rpm for 30 minutes, 10^7 NT2 cells). There are at least 3 visible layers and a relatively small cell pellet (shaded areas added to help visualise where the layers reside). The layers are representative of the regions enriched for different enucleation products. Despite optimisation, the clarity and purity of the products in each region is not 100% (i.e. each layer still contains a mixture enucleation products – karyoplasts, cytoplasts, and whole cells).

The mixing of enucleation products and difficulty in isolating just cytoplasts and just karyoplasts may be due to the fact that all the cells enucleated are not of uniform size or shape and therefore their enucleation products have varying properties. For instance, from microscopic analysis, there are karyoplasts with a very small bit of cell membrane around them and almost no cytoplasm, but then there are also some that appear to be small cells, karyoplasts that maintained about half of their cytoplasm. This means that while there are large cytoplasts that are roughly the size of a whole cell without a nucleus, there are also small cytoplasts containing about half the cytoplasm of a cell. A large cytoplast may therefore end up with the same density, and therefore in the same layer, as a karyoplast (see Figure 3.8). This may simply be a result of the composition of EC cells, which have been previously shown to contain a relatively high amount of high density components, such as glycogen (Damjanov et al. 1983).

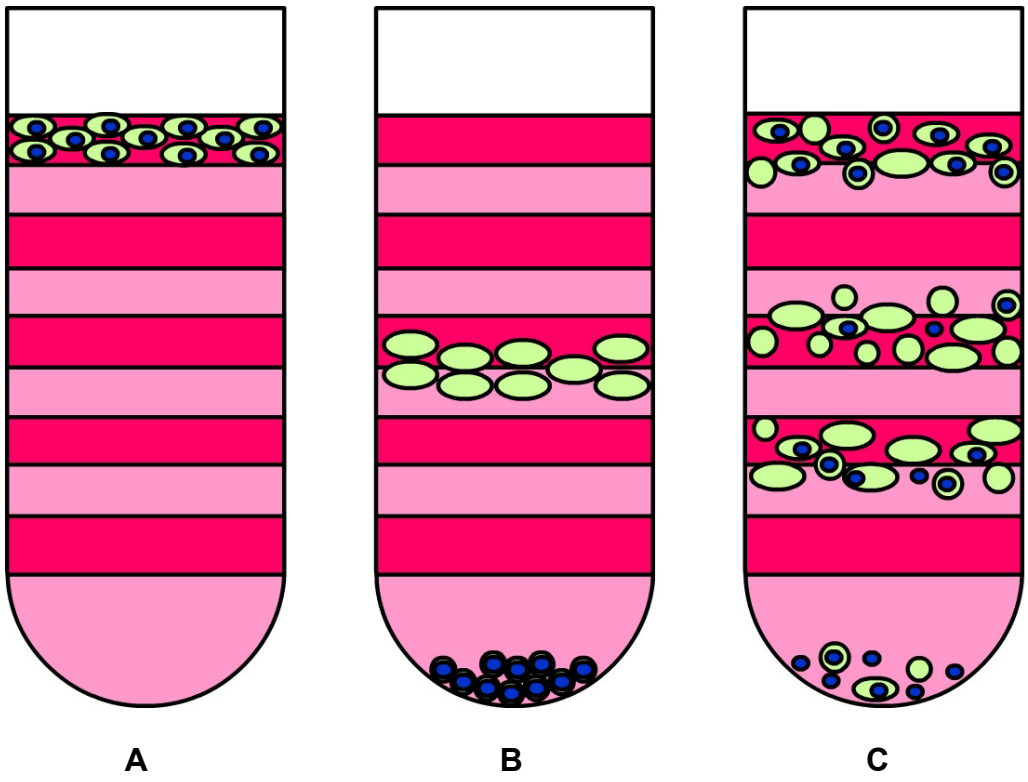

Figure 3.8: Enucleation Results – Expected vs Actual
A) Ficoll gradient loaded with cells. B) Predicted separation of whole cells into two distinct groupings of karyoplasts and cytoplasts. C) Actual results of semi-optimised enucleation procedure, many layers form, each layer tends to be enriched for particular enucleation products, however, no layer consists of only one enucleation product.

3.2.7 Detection of Cytoplasts Using FACS

After deciding upon baseline conditions, FACS analysis was implemented in an attempt to isolate a pure population of cytoplasts and learn more about the composition of the enucleation products generated. As shown in Figure 3.9, before each FACS run, 3 µm and 10 µm sizing beads were used to calibrate the machine, allowing for an estimate of the size of the enucleation products.

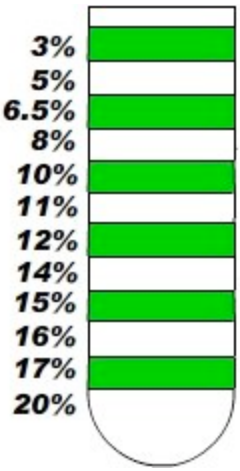

Layer Composition
3 mL 3% Ficoll in PBS + Cyto D + Cells
2 mL 5% Ficoll in PBS + Cyto D
2 mL 6.5% Ficoll in PBS + Cyto D
2 mL 8% Ficoll in PBS + Cyto D
2 mL 10% Ficoll in PBS + Cyto D
2 mL 11% Ficoll in PBS + Cyto D
2 mL 12% Ficoll in PBS + Cyto D
2 mL 14% Ficoll in PBS + Cyto D
2 mL 15% Ficoll in PBS + Cyto D
2 mL 16% Ficoll in PBS + Cyto D
2 mL 17% Ficoll in PBS + Cyto D
5 mL 20% Ficoll in PBS + Cyto D

Parameter	Setting
Speed	9,000 rpm (12,700 g)
Run Time	30 minutes
Temp	31^{o}C
Accel	1
Decel	1
Cells	1x10^{7} NT2 cells P53

The conditions shown above were used and the total contents of the gradient were diluted and washed in PBS three times, then stained in DMEM + 10% FBS with Hoechst 33342 for 15 minutes prior to running them through the MoFlow FACS [Beckman Coulter]. Before running enucleation products, sizing beads were used to calibrate the FACS (see Figure 3.9). Untreated NT2 cells were run first as a control, followed by NT2 cells enucleated as described above. FACS plots generated indicate that over 80% of the enucleation products generated have a 10-fold lower level of Hoechst 33342 compared to the control (see Figure 3.10 and see section 2.6 for explanation of how to read FACS graphs). The 10-fold lower levels most likely indicate that cells have been enucleated, but a low level of Hoechst has been activated by

mitochondria and possibly weakly by RNA. For clarity, Figure 3.11 shows an overlay of the Hoechst 33342 readouts of the control compared to the enucleated sample.

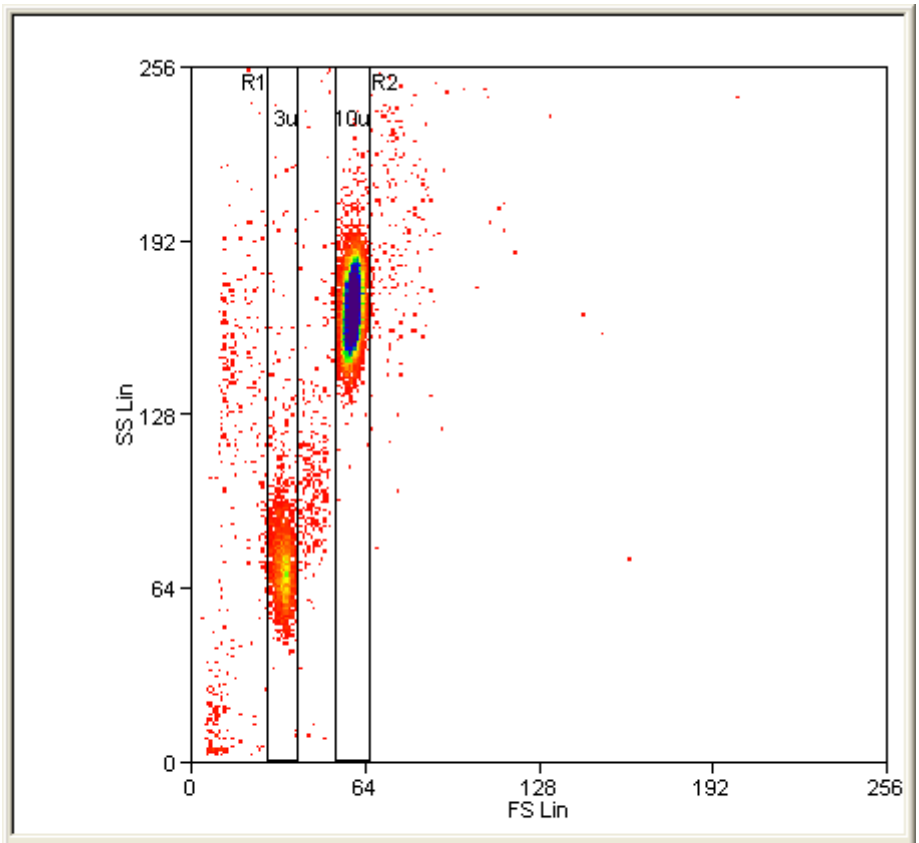

Region	% Hist	Median	Bounds
Total	100.00	59.00, 164.00	(0.00,255.00) (255.00,0.00)
R1	13.30	34.00, 71.00	(28.00,255.00) (40.00,0.00)
R2	82.33	59.00, 167.00	(53.00,255.00) (66.00,0.00)

Figure 3.9: FACS Sizing Beads
Before each FACS sorting run, 3µm and 10µm beads were put through the FACS in order to calibrate the machine and allow for approximation of the sizes of the events based on their forward scatter (FS Lin) read out.

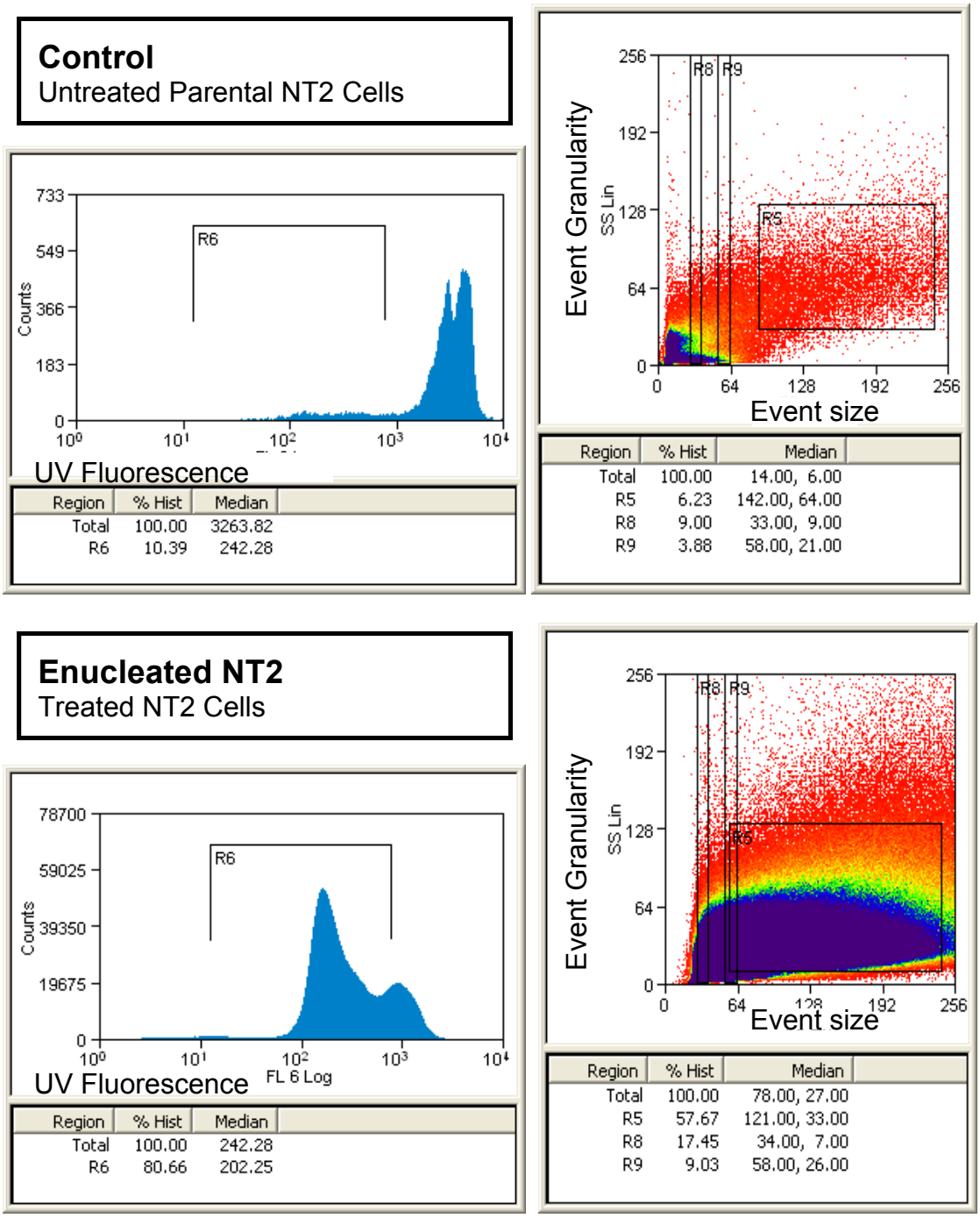

Figure 3.10: FACS – Control vs Enucleated NT2 cells
The sets of FACS plots above depict the relative level of Hoechst 33342 flourescence (FL 6 Log) on the left and the forward scatter (FS Lin - size) vs. side scatter (SS Lin - granularity) readouts on the right. The two vertical regions (R8 and R9) are representative of 3 µm and 10 µm, as checked using sizing beads prior to this analysis (Figure 3.9). As the graphs on the left clearly show, there is a downward shift in the general level of fluorescence per event post enucleation. The bimodal distribution of fluorescence in the parental sample (10^3-10^4) represents the cells in G1 and G2/M phase, while the bimodal distribution of the treated sample is indicative of enucleated cells (10^2-10^3) with the second small peak (~10^3) likely being representative of the karyoplasts and whole cells.

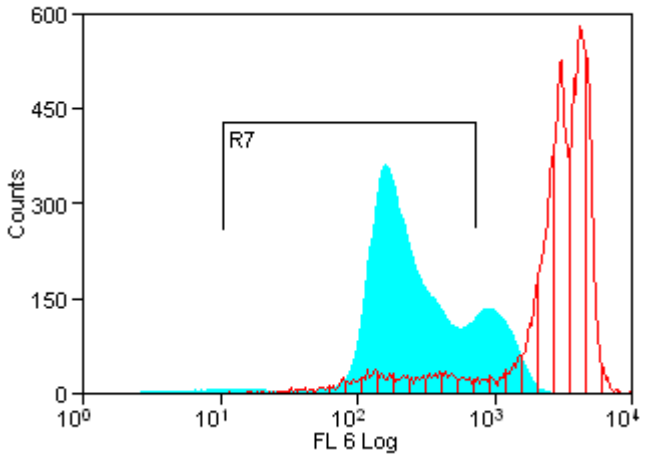

Figure 3.11: Overlay of Fluorescence graphs, NT2 vs Enucleated NT2
This figure shows the untreated NT2 control Hoechst 33342 readout (shaded with vertical lines) versus the enucleated sample's reading (solid). Enucleation has caused a significant increase in Hoechst negative samples (large solid peak), likely to be representative of our target cytoplast population. Also, notice the smaller peak at about 10^3, this population is likely to be representative of the karyoplast population. Due to an overall decrease in size and granularity, it appears that the average Hoechst readout per karyoplast is lower than the readout of a whole cell which owes some of its Hoechst signal to mitochondria and very weakly from RNA.

3.2.8 Isolation of cytoplasts using FACS

Following initial runs to calibrate the FACS and to get an idea of the properties of the events generated by centrifugal enucleation, individual sections of the gradient were carefully removed and analyzed.

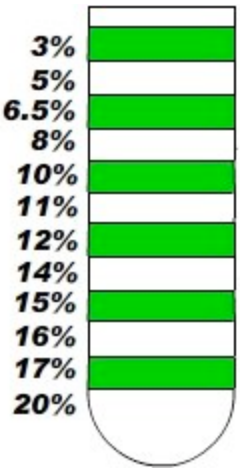

Layer Composition
3 mL 3% Ficoll in PBS + Cyto D + Cells
2 mL 5% Ficoll in PBS + Cyto D
2 mL 6.5% Ficoll in PBS + Cyto D
2 mL 8% Ficoll in PBS + Cyto D
2 mL 10% Ficoll in PBS + Cyto D
2 mL 11% Ficoll in PBS + Cyto D
2 mL 12% Ficoll in PBS + Cyto D
2 mL 14% Ficoll in PBS + Cyto D
2 mL 15% Ficoll in PBS + Cyto D
2 mL 16% Ficoll in PBS + Cyto D
2 mL 17% Ficoll in PBS + Cyto D
5 mL 20% Ficoll in PBS + Cyto D

Parameter	Setting
Speed	9,000 rpm (12,700 g)
Run Time	30 minutes
Temp	31^{o}C
Accel	1
Decel	1
Cells	1x10^{7} NT2 cells P55

The conditions shown above were used and the enucleation resulted in three visible layers (similar to Figure 3.7). The contents of the gradient were divided up into seven samples (taken carefully by pipette) and were taken from the following approximate locations within the gradient: 1) 3-5%, 2) 6.5%-8%, 3) 10-11%, 4) 12-14%, 5) 15-16%, 6) 17-20% 7) 20%+Pellet. The first six sample regions taken line up roughly with the same six sample regions taken as part of the centrifugation time analysis in section 3.2.6 with a seventh sample being taken at the base of the gradient that includes the pellet. Immediately after sampling, samples were diluted 5:1 in prewarmed (37^{o}C) PBS and mixed gently by inversion. Then samples were centrifuged at 250 rcf for three minutes, the supernatant was aspirated and the pellet was gently washed in 10 mL fresh medium, centrifuged down again and resuspended in 1 mL fresh medium with 10

µg/mL Hoechst 33342. Samples were incubated in Hoechst for 15 minutes before being put through the FACS for analysis.

The data shown in section 3.2.6 did not take into consideration the pellet, so it was added in this experiment. At the base of the tube we expected to find a population of events composed predominantly of karyoplasts since the nucleus is the major component of a karyoplast and has a higher density than other cell components. The FACS data below appears to strongly mirror the data obtained by eye, but unfortunately, cell clumps in the 3-5% region of the gradient caused blockages in the FACS machine and it was not possible to analyze that sample [sample 1]. It has also been noticed by direct observation that cell clumps congregate toward the top of the gradient and do not move through the layers in the same way as single cells.

The following set of figures (Figures 3.12 - 3.21) show the FACS graphs of the parental NT2 control group and the six sample groups that were analyzed without incident ([sample 2: 6.5-8%] – [sample 7: 20%+Pellet]). These samples represent the regions of the gradient described above and show much more clearly the spectrum of events that exist due to the fact that the FACS is able to tell the size, granularity, and level of fluorescence of each event in comparison to the parental cells. For ease, Hoechst 33342 positive events are shown in red while Hoechst 33342 negative events are in green.

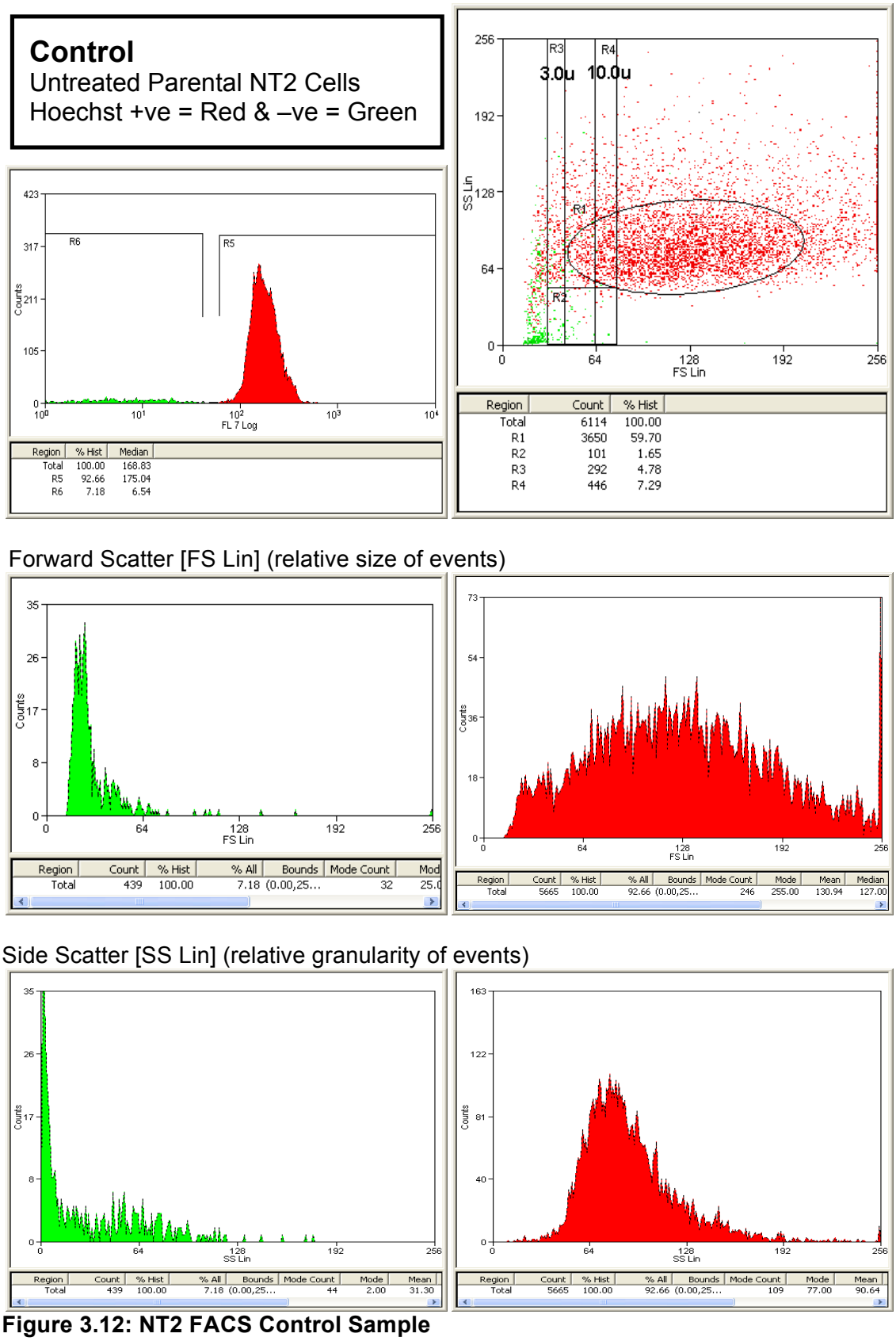

Figure 3.12: NT2 FACS Control Sample

Untreated, Hoechst 33342 stained NT2 cells typically appear as shown above. They are ~20 µm in diameter and clearly register as Hoechst 33342 positive (red events) with a fairly predictable level of granularity. The oval shaped gate was added to show where the average population of NT2 cells congregates; this was used as a point of comparison for subsequent samples. Each plot shows all events with Hoechst 33342 positive events in red and negative in green.

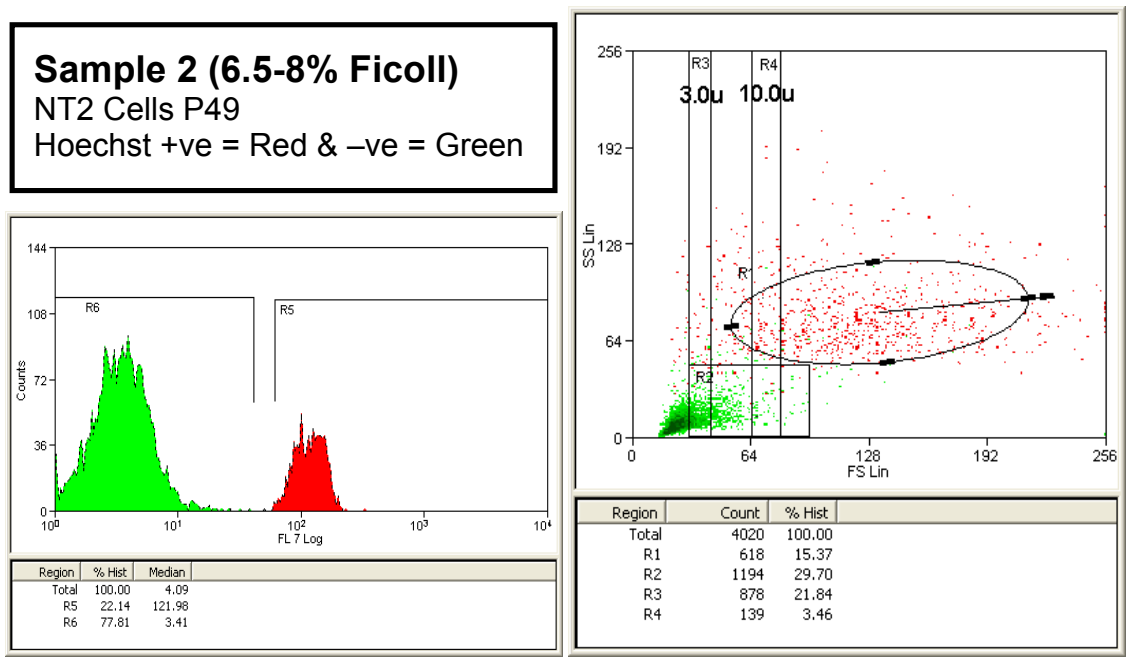

Forward Scatter [FS Lin] (relative size of events)

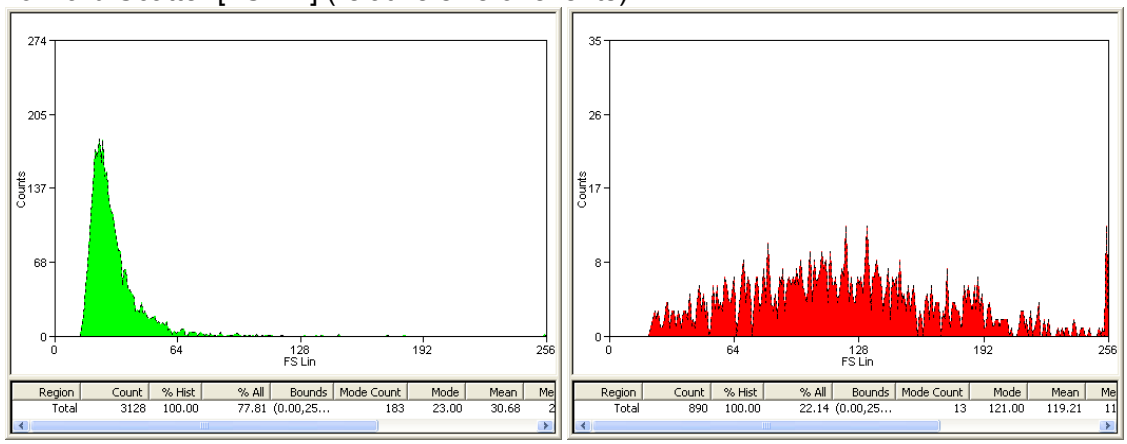

Side Scatter [SS Lin] (relative granularity of events)

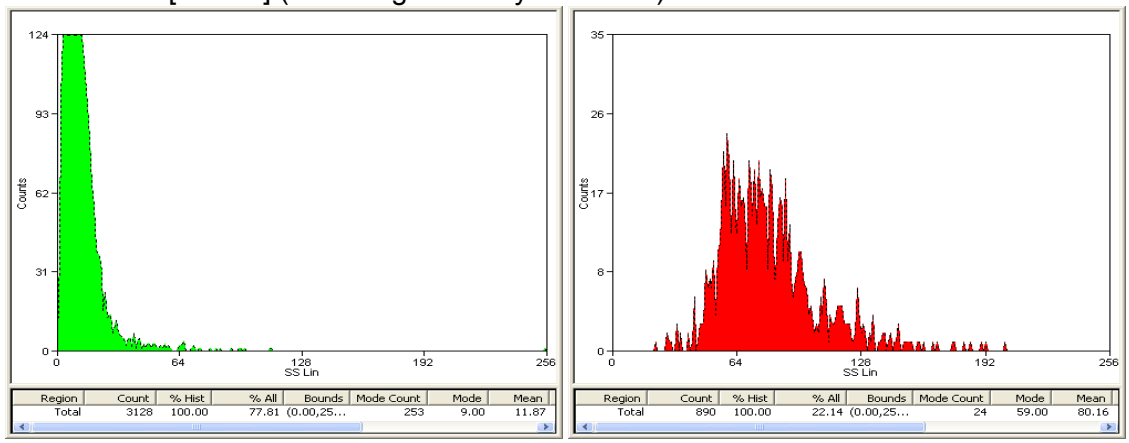

Figure 3.13: Enucleated Sample from 6.5-8% Ficoll Region

The small rectangular gate labelled ‘R2’ represents the predicted region where we estimated that cytoplasts would appear. Upon running the sample from the 6.5-8% Ficoll region, it was clear that there were a lot more Hoechst negative events than the control. Also, as seen in the gated graph, these green (Hoechst –ve) events are smaller and less granular than the control cells, and appeared in the predicted ‘R2’ region of the graph. We choose to sort out the green events in this R2 population, see Figure 3.14 for a phase contrast image of the sorted population.

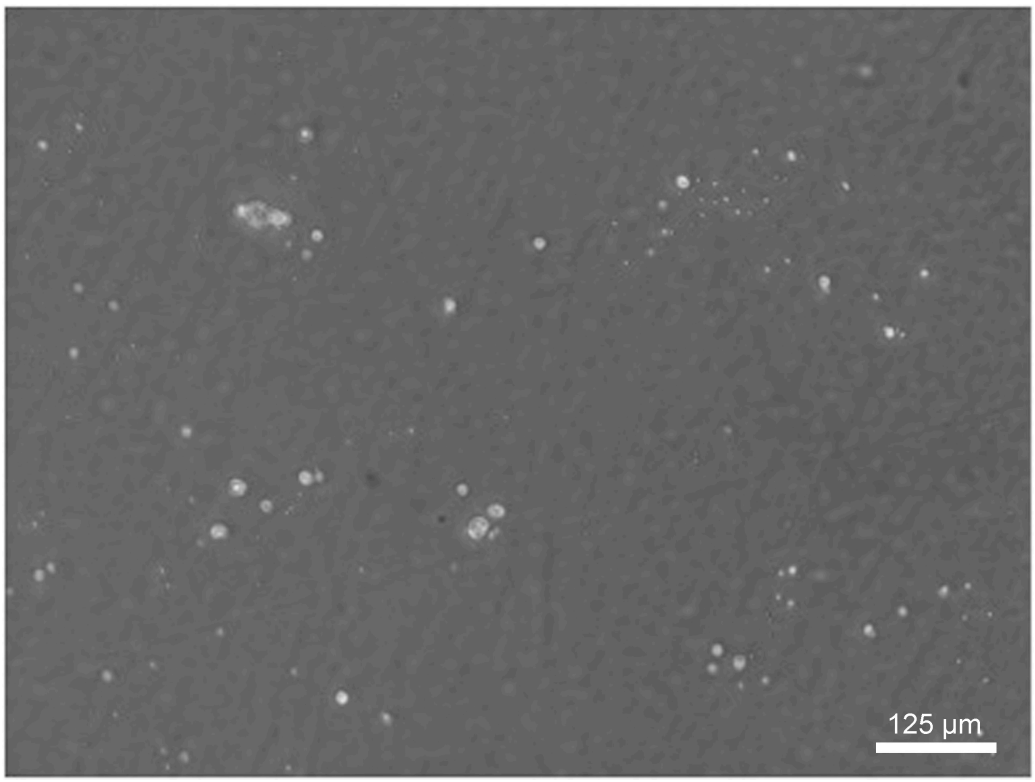

Figure 3.14: Hoechst Negative Events Isolated from Sample 2
This phase contrast photo, at 10x magnification, shows some of the events isolated by FACS from Sample 2. These results were sorted based on the fact that they were Hoechst 33342 negative (therefore devoid of nuclear DNA) and resided in the small rectangular "R2 gate" as shown in the main FACS plot (see Figure 3.13 – top right). These events are indeed Hoechst negative and appear to be just cytosol wrapped in a small proportion of cell membrane as expected, but due to their small cytoplasm to membrane ratio, each individual cytoplast has only a fraction of the total cytoplasm of a whole cell. Not knowing how much cytoplasm is needed to reprogram, it was assumed that it would take at least one cell's worth; therefore many small cytoplasts like those shown here would likely be needed. However, we speculated that the partition captured by sorting out events from the R2 gate was not where the largest cytoplasts reside, therefore further analysis of the other gradient regions was carried out.

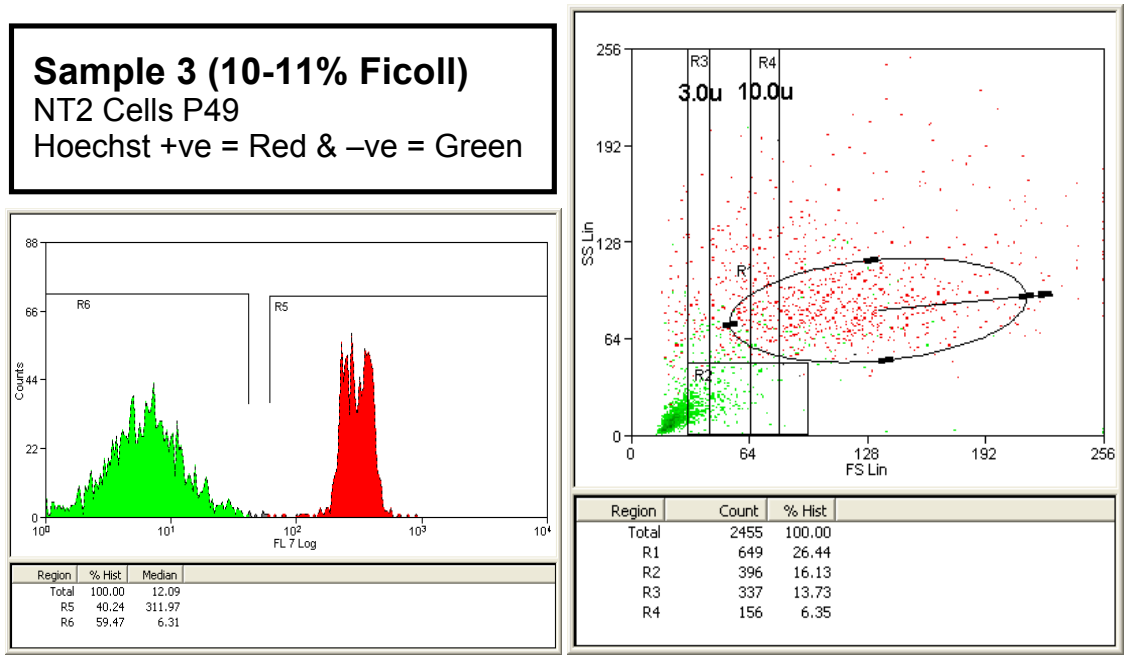

Forward Scatter [FS Lin] (relative size of events)

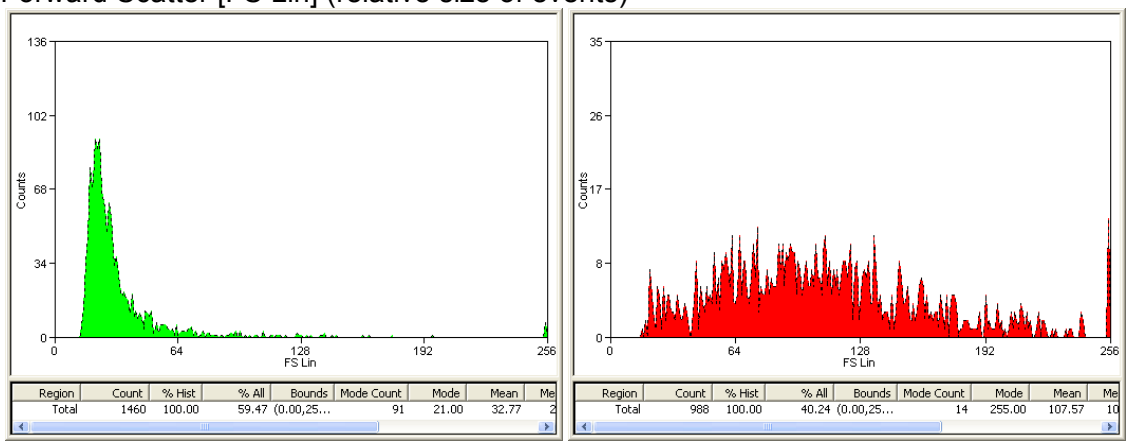

Side Scatter [SS Lin] (relative granularity of events)

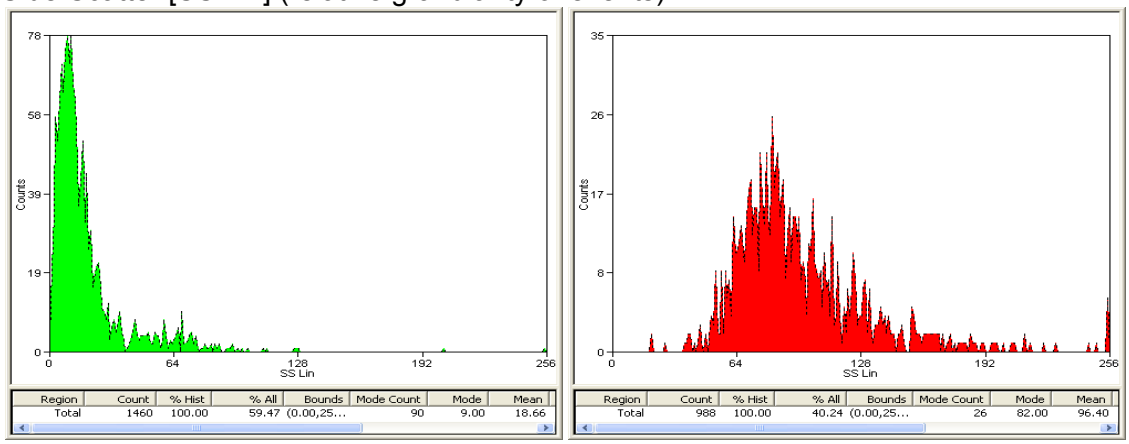

Figure 3.15: Enucleated Sample from 10-11% Ficoll Region

As seen in the previous experiment by eye, the 10-11% Ficoll region contained few events (see section 3.2.6), however, there does appear to be a slightly noticeable shift downward in the size of the Hoechst positive (red) events. It might be that these events are the counterparts of the small cytoplasts recorded in Sample 2, instead of splitting into large cytoplasts and karyoplasts consisting primarily of just a nucleus, it may be that they split into small cytoplasts and small cells/karyoplasts.

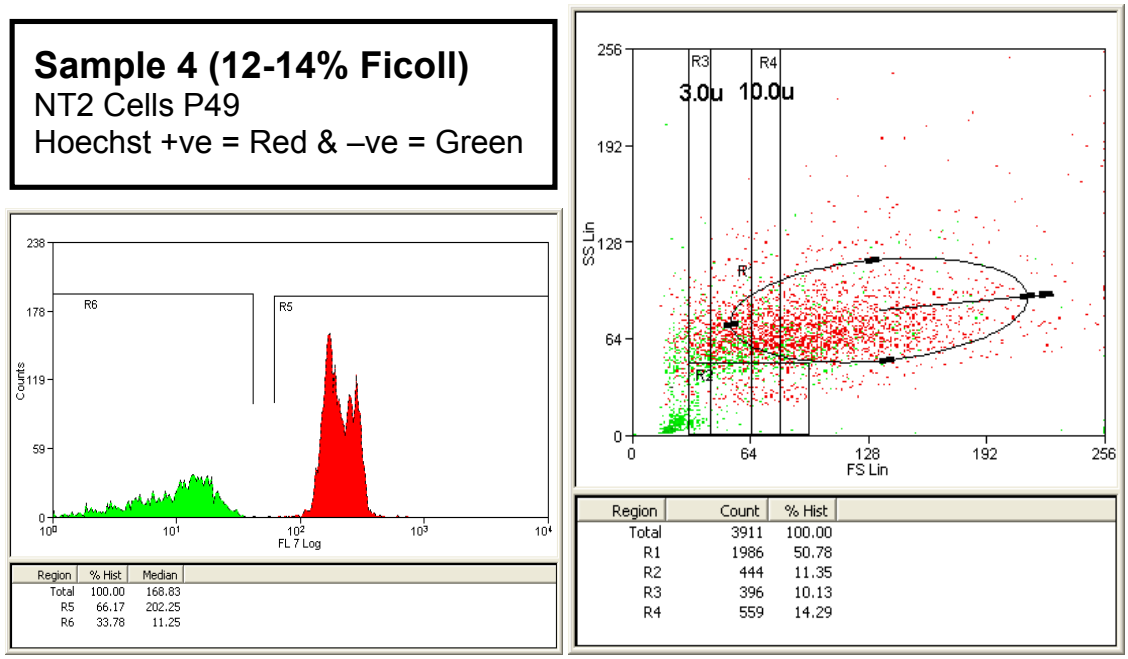

Forward Scatter [FS Lin] (relative size of events)

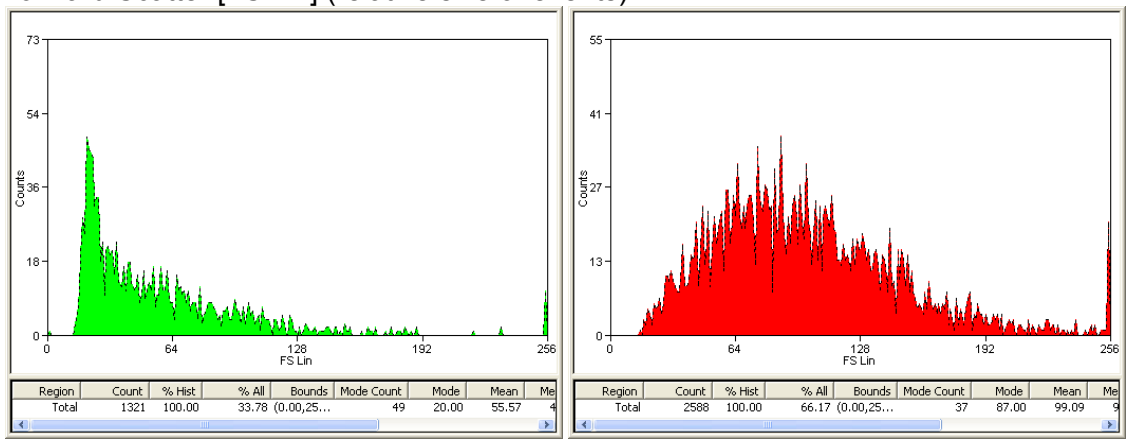

Side Scatter [SS Lin] (relative granularity of events)

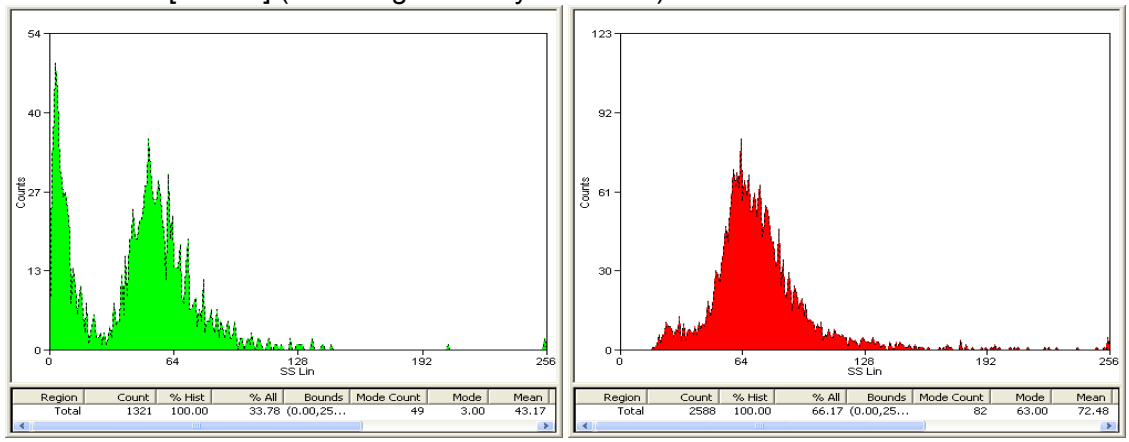

Figure 3.16: Enucleated Sample from 12-14% Ficoll Region

Green events have shifted both up and to the right in the main FACS plot, indicating that the events are larger and more granular. This indicates that cytoplasts are larger than those sorted from Sample 2 and the increased granularity (y-axis) can be attributed to the cytoplasts containing other cellular components such as mitochondria. Notice that the side scatter graphs show a new peak in the Hoechst negative events. Compared to the control, the shift in the red events is both down and to the left, indicating a decrease in size and granularity due to whole cells becoming karyoplasts.

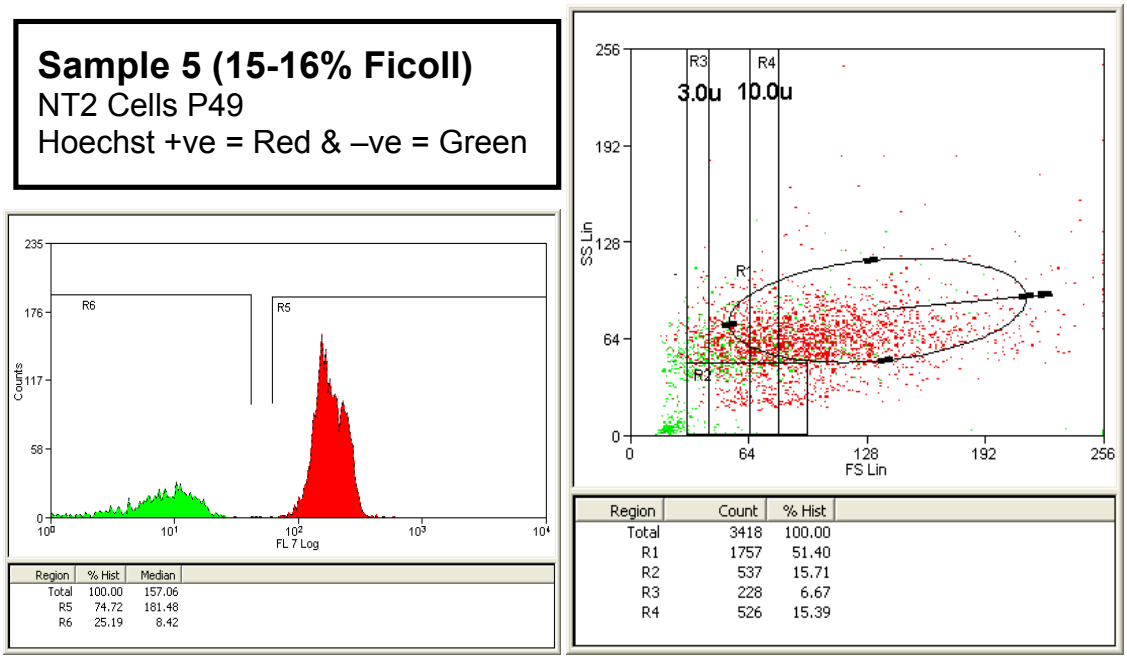

Forward Scatter [FS Lin] (relative size of events)

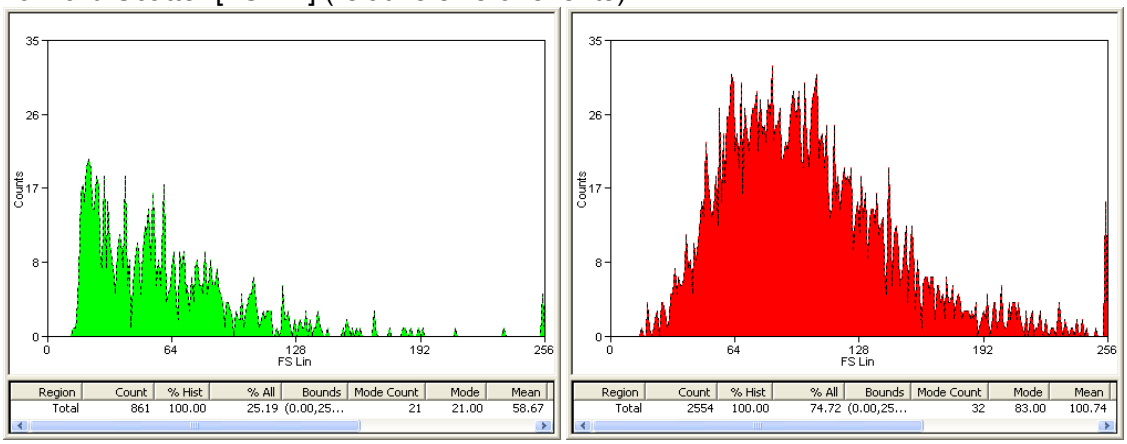

Side Scatter [SS Lin] (relative granularity of events)

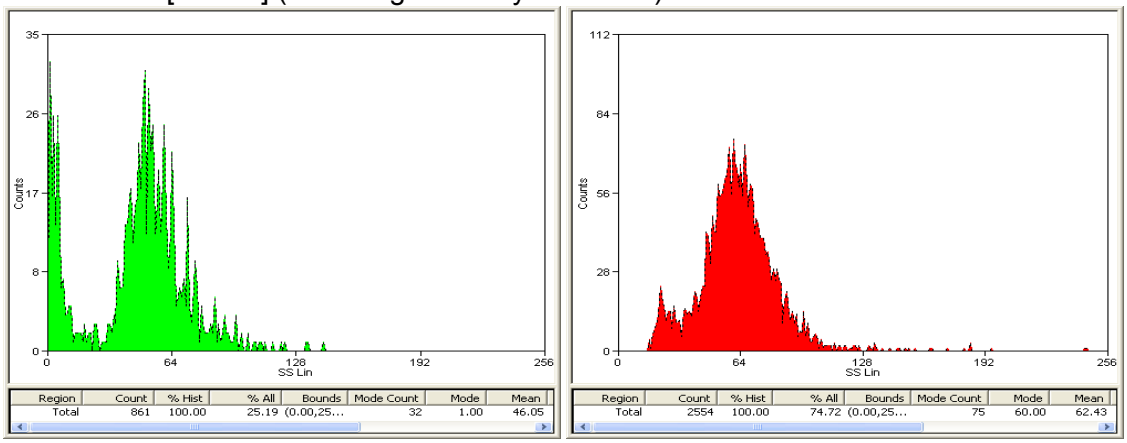

Figure 3.17: Enucleated Sample from 15-16% Ficoll Region

Similar to Sample 4, there is a noticeable increase in size and granularity in the Hoechst negative population compared to the control and earlier samples. There is also a corresponding decrease in size and granularity of the Hoechst positive events indicating that a significant proportion of cells have become karyoplasts.

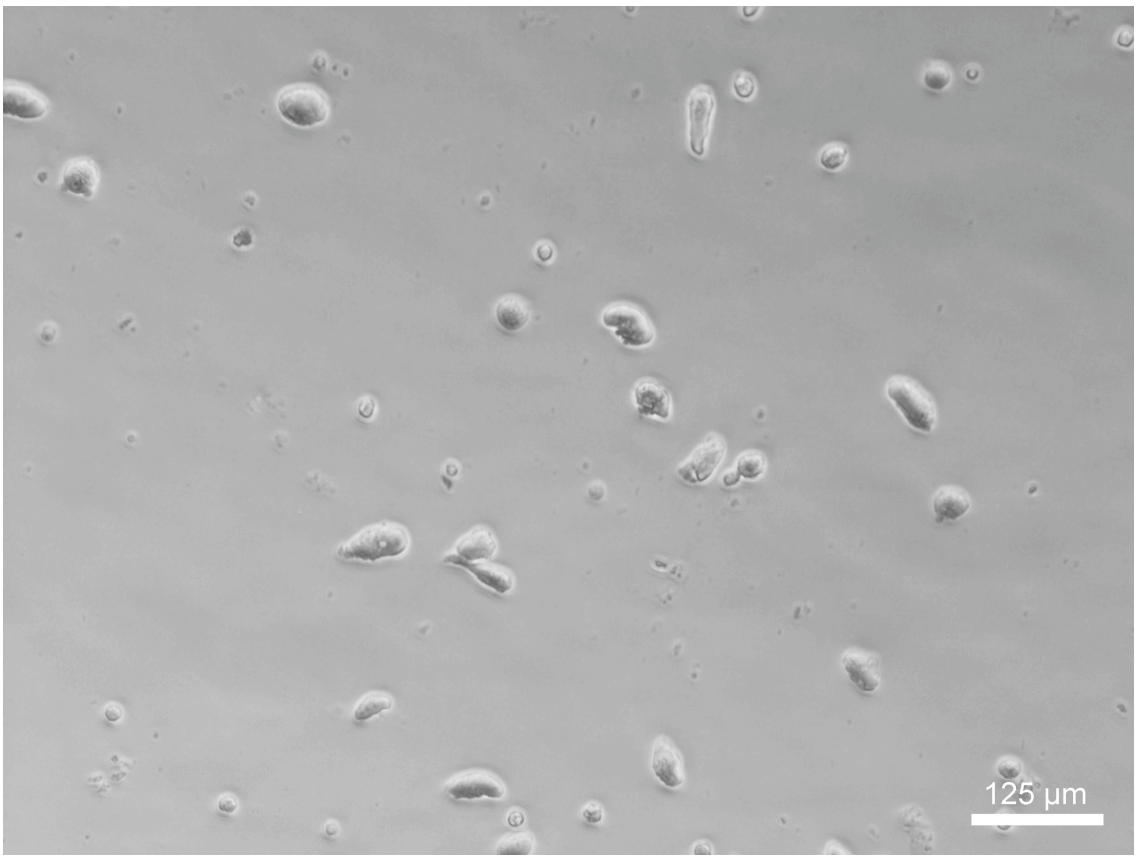

Figure 3.18: Phase contrast image of FACS sorted NT2 cytoplasts
Typical 10x phase contrast image of NT2 cytoplasts from the 12-16% region of the Ficoll gradient. Notice that these enucleated events are much larger than those isolated from Sample 2 (6.5-8% Ficoll), see Figure 3.14. Notice, unlike whole cells, cytoplasts do not show processes or typical cell spreading, but do attach to the culture flask.

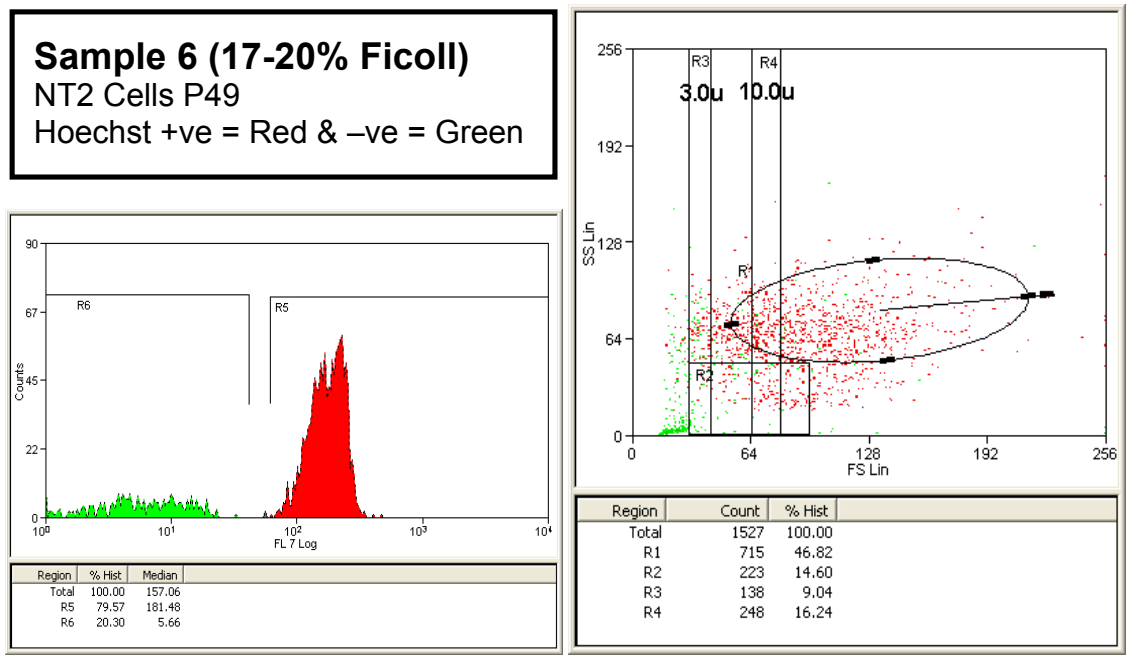

Forward Scatter [FS Lin] (relative size of events)

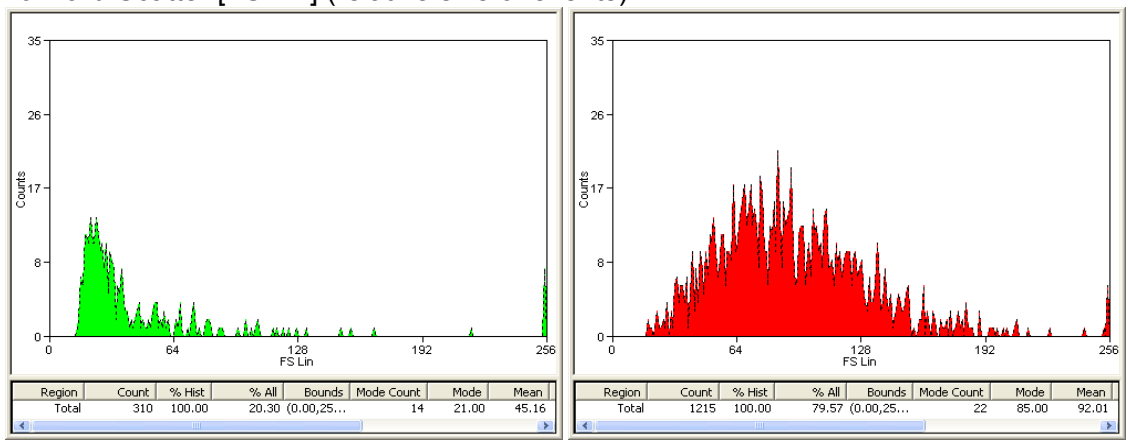

Side Scatter [SS Lin] (relative granularity of events)

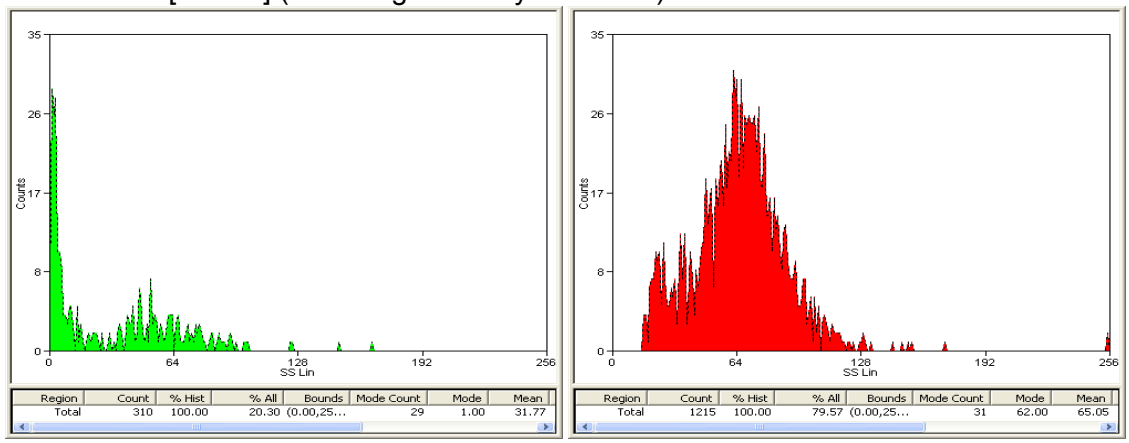

Figure 3.19: Enucleated Sample from 17-20% Ficoll Region
Sample 6 still contains some cytoplasts and karyoplasts, but for the most part, cytoplasts appear to have remained in the 12-16% region of the gradient, as seen by the decrease in the green forward and side scatter graphs. This layer at the base of the tube appears to be primarily karyoplasts with the red forward and side scatter graphs showing lower granularity, relatively smaller events which fits with the hypothesis that the heavier, dense nuclei go furthest through the gradient.

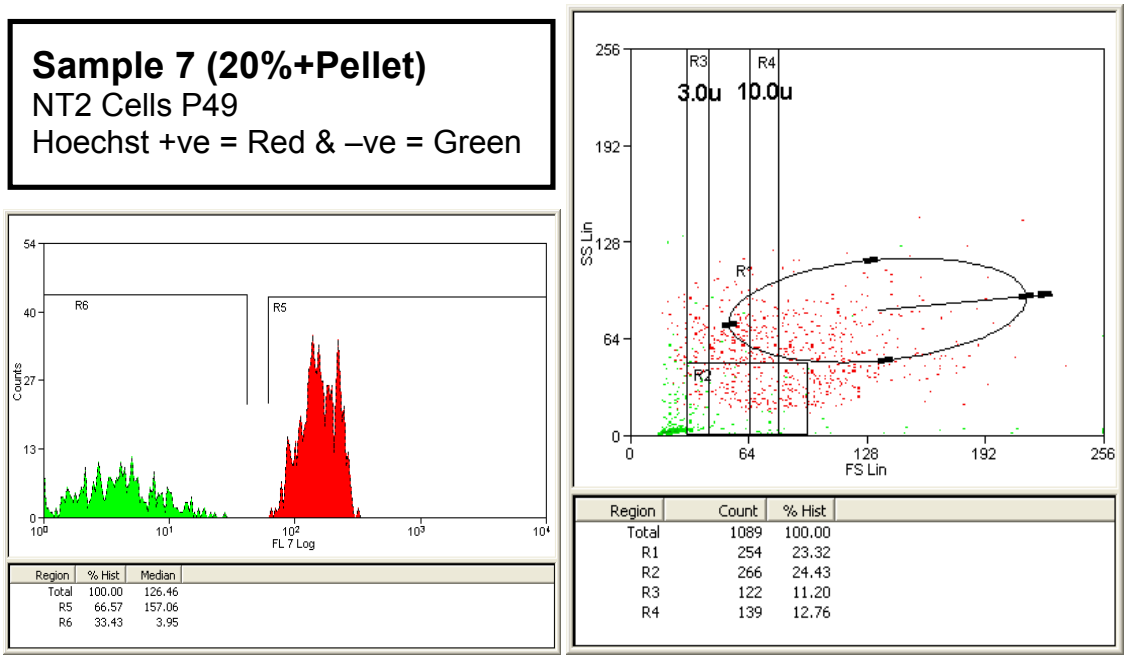

Forward Scatter [FS Lin] (relative size of events)

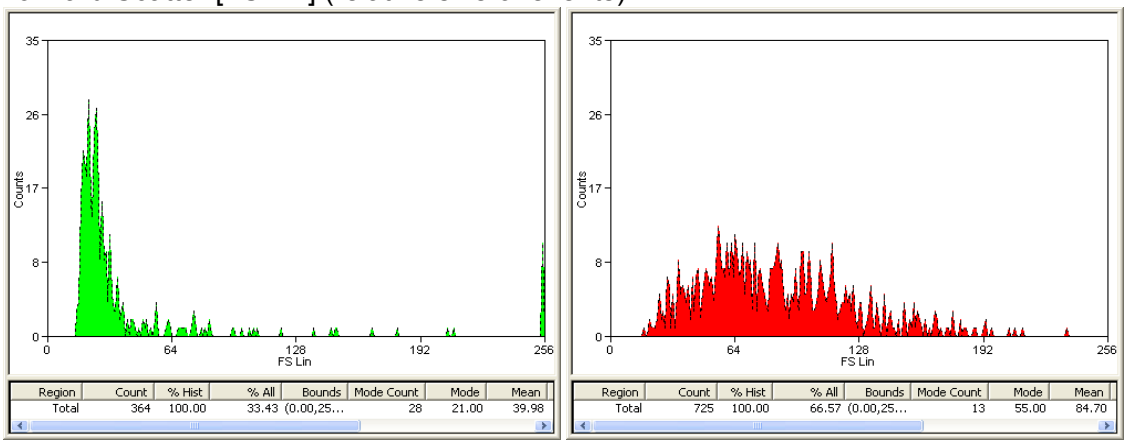

Side Scatter [SS Lin] (relative granularity of events)

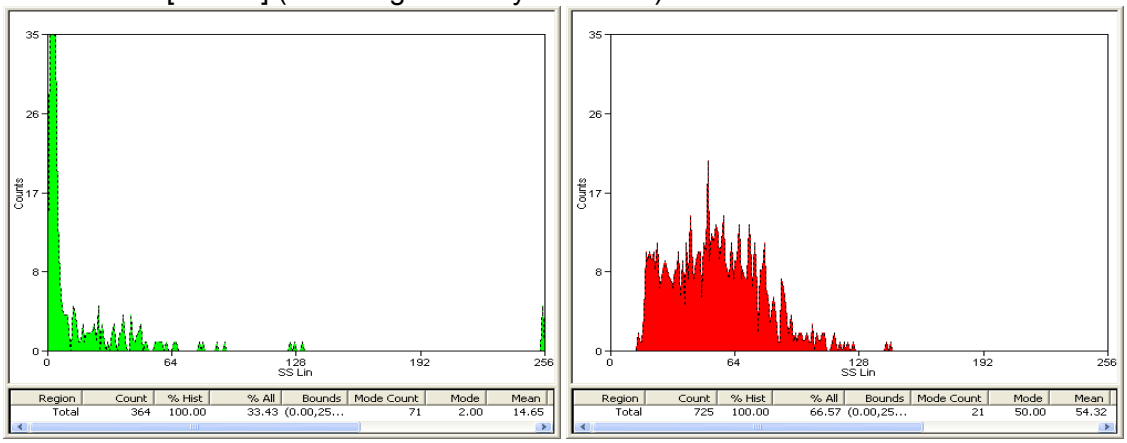

Figure 3.20: Enucleated Sample from 20%-Pellet Ficoll Region
The Hoechst negative (green) forward and side scatter graphs look very similar to the control, indicating that there are very few cytoplasts in the pellet. However, the Hoechst positive events are clearly much smaller and less granular, it is likely that this sample represents our purest population of karyoplasts, events consisting of little more than a nucleus encased in cell membrane. These results also match visual observations of the pellet (see Figure 3.21 below).

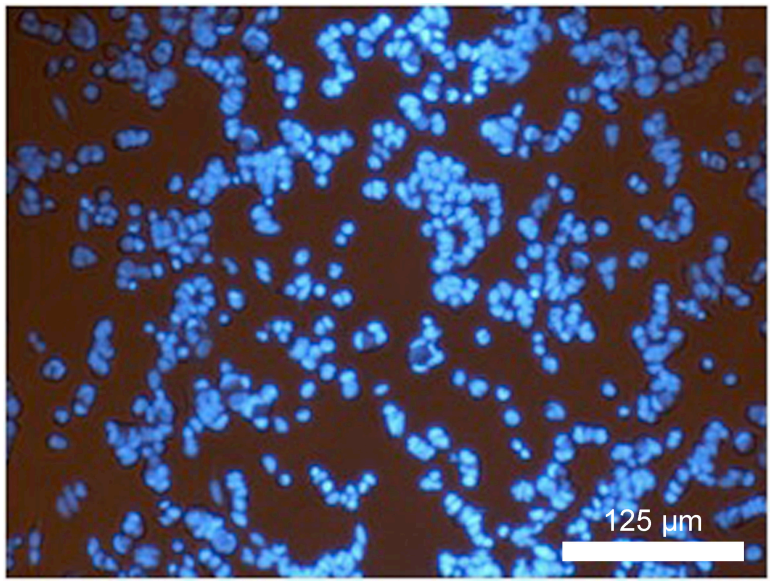

Phase Contrast + UV

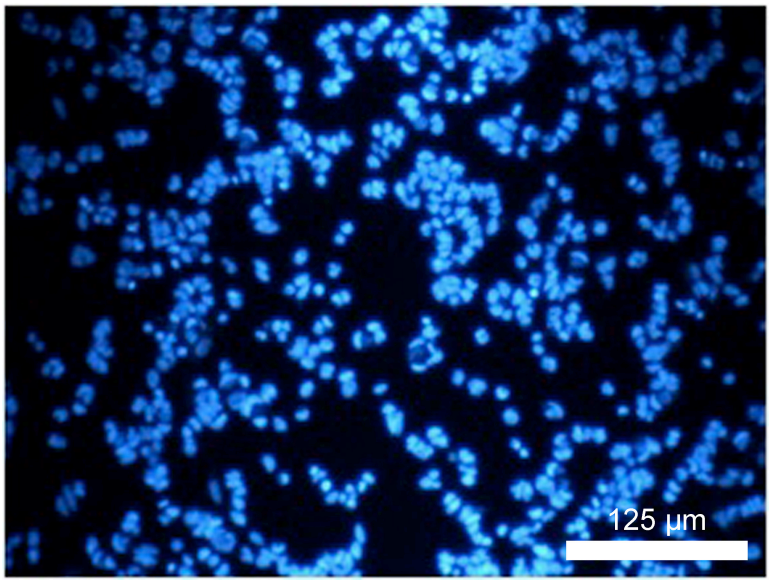

UV Flourescence

Figure 3.21: Karyoplasts and Hoechst positive events removed by FACS
Karyoplasts isolated as the unwanted fraction from a FACS sort of enucleated NT2 cells treated with Hoechst 33342. As expected, the majority of the events here are karyoplasts with simply a nucleus surrounded by a thin layer of cell membrane and very little if any cytoplasm or other cell components.

After FACS analysis, it was found that the 12-16% region of the gradient contained the most Hoechst 33342 negative events and also, very importantly, these events were generally larger than debris, suggesting that they are the population of cytoplasts we want. Multiple FACS runs confirmed this, however, there were still detectable events in nearly every partition that resembled karyoplasts or whole cells and in the interest of preventing contamination with NT2 nuclei, FACS sorting was performed using very stringent conditions. However, although using stringent conditions for isolating cytoplasts gave over 95% purity, the actual yield of cytoplasts was dramatically lower than what we detected in earlier experiments by eye. This could be due to the fragile cytoplasts breaking open as they move through the FACS machine, it could be due to the fact that seemingly Hoechst negative events by eye are counted as positive by the much more sensitive FACS equipment, or some other unaccounted for issue. Whatever the reason, it was found that 10 million NT2 cells would never produce anywhere near 10 million isolated cytoplasts using this process; in fact, some runs had a cytoplast yield of less than 10% (<1 million cytoplasts from 10 million NT2).

3.2.9 Improving Cytoplast Lifespan

After successfully sorting out the majority of cytoplasts with FACS and plating them out into flasks, they did not last long in normal culture conditions. Within 48 hours, cytoplasts sank, stuck to the bottom of the dish (but remained spherical, not spreading out like cells), then eventually shrivelled up or degraded entirely into what appeared to be cell debris. Even with multiple wash steps and increased serum concentration, isolated cytoplasts had a very short shelf life under culture conditions. The assumption was made that the cells may suffer from a low tolerance to Ficoll and that balancing the salts and pH within the gradient to more closely match culture conditions might improve cell, and therefore cytoplast, health. In order to achieve this, Hanks Buffered Salts Solution (HBSS) with bicarbonate was mixed with the PBS when making Ficoll. The bicarbonate allows proper pH buffering without the need for incubator supplied CO_2

which is not present during centrifugation. See Table 2.6 for the revised Ficoll formulation.

3.2.10 Effect of Ficoll on Cell Health

To test the effect of Ficoll on NT2 cell health and whether or not the addition of HBSS results in an improvement, three groups were tested in triplicate, in six well plates. Each group was exposed to Ficoll mixed with PBS alone (as done in previous experiments) and with the revised formulation including the addition of 10x HBSS (to a final concentration of 1x HBSS) for a set period of time at normal culture conditions (37^{o}C, 10% CO_2 in a humidified incubator). Then, after the given length of treatment time, the cells were carefully washed three times with PBS to remove the Ficoll, and then given fresh medium (DMEM +10% FBS) and a day to recover before assessing their viability. Viability was estimated by simply counting the cells before seeding them and again 24 hours after the removal of Ficoll and dividing the number of live attached cells at 24 hours post treatment by the pre-treatment (seed) cell count; this assumes that cells that attach are live, viable cells.

Ficoll led to a surprising amount of cell death with many cells found floating dead in the medium 24 hours after removal of the Ficoll. It may be that the Ficoll was not completely washed away by three PBS washes, but it appears that the HBSS had a marked affect on cell health.

Table 3.6: HBSS improves cell recovery following Ficoll treatment

Time	Ficoll + PBS	Ficoll + PBS + HBSS
1 hr	45% attached	80% attached
3 hrs	11% attached	78% attached
24 hrs	<1% attached	<1% attached

Results of cell viability based on attachment after Ficoll exposure. From this simple experiment, it was determined that the addition of HBSS would be made to all future formulations in an effort to help improve cell (and cytoplast) health.

3.2.11 Fusion & Isolation Protocol for Reprogramming

Having settled upon a satisfactory process for producing cytoplasts from NT2 cells, fusion methods that could be used to fuse cytoplasts to somatic cells and each other were tested. Various conditions were tested with the aim to find the right proportion of cytoplasts to somatic cells to result in reprogramming toward a pluripotent state.

First and foremost, the goal was to try to reproduce previous results, showing that NT2+somatic cell hybrids can result in reprogramming (Flasza et al. 2003), but through formulating a process for fusion it was realized that isolation of properly fused events also needed to be taken into consideration. To achieve isolation of reprogrammed cells, it was reasoned that a method to select *against* the parental cell types used in the fusion, and select *for* the fused phenotype was needed. Fortunately, Prof. Peter Andrews kindly allowed the use of the previously derived NT2.TG11 line. This NT2 sub-line is known as a universal fuser. It is morphologically, and, for all intensive purposes, identical to the NT2 line used up to this point, however, it has been genetically modified such that it is neomycin resistant, but sensitive to aminopterin. When cultured in hypoxthanine aminopterin (HAT) medium, NT2.TG11 cells are unable to grow and eventually die off, whereas mammalian cell types are typically able to utilise the amino acid salvage pathway and are left unaffected by medium containing HAT. Since NT2.TG11 is neomycin resistant, as long as the somatic cell fusion partner is not neomycin resistant, we can select against it with neomycin. Therefore, only hybrids that have the salvage pathway (to overcome HAT) and neomycin resistance will survive. To apply this to cybrids-somatic cell fusions, any potentially reprogrammed, ES-like events will have to be identified by morphology and checked karyotypically; HAT medium being used to prevent the growth of any NT2.TG11 cells.

The other issue we considered was which somatic cell line we should attempt to reprogram. Although we could select against cells that were not reprogrammed, we did not have a method of selecting for reprogrammed cells (somatic cells that have

successfully fused with cytoplasts). Despite the fact that we could test cells that grew out that we suspected of being reprogrammed, essentially we were left to select based on survival and morphology. With this in mind, we chose to initially attempt to reprogram K562 cells, a human immortalized myelogenous leukemia cell line that grows in suspension. The assumption was that this line would convert to the morphology of a pluripotent cell upon reprogramming, and therefore attach. This would mean that we could remove non-reprogrammed somatic cells by simply changing the medium and select against potential NT2.TG11 contamination with medium containing HAT. This only leaves potential contamination by hybrid fusions formed between unsuccessfully enucleated/sorted NT2.TG11 cells and K562 cells. In the case that a NT2.TG11 fused with a somatic cell, it would gain the ability to survive in HAT medium and would theoretically attach and grow in monolayer and would only be eliminated as an unsuccessful reprogramming attempt after karyotypic analysis.

3.2.12 HAT Testing

To test the ability of HAT to select against NT2.TG11 EC cells, a simple serial dilution concentration experiment was run comparing the survival of NT2 cells (which can process HAT) and NT2.TG11 cells (which have been modified so that they cannot survive when cultured in medium containing HAT). HAT is not as strong of a selection tool as typical antibiotics, such as neomycin, but is usually toxic to mammalian cell types in high concentrations. Therefore, it was important that the strongest HAT concentration that effectively selects against NT2.TG11 cells, but allows normal cells to survive and proliferate was known. as HAT in high concentrations is toxic, even to cells that are able to survive in the presence of HAT.

After culturing NT2 cells vs NT2.TG11 cells in triplicate with medium containing 0x, 1x, 2x, 4x, and 10x HAT concentrations (1x = 400 nM aminopterin), it was discovered that NT2 cells can maintain a normal rate of proliferation in medium with up to 2x HAT (800 nM aminopterin). At 4x and above, NT2 proliferation rate was slowed and led to cell

death. Also, as expected, NT2.TG11 cells died off faster at 2x HAT concentrations compared to 1x, although 4x and 10x HAT were no more effective than 2x. So a HAT concentration of 2x (diluted from 50x stock [Invitrogen]) was used for all experiments selecting against NT2.TG11 EC cells.

3.2.13 Development of the Fusion Protocol

Basing our own protocol on Norwood et al. (1976), PEG_{6000} was initially tested at the conditions which gave the best fusion efficiency with a cell survival rate over 70%, 41% PEG and 15% DMSO. After treating NT2 cells with this solution, both in monolayer and in suspension, for one minute, followed by 5 PBS wash steps and resuspension in fresh DMEM + 10% FBS, it was found that NT2 cells are more sensitive than those used by Norwood et al. (1976). Therefore, the level of DMSO was scaled back to 10% at which point the survival of the cells increased to within the 70-90% range with high levels of multinucleated cells present, this formula was then set as our standard fusion medium (see section 2.10.9.1 for the fusion medium formulation).

Initially, NT2 and NT2-GFP cells were used along with HeLa cells to test the ability and relative efficiency of PEG_{6000} fusion medium to fuse two different mammalian cell types. Using a one minute exposure time and the fusion medium described above, the level of fusion appeared to be frequent and reproducible (See Figure 3.22 for photos of fusions). Although one minute in this fusion medium led to widespread fusion of NT2 cells, it was noticed that the exposure time, and whether or not the cells were in monolayer or suspension, made a noticeable difference in the level of fusion and the number of nuclei that were found, on average, in each fused cell (see Figure 3.25). So, in an effort to optimise for the best fusion conditions, conditions that result in the highest number of the largest, surviving, multinucleated cells, NT2 cells were tested in monolayer and suspension at different exposure times. Times tested were based on anecdotal evidence, with two goals: 1) isolating large fused NT2 cells to test whether or not large cytoplasts could be efficiently made from them (i.e. bigger cytoplast = more reprogramming factors) and 2) finding the exposure time that resulted in the highest

fusion efficiency, balanced with moderate levels of cell death, based on the number of 4n+ events (cells with 2+ nuclei).

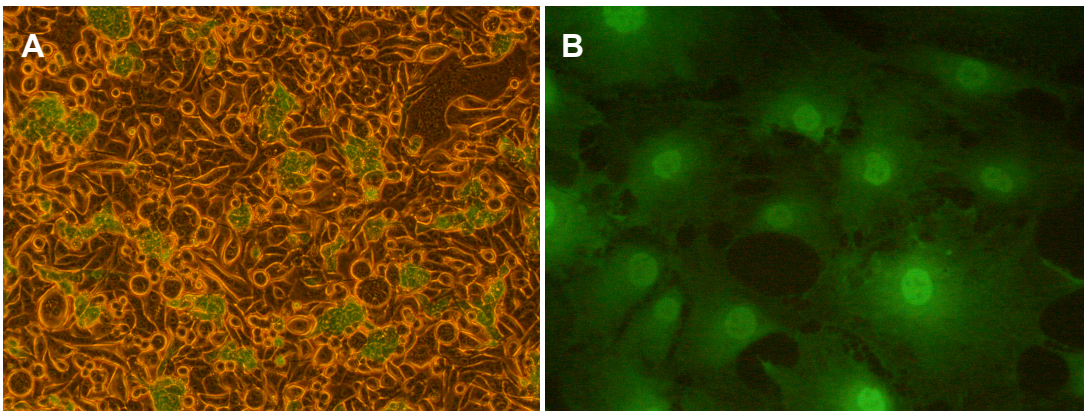

Figure 3.22: NT2-GFP + Hep2.5 (HeLa) Fusions
A) NT2-GFP cells fused with Hep2.5 (HeLa) cells at 1:1 ratio 48 hours post fusion using one minute of exposure to fusion medium (M&M section 2.10.9.1) in suspension. B) The NT2-GFP cell line was designed with a neomycin resistance gene, allowing for the selection of the NT2-GFP+HeLa fusions shown here. These slow growing cells appeared morphologically very different from either parental cell type, but retained GFP expression and neomycin resistance. The fusions shown in B are from approximately one month after the initial fusion experiment, shown at 48 hours in A.

3.2.14 FACS Analysis of Fused Cells

In order to assess the success of fusions using the FACS, it is important to understand how the FACS reads individual events, which should then enable us to understand how a fusion should appear on the FACS plot and how to differentiate fusions of different magnitude. With the help of Dr. Mark Jones, the CSCB FACS technician, an appropriate gating structure for the detection and isolation of fused events was formulated based on previous work he had done with multinucleated chicken erythrocytes (see Figure 3.23). First, sizing beads were run through the MoFlow to demarcate the 3 μm and 10 μm regions of the FACS plot, setting a point of reference for size (see Figure 3.9). As shown in Figure 3.24, the basic forward and side scatter FACS plot was supplemented with a Hoechst intensity graph, denoting DNA quantity per event, and a Hoechst pulse intensity versus pulse area plot (similar to the one shown in Figure 3.23 showing the erythrocyte data), this is meant to tweeze out the events that are actually multinucleated as opposed to those in late G2 phase, when the DNA content is naturally nearly double. Also, the pulse intensity versus area plot was designed with the intent to predict the number of nuclei an event should have and what percentage of the events had a particular number of nuclei, but, unlike the erythrocyte data, it proved to be very chaotic and we were only able to accurately estimate events with two or more nuclei.

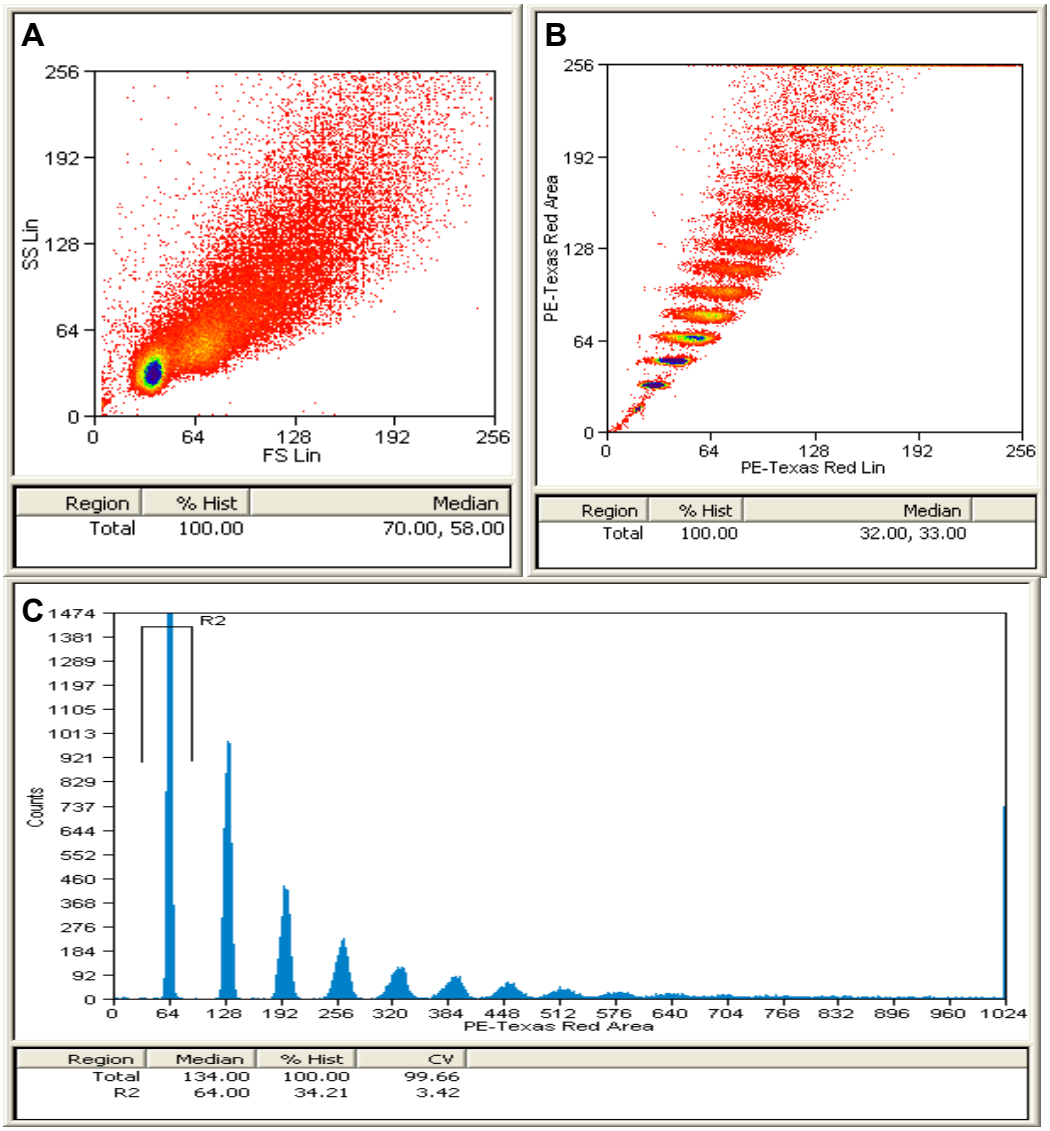

Figure 3.23: Multinucleated Chicken Erythrocyte Data
These FACS plots show the results of multinucleated chicken erythrocytes and were used with the assistance of Dr. Mark Jones, our FACS technician, to develop a model for isolation and quantification of multinucleated NTERA2 cells. A) This plot shows the standard forward (FS Lin) and side (SS Lin) scatter plot where the x-axis represents event size and the y-axis depicts event granularity. B) This plot shows how pulse intensity (x-axis) and pulse area (y-axis) can be used to isolate distinct groups of cells based on the number of nuclei they contain using a nuclear stain. C) This graph depicts the pulse area along the x-axis. From left to right, each peak represents a single nuclei increase (i.e. 64 = 1 nucleus, 128 = 2 nuclei, 192 = 3 nuclei, etc.). With this model, it should be possible to selectively sort groups of cells based on how many nuclei they contain.

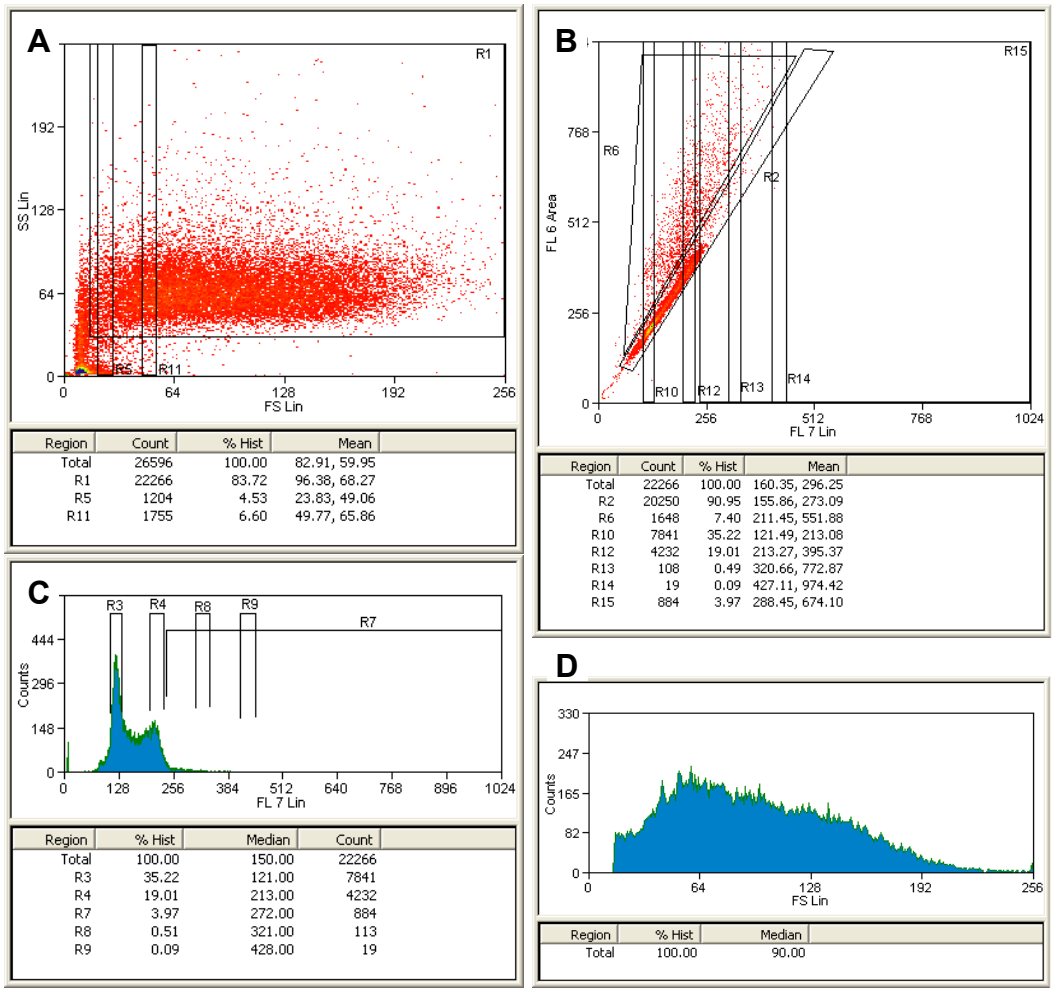

Figure 3.24: Parental NT2 FACS Plot

This set of plots and graphs represents the baseline for our fusion efficiency analysis study. Similar plots were generated for each fusion condition tested with the results summarised in Figure 3.26. A) This plot represents the standard forward scatter (FS Lin – x-axis) versus side scatter (SS Lin – y-axis) for untreated, unfused NT2 cells where forward scatter is an indication of event size and side scatter an indicator of granularity. B) The set up of this plot was designed to mimic the pulse intensity versus pulse area plot shown in Figure 3.23.B. Gates R10, R12, R13, and R14 were put in to capture events with 1, 2, 3, or 4 nuclei respectively while gate R6 was designed with the intention of capturing events that are greater in Hoechst intensity (and therefore DNA content) than normal cells, making them likely to be multinucleated. C) Mimic of Figure 3.23.C showing Hoechst intensity, relating to the number of nuclei in a given event. D) This plot shows the relative size of events (x-axis) with peak height (y-axis) referring to the number of events at that size. NOTE: Refer to the Appendix section A.1 for diagrams explaining how FACS reads multinuclear events and A.2 for the rest of the FACS plots which have been summarised in bar charts in Figure 3.25.

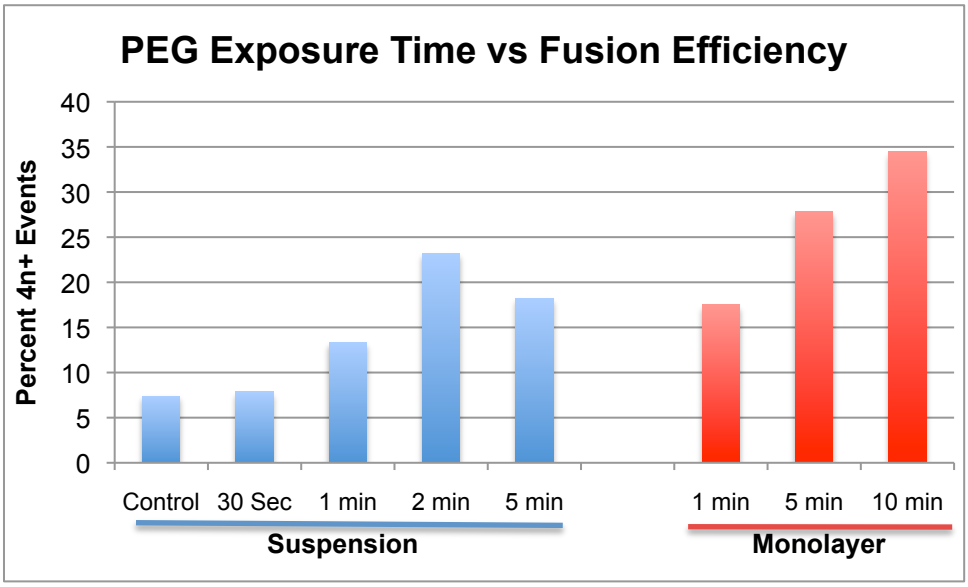

Figure 3.25: PEG Exposure Time vs Fusion Efficiency
Gate 'R6' from Figure 3.25.B was designed to capture events with two or more nuclei (4n+), the percentage of events in R6 is graphed above at varying fusion media exposure times. NT2 cells were fused both in suspension and monolayer. **Note:** each condition (column) shown represents a minimum of 10,000 events, sourced from 3 separate fusions.

3.2.14.1 Conclusions

Although the FACS data showed good correlation with what was witnessed down the microscope, some of the highest fusion efficiencies based on percentage of events in gate R6, turned out to be the same conditions that led to high levels of cell death. While further experimentation showed that the cells were able to cope with one to two minutes of fusion medium exposure, anything longer tended to result in more fusions but was followed by increased cell death at 24-48 hours later. Also, this FACS data was unable to take into consideration that at five or more minutes of exposure, many of the fusions were very large and their cell membranes appeared to 'bubble' or bleb out and become very fragile. It is highly likely that these cells lysed in the FACS analysis process. After balancing the conditions that resulted in the highest levels of fusion efficiency and lowest cell death, it was found that one minute of fusion medium exposure in suspension appeared to be the best, while five minutes in monolayer gives roughly the same level of fusion efficiency. These fusion times will therefore be used as standard when fusion is necessary.

3.2.15 Fusion Mediated Reprogramming

After settling upon protocols for the creation of cytoplasts, cell fusion, and isolation of successful fusions, we aimed to prove the hypothesis that cytoplasts from pluripotent cells are capable of catalyzing reprogramming upon fusion with somatic cells, given the correct amount of cytoplasts per somatic cell. As discussed in section 3.2.11, we initially examined the K562 cell line as a candidate for reprogramming based on the fact that it grows in suspension. We hoped that through fusion with NT2 cytoplasts, we might alter its gene expression patterns towards a pluripotent state, resulting in a phenotype similar to EC or ES cells, which typically attach and grow in monolayer. Then, selection would involve removing the floating K562 cells that were not reprogrammed by changing the medium and selecting against unfused NT2.TG11 cells by growing the fusions in medium containing 2x HAT. However, prior to attempting to

fuse K562 cells to NT2.TG11 cytoplasts, fusion was attempted directly between K562 and NT2.TG11 cells as a control to show that fusion can result in reprogramming.

After attempting to fuse K562 cells to NT2.TG11 cells, we found that K562 cells do not appear to fuse as readily as HeLa or NT2 cells and that, due to the compact, spherical morphology of K562 cells, it is very difficult to identify, by morphology alone, the difference between a tightly packed group of NT2.TG11 cells and a mass of fused cells consisting of a mixture between K562 and NT2.TG11. In an attempt to isolate hybrids and eliminate contaminating unfused NT2.TG11 cell, the resulting fusions were grown in medium containing 2x HAT. Unfused K562 cells remained growing in suspension while NT2.TG11-K562 cell fusions should gain the ability to survive in medium containing HAT. It was found that fusions appeared to grow for a short period of time, but there were a lot of unfused NT2.TG11 cells and as the HAT killed off these cells, nearby groups of cells, thought to be hybrids, died as well. It seemed that the NT2.TG11 cells released paracrine factors which induced apoptosis in nearby cells. However, some hybrids continued to slowly proliferate. These hybrids typically appeared fibroblastic in morphology (See Figure 3.26 F) and were much larger than parental NT2.TG11 or K562 cells. These hybrids were able to survive in medium containing 2x HAT more than a week after the disappearance of cells that resembled NT2.TG11, but did not survive passaging. Interestingly, some of the hybrids actually appeared to have K562 cells attached to them. Like small spherical bumps on the larger, fibroblastic cell's surface. These cells appeared to have K562 cells 'stuck' to them rather than their cell membranes becoming homogenous with the membrane of the fusion partner (see Figure 3.26 F). It was unclear whether or not fusion allowed these cells to survive, or a symbiotic relationship with K562s in close proximity.

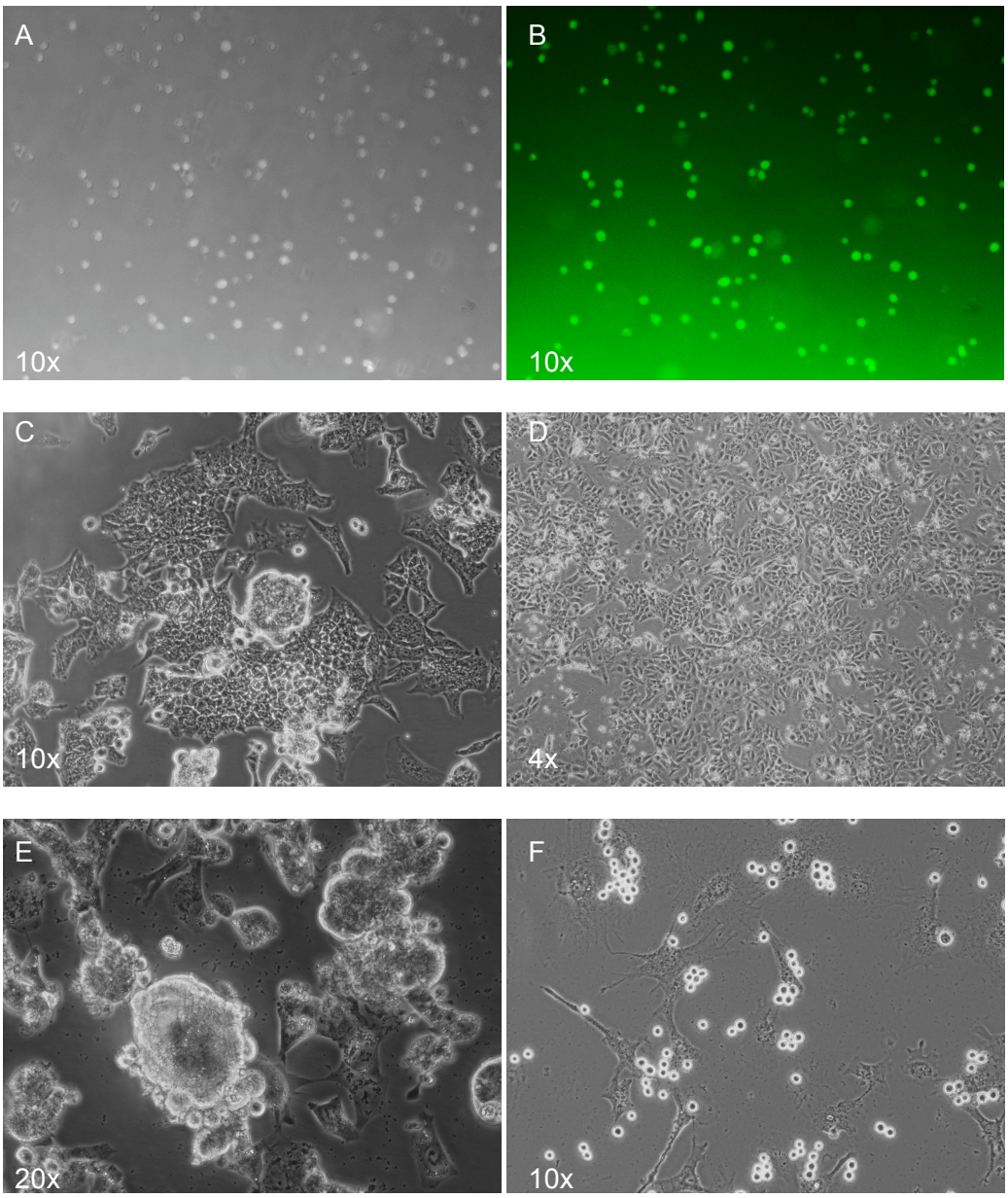

Figure 3.26: Fusion Partners – NT2.TG11 and K562 cells
A) K562 cells in suspension; B) K562 cells treated with CellTracker green under GFP fluorescence; C & D) Untreated NT2.TG11 cells growing in monolayer; E) 24 hours post fusion between NT2.TG11 and K562 cells, notice the 'nodules' that look similar to blebbing, but could be K562 cells; F) Fusions after one week of HAT selection.

3.2.16 Cell Tracker Staining of Fusions

Due to the morphologies seen post fusion (see Figure 3.26 E and F), there was concern that K562s may not be fusing properly and may even be helping NT2.TG11 cells survive HAT selection through being in close proximity, potentially allowing K562 cells to process the HAT medium and prevent the selection from working properly. In an effort to elucidate what was happening and whether or not true fusions were occurring, NT2.TG11 cells and K562 cells were stained using different colour cell tracker live cell staining dyes [Invitrogen, UK] followed by fusion.

NT2.TG11 cells were stained green and K562 cells were stained red prior to fusion (see section 2.10.10 for dye protocol), then epifluorescence photos were taken to show where the differing coloured dyes from each cell type co-localized, indicating a fusion. As shown in Figure 3.27, co-localization was detected, but even in these hybrids, and those isolated previously with HAT, the hybrids did not appear morphologically like pluripotent EC or ES cells and when attempts were made to grow the hybrids out, they would tend to last for only a few divisions before reaching a stagnant, non-proliferative state.

It was postulated that this lack of reprogramming may be due to the fact that NT2 cells are chromosomally very abnormal and that through fusion with K562, another cancer cell line, too many conflicts in gene expression may have occurred in the fused cells, leading to cell cycle checkpoint failures and ultimately apoptosis. However, it was decided that, without the abnormal chromosomal issues of NT2 being involved in cytoplast fusion, we would move forward with NT2.TG11 cytoplast + K562 fusions hypothesizing that the *non*-nuclear reprogramming factors will affect the K562 cells differently than whole NT2.TG11 cells.

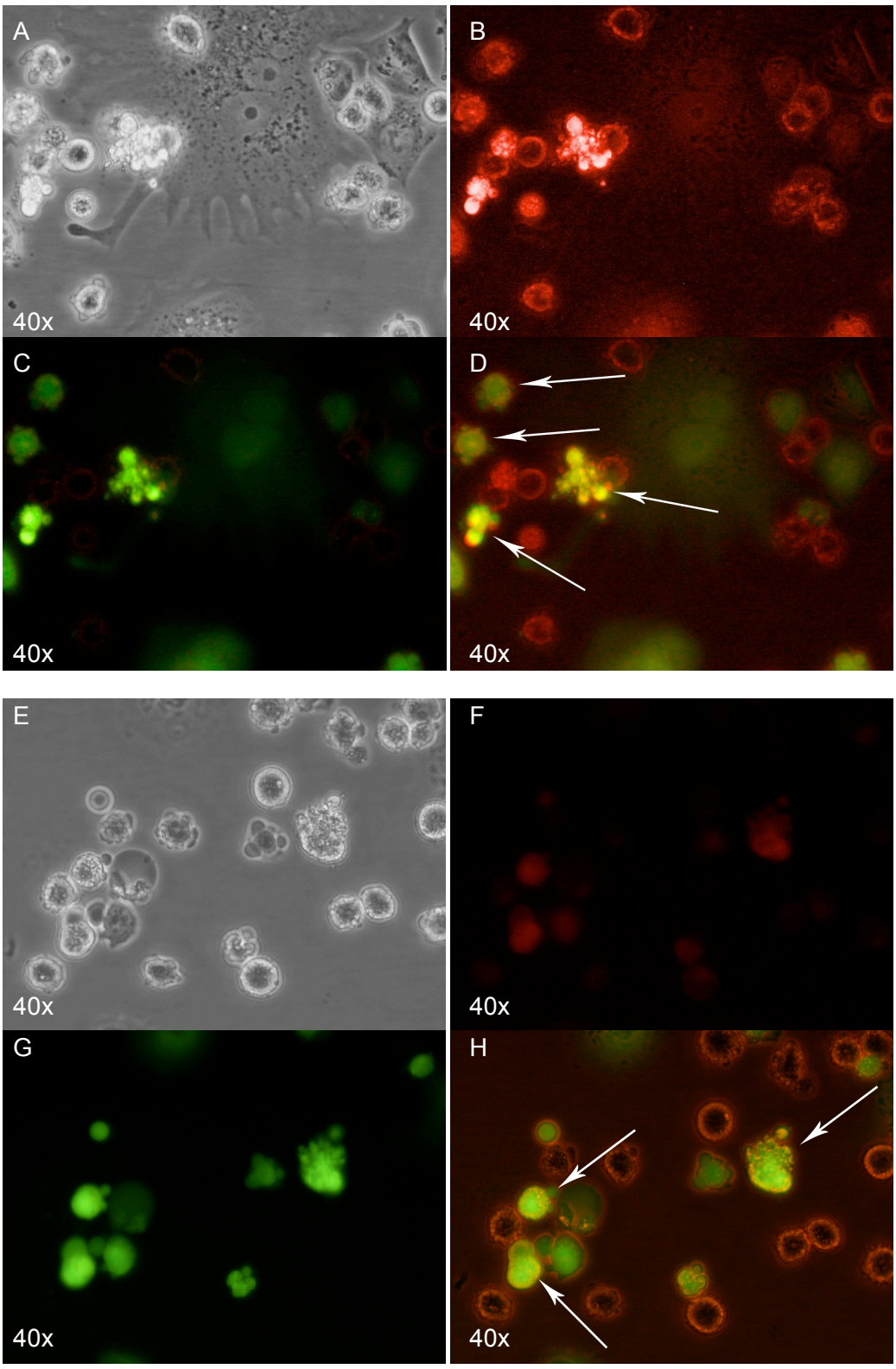

Figure 3.27: Cell Tracker Dye Fusions Between NT2.TG11 and K562 cells
In order to determine whether true fusions between NT2.TG11 and K562 cells were occurring, NT2.TG11 cells were treated with cell tracker green and K562 cells with cell tracker red, followed by PEG fusion for 1 min using the standard protocol (section 2.10.10). Arrows denote cells that showed both green and red fluorescence, indicating fusion. A and E) Phase contrast, B and F) red fluorescence, C and G) green fluorescence, D and H) red and green combined.

3.2.17 Fusion of NT2.TG11 Cytoplasts with K562 Cells

After verifying that fusions were occurring between K562 and NT2.TG11 cells, albeit without resulting in viable hybrid cells, NT2.TG11 cytoplast + K562 cell fusions were attempted. Similar to the fusions between NT2.TG11 cells to K562 cells, there were a number of cells that appeared to have K562 cells attached to the membrane's surface that did not fully integrate into the cybrid or hybrid cell (see Figure 3.28). Despite the unexpected morphologies of the resulting fusion products, they were able to grow in HAT medium and proliferated for a few passages, but ultimately, most of the fusions arrested. The remaining attachment cells that survived became apoptotic before enough could be expanded to characterize further. After similar repeated experiments, no fusions could be expanded and characterized. All cells that appeared to survive HAT selection did not appear morphologically similar to EC or ES cells. They typically divided only a few times, if at all, and despite attempts to transfer them into more nutrient rich medium, including DMEM/F12 +20% FBS and hES KO medium, they did not proliferate. Also, plating surviving cells in small well plates on gelatin or matrigel was attempted, but did not result in expansion.

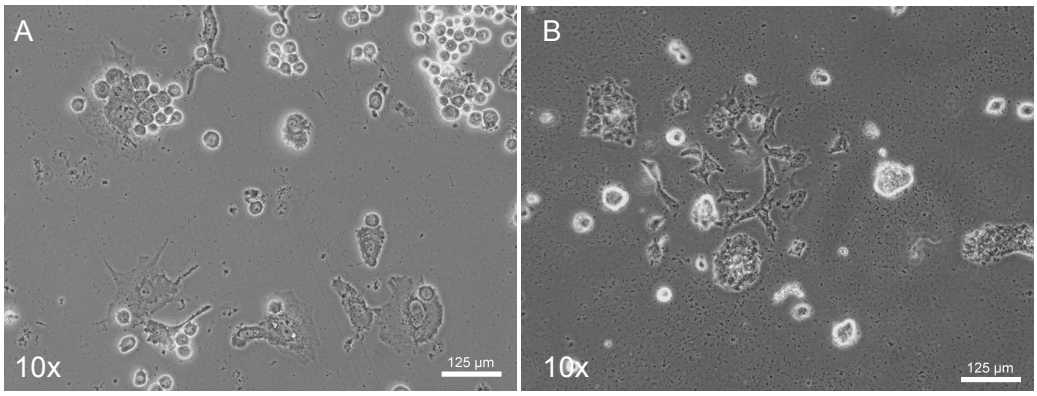

Figure 3.28: NT2.TG11 cytoplasts fused with K562s under HAT selection
After enucleation of NT2.TG11 cells followed by isolation of cytoplasts by FACS, cytoplasts were fused with K562 cells and fusions were selected for 7 days in HAT medium before taking these images. Unfortunately, despite multiple attempts, the sparse numbers of surviving cybrids/hybrid cells did not proliferate for more than a few divisions before reaching senescence.

3.2.18 Switching Cell Lines

After finding that K562 fusions did not result in any viable, isolatable cells, the ability of K562 cells to be successfully reprogrammed was questioned. This was compounded by the fact that these results also concur with other K562 reprogramming results done using a different methodology, shown in Chapter 4. Therefore it was decided that in order to move forward with our reprogramming work, other cell lines should be tested. Also, due to inability to gauge and monitor the reprogramming process, it was determined that, a reporter cell line with a fluorescent marker linked to a pluripotency gene would be ideal. This would then allow live cell monitoring in vitro and enable us to follow cell changes and isolate particular cells within a set of cells that show changes towards a pluripotent phenotype compared to the surrounding population.

3.2.19 Derivation of an OCT4-GFP Reporter Cell Line

After reviewing the current literature, human fibroblasts were settled upon as the somatic cell line of choice for reprogramming. The HuF1 human fetal fibroblast line, derived from a first trimester fetus, was used. They were of typical fibroblast morphology, reaching confluency within 4-5 days after splitting 1:5 and displaying a typical 'swirled' pattern with tight cell junctions with striated cell arrangement when confluent. Since these fibroblasts were highly proliferative and recently derived, it was decided that it should be possible to transfect them with a reporter construct and isolate a clonal reporter line before they reached senescence (which is typically around 20-30 passages, and the line was obtained at passage 7). See section 2.1.6 for more information.

An 'OCT4 minimal promoter'-GFP-Neo (OpGN) construct, used to derive a human ES OCT4 reporter cell line was constructed by Dr. Pete Tonge based on the construct used by Gerrard et al. (Gerrard et al. 2005). H7S6 human ES cells with this construct were clonally derived and express GFP as long as they remain undifferentiated, therefore detecting endogenous OCT4 expression. Also, neomycin resistance was

included to help select clones. This construct was then used to make a reporter line from the HuF1 human fetal fibroblast line. The construct works by having the human OCT4 minimal promoter driving GFP expression, such that, whenever OCT4 is being expressed, GFP is also expressed. The neomycin resistance gene is constitutively expressed under a separate (CAG) promoter. The intention being to create a fibroblast line that, when reprogrammed, should turn green due to the fact that endogenous OCT4 expression is a prerequisite for pluripotency.

HuF1 cells were transfected using the BTX ECM 830 electroporator [Harvard Instruments] according to the protocol shown in the Materials and Methods section 2.11.3. 3 µg of OpGN construct was shocked into 1 million cells and the cells were plated on a 10 cm dish. After three days of growth in DMEM + 10% FBS, 500 µg/mL neomycin was added to the medium to select for fibroblasts that took up and integrated the construct. After about three weeks of growth in neomycin, colonies began to proliferate.

After examining the cells that proliferated under neomycin selection, many of them were found to be GFP positive or partially GFP positive, which was surprising since HuF1 fibroblasts are not pluripotent and should not express OCT4 (See Figure 3.29 D). We wanted a reporter cell line that would turn green only when OCT4 was activated via reprogramming and was GFP –ve otherwise. So, three strategies were attempted: 1) to differentiate the existing hES OCT4 reporter line (H7S6+pOCT4-GFP) into fibroblasts (or similar somatic cell type); 2) to use FACS to sort the heterogeneous population of HuF1 fibroblasts containing the pOCT4-GFP construct into GFP positive and negative cells that survive neomycin selection; 3) to isolate single cell clones from the polyclonal population in hopes of being able to grow out a clone that would make a suitable reporter line.

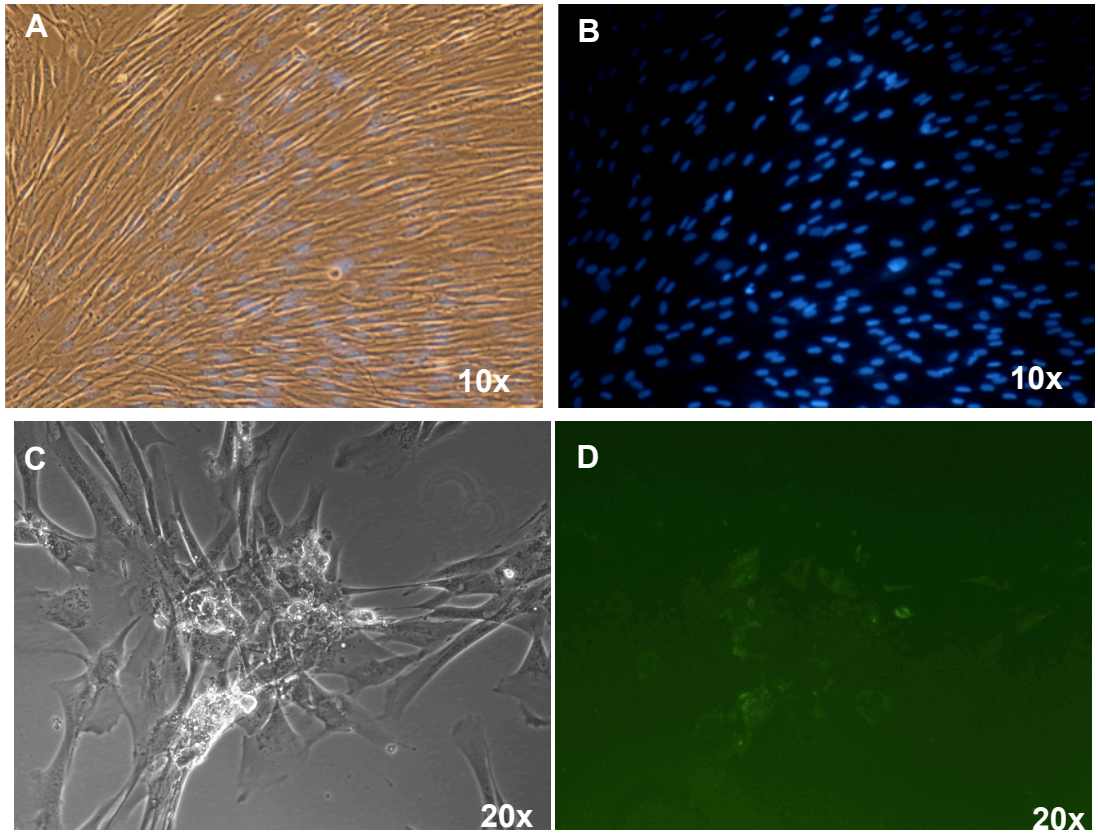

Figure 3.29: Initial HuF1 reporter cells unexpectedly express GFP
HuF1 fetal fibroblast cells (shown in A & B stained with Hoechst 33342) were transfected with the OpGN construct containing a human OCT4 minimal promoter driving the expression of GFP and providing ubiquitous neomycin resistance. These cells were designed to be a reporter of OCT4 expression, however, unexpectedly, some of the cells appeared to be completely or partially GFP positive (indicating OCT4 expression), as shown in C & D. However, these fibroblasts should not endogenously express OCT4. Further experiments and cloning attempts were made before isolation of a GFP-free, neomycin resistant OCT4 reporter could be established (as explained in 3.2.22).

3.2.20 Differentiation of H7S6+pOCT4-GFP into Fibroblasts

In attempting to differentiate H7S6+pOct-GFP, the publication “Immortalized fibroblast-like cells derived from human embryonic stem cells support undifferentiated cell growth” (Xu et al. 2004) was used as a guide. Instead of normal hES culture conditions, the reporter cells were shocked into an unfamiliar environment and treated as fibroblasts. They were grown on 0.1% gelatin with DMEM + 10% FBS at 10% CO_2, instead of their typical 5% CO_2. Many different phenotypes arose, cells differentiated into a number of undefined cell types, but over four to eight weeks in non-ES cell culture conditions, uniform cell types were manually isolated and cultivated. However, even after four to eight weeks of differentiation, many of the cells still showed GFP expression, indicating that the OCT4 was still activated, or that the construct itself was not a very reliable indicator of OCT4 expression. Assuming that the construct was not to blame, the cell types derived with the highest levels of GFP and least fibroblastic phenotype were discarded. After multiple rounds of manual passaging, a few flasks appeared to show uniform fibroblastic-like cells that did not appear to express GFP, or only did so at very low levels. This line, derived from H7S6+pOCT4-GFP appeared to be the solution to our problem, so we attempted to expand it and bank the cells down for future use. Unfortunately, within a few passages, the GFP negative cells became senescent and it was not possible to expand the cells enough to use them for reprogramming experiments.

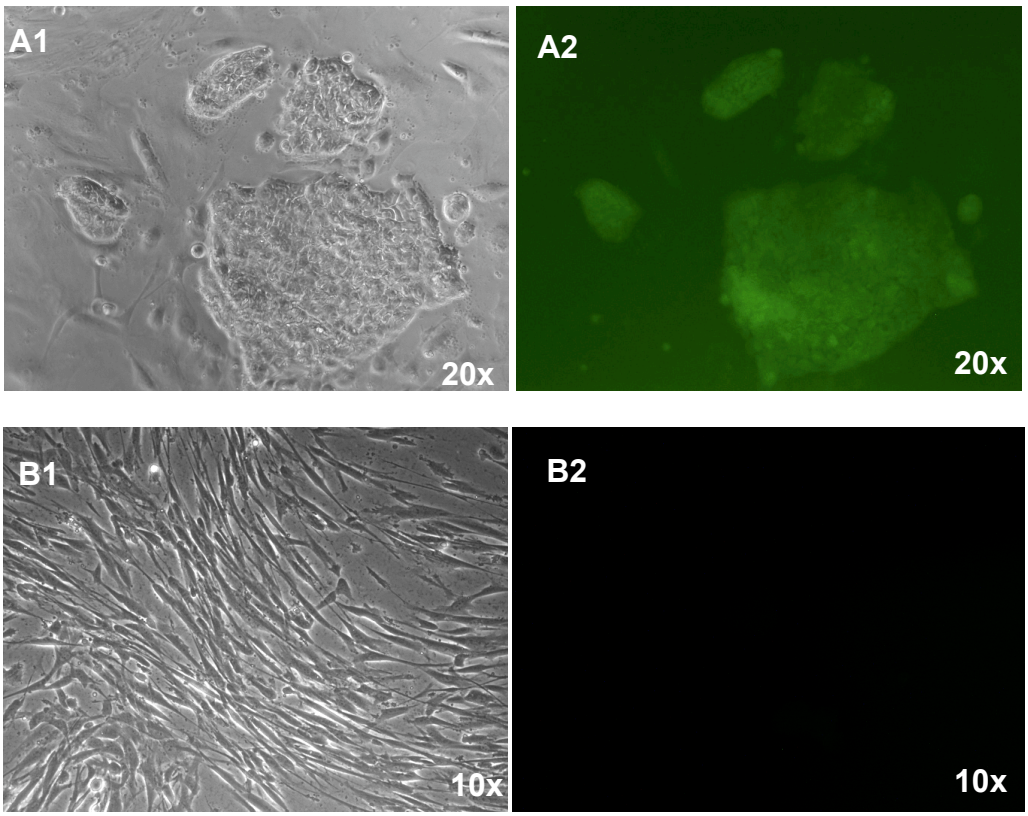

Figure 3.30: GFP Reporter line from H7S6-pOct-GFP line
H7S6 cells modified with the OCT4 minimal promoter driving expression of GFP (A) were differentiated over 8 weeks by manual isolation and expansion of fibroblastic cell phenotypes (B1). Eventually, no GFP could be detected (B2), inferring that any residule OCT4 expression ceased. However, within a few passages of deriving a fibroblast reporter line from these cells that maintained neomycin resistance (inferring that they still had the reporter construct in them), the cells senesced and could not be passaged further.

3.2.21 FACS Isolation of GFP -ve HuF1+pOCT4-GFP Cells

In addition to the differentiation of H7S6-pOCT4-GFP cells, the FACS was used to sort out the GFP negative HuF1 fibroblasts from those that expressed GFP in hopes that a neomycin resistant line could be isolated that would not be GFP positive, a line that would only turn green upon reprogramming and reactivation of endogenous OCT4 expression. Initially, this strategy proved to work well. The sorted cells were clearly GFP negative post-sort and still maintained the same morphology and proliferative capacity as the GFP positive fibroblasts. However, after a few passages in their normal growth medium (DMEM + 10% FBS), GFP positive cells were detected and within three to four passages, the culture was again a heterogenous mix of GFP positive and negative cells. Before giving up, the process was repeated twice more, but each time, from a population of FACS sorted GFP negative HuF1 fibroblasts, GFP positive cells would later emerge. These mixed cells were frozen down but deemed unusable for our purposes as a reliable reporter of reprogramming.

3.2.22 Isolation of GFP Negative HuF1+pOCT4-GFP Clones

The final strategy implemented for isolating an OCT4-GFP reporter was clonal derivation. Despite many attempts at plating out cells at low/clonal density, they failed to proliferate. HuF1 fibroblasts can grow in clumps at low density, but at densities where single cells were not within close proximity of other single cells, they senesced very quickly. The process was repeated at different densities to determine whether or not slight adjustments could improve the outcome, but each time it was found that either the density was too low and cells would become senescent or the density was too high, and single clones were difficult to isolate from the rest of the population. It was decided that the best available option was to isolate small colonies using cloning rings based on the assumption that a single colony was derived from a single clone, however, the lines derived cannot be said to be truly clonal.

After transfection, HuF1 cells were seeded into circular 10 cm diameter tissue culture dishes [Corning] and grown in fibroblast medium (see section 2.1.6) for 3 days. After 3 days, the medium was supplemented with 1000 µg/mL neomycin to select for cells that had taken up the plasmid. After approximately 21 days, individual colonies were isolated using cloning rings [Corning] as per manufacturer's instructions. Each isolated colony was treated as an individual clone and further grown under selection for several passages. All of the isolated lines appeared to grow uniformly and three of the eight lines maintained a GFP negative (but neomycin resistant) phenotype. These lines, clones C, E, and G, were expanded and banked down for future use. After FACS analysis and verification of promoter reactivation by fusion with pluripotent NTERA2 cells, clone E (HuF1b+pOCT4-GFP cl E) was chosen and used, where noted, throughout this study.

3.2.23 Fusion of TG11 and HOG Reporter Fibroblast Line

Having isolated and cultured successful HuF1+pOCT4-GFP (HOG) reporter clones, we wanted to test that the reporter was working by attempting reactivate it through reprogramming. Since fusion reprogramming is the simplest, most straightforward process available to us, we first attempted to fuse reporter fibroblasts to NT2.TG11 cells as discussed above, using our semi-optimised fusion protocol.

Different NT2.TG11 to HOG cell ratios were tested (1:1, 5:1, 10:1, and 20:1) and it was found that one of the 10 NT2.TG11 cells to 1 HOG cell culture had a small GFP positive colony in it after approximately seven days of post-fusion culture (See Figure 3.31). This proliferative colony appeared raised in appearance and was at least 20 cells across. It actually appeared as though the clump of cells was beginning to form an EB and might eventually detach from the tissue culture plastic.

Unfortunately, this colony, despite its high proliferative capacity early on, abruptly stopped growing. Attempts were made to manually remove the clump, dissect it, and passage it onto feeders, but the GFP positive cells only settled and remained stagnant. Cells with fibroblast and NT2.TG11 morphology were found to be growing out from the dissected clump of cells, but the GFP positive cells did not adapt to the hES cell conditions and these GFP positive hybrid cells eventually became undetectable. Several attempts were made using similar conditions and other GFP positive clumps were found, but each only reached a similar or smaller size before eventually becoming senescent. Attempts were made to dissect the clumps early on and also to let the clump just grow out naturally in DMEM + 10% FBS, but these strategies failed to yield a GFP positive hybrid line.

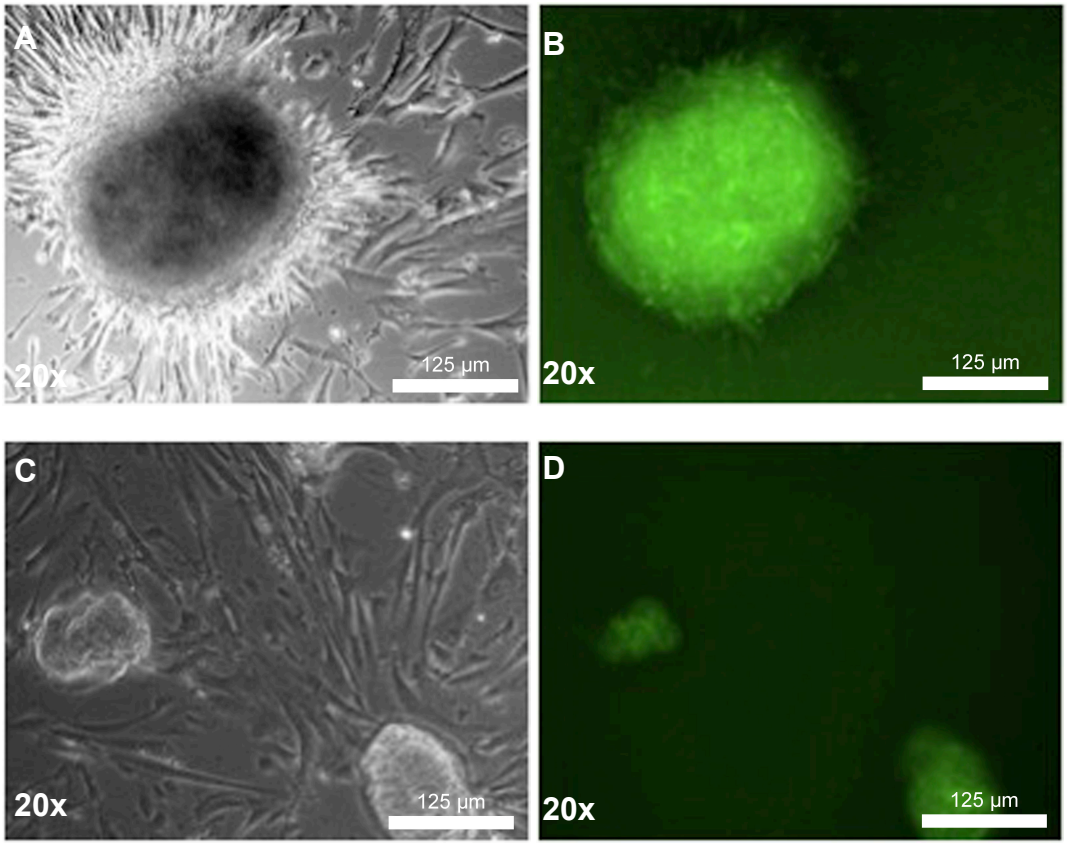

Figure 3.31: GFP Positive Cell Clumps from NT2.TG11 + HOG Cell Fusions
A & B depict the initial GFP positive clump that arose from fusion between NT2.TG11 cells and HuF1-pOCT4-GFP cl E cells after 7 days in culture. C & D show similar, smaller clumps found in replicates using the same fusion conditions.

3.2.24 Cytoplast + OCT4-GFP Reporter Fusion

After successfully fusing NT2.TG11 and HOG cells and getting OCT4 reactivation as detected by GFP expression, it was decided that the next logical step was to apply our cytoplast fusion protocol to these reporter cells. Using the semi-optimised enucleation and fusion protocols derived, NT2.TG11 cytoplasts were fused with HOG cells. Within a few days, HAT selection was initiated.

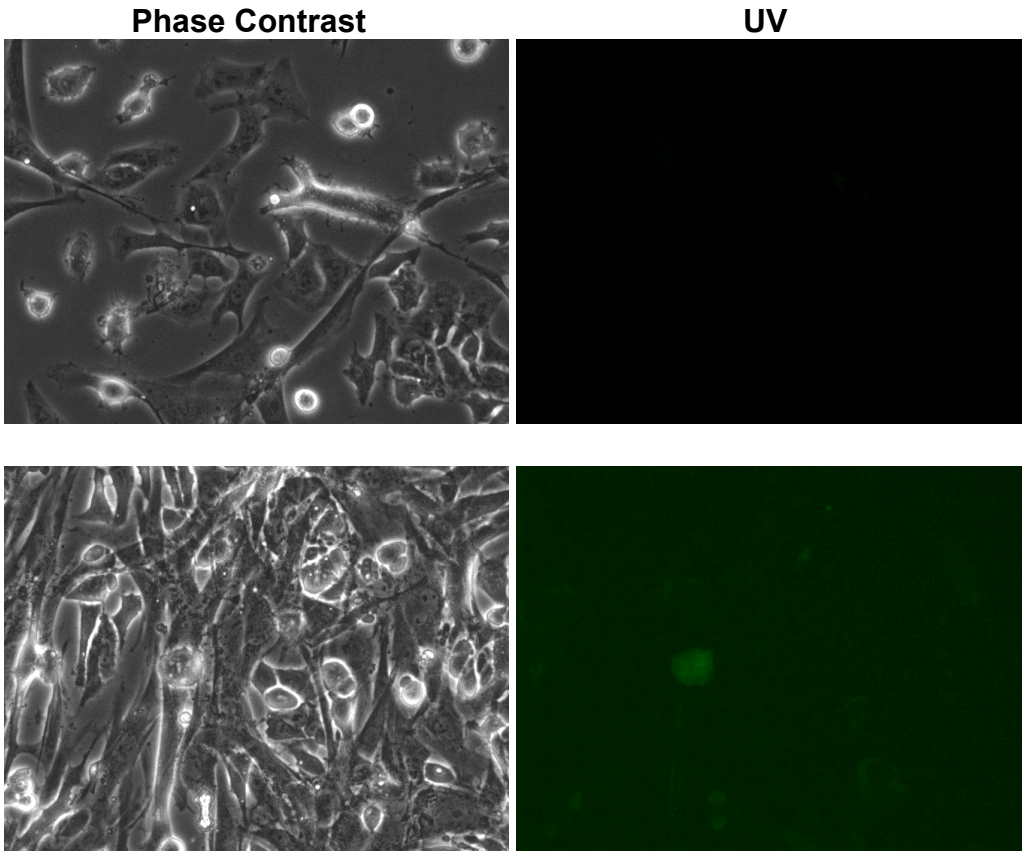

Figure 3.32: Cytoplast + HuF1+pOCT4-GFP Fusion
Unfortunately, the only detectable GFP positive cells post-fusion were only barely GFP positive compared to hES cell controls and did not remain GFP positive. Despite multiple attempts and keeping the cells in both hES and EC conditions for 2-3 weeks, following HAT treatment, remaining live cells were not GFP positive or of ES cell morphology.

3.3 Chapter Discussion

A number of issues arose over the course of this set of experiments. While some were solved or ameliorated by optimisation, the issue of cytoplasts being produced in varying sizes and levels of granularity remained. This led to them residing in the same areas of the gradient as karyoplasts and made isolation of pure cytoplasts very difficult and making FACS a necessary part of the process. According to Andrews et al., NT2 cells have relatively high glycogen levels as compared to other mammalian cell types; glycogen, being relatively heavy and dense, may be causing cytoplasts to acquire densities in a similar range to nuclei (Damjanov et al. 1983; Andrews et al. 1985). While Pralong et al. (2005) reported successful enucleation of mouse ES cells, they used an ultracentrifuge. While our centrifuge provided similar levels of relative centrifugal force, there may be other advantages to using an ultracentrifuge, such as faster spin-up times, that may allow for more uniform enucleation. Other lower cell densities were also briefly experimented with, but no further significant improvements on the process were reached.

While we are not certain why the cytoplast strategy did not result in full somatic cell reprogramming, Wakayama *et al.* has shown that the amount of cytoplasm in an oocyte relates directly to its chances of developmental success. Their study showed that oocytes need a minimum of half their cytoplasm to result in a successful embryo, any less and it will fail (Wakayama et al. 1998b). It may be that this principle holds true in terms of an oocyte's ability to catalyze reprogramming; in our experiments, perhaps there was not enough cytoplasm containing the necessary factors in the right proportions. Although various concentrations of cytoplasts to somatic cells were attempted, there is a limit to the rate and frequency of fusion before PEG induced apoptosis becomes a serious issue. It is quite reasonable to assume that we might have achieved partial reprogramming, but that key elements present in the cytoplasm were not sufficient enough to overwhelm and ultimately reprogram our somatic cells. It

may also be that the process, as it stands, is not optimised enough to fuse a single somatic cell to enough cytoplasts to catalyze reprogramming.

We postulated that the nuclear factors and the nucleus itself were not the limiting factor for reprogramming, as suggested by Egli et al. (Egli et al. 2007), but if nuclear factors are the missing element, it is known that there are various 'nuclear factors' which dissociate from the chromatin during M-phase of the cell cycle and it may be that we need to optimise for cell cycle timing to better coordinate the isolation and administration of cytoplasts with this phase. While many questions still remain, with new evidence that alternative methods, such as RNA and viruses, may be more successful, the choice was made to move in a different direction.

3.3.1 Cytoplast Isolation and Fusion as a Microbiology Tool

Although the cytoplast fusion strategy did not produce the results hypothesised, with more time, there are a number of other potential applications for this process, namely, directed differentiation, transdifferentiation, and study of non-nuclear cell components. Studies have shown that co-culturing stem cells with specific cell types can often drive stem cells towards a similar cell state (Mummery et al. 2003; Jang et al. 2004; Qin et al. 2005; Mummery et al. 2007). Through differentiation, a stem cell would need to eventually take on the gene expression profile of the cell type it is differentiating into before differentiation is complete. Cytoplasts could be fused to stem cells and thereby provide the proteins and RNA from a desired somatic cell type. Used in high enough proportion, the cytoplast contents could serve to overwhelm the stem cell's natural RNA and protein levels, thereby giving the stem cell a gene expression signature of the cell type the cytoplast was derived from, potentially giving similar or potentially more effective results than those seen using co-culturing methods. Similarly, multipotent cells and somatic cells with cell state plasticity might be able to be pushed from one cell state to another through cytoplast fusion. A similar procedure using mouse

cardiomyocyte cell extracts has been shown to catalyse transdifferentiation of human adipocyte stem cells into cardiomyocytes (Schimrosczyk et al. 2008).

This cytoplast isolation strategy could also be used to make and isolate microcells, cells that consist of one or few chromosomes surrounded by a portion of the cell membrane. Microcells have been used before to isolate and study the effects of individual chromosomes (Lugo et al. 1987; Schultz et al. 1987; deJong et al. 1999; Liu et al. 2003). With a slightly altered process, one could selectively isolate particular chromosomes and fuse them to other cells to supplement their chromosome count, thereby creating potentially interesting mutants. In this way, chromosomal abnormalities could be promoted in a relatively controlled way in vitro. Human embryonic stem cells and embryonal carcinoma cells often gain mutations over time from in vitro culture, such a system might allow a more in depth study of why and how chromosome copy number of certain chromosomes leads to in vitro advantages.

3.3.2 Conclusions

Cytoplasts themselves need more study, the available literature does little to define them more than we have here and it would be interesting to determine what a cytoplast actually contains, what RNA it holds, what proteins are typically encapsulated, etc. However, due to the limited reprogramming results obtained, this line of research was abandoned in favour of RNA mediated reprogramming (see Chapter 4). It was hypothesised that the amount of factors getting through (per somatic cell) was lacking and that by using RNA transfection, it might be possible to force more factors in per cell with higher reproducibility.

Having had difficulties with the K562 cell line and isolation of viable fusions, Total RNA transfection was considered as a possible alternative to cytoplasts. Total RNA, in theory, should contain the instructions and machinery for a given cell's production of

proteins and might be able to redefine a cell's state by causing production of all the proteins a pluripotent cell would contain. Since Total RNA has been used historically to understand the expression profile of a cell or set of cells, it seemed a logical assumption that if we can make a set of somatic cells express the RNA from a set of pluripotent cells long enough, this might catalyse the somatic cells to change their gene expression patterns permanently to support the pluripotent cell state catalyzed by the Total RNA. Due to her previous experience with RNA and transfection techniques, Dr. Jie Na agreed to collaborate on the development of a system to isolate and transfect Total RNA in relatively large quantities, keeping the same ultimate goal in mind, to reprogram somatic cells without genetic addition or modification. We also recognized that RNA has the added benefit of being inherently transient; RNA is read, translated into protein, and then degraded, leaving no lasting effect on the DNA and unlike the cytoplast method, there's no transfer of mitochondrial DNA, making it potentially a safer alternative to cytoplast fusion.

Chapter 4 – RNA Mediated Reprogramming

4.1 Introduction

After investigating the pluripotent potential of cytoplasts with limited success, we moved forward by asking, what are the key factors within cytoplasts, oocytes and pluripotent cells that are responsible for somatic cell reprogramming? Is there a better, more efficient way to isolate and administer these factors? We hypothesized that the bulk of the reprogramming factors present at any given time in cytoplasts, oocytes, and pluripotent cells are likely to be in the form of proteins and RNAs. Since proteins are coded from mRNA, it followed logically that the total RNA from a pluripotent cell should hold all the instructions needed to code for all the pluripotency proteins present at a given point in time. The total RNA also contains tRNA, rRNA, microRNAs, and other regulatory RNA components that could potentially contribute to the process of reprogramming by shifting the intracellular environment towards that of a pluripotent cell. Plus, total RNA has the benefit of being easier to isolate than cytoplasts, there is a lower risk of DNA contamination, FACS is not required, and it can be done so in bulk without PEG or Ficoll, which is relatively messy.

While we did not know the exact combination of factors necessary to catalyse reprogramming, we felt it logical to assume that if one could reproduce the intracellular environment of a pluripotent cell within a somatic cell, it might be enough to catalyze epigenetic change leading to a change in cell state towards pluripotency. Therefore, if we can show that the somatic cell's machinery is capable of taking up and translating the RNA from a pluripotent cell, it would then be subjected to the same proteins present in the pluripotent cell and, at least to some extent, mimic the intracellular environment of the pluripotent cell. Assuming the right balance of factors are amongst the RNA translated, it may be enough to push the somatic cells toward a pluripotent phenotype.

After reviewing the literature, we found a parallel trend between the development of our fusion/cytoplast work and the evolution of cancer vaccines, which moved from using dendritic cell/tumour cell hybrids derived through fusion as a vaccine (Phan et al. 2003) to transfecting dendritic cells with tumour RNA (Mu et al. 2003) to achieve the same or better results. Using the RNA from a patient's tumour, the patient's dendritic cells were transfected and matured, resulting in cells that cause T-cell activation upon contact with tumour cell antigens (Mu et al. 2003; Markovic et al. 2006). Not only was the RNA just as effective as cell fusion for this application, but also it is inherently safer due to the elimination of tumour DNA and as part of the vaccine and has already been used successfully in phase I/II clinical trials (Kyte et al. 2006).

Although RNA transfection is typically ignored in favour of DNA vector transfection, for reprogramming its transient nature is an advantage. However, whether or not RNA can act transiently to catalyse permanent changes in cell state has not been previously tested beyond the dendritic cell work described above. The work using dendritic cells indicates that RNA from one cell type can be transfected and translated by another cell type, if this holds true with RNA from a pluripotent cell in a somatic cell, corresponding changes in phenotype and potentially dedifferentiation towards the pluripotent cell state might occur.

At this point in the project, Dr. Jie Na, a colleague from the CSCB, kindly lent her assistance as she has prior experience electroporating mouse embryos with RNA to study the effects on development. Together, we mapped out a plan to transfect RNA from NT2 cells into somatic cells, using the literature on dendritic cell transfection as a starting point.

4.1.1 Transfection of K562 Cells with Total RNA

Prior to the completion of the work described in Chapter 3, testing RNA as a pluripotency catalyst was already underway. At this time, our primary goal was the reprogramming of K562 human immortalised myelogenous leukaemia cells, cells that grow in suspension. The fact that K562s expand in suspension was seen an inherent advantage because it was hypothesized that reprogrammed K562 cells would take on a typical pluripotent phenotype, including a propensity to attach, therefore allowing us to remove cells that did not get reprogrammed by simply changing the media. Although we were unable to isolate reprogrammed K562 cells through cytoplast fusion, we felt that this might be in part due to the dosage of reprogramming factors being too low. However, by isolating just the RNA and concentrating it, it should be possible to administer a greater amount of reprogramming factors on a per cell basis than possible through cytoplast or cell-cell fusion.

4.1.2 Chapter Aims

I. To optimise RNA isolation and transfection conditions.

II. To test whether or not transfected RNA is making it into cells efficiently.

III. To test whether or not transfected RNA is being translated into protein.

IV. To test total RNA from pluripotent cells as a catalyst for reprogramming.

4.2 Results

4.2.1 Development of Electroporation Protocol

K562 cells were transfected with RNA isolated from pluripotent cells using electroporation. In contrast to other popular transfection methods, such as lipofection, electroporation has been shown to give high transfection efficiency using both suspension *and* attachment cells. However, electroporation conditions vary depending on cell type and need to be optimised.

As a starting point, the Guide to Electroporation and Electrofusion by Chang et al. was used to help identify the best base conditions and test conditions for optimal RNA delivery by electroporation, specifically Chapter 27, “Protocols for Using Electroporation to Stably or Transiently Transfect Mammalian Cells” by Huntington Potter (Chang et al. 1992). Many of the contributors of this book worked with or for BTX, the company which manufacturers the electroporator that we chose to use the BTX ECM 830 [Harvard Instruments]. According to Chang et al., first and foremost, it is important that mammalian cells be transfected in “mid to late log phase” (Chang et al. 1992), therefore K562 cell growth was monitored under standard growth conditions to determine the best time point for electroporation.

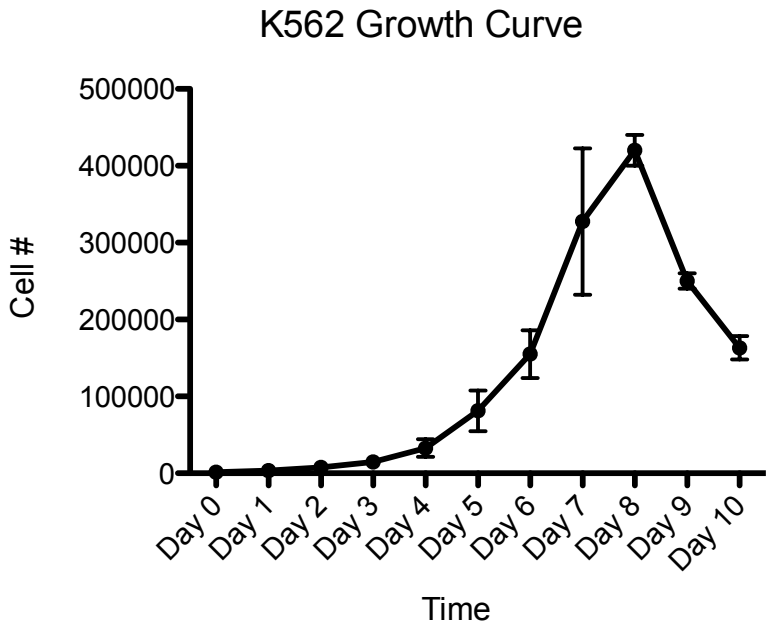

Figure 4.1: K562 Growth Curve
According to the Guide to Electroporation and Electrofusion (Chang et al. 1992), and confirmed by our own work, it is important to electroporate mammalian cells while they are in their exponential growth (log) phase. Growth was therefore monitored (without passaging) to determine the optimum range for transfection, which, as shown above, is typically between 5 and 8 days after passaging 1:100.

Having successfully identified the mid to late log phase for K562 cells under typical growth conditions, we attempted to identify the best electroporation conditions by testing a range of parameters including voltage, pulse length, and number of pulses. In order to assess transfection efficiency under various conditions, K562 cells were transfected with a GFP plasmid driven by the CAG promoter and the percentage of GFP positive cells were calculated by FACS 72 hours after electroporation. Results shown in Figure 4.2, see Materials and Methods section 2.11.3 for electroporation protocol.

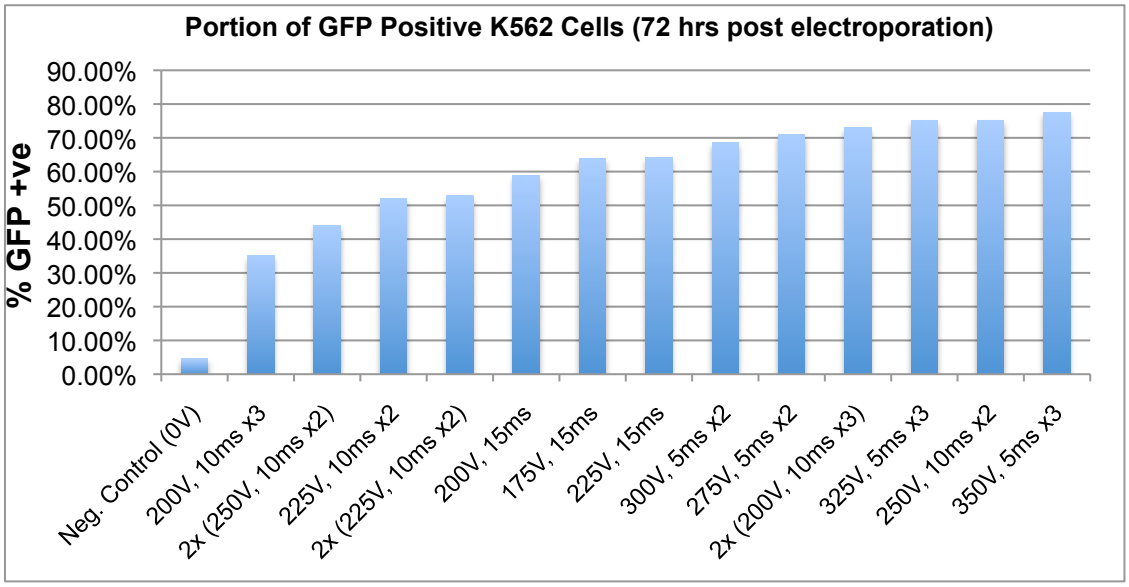

Figure 4.2: K562 Electroporation optimisation

The 12 conditions tested have been arranged in ascending order by the percentage of GFP positive events, as calculated by FACS at 72 hours post electroporation. Three pulses of 350 Volts for 5 milliseconds gave the highest transfection efficiency. While this read out gave a good indication of what conditions result in high GFP uptake, it did not take into consideration cell survival. Therefore, FACS analysis was used to determine the best balance between transfection efficiency and cell survival. Ultimately, two pulses of 275V for 5 milliseconds was settled upon as the best condition, resulting in high transfection efficiency (>70%) and minimal cell death.

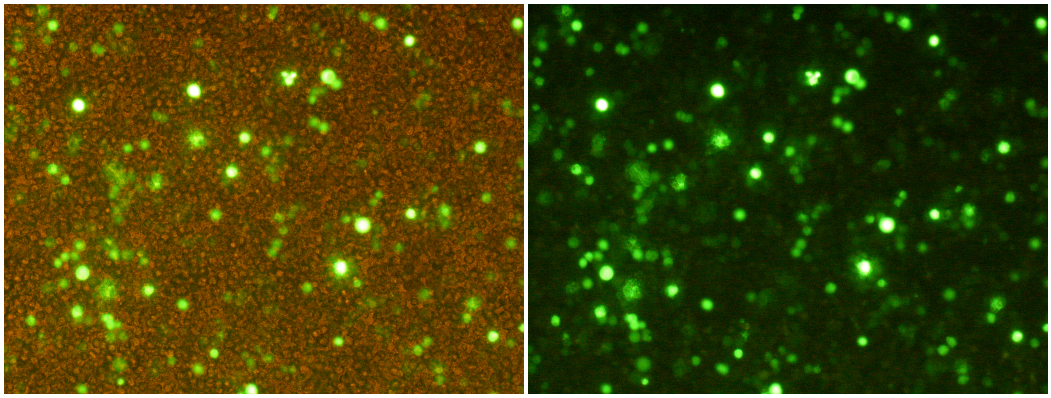

Figure 4.3: K562 Electroporated with GFP

K562 Cells transfected with a CAG driven plasmid coding for GFP, 72 hours after electroporation.

K562 Electroporation Optimization using pGFP		
CONDITION	**PERCENTAGE GFP +ve**	**TOTAL VOLTAGE**
Neg. Control (0V)	4.57%	0
200V, 10ms x3	35.25%	6000
2x (250V, 10ms x2)	44.13%	10000
225V, 10ms x2	51.96%	4500
2x (225V, 10ms x2)	52.91%	9000
200V, 15ms	58.77%	3000
175V, 15ms	63.91%	2625
225V, 15ms	64.29%	3375
300V, 5ms x2	68.63%	3000
275V, 5ms x2	70.99%	2750
2x (200V, 10ms x3)	73.09%	12000
325V, 5ms x3	75.09%	4875
250V, 10ms x2	75.22%	5000
350V, 5ms x3	77.57%	5250

Table 4.1: Further Optimisation of Electroporation Conditions
To optimise the best conditions for electroporation, the 'total voltage' for each condition was assessed ([Voltage] x [Pulse Length] x [# of Pulses]). It was discovered that 350V, 5ms x3 was the best in terms of efficiency, but that similar efficiency with significantly lower levels of cell death could be achieved at 275V, 5ms x2. This was noticed under the microscope and confirmed by cell counts. However, for some experiments, where cell number was not a limiting factor and transfection efficiency was deemed most important, 350V, 5ms x3 was used.

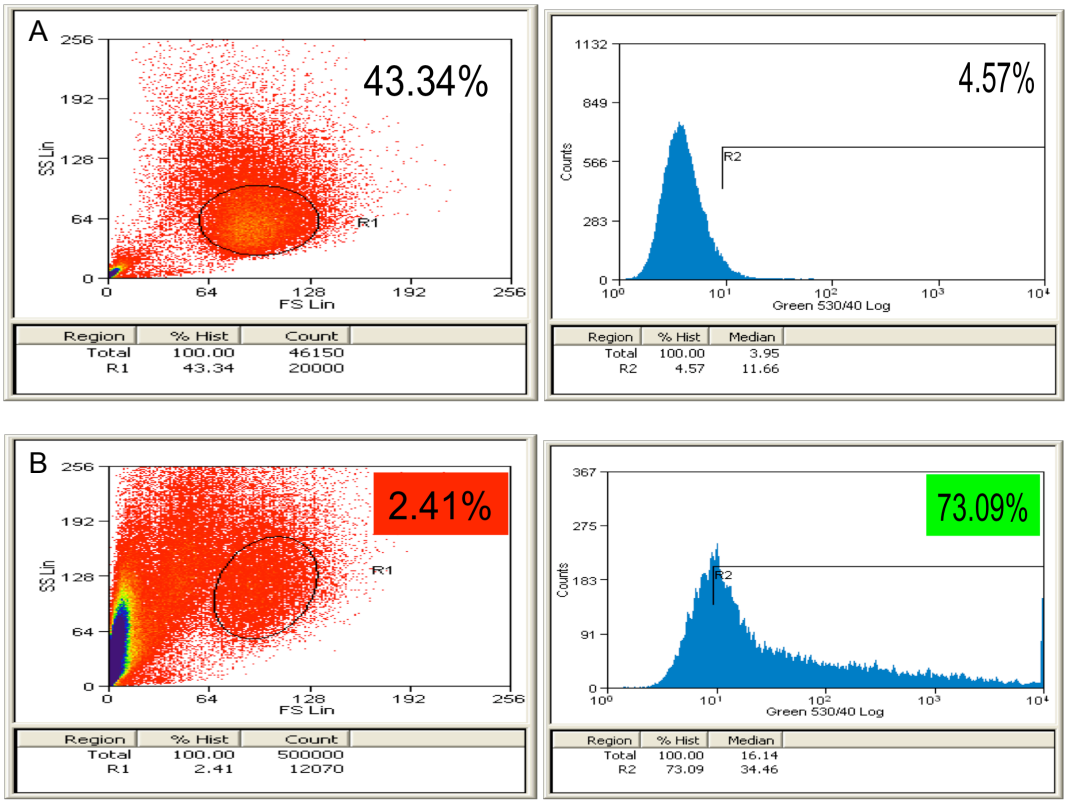

Figure 4.4: FACS plots from Electroporated K562 showing high cell death
A) These plots show the K562 control cells, these cells received no electroporation. The graph on the right shows GFP fluorescence. B) This set of plots is representative of one of the best electroporation conditions in terms of transfection efficiency (notice the shift in GFP), however, it was also the highest in terms of cell death. Comparing the A and B forward and side scatter plots; the majority of the events are smaller and more granular on the B plot, indicating apoptosis; also, notice the large blue section on the very left of the B plot, indicating a sharp increase in small, somewhat granular particles, typically representative of cellular debris. These plots, coupled with visual observation and cell counts, lead us to choose 275V, 5ms x2 pulses as the best condition for electroporation of K562 cells when taking cell death into account. The plot for 275V, 5ms, x2 (not shown) shows cell debris levels comparable to the control group (A) with over 70% transfection efficiency, which is relatively high in comparison to most published mammalian cell electroporator based transfection data.

4.2.2 Testing the Effects of NT2 Total RNA on K562 Cells

After several rounds of electroporation and various electroporation conditions, we found that three 5ms pulses at 350V gave the highest transfection efficiency, while two 5ms pulses at 275V gave the best compromise between transfection efficiency and cell survival. With these optimized electroporation conditions, we moved forward by adding NT2 Total RNA in varying amounts in an attempt to determine whether or not the RNA had an effect in terms of toxicity, phenotype, or ability to boost expression of pluripotency genes.

Following five similar experiments, it was found that all concentrations of NT2 Total RNA tended to increase the levels of GFP expression compared to the control. Figure 4.5 shows the results of electroporating 75 µg, 250 µg, and 500 µg of NT2 Total RNA. Further testing determined that the increase was roughly linear up until about 200 µg total RNA (data not shown), after which point there was no further increase in GFP expression according to FACS analysis and above 200 µg cytotoxicity typically became an issue, which explains the lower GFP levels in the 500 µg sample (Figure 4.5). This phenomenon of total RNA boosting expression may be due to the transfected tRNAs, rRNAs, and microRNAs working to assist in the translation of GFP up to the point of saturation or it might be that the RNA is translated into proteins that help bolster the cell health, preventing or limiting cytotoxic effects from GFP and stress induced by electroporation, but the mechanism is an unclear side effect that requires more study.

In an attempt to determine how much RNA the cells could handle and judge whether or not more RNA lead to better or quicker changes in phenotype, the levels of RNA used were tested from 50 µg up to 500 µg. 500 µg total RNA was found to be the upper limit for a single electroporation of 1 million cells, limited in part by RNA concentration and partly due to high levels of cell death (data not shown). Although some cells would survive up to 500 µg NT2 Total RNA, after repeated attempts it was found that over 400 µg NT2 Total RNA per million cells resulted in high levels of cell death (>70%).

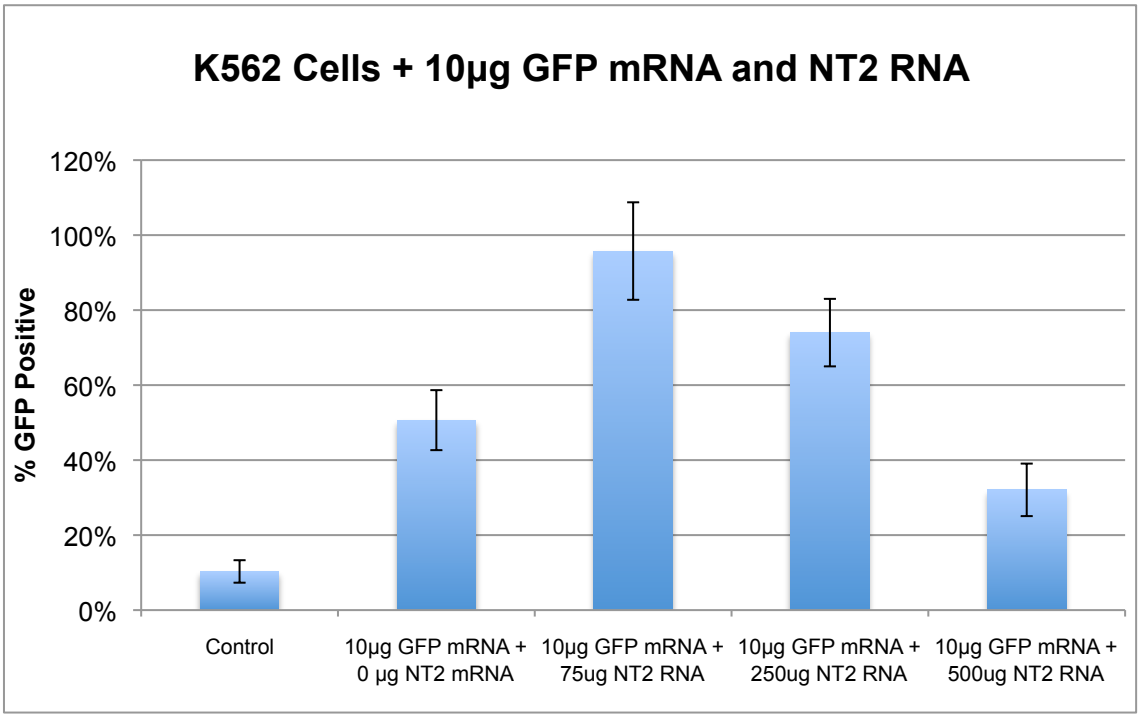

Figure 4.5: FACS results of K562s 4 days post-electroporation with GFP mRNA and NT2 Total RNA

K562 cells were transfected with GFP mRNA and varying amounts of NT2 Total RNA (shown). The GFP was initially added as an indicator of transfection efficiency; however, we noticed that the level of GFP expression appeared to be consistently higher in groups with NT2 Total RNA added. NT2 RNA helps increase the percentage of live cells that express GFP as compared to GFP alone, however it is unclear whether NT2 RNA is helping the GFP translation process, preventing cytotoxic effects of GFP, or some other mechanism is responsible. Interestingly, when a similar experiment was performed with GFP plasmid DNA instead of GFP mRNA (the same CAG driven plasmid used to optimise transfection conditions), NT2 total RNA did not result in the same boost in GFP expression, inferring that the NT2 total RNA is lending 'helper' RNAs to the transfected cells which bolster the expression speed and capacity of the cells. NOTE: n = 3 and error bars represent 1 standard deviation.

4.2.3 K562 Cells Show Uptake of OCT4 from NT2 Total RNA

In order to test the efficiency and relative level of RNA uptake, K562 cells electroporated with NT2 total RNA were then tested by PCR 24 hours later. As shown in Figure 4.6, a million K562 cells were shocked with 100 µg of NT2 total RNA and tested positive for OCT4 mRNA 24 hours post-electroporation, indicating that a substantial level of RNA is successfully making it into the K562 cells. Although this does not prove that the mRNA is being translated into protein, it assured us that it is getting into the cells at a readily detectable level.

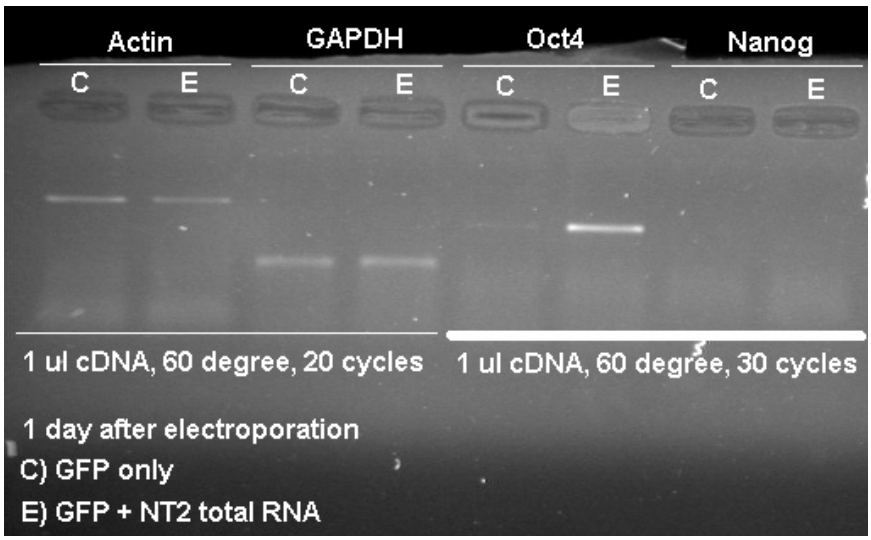

Figure 4.6: K562s 24hrs Post-electroporation of GFP mRNA and NT2 Total RNA
K562 cells were tested for Actin, GAPDH, OCT4, and NANOG by PCR 24 hours after electroporation with 10 µg GFP mRNA (control) and 10 µg GFP mRNA + 100 µg NT2 Total RNA. As shown above, NT2 total RNA is able to enter the cells via electroporation and OCT4 mRNA (from NT2 total RNA) is detectable 24 hours later.

4.2.4 NT2 Total RNA vs NT2 Total mRNA

After a number of experiments involving electroporation of K562 cells with NT2 total RNA, we did not detect any changes in K562 morphology, cell attachment, or phenotype. Although we detected OCT4 mRNA in the K562s electroporated with NT2 total RNA, we were not seeing the changes towards pluripotency that we had anticipated. Despite increasing the levels of NT2 total RNA as much as we could, it did not seem to be making a difference. So, we attempted to determine how we might be able to increase the potency of the pluripotency factors within the RNA we were electroporating into the cells on the basis that more pluripotency factors might be the key to catalysing reprogramming.

Although we were not certain which factors within the total RNA were involved in reprogramming, we know that mRNA is responsible for all the proteins transcribed in the cell. Therefore, mRNA was hypothesised to be the key component of total RNA responsible for the proteins that ultimately catalyse intracellular changes and potentially cause reprogramming. Since mRNA is only 1-5% of total RNA, we hoped to increase the amount of pluripotency factors we could transfect 20 to 100 fold. To isolate mRNA from total RNA we used Oligotex beads [Qiagen] and followed the manufacturer's instructions (See Section 2.11.2). After purifying NT2 total mRNA from total RNA, we tested it in parallel with NT2 total RNA by PCR and found that 40 µg (~10x the amount) of NT2 total RNA contained roughly the same amount of detectable GAPDH, Actin, OCT4, and NANOG mRNA as 4 µg of our purified NT2 total mRNA, inferring that the total mRNA isolation enriches the factors by approximately 10 fold. This increased our confidence that the total mRNA was more or less a concentrated equivalent to total RNA in terms of the effective mRNA content.

4.2.5 Total mRNA Transfection

To determine if the increase in factor concentration by mRNA isolation would allow us to transfect more factors per electroporation, K562 cells were electroporated with 5 µg to 100 µg of NT2 total mRNA (roughly equivalent to 50 µg to 1000 µg of total RNA) and monitored for changes towards a pluripotent phenotype. After growth in K562 and NT2 culture conditions for up to 3 weeks post-electroporation, no significant changes were witnessed. However, western blotting for OCT4 at 4 days post-electroporation showed that pluripotent total RNA and total mRNA was being translated into protein, albeit at low levels compared to the control (see Figure 4.7). At this point, it was unclear how to proceed. After discussion, the conclusion was reached that the K562 cell line may simply be less amenable to reprogramming and/or may inherently be a difficult line to reprogram based on other factors such as gene expression profile or sensitivity to electroporation or RNA factors.

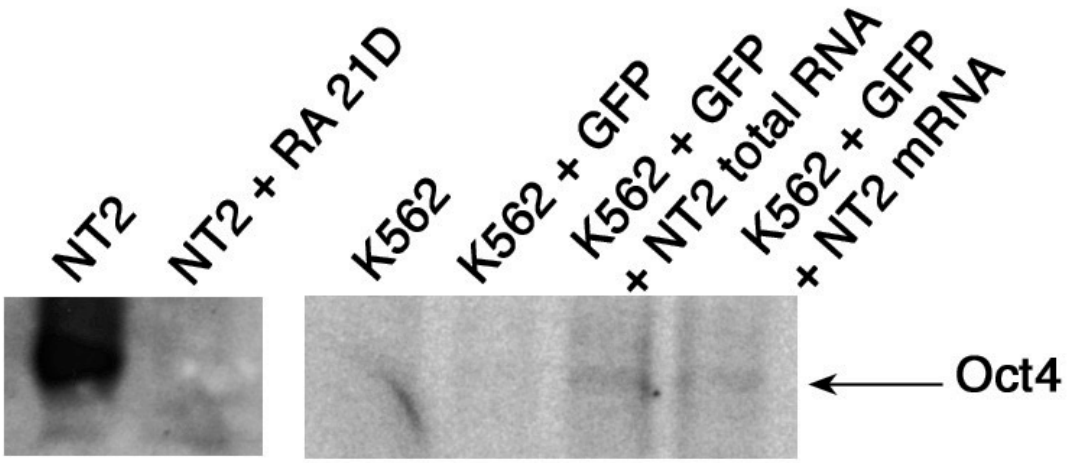

Figure 4.7: Western Blot 4 days post-electroporation with total RNA and mRNA
The block on the left shows the NT2 controls, the one on the left showing OCT4 positive NT2 cells and the other showing OCT4 negative NT2 cells after 21 days of retinoic acid induced differentiation. The four samples on the right show groups of 1 million K562 cells with no RNA, 10 µg GFP mRNA, 10 µg GFP mRNA plus 100 µg NT2 total RNA, and 10 µg GFP mRNA plus 10 µg NT2 total mRNA. The total RNA and total mRNA samples show small amount of OCT4 detected. NOTE: Later experiments (shown in chapter 5) indicate that electroporated RNA is translated into protein, which only lasts until 4 days post electroporation.

4.2.6 Change of Somatic Cell Type

After a number of electroporations with varying amounts of NT2 total RNA and total mRNA without any signs of change in K562 growth rate or phenotype towards pluripotency, the ability of K562 cells to be reprogrammed was brought into question, particularly after fusion experiments did not yield any cell lines or cells that appeared morphologically like pluripotent cells (see Chapter 3). Although we could verify that K562 cells were taking up NT2 mRNA and translating at least some if it in to protein, we were unable to detect any other evidence that changes towards pluripotency had occurred. Also, around this point in time (late 2007), a number of virus induced reprogramming papers were published (supporting the work published in 2006, (Takahashi 2006)) successfully using specific reprogramming factors to induce pluripotency in human fibroblasts. Therefore, we chose to switch to human fibroblasts as our somatic cell type of choice. Also, we began creating constructs to allow us to make mRNAs corresponding to the specific factors shown to induce reprogramming (Takahashi et al. 2007; Yu et al. 2007).

4.2.7 Optimisation of Fibroblast Electroporation

We were able to readily acquire two fetal fibroblast cell lines, similar to those used in reprogramming publications, WI-38 and HuF1. WI-38 cells were derived from normal embryonic (3 month gestation) human female lung tissue and HuF1 fibroblasts were derived from a normal karyotype female first trimester fetal skin and were shown to support the growth of human ES cells. In order to determine which line was best suited for RNA transfection by electroporation, both lines were electroporated across a range of voltages from 0 to 300V with plasmid GFP and the transfection efficiency was compared. Following transfection, it was found that WI-38 and HuF1 cell lines were both amenable to transfection, but HuF1 cells were significantly more robust, surviving electroporation better with higher transfection efficiency than WI-38 cells based on GFP expression levels (both GFP plasmid and GFP mRNA were tested). This was easily seen by eye under UV fluorescence and verified also by FACS (see Figure 4.8). The optimal electroporation conditions for HuF1 were found to be three 5ms shocks at 250-275V (see Figure 4.9). These conditions were used as standard for all future electroporation experiments using HuF1 cells.

HuF1 cells were subsequently used to derive a reporter line linking the OCT4 promoter to GFP expression (see Chapter 3 section 3.2.22), the goal being to optimise the electroporation procedure with HuF1 cells and then use the small stock of OCT4 reporter HuF1 cells to help identify cells that were undergoing reprogramming. Due to the fact that it took a number of passages to isolate the limited number of HuF1+pOCT4-GFP clones, we used them as sparingly as possible as they would only proliferate for 4-6 passages before reaching senescence.

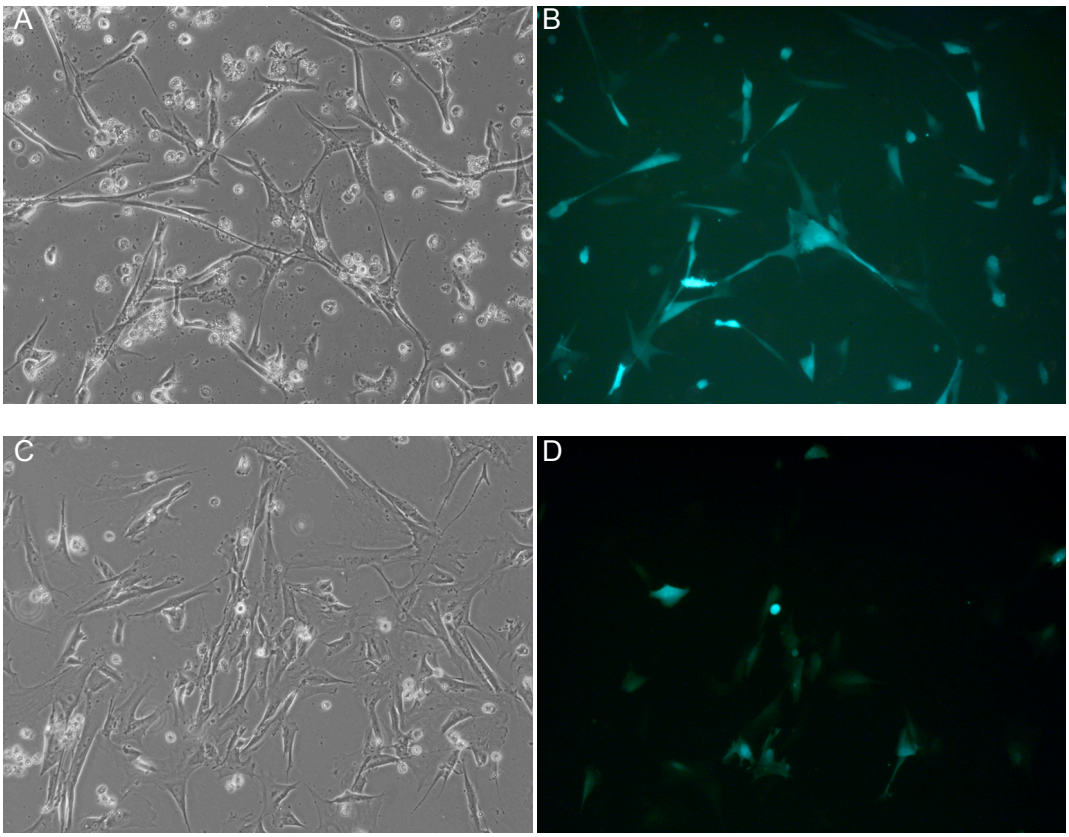

Figure 4.8: WI-38 versus HuF1 fetal fibroblasts
Groups of 1 million HuF1 and WI-38 cells were electroporated with 3 µg GFP plasmid from 0V to 300V, photos of the best conditions 24 hours after electroporation are shown above. A) Phase contrast photo of HuF1 cells, B) HuF1 cells under UV fluorescence, C) WI-38 Phase Contrast, D) WI-38 under UV Flourescence.

A

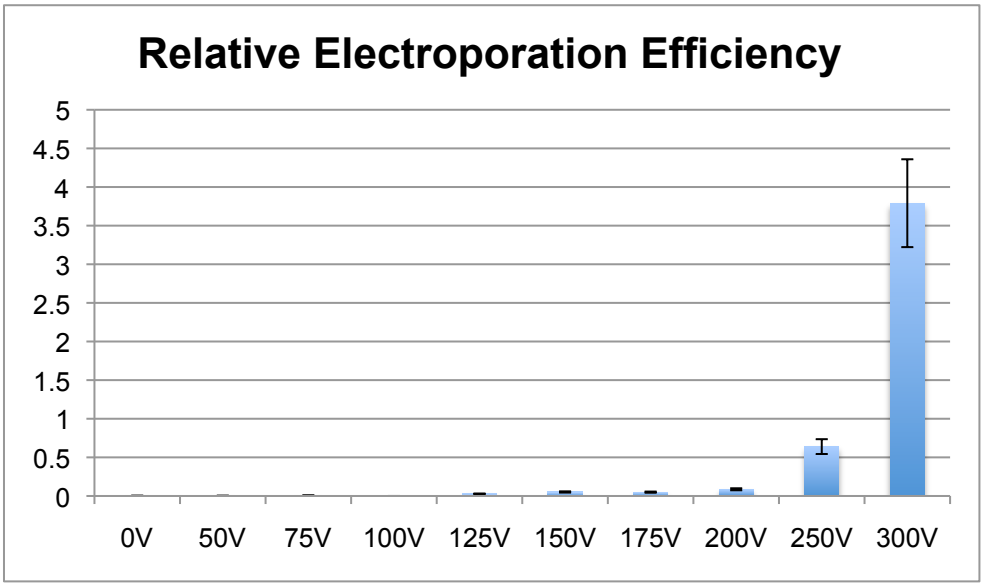

B

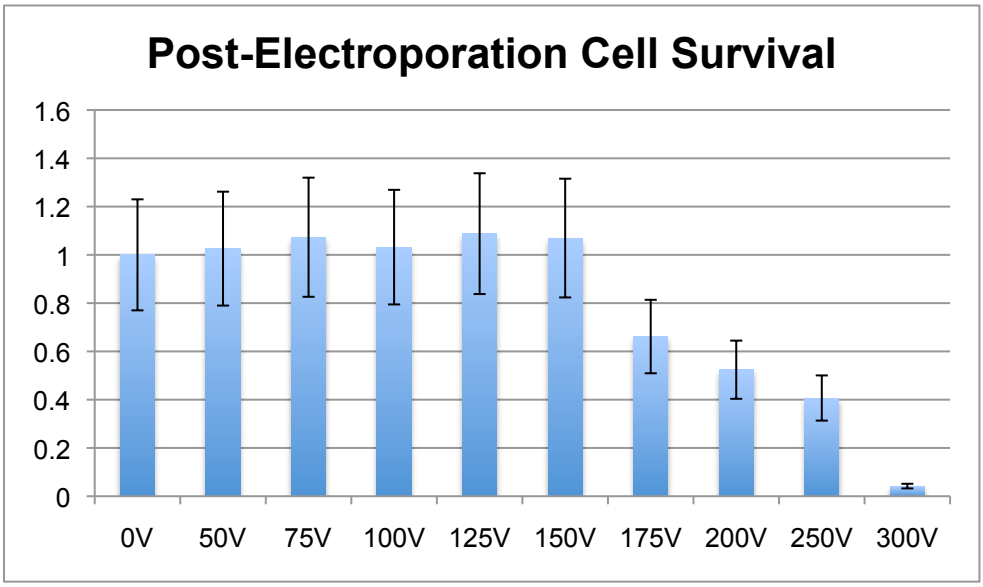

Figure 4.9: HuF1 Electroporation Optimisation
Groups of 1 million HuF1 cells were shocked 3x with 5ms pulses 100 ms apart at the voltages shown above. A) After 3 sets of electroporation at each condition, the average efficiency (percentage of GFP positive cells) was calculated and results were normalised. B) To reconcile transfection efficiency with cell survival, cell counts were normalised post-electroporation against a non-electroporated control group. Although 300V showed the highest efficiency, it also nearly killed all the cells. Further analysis revealed 250-275V as the best range for HuF1 fibroblast transfection by electroporation, resulting in approximately 70% of surviving cells being successfully transfected. NOTE: columns represent mean of 3 replicates (n = 3).

4.2.8 Transfection of HuF1 Fibroblasts with Total RNA

Following electroporation optimisation, HuF1 cells were initially electroporated with Hues1 human ES cell and NT2 total RNA and total mRNA. Based on the assumption that, if HuF1 cells could be overwhelmed with pluripotent RNA (i.e. more pluripotent RNA than endogenous RNA), the gene expression profile would theoretically match that of the pluripotent RNA administered and eventually take on characteristics of pluripotent cells and potentially catalyse full, permanent reprogramming.

A fundamental issue with this approach is RNA dosage. Unfortunately, there is no past precedence on what amount of RNA should be used, therefore it was postulated that approximately 10 cells worth of RNA per somatic cell should to be more than enough to overwhelm a HuF1 cell, taking into consideration that some is lost and approximately 50% of cells die from electroporation. Based on the fact that there is approximately 1 x 10^{-5} µg total RNA in a mammalian cell, with only 1-5% of that being mRNA (1-5 x 10^{-7} µg mRNA/cell), 100 µg of total RNA is roughly equivalent to 10 million cells worth of total RNA (Gardner et al. 2004). Based on this, two groups of 1 million cells were initially electroporated with 100 µg total RNA each, one group with NT2 derived total RNA and the other with Hues1 human ES cell derived total RNA. In addition, 10 µg of NT2 and Hues1 total mRNA was electroporated into two additional groups; equivalent to approximately 10 cells worth of mRNA per somatic cell (based on PCR comparison of Total mRNAnvs Total RNA potency). Following electroporation, the cells were carefully monitored for changes in morphology and growth rate. At 24 hours post-electroporation, cells either appeared similar to the GFP control, or sparser with higher levels of cells death.

Subsequently, two additional groups of 1 million HuF1 cells were electroporated with 40 µg of human ES and NT2 cell total RNA and 5-50 µg NT2 and HUES1 Total mRNA on the basis that the previous dosages tested may have been incorrect. After 2-3

weeks in culture, no changes were seen in any group, and in some samples cells simply senesced. This lead us to conclude that, if there are indeed reprogramming factors present in the RNA, they are not enough to override the endogenous somatic cell gene expression profile and may even be catalysing apoptosis. Initially, we had hoped that we simply needed more RNA per cell, but pursuing this line of testing only lead to increased levels of apoptosis post-transfection.

Around this point in time, constructs to produce specific mRNAs in vitro based on the factors shown to be successful in Yamanaka and Thomsons' publications (OCT4, SOX2, cMYC, KLF4, LIN28, and NANOG) were in the process of being made (Takahashi et al. 2007; Yu et al. 2007). Therefore, we choose to abandon this less specific approach for a more targeted, specific mRNA approach mimicking the viral work but using transiently expressed mRNA of the key factors instead.

4.3 Chapter Discussion

This set of experiments represents a transitional phase in this research project as a whole. Switching from cytoplast mediated reprogramming to an RNA transfection based approach took a considerable amount of time, learning of new techniques, and many iterations of optimisation were required. This work was done in parallel with some of the Chapter 3 work and bridges the gap between the cytoplast work and the use of specific mRNA factors as a means of catalysing phenotypic change. While more work could have been done with total RNA and its affects on bolstering GFP expression, the four factor iPS strategy work prompted us to change the course of our research in an effort to remain at the forefront of current research techniques.

A few of the major issues faced using this RNA transfection approach were dosage and time. Until the publication of Yamanaka and Thomsons' work using viruses, there was no time scale data for reprogramming other than from oocyte and pluripotent cell fusion. While fusion work indicated that reprogramming could occur in as little as 48 hours, the viral approach was initially shown to take 3+ weeks of culture before resulting in iPS cells at a very low rate (~0.01%). At this point in the work, it was assumed that readily apparent changes in cell morphology should occur within a week or two at most, based primarily on fusion and oocyte studies. A large, easily detectable change was expected, but very few changes occurred at all.

Importantly however, through this brief set of experiments, we were able to develop a protocol for administering RNA and mRNA to large numbers of cells. Furthermore, we were able to subsequently detect the mRNA transfected up to 3 days after electroporation and also found that protein derived from the ectopically administered RNA was present at 4 days post-electroporation.

Although there are certainly more subtle changes caused by RNA, which need further study to elucidate, for some applications (such as dendritic cell transformation) RNA transfection is a viable option for affecting cell expression. It may be that the change from somatic to pluripotent is not a simple, one step change, but likely a complex, step wise reversal through a hierarchy of progenitor states, states which need time and a correct balance of factors to accomplish. It may well be that this methodology is better suited for differentiation as opposed to de-differentiation. It would have been interesting to transfect a variety of total RNA samples from various cell types (such as neuronal, hepatic, pancreatic, etc.) into pluripotent cells in an effort to catalyse directed differentiation.

While DNA transfection by electroporation is a fairly well understood process, the use of RNA for the purposes of catalysing forced expression in a large population of cells is not as well understood. However, this work serves as a useful tool, a starting point for the transfection of any variety of RNA into mammalian cells for the purposes of causing temporary gene expression changes. While most applications, such as the derivation of a reporter cell line or study of a specific gene mutation, benefit from transfection of a DNA construct, other applications beyond those suggested here may benefit from a transient gene upregulation and allow for cells to be ‘pulsed’ with specific, dosed levels of RNA that can subsequently be analysed. Unfortunately, all the avenues of research that were pondered could not be explored, instead we moved forward by using specific mRNAs in place of total RNA.

Chapter 5 – Specific mRNAs for Reprogramming

5.1 Introduction

The landmark studies by Yamanaka and Thomson et al. opened up the field of somatic cell reprogramming by showing that only four genes are necessary to catalyse somatic cell reprogramming (Takahashi et al. 2006; Okita et al. 2007; Takahashi et al. 2007; Yu et al. 2007). These initial studies led to a near exponential increase in somatic cell reprogramming publications and review papers. While the long term aim for many researchers is to see the benefits of reprogramming reach patients through regenerative cellular therapies, the methods employed by Yamanaka and Thompson et al. involve using lenti- and retro-viruses that irreversibly alter the genome and have been linked to oncogenesis (Okita et al. 2007). While viruses are effective for deriving cell lines that stably express a gene or set of genes, the problem comes when cells are reprogrammed and the viral insertions are no longer needed. Also, when considering the adaptation of the process to a clinical setting, it is highly unlikely that a regulatory body would approve the use of cells in a patient that contained viral insertions, particularly cMYC, which has been associated with many forms of cancer (Ruggero 2009).

In an effort to activate the reprogramming genes, while avoiding the side effects of viral transduction, we attempted to breakdown the process of reprogramming and this led to the concept of using mRNA transcripts of the key reprogramming factors in place of viruses. By using mRNA instead of viruses, it should be possible to transiently express the factors, cause the same epigenetic changes as the viruses, and then once reprogramming has reached completion, isolate reprogrammed cells based on morphology, leaving the DNA unaltered (See Figure 5.1 for an overview).

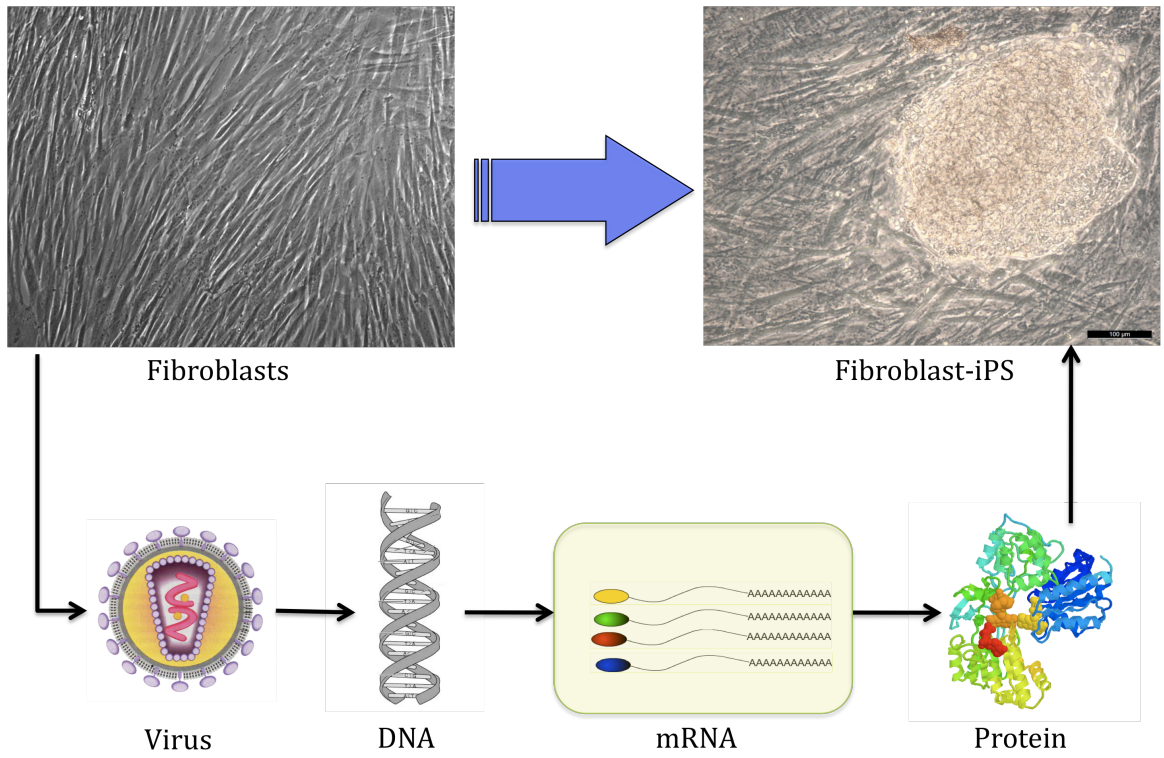

Figure 5.1: Simplified Reprogramming Overview
The figure above shows a simplified overview of the steps involved in somatic cell reprogramming as defined by the process invented by Takahashi et al. (Takahashi et al. 2006). First, fibroblasts are treated with viral particles containing constructs that express the reprogramming factors. Then, the viruses integrate into the fibroblast's genome, causing a permanent change to the DNA and upregulating the expression of the reprogramming factors. Next, the integrated reprogramming factors are copied from the DNA into mRNA. mRNA is subsequently translated into protein. The raw protein reprogramming factors bind, react with, and upregulate many other factors and catalyse changes in the cells' epigenetics, ultimately leading to endogenous production of the genes responsible for the activation and maintenance of pluripotency. Working from this model, we chose to make mRNA in vitro (depicted by the highlighted box) and transfect it directly into somatic cells, circumventing viral integration and preventing permanent changes in genomic DNA. NOTE: The picture on the top left shows MRC5 human fibroblasts and the picture on the top right shows MRC5 iPS cells made in our lab using lentiviral vectors.

5.1.1 The Constant Evolution of Reprogramming Strategies

This chapter represents the largest proportion of this project and it was carried out over the course of approximately two years, from fall 2007 to fall 2009. During this time, rapid developments in the field of somatic cell reprogramming occurred. In an attempt to remain at the forefront, the techniques used were continually adapted and updated to compensate for the improvements published by other groups. To put the speed of development into perspective, Yamanaka's group published the first paper showing that viruses could induce pluripotency in somatic mouse cells in mid-2006; by 2008, Harvard and universities in Toronto and Kyoto devoted whole facilities to iPS cell research, and at the endpoint of this work in late 2009, according to PubMed, over 200 scientific papers and articles have been published on the subject of iPS cells and reprogramming. While it took 17 years from the initial derivation of mouse embryonic stem cells in 1981 until the derivation of their human counterparts, it took only 6 months for iPS cells (Baker 2009). Keeping up with this type of growth and trying to stay ahead of the competition became a central concern throughout this project and required constant examination of the literature and changes to our methods.

While many groups showed that they could achieve reprogramming in a similar manner as reported initially by Yamanaka's group (Takahashi et al. 2006; Yu et al. 2007; Brambrink et al. 2008; Duinsbergen et al. 2008; Maherali et al. 2008a; Maherali et al. 2008b), the majority of publications that followed from the initial 4-factor publication were aimed at improving the reprogramming process, typically by the addition of small molecules, supplementing the factors used with additional 'helper' genes, or altering the growth and iPS isolation conditions (Aoi et al. 2008; Epsztejn-Litman et al. 2008; Hockemeyer et al. 2008; Huangfu et al. 2008a; Huangfu et al. 2008b; Merrill 2008; Nakagawa et al. 2008; Zhao et al. 2008; Baker 2009; Kaji et al. 2009; Kim et al. 2009b; Page et al. 2009). Considering that viruses are highly developed and efficient vehicles for gene integration and upregulation, it was anticipated that our mRNA approach would be, at least initially, less efficient than Yamanaka and Thomson's systems which

was used as a model. With this in mind, we attempted to make use of every additional piece of information we could gather concerning the improvement of reprogramming efficiency.

While initial experiments involved simple testing of the four factors used by Yamanaka's group (OCT4, SOX2, cMYC, and KLF4) (Takahashi et al. 2007), we eventually NANOG and LIN28 were incorporated as suggested by Thomson's group (Yu et al. 2007). Then, in an effort to increase efficiency further, SV40 Large T (LT) was tested (Park et al. 2008b). Beyond additional mRNA transcripts to upregulate key genes, a variety of small molecules that were shown to increase the efficiency and speed of reprogramming were also experimented with, including: 5-Aza-2'-deoxycytidine (5Aza), Tricostatin A (TSA), Valproic Acid (VPA), and BIX-01294 (Li et al. ; Huangfu et al. 2008a; Mikkelsen et al. 2008; Ruau et al. 2008; Shi et al. 2008b; Feng et al. 2009). While other genes and molecules beyond those listed have been implicated in improved efficiency, it was not possible to test every compound reported and only a handful of compounds reported to increase reprogramming efficiency by at least 10-fold were experimented with. These small molecules have all been shown to act on mammalian cell epigenetics, modifying the arrangement or state of the chromatin and subsequently affecting gene expression. Previously, the process of differentiation was initially thought to be irreversible as sections of the chromatin coding for pluripotency genes are gradually blocked off via chromatin and histone methylation and acetylation; however, these small molecules prevent the generational transfer of methylation and acetylation patterns during cell division in a non-specific way, causing changes in the chromatin structure that can result in activation of previously silenced genes, albeit in a relatively uncontrollable, erratic fashion.

In an effort to maintain consistency in an ever-changing field of study, we decided early on to use OCT4 as our primary marker for pluripotency with alkaline phosphatase added as a precursor marker of pluripotency as it became apparent that it was one of

the first markers to be activated during the reprogramming process (Brambrink et al. 2008).

5.1.2 Chapter Aims

I. Construct the necessary plasmids and develop a process to produce mRNA in vitro.

II. Validate that mRNA can be effectively transfected into human fibroblast cells.

III. Test that the mRNA is being translated and converted to protein.

IV. Determine whether or not mRNA transfection is resulting in changes that catalyse pluripotency in fibroblasts.

V. Attempt to isolate iPS cells from fibroblast cultures treated with mRNA factors.

5.2 Results

5.2.1 Designing Specific mRNAs

Based on the genes used by Yamanaka (Takahashi et al. 2007) and Thomson's (Yu et al. 2007) groups, constructs were designed using total RNA from HUES1 human ES cells as a template for making cDNAs of the coding regions of the genes of interest (OCT4, SOX2, cMYC, KLF4, LIN28, and NANOG) with the assistance of post doc, Dr Jie Na. Later, SV40 large T (LT) cDNA, a generous gift from Dr. Robert Weinberg, was used to make a construct for the production of LT mRNA as well. The cloning primers were designed using Invitrogen's Oligo Perfect custom primer design tool (http://tools.invitrogen.com/content.cfm?pageid=9716) and are listed Table 5.1. The process used is outlined in Figure 5.3 and covered in more detail below.

Table 5.1: Cloning primers used

Gene	Accession	Cloning Primers
cMYC	NM_002467	F: gaggctattctgcccatttg R: ctcagccaaggttgtgaggt
KLF4	NM_004235	F: agaaggatctcggccaattt R: atccagtcacagaccccatc
LIN28	NM_024674	F: gtgcgggggaagatgtag R: catggcagtgccaactagc
NANOG	NM_024865	F: gactgagctggttgcctcat R: aaccagaacacgtggtttcc
OCT4	NM_002701	F: caagccctcatttcaccag R: caaaaaccctggcacaaact
SOX2	NM_003106	F: ttcttcgcctgattttcctc R: cccatttccctcgtttttct

Table 5.2: Primers for subcloning into RN3P

Gene	Subcloning Primers
cMYC	F: (EcoRI-Kozak-MYC) gcGAATTCcgccaccATGCCCCTCAACGTTAGCTT R: (MYC-NotI) atGCGGCCGCttacgcacaagagttccgta
KLF4	F: (EcoRI-Kozak-KLF4) gcGAATTCcgccaccATGGCTGTCAGCGACGCGCT R: (KLF4-NotI) atGCGGCCGCttaaaaatgcctcttcatgt
LIN28	F: (EcoRI-Kozak-LIN28) gcGAATTCcgccaccATGggctccgtgtccaac R: (LIN28-NotI) atGCGGCCGCtcaattctgtgcctccgg
NANOG	F: (EcoRI-Kozak-NANOG) gcGAATTCcgccaccATGAGTGTGGATCCAGCTTG R: (NANOG-NotI) atGCGGCCGCtcacacgtcttcaggttgca
OCT4	F: (Sal I-Kozak-OCT4) gcaGTCGACcgccaccATGGCGGGACACCTGGCTTC R: (OCT4_NotI) atGCGGCCGCtcagtttgaatgcatgggag
SOX2	F: (Xho I-Kozak-SOX2) gcctcgagcgccaccatgtacaacatgatggagac R: (SOX2_NotI) atGCGGCCGCtcacatgtgtgagaggggca

Single stranded cDNAs were converted into double stranded DNA using the One-step RT-PCR kit [Invitrogen]. The products of reverse transcription were run on a 1% agarose gel, then bands corresponding to the double stranded gene fragments of interest were carefully excised from the gel using a scalpel and purified with the QIAquick Gel Extraction kit [Qiagen]. Purified DNA fragments for each gene were expanded using the High Fidelity Expansion PCR system [Roche]. For further purification, the High Fidelity PCR products were run on a 1% agarose gel, followed by excision and purification using the QIAquick Gel Extraction kit. The cloning primers used added unique specific restriction sites (Age1 or Sal1 or EcoR1, and Not1 or Xho1) to the ends of the coding regions for ligation into RN3P. After digestion of the DNA fragments, fragments with appropriate 'sticky ends' containing the coding regions for each gene were individually ligated into the RN3P plasmid. RN3P was derived from pBluescript RN3, and genes were inserted between a T3 RNA polymerase promoter and a recombinant polyA tail derived from Xenopus globin (Lemaire et al. 1995) (see section 2.12.1 for ligation protocol). RN3P plasmid was expanded in E. coli and isolated using mini- and maxi-prep kits [Qiagen]. The identity of each gene was confirmed by sequencing [Geneservice Sequencing]. Master stocks of RN3P plasmid for each sequenced gene were stored at -20^{o}C and all mRNA synthesised in vitro was made from this stock. For mRNA in vitro transcription, the plasmids were linearised with Sfi1 enzyme (as linearization improves in vitro transfection efficiency), and capped mRNAs were synthesised using an AmpliCap-Max T3 High Yield Message Maker kit [Epicentre] (see Figure 5.2 for a diagram of RN3P), for more details, see section 2.12.3.

After in vitro transcription, mRNA products were treated with DNAse (0.5 units/10 µL) for 15 minutes at 37^{o}C to remove the template; DNAse was then heat inactivated. To remove salts, left over dNTPs, and other potential contaminants, the mRNA was purified using Illustra S-200 HR Microspin columns [GE Healthcare, 27-5120-01]. Phenol:chloroform extraction was used to isolate and further purify the mRNA (see

section 2.12.5). mRNA was then resuspended in ddH_2O and stored at -80^oC until needed for transfection. To test for contaminants, 1 µL from each sample of mRNA was checked on a 1% agarose gel. mRNA concentration was quantified by spectrophotometer (see Materials and Methods section 2.4.1.3), mRNA stocks were typically stored at 1-5 µg/µL and aliquots were made as needed.

From our stock of RN3P plasmids, we were able to produce a large stock of mRNA for each of the genes of interest. This stock tended to be replenished about every three to six months from the same plasmid stock, ensuring reproducibility between mRNA batches.

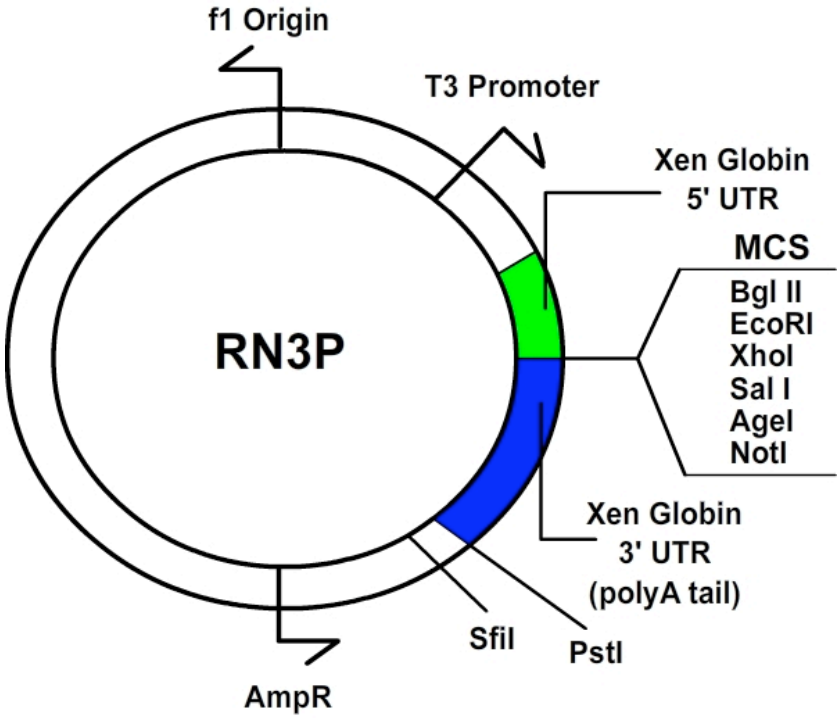

Figure 5.2: RN3P Vector Map
The coding region (cds) for each gene of interest was cloned from HUES1 human ES cell Total RNA using reverse transcription modified to incorporate a kozak region and the appropriate restriction sites for ligation, then inserted into the multiple cloning site (MCS). Prior to in vitro mRNA synthesis, RN3P was linearised using Sfi1 enzyme. T3 RNA polymerase was then utilised to make multiple copies of our gene of interest with Xenopus Globin cap and tail sequences.

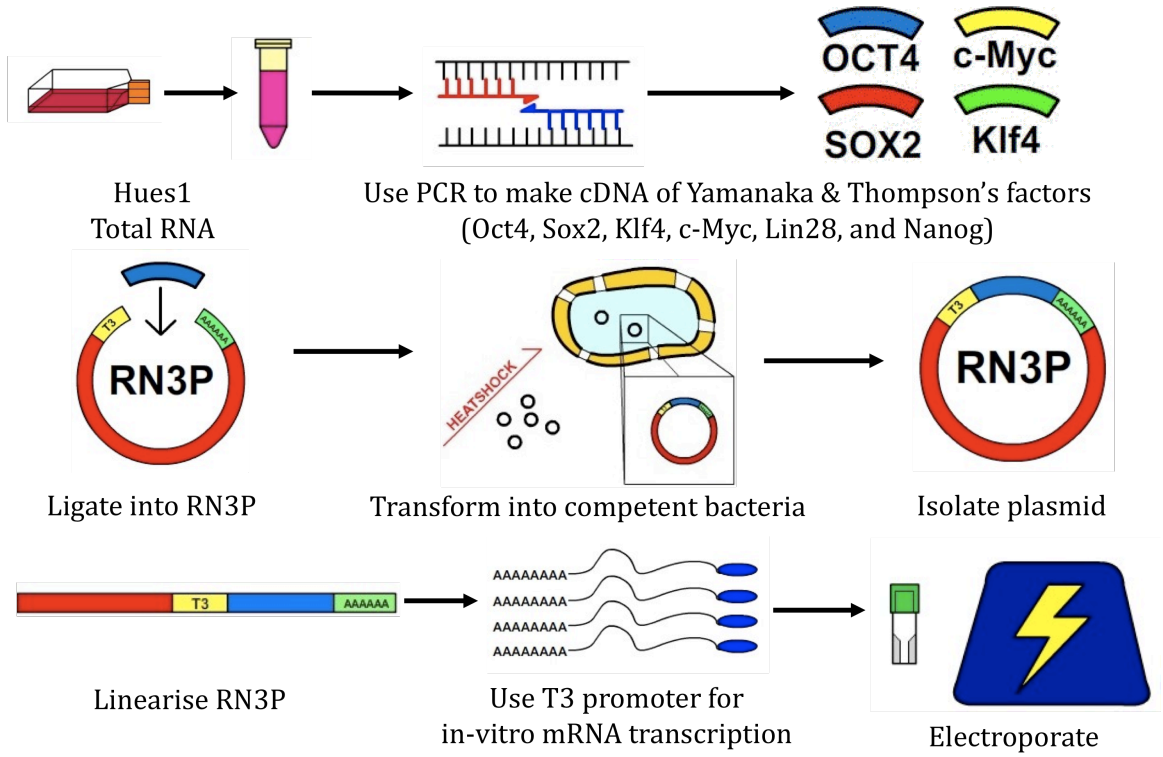

Figure 5.3: Simplified Overview of In Vitro mRNA Production Process
Using Trizol, the total RNA from HUES1 hES cells was isolated and used as a template for making cDNA using gene specific primers. cDNA was then made into double stranded templates and one by one, templates were made for each reprogramming factor. These individual gene templates were then expanded by PCR and the ends were trimmed with enzymes to create specific sticky ends that enabled ligation of the gene templates into RN3P, a plasmid designed for in vitro production of mRNA with a T3 promoter, mRNA cap protein and a polyA tail built in. RN3P was then used to transform competent E. coli via heat shock. Transformed bacteria were plated on agar under penicillin selection, and then individual clones were isolated and tested by restriction mapping followed by gene sequencing. Once we were able to identify clones containing the correct plasmid sequence for each reprogramming factor, we expanded and banked the clones and made a stock bank of RN3P plasmids for each reprogramming factor. RN3P plasmids were linearised using the sfi1 enzyme in preparation for in vitro reprogramming. Using the AmpliCap Max T3 kit [Epicentre], mRNA was transcribed in vitro for each reprogramming factor from the linearised template. mRNA factors were then purified, concentrated, and quantified before eventually being transfected into fibroblasts. NOTE: refer to Materials and Methods section 2.12 for in depth protocol information.

5.2.2 Initial Electroporation of Specific mRNAs into HuF1

Once specific mRNAs for OCT4, SOX2, cMYC, and KLF4 were made, an initial electroporation of all four factors into HuF1 fetal fibroblasts was performed. At the start, there was no basis of comparison. However, it was previously found through electroporation optimisation experiments (section 4.2.7) that approximately 10 µg of GFP mRNA appeared to be the amount needed to visually detect GFP expression under UV fluorescence (see Figure 5.6 for an example) and 10 µg mRNA electroporated into 1 million cells is approximately equivalent to 10 cells worth of mRNA per cell (based on calculations shown in section 4.2.8). Also, from repeated electroporations with total mRNA, toxicity from total mRNA was typically reached at approximately 200 µg mRNA per million cells and above (see section 4.2.2 for more details).

Initially, two groups of 10 µg and 20 µg of each factor (OCT4, SOX2, cMYC, KLF4) along with 10 µg GFP mRNA to visualise transfection efficiency were tested (50 µg and 90 µg mRNA total), with a 10 µg GFP mRNA only group as a control. The previously described optimal electroporation conditions were used (see section 4.2.7), 275V 3x 5ms (see section 2.11.3 for electroporation protocol). It was anticipated that the specific reprogramming factors would quickly catalyse morphological and phenotypic changes, and possibly reprogramming. The expectation was that reprogramming would likely progress in a similar fashion as reported by Yamanaka and Thomson's groups, taking roughly four weeks to detect fully reprogrammed fibroblasts that appear ES-like; or possibly faster, since there are no viral integration and transcription steps.

After electroporating both groups with a mix of OCT4, SOX2, cMYC, and KLF4, it became clear that the mRNA was having a different effect on the fibroblasts than the viral system. As shown in Figure 5.4, a 1:1:1:1 ratio of the factors caused high levels of cell death at 24 hours post-electroporation compared to the GFP control. Instead of boosting cell survival or proliferation, only 15-20% of cells treated with 10 µg of each

factor and 1% of cells treated with 20 µg of each factor survived (as judged by counts of the cells that attached at 24 hours post-electroporation versus the number of cells electroporated). By 72 hours post-electroporation, all cells in the 20 µg group were no longer viable. Since a mix of equal amounts of each factor did not catalyse any changes, only cell death. It was suspected that one or more of the factors was out of balance with the others, resulting in increased levels of apoptosis. To move forward from this point, cells were transfected with each factor individually, comparing the cell survival, and monitoring for changes in proliferation and morphology.

A

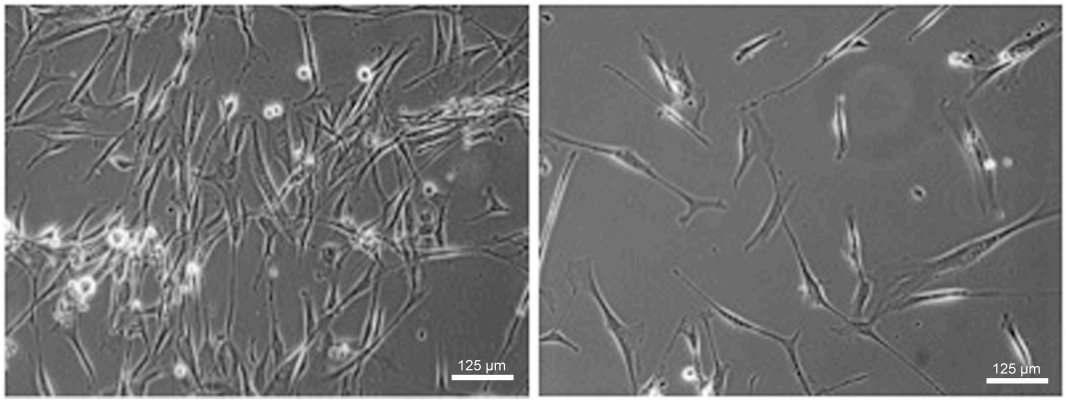

10 µg GFP only (10x) 10 µg of each factor + 10 µg GFP (10x)

B

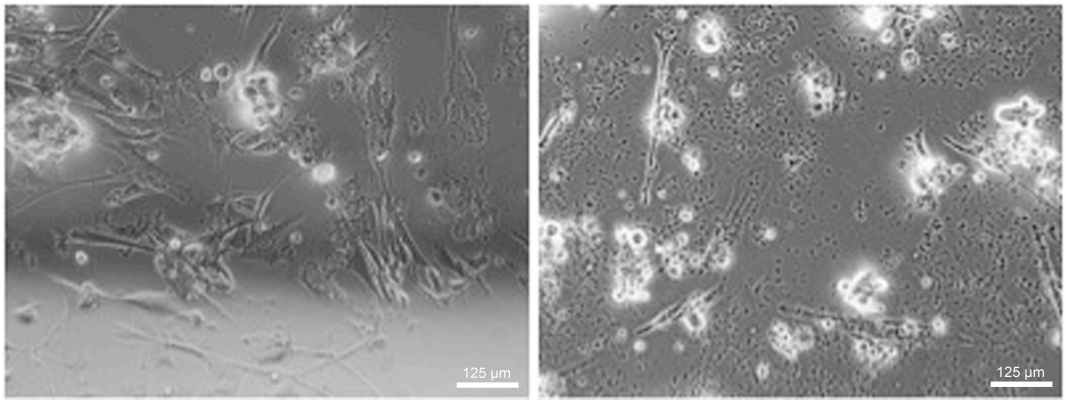

20 µg GFP only (10x) 20 µg of each of the 4 factors (10x)

C

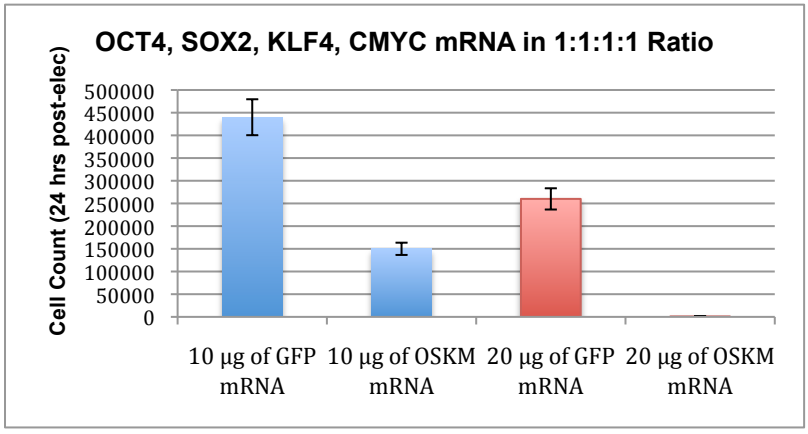

Figure 5.4: Initial test of Yamanaka Factors on HuF1 fibroblasts
A) Compared to the GFP control, OCT4, SOX2, KLF4 and cMYC (OSKM) in equal amounts (10 µg each) resulted in significantly higher levels of cell death and no signs of morphological change. B) Increasing the amount of the factors to 20 µg each, only increased the level of cell death, leaving approximately 1% of cells surviving at 24 hours post-electroporation and no surviving cells by 72 hours post electroporation. Notice that 20 µg GFP is relatively toxic, however, the majority of the field of cells treated with 20 µg of reprogramming factors contains cell debris with very few attached cells. C) Cell counts from 24 hours post-electroporation.

5.2.3 Electroporation of Individual mRNA Factors

After multiple attempts, it was found that a 1:1:1:1 ratio of OCT4, SOX2, cMYC, and KLF4 led to apoptosis; therefore, each of the factors was tested individually. Constructs for producing LIN28, NANOG, OCT4-GFP, OCT4-Cherry, and OCT4-3HA mRNA in vitro were also made, so these were tested individually as well. OCT4 fusion protein mRNA constructs were designed by Dr. Jie Na for the purposes of tracking OCT4 localisation and estimating transfection efficiency. They were made by replacing the OCT4 stop codon with a linker sequence connected to GFP, Cherry, or 3HA under the control of the same OCT4 promoter.

Groups of 1 million cells were electroporated as described in section 2.11.3 (1 million HuF1 in 200uL cell projects buffer + mRNA, shocked at 275V, 3x 5ms) with 10 µg of individual reprogramming factors (OCT4 wt, OCT4-GFP, OCT4-Cherry, OCT4-3HA, SOX2, cMYC, KLF4, LIN28, and NANOG). Photos were taken 24 hours later and cells were fed DMEM +10% FBS every four days and monitored daily over the course of four weeks (or until senescence) for changes in fluorescence, morphology, and rate of proliferation.

5.2.3.1 OCT4 mRNA Temporarily Boosts Proliferation

Four variants of human OCT4 were tested, OCT4 wild type (wt), OCT4-GFP, OCT4-Cherry, and OCT4-3HA. The tagged forms of OCT4 were designed for the purpose of visualising both the transfection efficiency and the localisation of OCT4 within the cell. At just 24 hours post-electroporation, it was clear that the cells transfected with 10 µg of all variants of OCT4 survived better and/or proliferated more quickly than any of the other groups, including the GFP mRNA control (see Figure 5.6, 5.7, and 5.8). Also, as shown in Figure 5.7 (B, C, and D), the OCT4 variants appeared to be localising correctly within the cell, residing primarily in the nucleus.

Within 48 hours of electroporation some of the sample groups treated with OCT4 mRNA appeared to form tight groups (as shown in Figure 5.7 C) and appeared 'piled up' or raised with indistinct cell boundaries. Judging by the red cherry stain in Figure 5.7 C2, it's as though the cells electroporated with OCT4-Cherry mRNA migrated towards each other and bundled together. Over the course of monitoring the cells, it was noticed that the fluorescence intensity tended to drop below visible levels by four days post transfection.

To test OCT4's effect on cell survival and proliferation, groups of human fetal lung fibroblasts were transfected with 1, 5, 10, and 20 µg OCT4 wt mRNA in triplicate, then cell counts were taken every other day to assess what effect, if any, OCT4 mRNA has on fibroblast proliferation and survival post-electroporation. As shown in Figure 5.5, all levels of OCT4 tested showed increased proliferation as judged by the slopes of the OCT4 treated samples compared to the GFP and non-mRNA treated controls. Also, OCT4 mRNA does not show increased survival, and in some cases (>5 µg), cell number initially decreases. Higher levels of OCT4 mRNA appear to slow or may even kill cells before eventually boosting proliferation for up to 5 days post transfection. Although the data is not shown here, groups receiving >10 µg of OCT4 mRNA showed continued proliferation for up to 2 days longer than those treated with $\leq$5 µg.

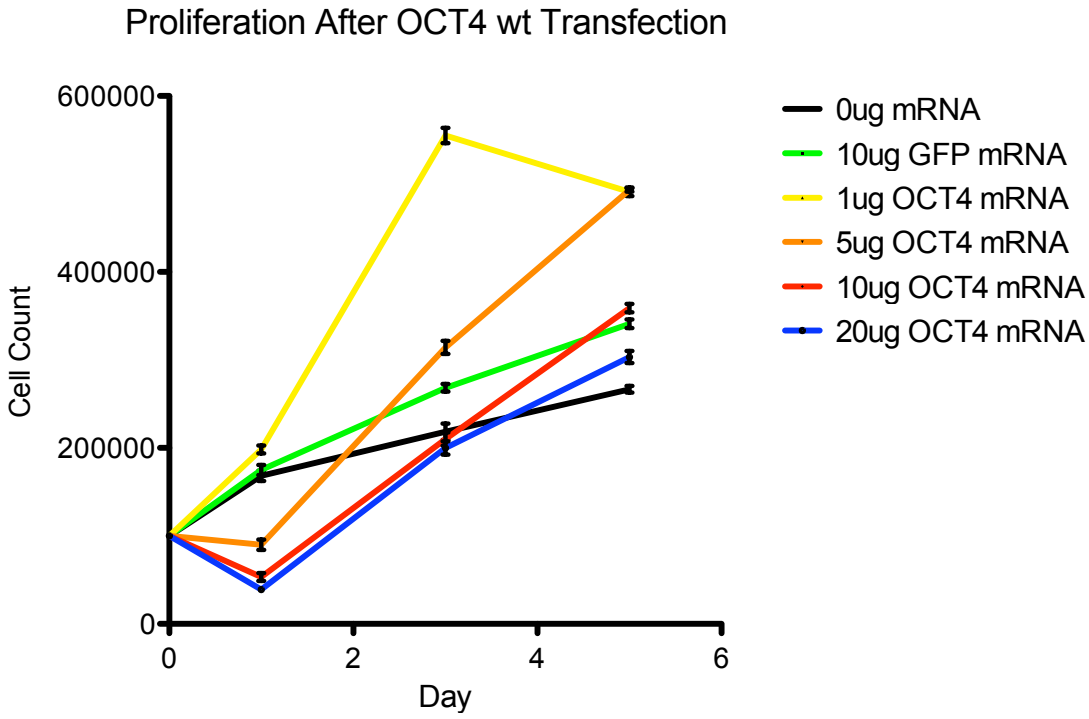

Figure 5.5: OCT4 mRNA boosts proliferation
Electroporation of fibroblasts with OCT4 mRNA resulted in increased, short-term proliferation. The black line indicates the control, notice how all treated groups have a steeper growth curve, indicating an increased rate of proliferation. Although 10 and 20 µg groups appear to have suffered from mRNA toxicity, they still quickly recovered and proliferated to higher levels than the control by day 5 post-transfection.

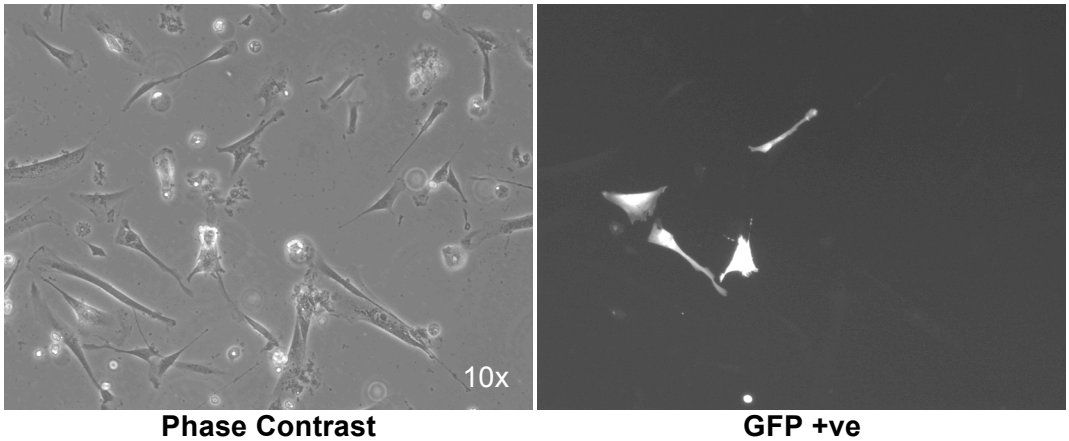

Figure 5.6: 10 µg GFP mRNA control - 24 hours post-electroporation
This figure has been included as an initial point of reference. The cells were electroporated with 10 µg GFP mRNA as a control and compared to other populations of cells shocked with 10 µg of individual factors.

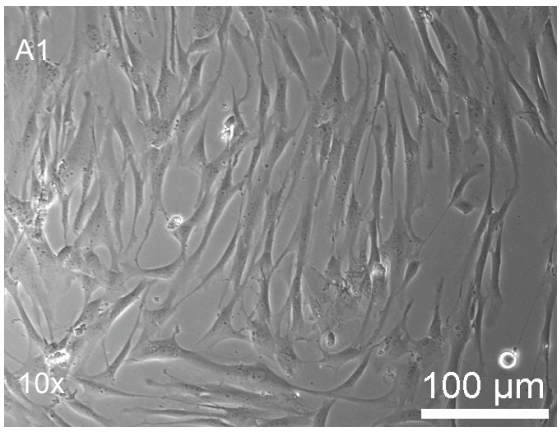

Figure 5.7: 10 µg OCT4 mRNA in HuF1
A) HuF1 fibroblasts electroporated with OCT4 wt, B) HuF1 transfected with OCT4-GFP showing nuclear localisation, C) OCT4-Cherry causes aggregation of HuF1 cells within 48 hours, D) OCT4-Cherry shows nuclear localisation in HuF1 cells.

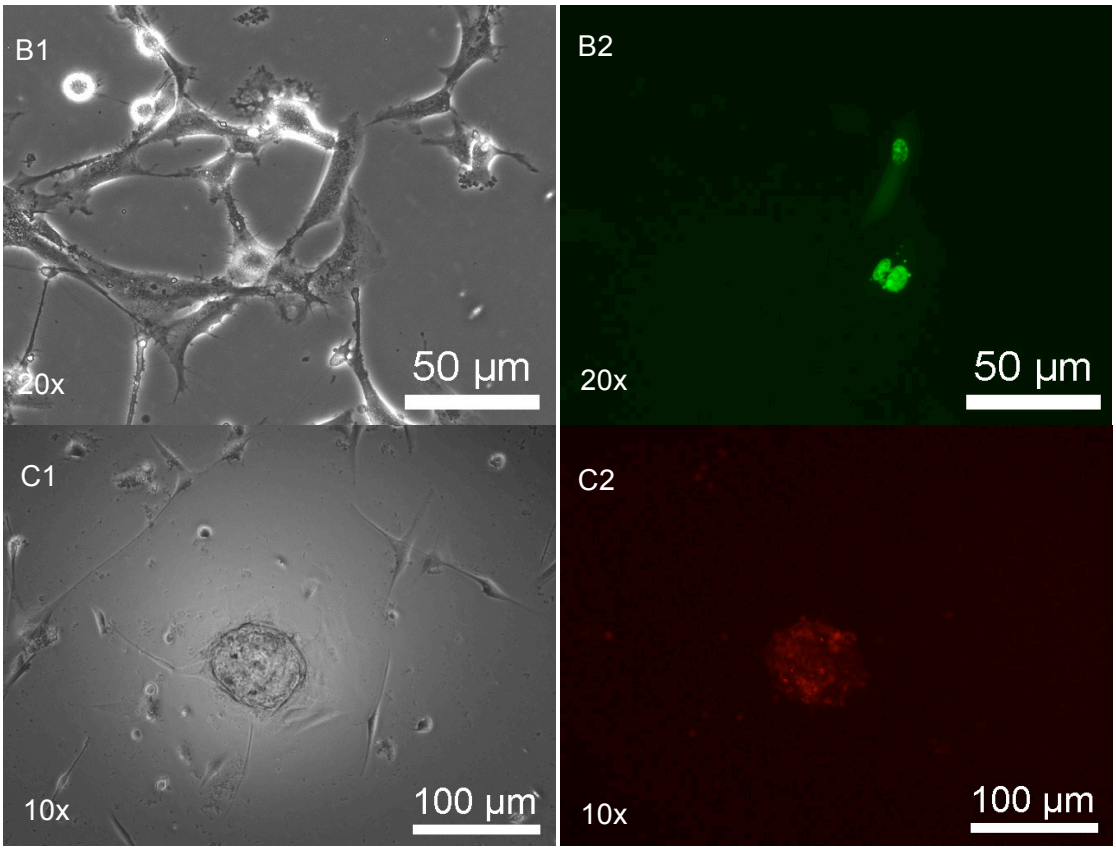

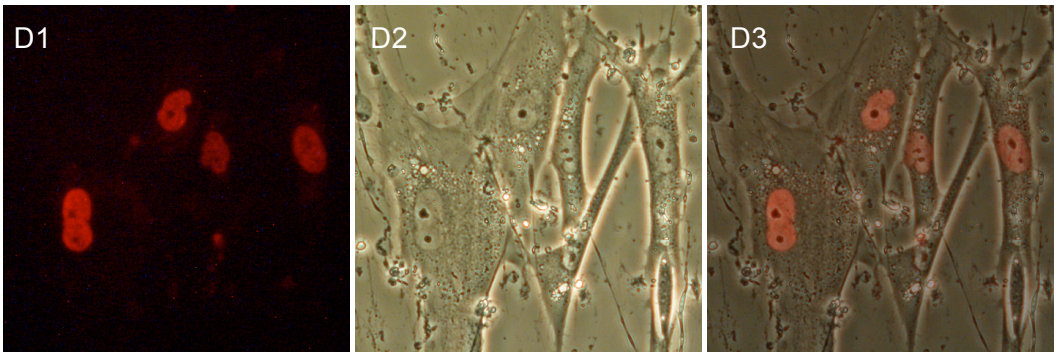

5.2.3.2 SOX2 mRNA Holds Fibroblasts in S phase

After transfecting HuF1 fibroblasts with 10 µg SOX2 mRNA, it was noticed that SOX2 reduced cell proliferation. By day 3, cells transfected with SOX2 were markedly less confluent (see Figure 5.8). Cell counts confirmed that, by 3 days post transfection, the number of SOX2 treated cells was approximately 50% that of the GFP control and less than 25% as compared to OCT4 treated cells (data not shown). Also, cells formed radial patterns more frequently than controls and other factors tested (See Figure 5.10). Although the cells did not clump or bunch together as seen in the OCT4 groups, the SOX2 did influence the orientation of the cells in relation to each other, frequently forming small tight clusters. Typically the diameter of these clusters was noticeably less than that of aggregates seen in OCT4 treated samples. This clustering effect may relate to the role SOX2 plays in neuronal cell lineages since neurons are known to form rosettes in culture that have a similar radial orientation.

To further investigate the role of SOX2 on fibroblasts, with the help of Jie Na and Mark Jones, the effects on cell cycle were examined using propidium iodide (PI) and FACS. As shown in Figure 5.9, groups of 10^5 human fibroblasts were treated with 5 µg GFP, OCT4, or SOX2 mRNA then their cell cycles were monitored. After 3 days, no marked change was seen, but at day 4, when evidence of products from mRNA typically drops (i.e. lack of GFP fluorescence and detection of protein), an increased number of SOX2 treated cells were found to be in S-phase (see Figure 5.9).

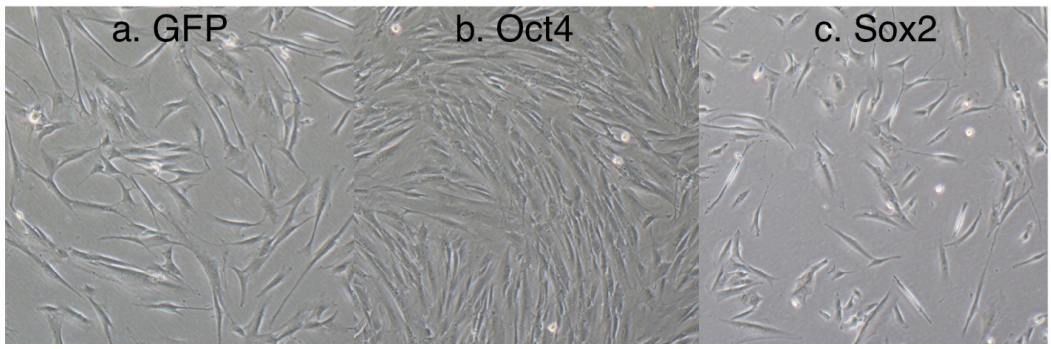

Figure 5.8: Comparison of fibroblast proliferation 3 days post mRNA transfection
Equal numbers of cells were each transfected with equal amounts of each mRNA shown above and photographed at 3 days post transfection. As shown, SOX2 treated cells are markedly less confluent than controls and do not confer the proliferation boost like OCT4 mRNA.

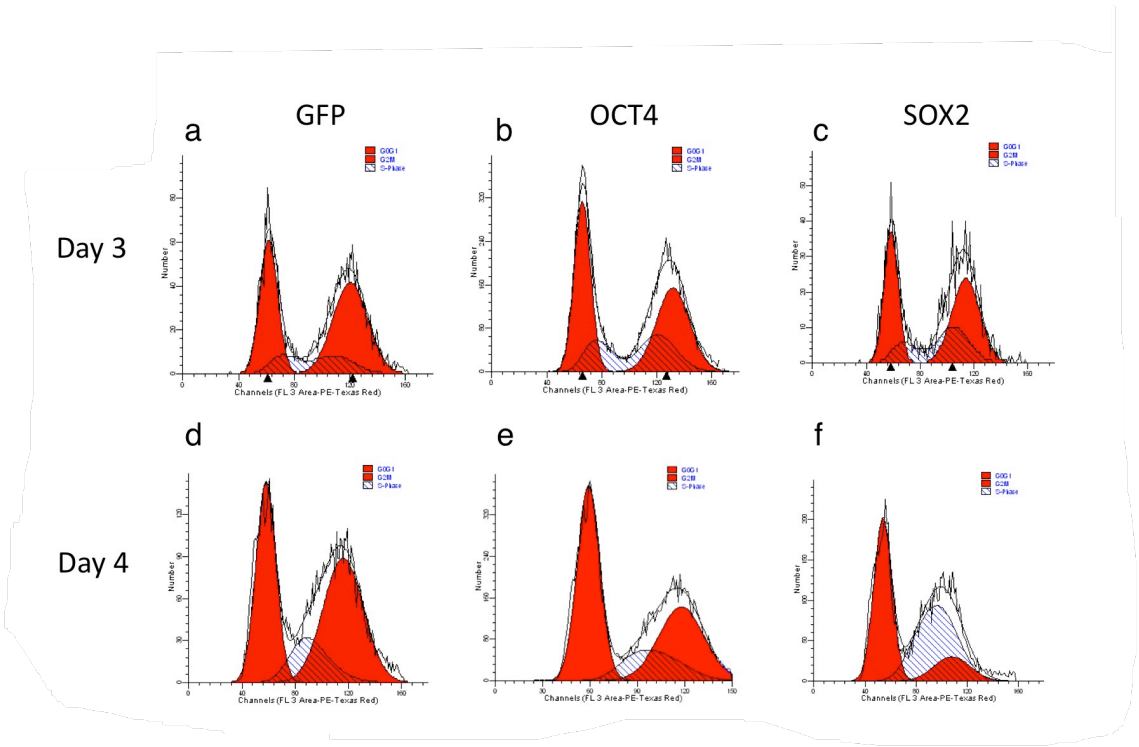

Figure 5.9: Propidium Iodide and FACS reveal that SOX2 holds cells in S-phase
Groups of 10^5 human fibroblasts were transfected with 5 µg mRNA (GFP, OCT4, or SOX2) and there cell cycles were monitored by FACS using propidium iodide. Plots a-c represent 3 days post transfection, and d-f are 4 days post mRNA transfection. The first red peak in each graph represents the G0/G1 phase, the second red peak is G2M phase, and the blue and white areas represent cells in S phase. The increased number of cells in S-phase was noted as significant compared to GFP control, as well as the other factors tested, including OCT4, cMYC, and KLF4 (data not shown).

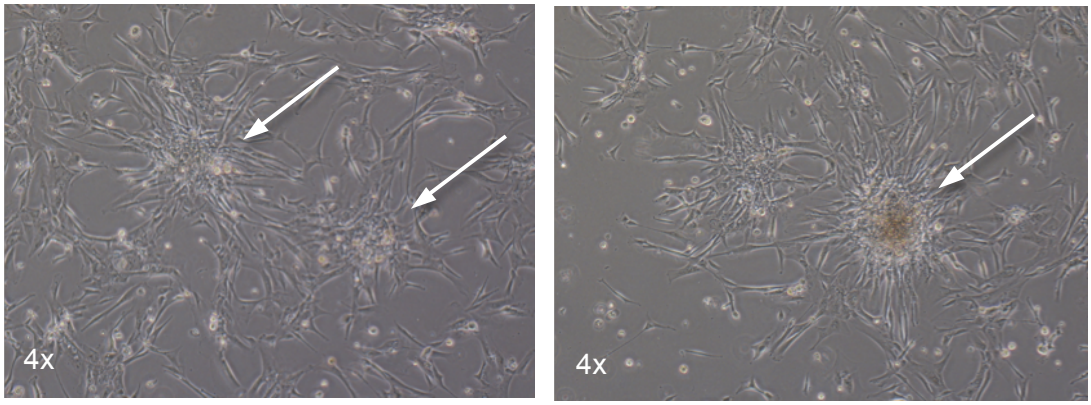

Figure 5.10: HuF1 cells Electroporated With 10 µg SOX2
At 24 hours post-electroporation with 10 µg SOX2 mRNA, the subtle change in cell orientation toward a radial pattern is shown above. Subsequent electroporations revealed that higher doses of SOX2 increase the frequency of radial clusters.

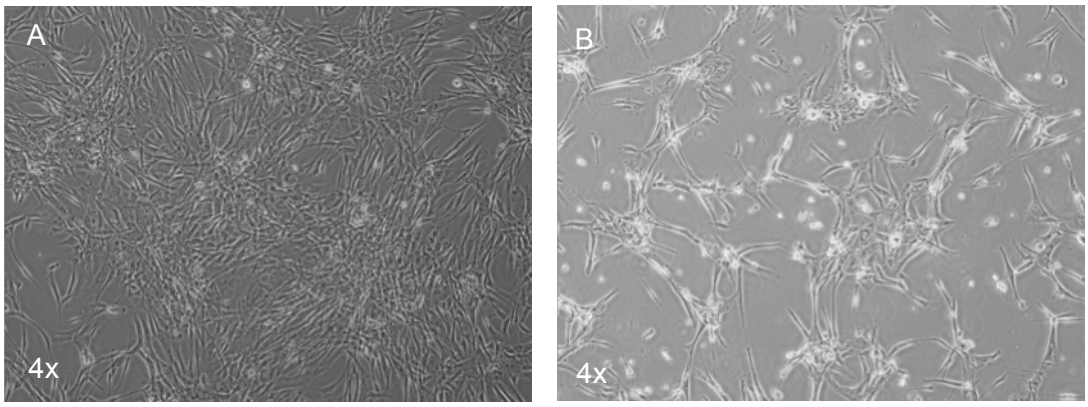

Figure 5.11: OCT4 vs cMYC mRNA
These photos show HuF1 cells 24 hours after electroporation with A) 10 µg OCT4 mRNA and B) 10 µg cMYC mRNA. Notice the marked difference in cell density and number. Interestingly, when mixed in equal proportions, the negative effects of cMYC on proliferation overrode the positive effect of OCT4 (as in Figure 5.4 A).

5.2.3.3 cMYC mRNA has Negative Effect on HuF1 Proliferation

Whereas OCT4 appeared to have an immediate positive impact on HuF1 fibroblasts, 10 µg cMYC mRNA had an obvious negative effect (see Figure 5.11). Noticeably less cells survived and attached after transfection and unlike the other factors tested, cells transfected with cMYC did not recover well and in most samples, all cells reached senescence or apoptosis within a week of electroporation, preventing accurate cell counts. This result was surprising given that cMYC has been linked to increased proliferation, oncogenesis, and immortalisation (Biro et al. 1993; Boxer et al. 2001).

5.2.3.4 KLF4 mRNA has no Noticeable effect on HuF1

Samples of 1 million HuF1 fibroblasts were electroporated with 10 µg KLF4 mRNA and at 24 hours post transfection, the cell population looked largely unaffected in relation to the control; no changes in morphology or proliferation were detected compared to control cells electroporated with 10 µg GFP mRNA.

5.2.3.5 Effect of 10 µg NANOG mRNA on HuF1

Cells transfected with 10 µg NANOG mRNA were noted to have a lower plating efficiency than the GFP control, however, it was not until 2-3 days post transfection that it became clear that the NANOG was having an effect. They appeared normal and remain attached, but compared to controls, the cells proliferated at a noticeably slower rate. This effect may parallel the effect of SOX2, but NANOG was not included in that analysis. Further analysis is needed to determine how NANOG is linked to slower cell proliferation.

5.2.3.6 Effect of 10 µg LIN28 mRNA on HuF1

Transfection of 10 µg LIN28 mRNA, like KLF4, did not appear to have any noticeable affect on the cells. They attached and proliferated at the same rate as the control with no noticeable changes in morphology as they grew out.

5.2.3.7 Conclusions

After electroporating 10 µg of each individual factor into samples consisting of one million HuF1 cells, we concluded that OCT4 improved proliferation and survival while cMYC had a noticeably detrimental effect and NANOG resulted in limited proliferation of HuF1 cells in vitro. SOX2 contributed to changes in morphology that may be linked to its association with neural phenotypes. These results prompted further experimentation concerning dosage of each factor and how that plays into the reprogramming process.

In order to determine what levels of the factors were best for reprogramming, we attempted to look for a positive control amongst published data. One of the main issues encountered was that no other group has published data showing the actual process of reprogramming, the step by step gene changes that occur over time after transfection with virus or any other form of the reprogramming factors. Therefore, it was unclear as to what amounts of the factors are necessary to catalyse the changes desired. In the case of viral transduction, it seems that there is a sort of 'lottery' aspect to the process where one is giving all the necessary ingredients for reprogramming to the cells and about 1 in 10,000 (0.01%) actually takes up the necessary combination of viral integrations with the correct levels of expression to provide the proper amounts of each factor required to result in reprogramming. While the number of viral integrations has been reported in some publications, this information is not a good representation of the actual level of viral gene transcription and is a poor indicator of the proportions of the factors needed.

5.2.4 Protein Levels of Factors after mRNA Transfection

Previously published data has shown that fusion between a human ES cell and a fibroblast can result in reprogramming (Cowan et al. 2005); therefore, we decided to test for the inherent protein levels of the reprogramming factors in the fibroblasts and compare them with HUES1 human ES cell levels by Western blot. HuF1 fibroblasts were found to have very little (if any) endogenously expressed OCT4, SOX2, cMYC, KLF4, NANOG, and LIN28 protein compared to HUES1 human ES cells (as shown in Figure 5.12). In order to determine how much electroporated mRNA is translated into protein, samples of 1 million cells were electroporated with 10 µg of mRNA of each factor. Then, at 48 hours post-transfection, 200,000 cells from each group were taken for Western blotting (as shown in Figure 5.13). From this western blot, we were able to estimate the amount of protein expressed from 10 µg mRNA in HuF1 cells as compared to a human ES and NT2 control. As the data shows, 10 µg of mRNA does not result in equal levels of translation into protein. For instance, 10 µg of cMYC appeared to result in the largest band, indicating that a small amount of cMYC is more than enough to equal or surpass human ES levels. From this data, a set of the estimated ratios between human ES cell expression and HuF1+10 µg mRNA expression was made:

Factor:	**HUES1:HuF1+10 µg mRNA**
OCT4	1:0.25
SOX2	1:0.2
KLF4	1:10
cMYC	1:20
NANOG	1:2
LIN28	1:0.1

Even though the endogenous levels of cMYC and KLF4 in human ES cells appear very low by western blot (Figure 5.12), we were able to detect them by PCR (data not shown). Also, although OCT4-GFP was picked up by western blot with the OCT4 wt antibody, the OCT4-3HA and OCT4-Cherry forms of OCT4 were not detected (Figure 5.13). It was concluded that the antibody used to detect OCT4 was unable to bind due to the 3HA and Cherry fusion protein tails interfering with the interaction. Whether or

not our fusion protein tails have affected the functionality of OCT4 is unclear, but we know from fluorescence that the OCT4-Cherry is correctly localising (Figure 5.7) and using a 3HA antibody, that OCT4-3HA protein is being translated (Figure 5.13). This effect may just be related to how the antibody binds to the OCT4 protein and not necessarily indicative of altered protein function. However, where possible, OCT4 wt mRNA has been used to prevent confounding results.

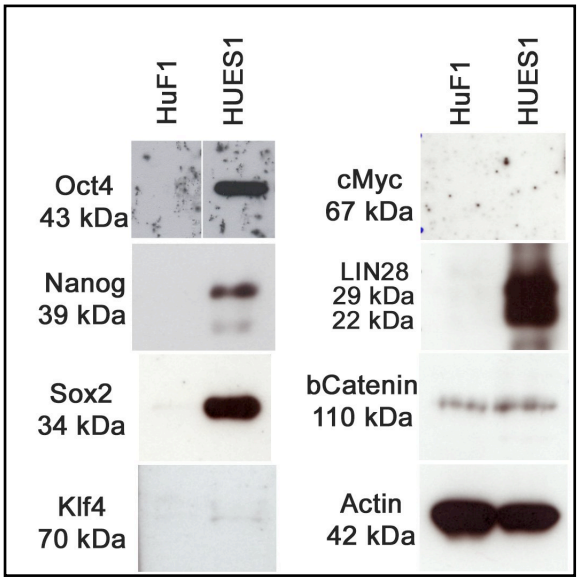

Figure 5.12: Western blot comparing protein levels in HuF1 and HUES1
As an initial basis of comparison, HuF1 fibroblasts and HUES1 human ES cells were taken for Western blot analysis to gauge the levels of inherent, endogenous reprogramming factor protein production (see M&M section 2.8 for Western protocol).

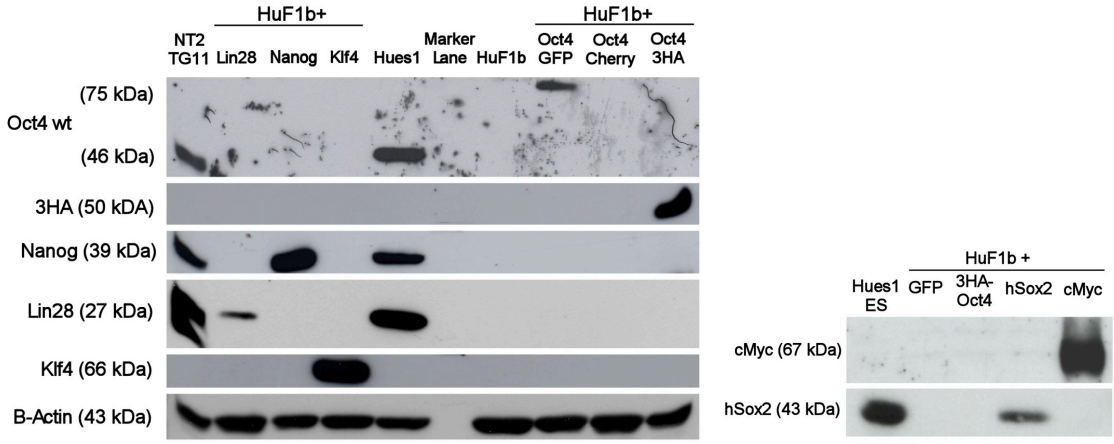

Figure 5.13: Comparison of mRNA transfected HuF1 to Pluripotent Cell Lines
48 hours after transfection with 10 µg of each of the individual mRNA factors listed under 'HuF1b+', 200,000 cells from each group were tested for protein expression by Western blot. Hues1 human ES cells and NT2.TG11 EC cells were used as controls. HuF1 cells electroporated with mRNA factors expressed the appropriate proteins. Correct protein sizes listed in parentheses. NOTE: OCT4-GFP fusion protein is larger due to the GFP fusion protein. Only OCT4-Cherry was not detected, this is likely due to the Cherry fusion protein tail interfering with the antibody used for detection. Localisation experiments show that it is expressed and does properly localise in the nucleus.

5.2.5 Optimisation of Amounts of mRNA Factors

After successfully detecting the uptake and translation of the mRNA transcription factors individually, the aim was to optimise levels of the factors to prevent apoptosis and improve levels of cell survival and proliferation. Based on the western blot data, we attempted to match the amounts of each mRNA factor to the amount detected in HUES1 human ES cells. However, this combination still led to over 50% cell death. Therefore, anecdotal evidence from electroporation of the factors was used, it was decided that an increase in the amount of OCT4 mRNA and a decrease in the amount of cMYC mRNA should be beneficial and decrease apoptosis. While 10 µg KLF4 mRNA showed higher expression than the HUES1 control, KLF4 did not appear to have a significant detrimental effect when tested individually on HuF1 cells and was therefore left at the 10 µg dosage. SOX2 was also initially left unaltered at 10 µg per 10^6 cells.

After testing a range of mRNA combinations, we found that 20 µg OCT4, 10 µg SOX2, 1 µg cMYC, and 10 µg KLF4 not only prevented the apoptosis seen previous, but actually led to increased cell survival and proliferation compared to the GFP control as judged by cell counts done at 24 and 96 hours post-electroporation (see Figure 5.14). From the groups tested, cMYC appeared to be the primary contributor to cell death with groups receiving less than 5 µg cMYC per million cells surviving and proliferating, while more than 5 µg per million cells led to near complete apoptosis or senescence within a week of electroporation.

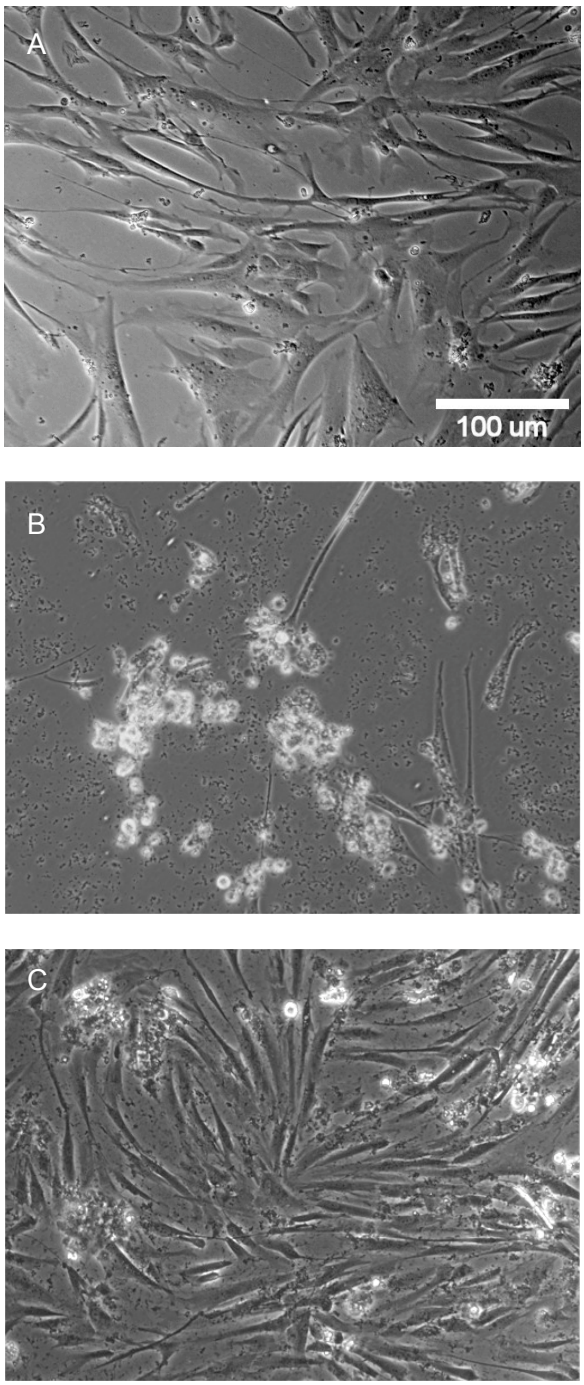

Figure 5.14: Optimisation of Yamanaka factors
HuF1 cells were electroporated with A) no mRNA (mock transfection), B) 20 µg each of OCT4, SOX2, KLF4, and cMYC. C) The mix of factors was adjusted following individual mRNA factor experiments to: 20 µg OCT4, 10 µg SOX2, 1 µg cMYC, and 10 µg KLF4. Which lead to increased proliferation and cell survival.

5.2.5.1 Conclusions

Despite cMYC's association with proliferation and anti-apoptotic effects, it has also been shown to cause oxidative damage to DNA and trigger apoptosis through the p53 pathway (Vafa et al. 2002). While the relationship between OCT4 and proliferation is not well studied, in the case of our fibroblasts it is obvious that it is having a beneficial effect on proliferation and possibly cell survival following the stress of electroporation.

5.2.6 mRNA Leads to Cell Aggregates

After discovering a combination of the Yamanaka factors that resulted in proliferation as opposed to cell death, treated cells were monitored for changes in morphology. However, instead of witnessing the formation of iPS colonies, only cell aggregates were detected. These aggregates appeared to proliferate at a higher rate (although only temporarily), they had much tighter cell junctions, and they would often appear somewhat raised or piled up in comparison to the monolayer of fibroblasts around them. They would typically reach a nominal size and then senesce, gradually 'browning' once they reached their maximum size (see Figure 5.15). From these aggregates, it was implied that the mRNA was causing gene expression changes, but that more optimisation was needed.

Initially, attempts were made to manually excise the aggregates from the surrounding fibroblasts and transfer them to human ES cell medium on MEFs. By treating them as ES cells, the thought was that they might grow out and adopt an ES cell phenotype. However, despite excision and attempted growth of over 30 cell aggregates in various growth conditions including growth on MEFs, Matrigel, and gelatin in human ES, fibroblast, and high nutrient DMEM/F12 medium, only fibroblasts grew out from the isolated aggregates. The centre of the aggregates would typically erode as the cells grew out, or turn brown and reach senescence within 3-4 weeks following electroporation.

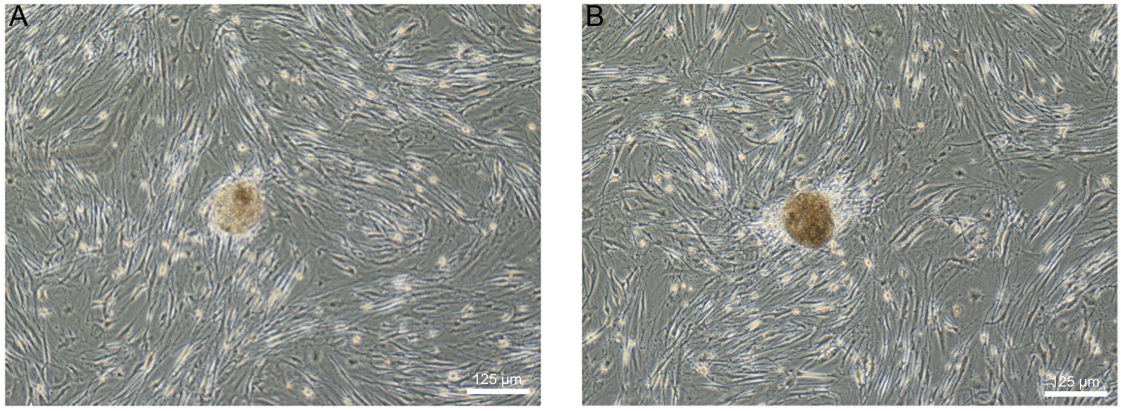

Figure 5.15: mRNA Leads to Aggregate Formation
A) Aggregate pictured was induced by a single electroporation of 10 µg OCT4, 20 µg SOX2, 1 µg cMYC, and 10 µg KLF4 mRNA. B) Senescent, mRNA derived aggregate approximately 3 weeks post electroporation, notice how it has become brown in colour.

5.2.7 Incorporation of LIN28 and NANOG mRNA

Since we were unable to obtain proliferative cells from the isolated aggregates, LIN28 and NANOG mRNA were added in an effort to improve the probability of achieving reprogramming. Due to the fact that NANOG slowed down growth when tested individually on HuF1 cells, it was tested at 1, 5, and 10 µg while LIN28 was used at 10 µg as it previously showed no negative effects. Cells were transfected with 20 µg OCT4, 10 µg SOX2, 10 µg LIN28, and NANOG (the same set of factors used by Thomson's group to successful reprogram human fibroblasts with lentiviral vectors)(Yu et al. 2007). Following treatment, cells were cultured and monitored for 4 weeks. However, only a few aggregates were detected and in the group that received 10 µg NANOG, the cells senesced prior to reaching the 4-week time point. Again, none of the aggregates expanded and due to significantly lower numbers of aggregates as compared to the Yamanaka set, we chose to move forward without NANOG and LIN28.

5.2.8 Detection of Initial Stages of Reprogramming

In an effort to test whether or not the cell aggregates were representative of a partially reprogrammed phenotype, TRA-2-54 staining was employed. TRA-2-54 is an antibody that detects alkaline phosphatase, which has been used as a general cell surface marker of ES cells and other primitive cell types (Draper et al. 2002). While it is not a good enough marker on its own to denote pluripotency, high levels of alkaline phosphatase are typically a marker of pluripotency (Draper et al. 2002). Data from colleagues has also shown that it is typically expressed even after many other pluripotency markers disappear during the differentiation process (data not shown) and it has been shown to be one of the first markers activated during viral mediated reprogramming, typically over two weeks before OCT4 or NANOG (Brambrink et al. 2008). As shown in Figure 5.16, flasks of HuF1 cells containing aggregates were stained with TRA-2-54 seven days post-electroporation with 20 µg OCT4, 10 µg SOX2,

1 µg cMYC, 10 µg KLF4 and found to be positive for alkaline phosphatase expression, brightly expressing the FITC secondary conjugate antibody. Positive detection of TRA-2-54 (alkaline phosphatase) at 7 days post electroporation showed that mRNA was having a significant effect, even after the mRNA was degraded (as judged by loss of fluorescence from GFP mRNA by 3 days post transfection).

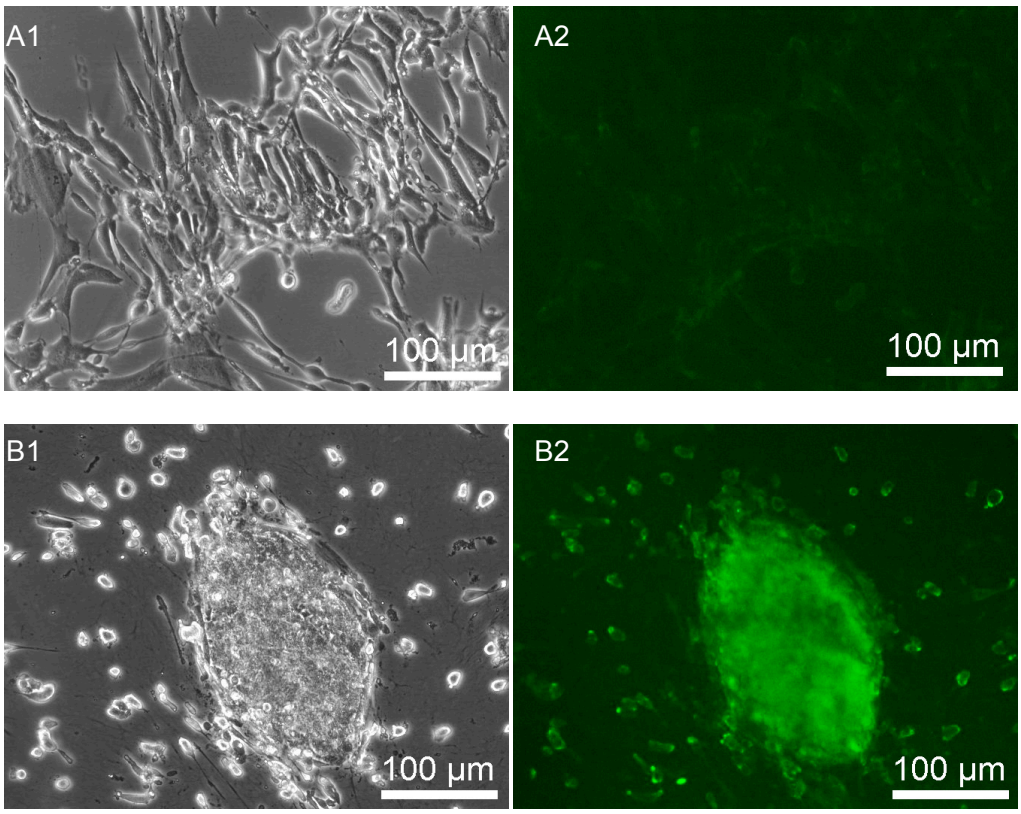

Figure 5.16: TRA-2-54 staining of HuF1s 7 days post-electroporation with mRNA
A) Untreated HuF1 fibroblasts were stained with TRA-2-54 antibody as a control. B) TRA-2-54 staining of HuF1 fibroblasts 7 days after electroporation with: 20 µg OCT4, 10 µg SOX2, 1 µg cMYC, and 10 µg KLF4 mRNA.

5.2.9 Use of Small Molecules to Enhance Reprogramming

Unable to isolate proliferative, ES-like cells from the aggregates detected, additional enhancements to aid in reprogramming were sought. Within a few months of the initial publication of human iPS cell derivation, many groups began to publish data showing that small molecules could be used to activate endogenous expression of reprogramming factors and in many cases improve the speed and efficiency of reprogramming. The first of these papers showed that tricostatin A (TSA) [Sigma, T8552], a histone deacetylase (HDAC) inhibitor, and 5-Aza-2'-deoxycytidin (5Aza) [Sigma, A3656], a DNA methyltransferase inhibitor, could activate pluripotency genes OCT4, KLF4, and NANOG in neurosphere cells, which constitutively express SOX2 and cMYC (Ruau et al. 2008). These small molecules are epigenetic modifiers (also known as chromatin modifying agents), and have been shown to interfere with epigenetic imprinting from one generation to the next (Furumai et al. 2001; Gottlicher et al. 2001; Christman 2002; Kubicek et al. 2007). This is typically through alteration or blocking of chromatin and/or histone methylation or acetylation during cell division. In somatic cells, pluripotency genes are epigenetically silenced. Specifically, the region of the genome containing the genes associated with pluripotency has been found to be mostly methylated in somatic tissues (Surani et al. 2007; Hayashi et al. 2009). This methylation forms a physical barrier, preventing promoter binding and blocking gene expression. This methylation 'block' is also sometimes supplemented by an additional barrier caused by the arrangement of histones. The chromatin is wrapped tightly around histones and depending on their structure and methylation or acetylation state, certain regions of the chromatin can be blocked off (such as OCT4), preventing transcription (Shi et al. 2008a; Shi et al. 2008b; Shi et al. 2008c; Hochedlinger et al. 2009). While there is currently no known small molecule to specifically remove these barriers in the region of embryonic genes, TSA and 5Aza have successfully been used to inhibit the general imprinting process during cell division and in some cases this leads to embryonic genes being 'unlocked' (Ruau et al. 2008). Since it has already been shown that many of the genes that regulate pluripotency, such as OCT4, have a

strong affinity to their own promoter regions and are self regulatory (Babaie et al. 2007); by unlocking these regions and introducing the factors via mRNA, the proteins translated from the mRNA should promote endogenous expression of the pluripotency genes if they have been properly demethylated.

In an attempt to remove these epigenetic barriers and assist in the activation of endogenous pluripotency genes, HuF1 fibroblasts were treated with small molecules. Based on the work of Ruau et al. (2008), TSA and 5Aza were used together to have maximum effect. Adding 500 nM 5Aza and 150 nM TSA to the culture medium for 48 hours (as published), HuF1 cells responded initially by slowing in proliferation rate as well as appearing unhealthy (similar to fibroblasts just before reaching senescence, with less compact morphologies and more spindly processes), but by 2-3 weeks following small molecule treatment (no mRNA treatment), aggregates were detected. These aggregates were uniform in morphology and noted to be typically approximately half the diameter of aggregates derived from mRNA (data not shown).

It was thought that the slowed growth might be a result of the dosages used. Therefore, 5Aza and TSA were tested on HuF1 cells individually and the growth rates were monitored for 7 days following 48 hour treatment. While HuF1 cells did not appear to be sensitive to concentrations of 500nM 5Aza or below, they were very sensitive to TSA at all concentrations tested, even as low as 50 nM (data not shown). In order to assess the effect of the small molecules together and to help determine what dosage of TSA was actually necessary, HuF1 cells were treated with 500nM 5Aza and a range of concentrations of TSA for 48 hours, then 24 hours later cells were taken for QPCR analysis to check for activation of OCT4 and NANOG. As shown in Figure 5.17, compared to non-treated and DMSO controls, 500nM 5Aza with 200nM TSA resulted in a 10 and 13 fold increase in OCT4 and NANOG respectively. While these levels do cause the cells to look unhealthy, they also seem to have the greatest effect in terms of OCT4 and NANOG activation. However, following further analysis,

endogenous OCT4 was found to be only 1/400th the level of HUES1 human ES cells following TSA and 5Aza treatment (see Figure 5.17). This may be an artefact of pooling the cells for QPCR; i.e. a small number of cells could be expressing OCT4 at high levels, but the larger proportion of cells without OCT4 reactivation may have diluted the signal.

In an attempt to confirm the increase in OCT4 detected by QPCR and determine whether or not this effect was uniform across the cells treated, or as hypothesised, confined specifically to those that aggregate together, HuF1+pOCT4-GFP cells were treated with 500nM 5Aza and 200nM TSA. The HuF1+pOCT4-GFP OCT4 reporter line does not normally express GFP, but has been shown to turn green upon fusion with NT2 cells (see section 3.2.23). Following 48 hours treatment with 500nM 5Aza and 200nM TSA, HuF1+pOCT4-GFP were monitored for changes in fluorescence. Within 1 week, mildly GFP positive cells were detected, indicating OCT4 expression (see Figure 5.18). Some non-aggregated cells were GFP positive and not all aggregates were GFP positive, but the brightest GFP positive cells were part of aggregates. Continued monitoring revealed that within two weeks after 48 hours of small molecule treatment, the cells reverted to non-GFP positive state. Attempts at isolating and expanding GFP positive cells were unsuccessful, despite trying a number of pluripotent cell friendly growth conditions including Matrigel, MEFs, DMEM/F12, and using MEF conditioned human ES medium.

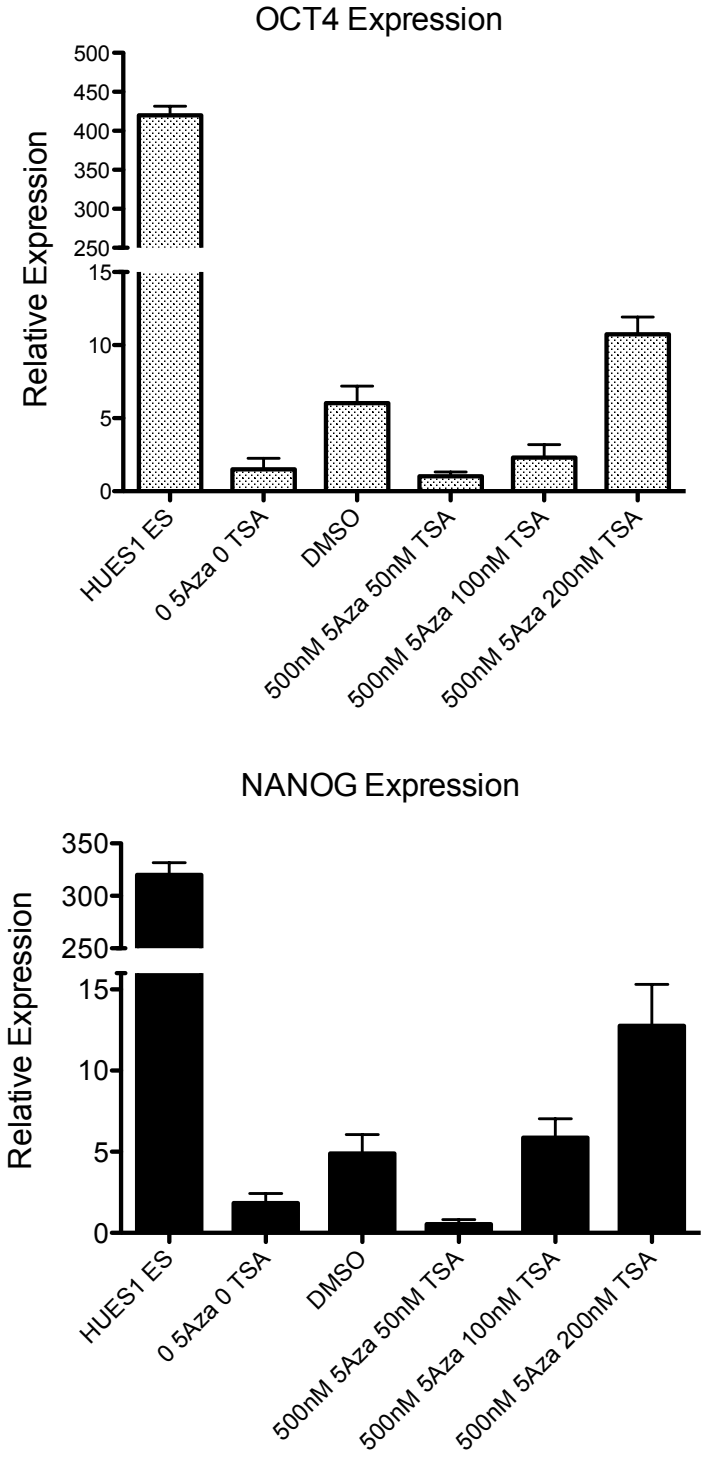

Figure 5.17: QPCR of HuF1 cells 24 hours after 48hr treatment with 5Aza and TSA
The two charts above show OCT4 and NANOG expression of HuF1 human fibroblasts after 48 hours treatment with combinations of the small molecules 5Aza and TSA. HUES1 ES cells, untreated HuF1 cells, and DMSO treated HuF1 cell were used as controls. 500 nM 5Aza and 200 nM TSA were found to result in the greatest increase in OCT4 and NANOG, but expression levels were still modest compared to the HUES1 control. It was concluded that the expression levels detected n HuF1 cells were diluted by surrounding fibroblast cells.

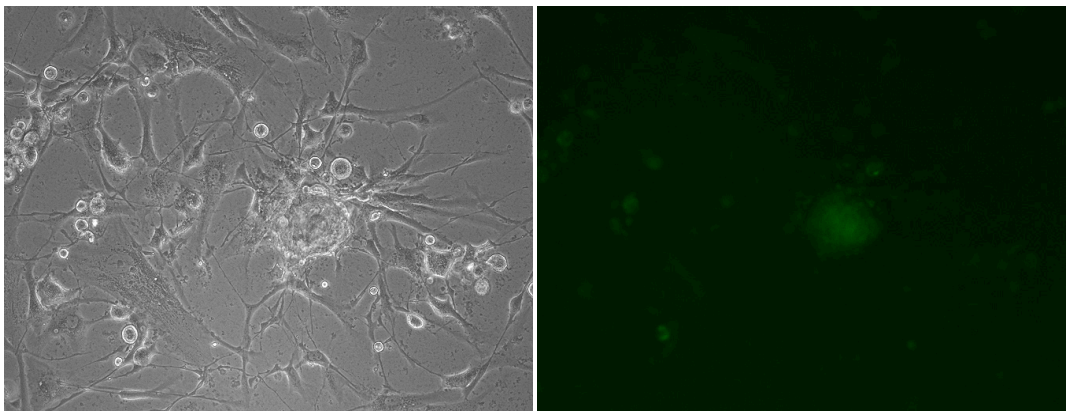

Figure 5.18: Endogenous OCT4 in HuF1-pOCT4-GFP cells from 5Aza+TSA
HuF1 cells modified to turn green upon OCT4 activation became mildly GFP positive after 48 hours treatment with 200nM TSA and 500nM 5Aza added to the medium.

While experimenting with TSA and 5Aza, two additional compounds were published as significantly increasing iPS cell generation, BIX-01294 (BIX) [Sigma, B9311] and Valproic Acid (VPA) [Sigma, P4543]. Interestingly, BIX, an inhibitor of G9a histone methyltransferase, was shown to replace OCT4 as well as enable the derivation of iPS cells using only OCT4 and KLF4 (Shi et al. 2008b; Shi et al. 2008c). VPA, an HDAC inhibitor similar to TSA, was similarly shown to allow the derivation of iPS cells using only two factors, OCT4 and SOX2 (Huangfu et al. 2008a; Huangfu et al. 2008b). Therefore, combining BIX's ability to replace OCT4 and VPA's ability to play the role of cMYC and KLF4, the effect should be synergistic, as seen with TSA and 5Aza.

Initially, BIX and VPA were tested on HuF1 cells individually to assess tolerance; then, different combinations within the tolerance range were tested similarly to TSA and 5Aza (see Appendix, section A.3 for Q-PCR results). Following 48 hours treatment with the various combinations (by addition to the culture medium), HuF1 cells were given 24 hours to recover before being taken for Q-PCR analysis. HUES1 human ES cells were used as a control and levels of OCT4, SOX2, cMYC, and KLF4 were tested (see Figure 5.19). Compared to TSA and 5Aza, HuF1 cells responded better, with lower levels of cell death and growth rate similar to the controls (data not shown). Also, unlike TSA and 5Aza treated cells, following BIX and VPA treatment, most cells were still proliferative.

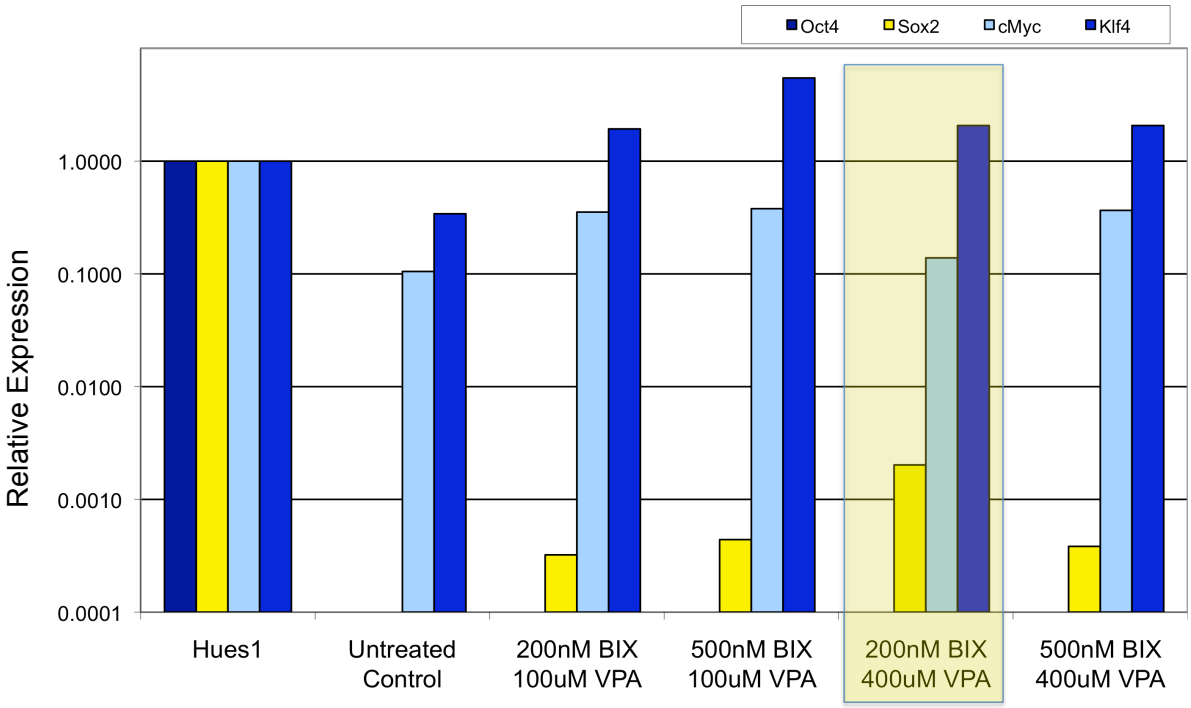

Figure 5.19: Q-PCR of HuF1 cells treated with combinations of BIX and VPA
We have found that treatment with DNA methyl-transferase, histone methyl-transferase, and histone deacetylase inhibitors, individually, does not result in OCT4 or SOX2 activation (See Appendix A, section A.3). However, as this graph shows, fibroblasts treated for 48 hours with a combination of VPA and BIX resulted in endogenous SOX2 activation (shown in yellow). After testing a variety of conditions, low BIX (200 nM) and high VPA (400 µM) was chosen as the best concentration as it resulted in the highest increase in SOX2 expression and most closely matched the ES control. Results were normalised against HUES1 human ES cells. While the upregulation is modest in comparison to HUES1 and OCT4 is at such low level as not to be detectable in this graph, the expression infers that, in at least a proportion of cells, the promoter regions for the reprogramming factors have been opened up. Protein coded from mRNA should then be able to bind to the endogenous promoter regions of these genes, promoting establishment of the pluripotent phenotype. NOTE: Data shown is an average of 3 replicates (n = 3). Graphs produced using BioRad software for Q-PCR analysis.

5.2.10 Combining Small Molecules and mRNA

On their own, neither mRNA nor small molecules resulted in iPS cells, even after 4 weeks growth in ES conditions. Therefore, small molecules were used following mRNA treatment in an effort to help 'unlock' the embryonic transcriptome and catalyse reprogramming. Cells were first electroporated with mRNA as done previously, then 24 hours later, followed with 48 hours of small molecule treatment. This was primarily so that the protein translated from the mRNA was in the cell at the same time that the chromatin regions were being opened up by the small molecules so that the factors had the highest chance of binding to the chromatin and catalysing endogenous pluripotency genes.

Fibroblasts were electroporated with 20 µg OCT4, 10 µg SOX2, 1 µg cMYC and 10 µg KLF4, followed by 48 hour treatment with 500 nM 5Aza and 200 nM. This resulted in proliferative aggregates that were equal to or typically larger than those previously derived from mRNA alone (NOTE: initial experiments were done with TSA and 5Aza, VPA and BIX later replaced TSA and 5Aza after comparison studies were done, as discussed in section 5.2.9). Aggregates occurred more frequently from combination treatment and also appeared more ES-like than previous attempts using mRNA or small molecules alone (see Figure 5.20). While some cells simply appeared to be more compact compared to the surrounding fibroblasts, most aggregates took on a rounded shape and looked raised up, as if they would eventually detach like embryoid bodies (EBs). However, similar to previous attempts, these larger aggregates, which occasionally contained cells with more prominent nucleoli like ES cells, also tended to senesce within 4 weeks of electroporation.

Again, attempts were made to isolate cells from the aggregates. Dr. Behrouz Aflatoonian, a postdoctoral researcher that specialises in the derivation of human ES cells, was recruited to help isolate and expand the aggregates. Cells were carefully manually dissected using pulled Pasteur pipettes and then transferred to in vitro

fertilisation (IVF) cell culture dishes coated in MEFs and treated like newly derived human ES cells. While some aggregates grew out briefly, within 3-4 weeks following transfer into human ES conditions, all aggregates stopped proliferating and in some cases the aggregates would appear to dissolve into or revert back to fibroblasts that would then often take over the culture dish. See Figure 5.21 for pictures of aggregates from mRNA and small molecule treatment.

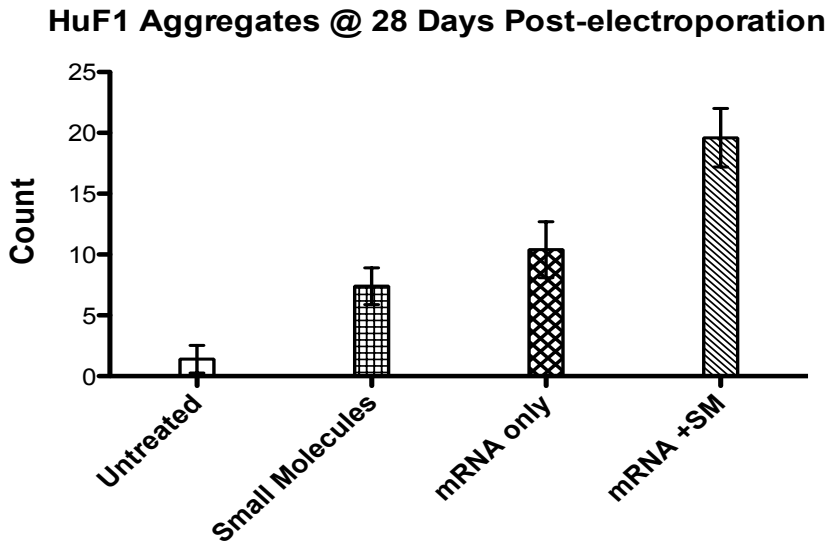

Figure 5.20: Number of HuF1 Aggregates after treatment with SM and/or mRNA
HuF1 cells were treated for 48 hours with small molecules (500 nM 5Aza and 200 nM TSA), mRNA (20 µg OCT4, 10 µg SOX2, 1 µg cMYC, and 10 µg KLF4) or both in combination (mRNA day 0, SM Day 1 & 2) and aggregates were counted at 28 days post-electroporation. Columns represent the mean of five experiments with error bars depicting standard deviation.

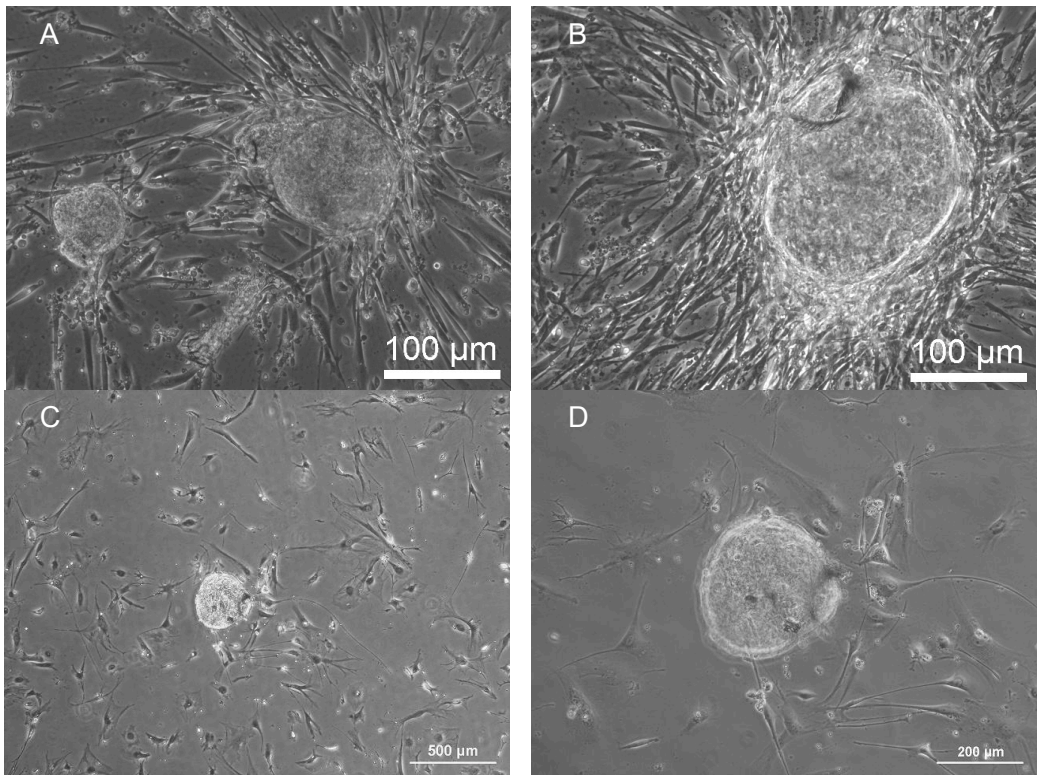

Figure 5.21: mRNA Factors and Small Molecules show Improved Results
A and B are photos of aggregates derived from HuF1 cells treated with OCT4, SOX2, cMYC, and KLF4 mRNA followed by 48 hour treatment with TSA and 5Aza. C and D show an aggregate that has been manually dissected and replated onto MEFs in human ES conditions.

The larger aggregates derived from small molecule and mRNA treatment continued to proliferate longer before reaching senescence as compared to aggregates detected from small molecules or mRNA treatment alone. Aggregates were either left to grow until senescence or dissected and replated, yet in both cases, cells would either lose their compact morphology or senesce within a few weeks of detection. Various types of culture conditions were also tried, including use of human ES KO medium, F12/DMEM, DMEM, and MEF conditioned hES medium. However, no stable lines grew out as all cells eventually reached senescence.

Previously, small molecules showed an upregulation in OCT4 levels by QPCR and activated GFP expression in the HuF1-pOCT4-GFP reporter line. To test whether or not these larger aggregates were also OCT4 positive, the reporter line was electroporated with 20 µg OCT4, 10 µg SOX2, 1 µg cMYC, 10 µg KLF4 (OSKM), then treated with 500nM 5Aza and 200nM TSA or 24 hours later for 48 hours. Cells were then grown out in standard fibroblast medium (DMEM +10% FBS). 14-16 days after electroporation, GFP positive proliferative aggregates were detected (see Figure 5.22 A).

All of the GFP positive aggregates appeared noticeably brighter and larger than those detected after small molecule treatment alone. There was an obvious synergistic effect from the combination of mRNA and small molecules, but while some isolated sections from the aggregates continued to grow out for up to two weeks, ultimately, they senesced. Also, comparing the brightness of the aggregates to a human ES cell line with the same reporter construct and also to cells derived from the HuF1 reporter line fused to NT2 cells, and it was found that the aggregate cells were not nearly as bright (see Figure 5.22 B and C).

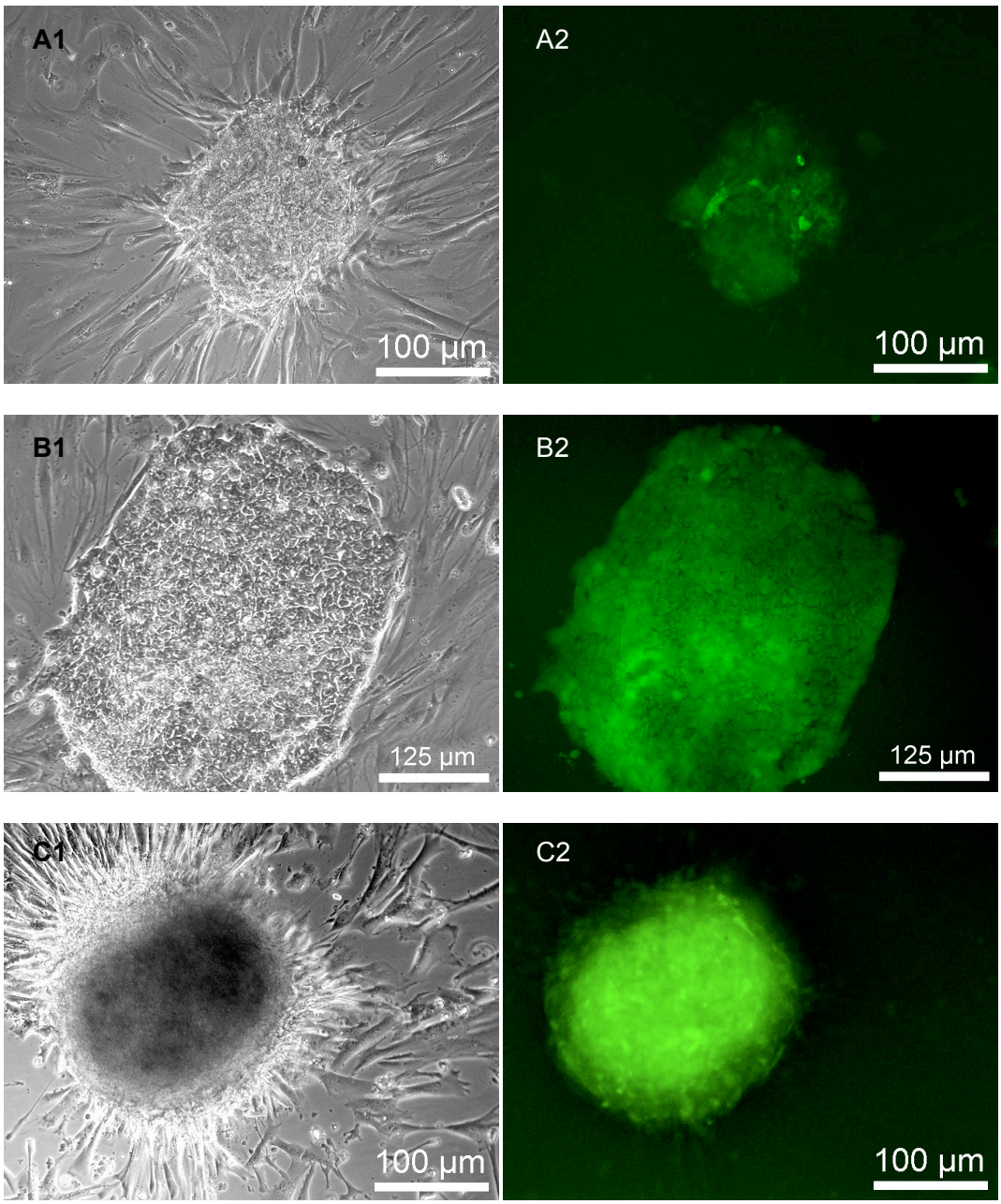

Figure 5.22: HuF1+pOCT4-GFP GFP +ve after mRNA & small molecule treatment
A) HuF1+pOCT4-GFP cells treated with OSKM mRNA, then 48 hours in TSA and 5Aza. B) H7S6+pOCT4-GFP human ES cells. C) HuF1+pOCT4-GFP cells fused with pluripotent NT2.TG11 cells. Although mRNA transfection followed by small molecules treatment resulted in the activation of GFP expression in the OCT4-GFP fibroblast reporter line, the level of GFP detected was noticeably lower than that of human ES cells containing the same reporter construct (B), and reporter cells fused to pluripotent NT2.TG11 cells (C).

5.2.10.1 Conclusions

Small molecules did seem to help the reprogramming process, leading to larger aggregates, an increased number of aggregates, and also showing an upregulation in OCT4, as judged by our reporter cell line. However, the small molecules themselves seemed to be detrimental to the cell health if used for more than a few days or if they are dosed too high. While TSA and 5Aza had a greater effect, they also caused more cell death. BIX and VPA have been found to be better suited overall to increasing efficiency while also preserving cell viability. It was hypothesized that epigenetic modifiers are the key to opening up the genome, allowing the proteins translated from the mRNA to bind to the opened chromatin and catalyse reprogramming.

While small molecules typically resulted in aggregates between 100 µm and 300 µm in diameter, the largest aggregate detected from mRNA alone was approximately 500 µm across. However, by combining small molecules and mRNA, most aggregates detected were at least 500 µm in diameter and some were up to 1500 µm across (data not shown). However, all attempts at growing out cells from these proliferative aggregates failed to result in anything resembling an ES line.

5.2.11 Multiple mRNA Transfection of HuF1

After repeatedly transfecting HuF1 cells with mRNA along with small molecule treatment, we consistently witnessed the formation of what we have termed 'proliferative aggregates.' However, despite efforts to isolate cells from these aggregates, to grow them out into a stable line, the aggregates would consistently reach a nominal size and then stop proliferating. Therefore, the process was again compared to the viral system and it was determined that one of the fundamental differences was the cells length of exposure to the factors. While viruses can integrate and provide a generally stable, consistent level of expression for long periods of time, our mRNA is much more transient. While we can more accurately dose the cells with a specific amount of mRNA, the mRNA and the protein it produces is typically degraded or used up within 4 days. Results published by Jaenisch's group show that, using viruses, iPS derivation from mouse fibroblasts requires a minimum of 8 days exposure before endogenous expression will take over, and additional expression time increases the efficiency of iPS colony formation (Brambrink et al. 2008).

In human cells, it typically takes approximately four weeks for reprogramming to occur using the Yamanaka factors (Takahashi et al. 2007; Nakagawa et al. 2008; Park et al. 2008a; Park et al. 2008b). It is also known that changes in epigenetics (and hence gene expression) typically occur at the point of cell division (Hochedlinger et al. 2009). So, proliferation plays an important role in reprogramming; without proliferative cells, there is less opportunity to alter gene expression through epigenetic modification from one generation to the next. Since GFP and OCT4-GFP protein expression typically dropped off by four to five days post electroporation, it was concluded that, at best, the factors were only present within the cells for 4 cell divisions. This contrasts greatly with virally treated cells, which have over 3 weeks or 20+ population doublings with relatively consistent expression of the factors. Not only does that mean that the viral genes have a much greater opportunity to affect cell fate, but it also means that the expression level should remain stable, as opposed to our mRNA, which is diluted with

each cell division. Despite these disadvantages, if mRNA could be transfected into HuF1 fibroblasts multiple times, it could potentially mimic, to a degree, the expression profile utilised by virus and catalyse reprogramming.

In order to test this, the best conditions previously tested were used and the electroporation procedure was repeated every 4 days. HuF1 cells were electroporated with 20 µg OCT4, 10 µg SOX2, 1 µg cMYC, and 10 µg KLF4, then treated 24 hours later with 200nM BIX and 400 µM VPA for 48 hours. Four days after the initial electroporation, cells were trypsinised and electroporated again with the same four factors. Following the second shock, most cells did not look healthy, growth rate appeared to slow, and the cells in each flask looked more sparse than they normally do following electroporation. Some flasks were combined to bring the confluence up, in hopes that this would prevent senescence. Eight days after the initial electroporation, some of the cells that looked healthier were taken for a third round of mRNA transfection, while some were left to grow out.

Cells shocked three times did not recover. It is likely that the electroporation procedure was either too hard on them or possibly that the cells were overloaded with RNA factors. The cells that only received two shocks did grow out and formed a few aggregates, but they looked slightly different than the typical aggregates. They appeared to have less defined aggregate borders and looked more like patches of compact fibroblast cells surrounded by fibroblasts of typical HuF1 morphology (see Figure 5.23).

5.2.11.1 Conclusions

The multi-electroporation treatment had a highly detrimental effect, each subsequent shock leading to higher levels of cell death until after 3 shocks, complete cell death or senescence occurred. Since the aggregates that did grow out from two shocks lasted longer than any previous aggregates, it was decided that better results might be

reached with additional rounds of transfection. However, the electroporation conditions were too harsh, so alternative methods of transfection were sought out with the aim to increase mRNA uptake and reduce cell death.

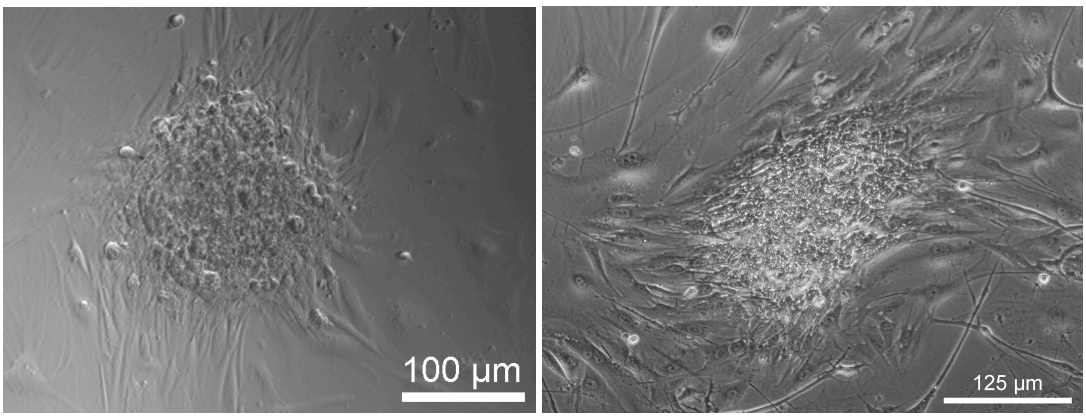

Figure 5.23: Aggregates persist longer after BIX+VPA & two doses of mRNA
These photos, taken at approximately 52 days after the initial electroporation, show surviving HuF1 cells after mRNA and small molecule treatment. These aggregates were removed and replated onto MEFs in an effort to boost their survival. In this instance, the aggregate cells appeared to grow out very slowly, but although they did not turn brown and become stagnant as had been typical in other experiments, they did not retain their compact morphology. Continued culture in MEF conditioned human ES medium on MEFs did not sustain them and eventually fibroblasts of typical HuF1 morphology took over the culture.

5.2.12 Replacement of HuF1 with MRC5 Fibroblasts

Having successfully created OCT4 positive cell colonies as shown by the HuF1+pOCT4-GFP reporter line, full reprogramming seemed an achievable goal. However, around this time, a number of publications inferred that reprogramming might simply be an artefact of cell culture, that the process may simply selecting for stem cells within a heterogeneous population (Kanatsu-Shinohara et al. 2004; Guan et al. 2006; Jaenisch et al. 2008; Guan et al. 2009). It was decided that, before getting any further into the work, it would be best to switch to a fibroblast line that was more defined, one that had been used successfully previously, and would be difficult for potential critics to find fault with.

After reviewing the published iPS literature and the available fibroblast lines, we settled upon MRC5. MRC5 human lung fibroblast cells were previously reprogrammed using virus by Daley's group, they were derived from lung tissue, have been used for vaccine production similar to the IMR90 line used by Thomson's group, and have a long history for being a stable and uniform fibroblast line (Yu et al. 2007; Park et al. 2008b). Passage 5 MRC5 cells were ordered from ATCC with the initial aim of replicating the results witnessed using HuF1 cells with MRC5 cells.

5.2.13 Optimisation of Transfection Using MRC5

After settling upon MRC5 fibroblasts as our somatic cell line for future reprogramming experiments, the best conditions found for deriving aggregates were repeated using MRC5. It was found that MRC5 cells did not form aggregates as readily as the HuF1 line, were very sensitive to TSA, and were similarly sensitive to electroporation. It was clear that a more effective, less detrimental method of transfection was needed if we were going to be able to provide MRC5 cells with repeated doses of mRNA. In order to accomplish this, we reviewed what technologies were available and tested the following methods:

1) Nucleofection
2) Lipofection
3) Polymersomes
4) Microporation

with the goal being to repeatedly transfect MRC5 fibroblasts without triggering apoptosis.

5.2.13.1 Nucleofection

Having compared the Amaxa Nucleofector to our BTX Electroporator, it was found that the Nucleofector was an easy to use device capable of transfecting fibroblasts with up to ~80% transfection efficiency. However, the nucleofector only used preset programs, making it difficult to vary the conditions or even know what exact conditions the cells were being subjected to. Ultimately, it was found that, with optimisation, the BTX electroporator could produce similar transfection efficiency (see Figure 5.24). Also, both devices led to similar levels of cell death. Due to our findings, we deemed that the Amaxa Nucleofector was no better than our current transfection system.

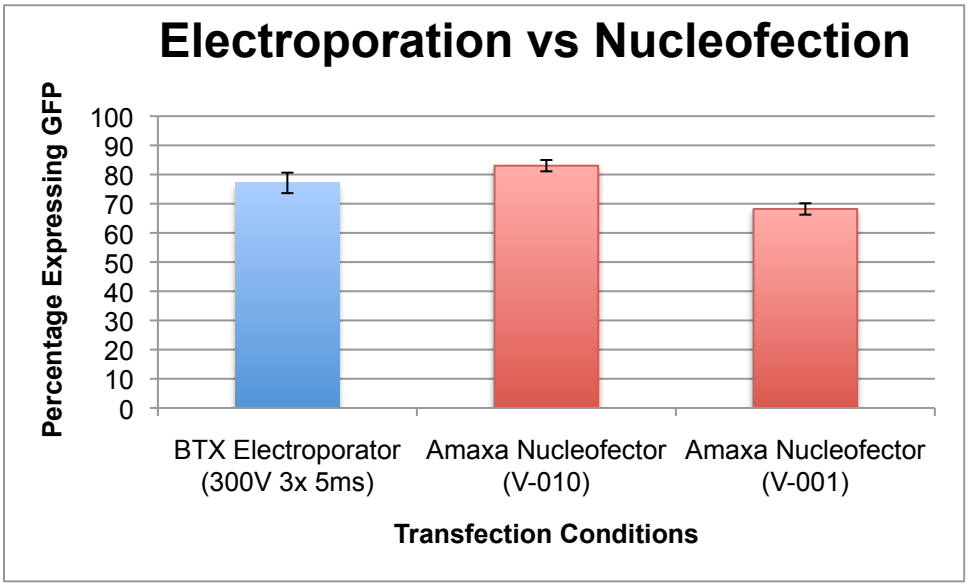

Figure 5.24: Electroporation versus Nucleofection
After transfection of HuF1 fibroblasts using both the BTX Electroporator (which we already owned) and the Amaxa Nucleofection system, it was decided that the Amaxa Nuclefector was not significantly better than the electroporator already owned by the lab. Also, the BTX offers full control over electroporation conditions while the Amaxa system only comes with pre-programmed parameters. The two best parameters tested are shown above compared to the best conditions found using the BTX system. The data shown is representative of three replicates with error shown as one standard deviation and transfection efficiency judged by the percentage of cell expressing GFP.

5.2.13.2 Lipofection

From our experience handling fibroblasts, it was concluded that the process of removing the fibroblasts from the tissue culture dish with trypsin, followed by centrifugation and shocking, puts the cells through a high level of stress, which is a major contributor to apoptosis and why cells do not survive multiple rounds of transfection. In contrast, lipofection reagents allow transfection of cells without detaching them from to the culture dish. A selection of transfection reagent samples were ordered and tested as per the manufacturer's instructions. Five lipofection reagents were tested:

1. Lipofectamine 2000 (Invitrogen, UK)
2. TransIT-siQuest (Mirus, US)
3. TransIT-TKO (Mirus, US)
4. TransIT-mRNA (Mirus, US)
5. GeneJammer (Stratagene, UK)

All manufacturer's instructions gave a range in terms of amount of reagent to use, each product was tested using GFP mRNA at three levels spanning the suggested range with 3 samples per condition. All wells were seeded at 50,000 cells per well, making them approximately 80% confluent 24 hours later, when they were transfected. 48 hours after lipofection, cells were analysed by FACS to determine the best condition, and cell counts were taken to assess cell viability. Table 5.3 shows a summary of the data, values are an average of the 3 samples from each condition tested.

	Amount of Reagent (uL)	% GFP +ve @ 48 hrs	% Viable Cells @ 48 hrs
Lipofectamine 2000	1.0	1%	81%
	1.5	21%	74%
	2.0	**43%**	**53%**
TransIT-siQuest	3.0	3%	90%
	6.0	17%	78%
	9.0	23%	67%
TransIT-TKO	4.0	1%	105%
	8.0	27%	62%
	12.0	11%	13%
TransIT-mRNA	1.0	2%	93%
	3.0	38%	22%
	5.0	21%	<1%
GeneJammer	1.0	4%	69%
	1.5	30%	54%
	2.0	51%	31%

Table 5.3: Summary of HuF1 Lipofection Results
Human fibroblasts were treated with a range of different lipofection products at different concentrations (based on manufacturer's suggestions). Percent of cells positive for GFP was used to gauge transfection efficiency with the percent of live cells being judged by counts of cells that were attached 48 hours after transfection compared to the number of cells seeded prior to lipofection [minimum of four 4x4 fields counted, results rounded to nearest %].

All products and conditions tested either resulted in very poor cell survival or very poor transfection efficiency, or both. Using 2.0uL Lipofectamine 2000 resulted in the best balance of GFP positive cells and cell viability (bolded). However, considering that half the cells were killed in the process, 43% is not actually very efficient considering we have achieved up to 77% transfection efficiency with approximately 50% cell death using electroporation. Overall, the lipofection reagents were disappointing and did not perform as well as manufacturers' reports. This may be down to MRC5 cells, inefficiency during the complexing of the mRNA and reagent, or potentially other unknown factors.

Following this experiment, Lipofectamine 2000 was tested again to see how cells reacted following multiple lipofections. Cell were transfected every 4 days using 2uL Liopofectamine 2000. Following two lipofections, cell health severely declined and no cells survived following a third lipofection.

5.2.13.3 Polymersomes

Having found that the transfection efficiency and toxicity associated with Lipofectamine 2000 [Invitrogen] and other similar lipofection reagents was higher than using electroporation, an alternative was offered by Dr Giuseppe Battaglia, a colleague in the University of Sheffield department of chemistry. They have developed a mammalian cell transfection protocol using a synthetic polymer based transfection technique that boasts >90% transfection efficiency of DNA in mammalian cells with very low levels of cell death (Lomas 2007; Lomas et al. 2008). They referred to the transfection reagent as polymersomes. Polymersomes are made up of pH-sensitive poly(2-(methacryloyloxy)ethyl-phosphorylcholine)-*co*-poly(2-(diisopropylami-no)ethyl methacrylate) (PMPC–PDPA) diblock copolymers. The PMPC block is highly biocompatible, while the PDPA block is pH-sensitive (p*K*a ~ 5.8–6.6, depending on the ionic strength) (Giacomelli et al. 2006; Lomas 2007). While Invitrogen reports that Lipofectamine 2000 is made up of cationic lipids and polymers, the formulation is

proprietary. However, polymersomes work in a similar way, forming micelles around DNA and being taken up through the cell membrane after addition to the culture medium. This is a benefit over electroporation in that it does not require the cells to be trypsinised from the flask or centrifuged, therefore potenitally making it less stressful on the cells being treated. The key difference with polymersomes is that they encapsulate nucleic acids depending on pH. At low pH, the diblock polymers are non-polar, but as pH goes over 6, the PMPC-PDPA polymer starts to become polar, forming stable, typically spherical, micelles or polymer capsules at pH 6.4 and above.

Polymersomes encapsulate DNA and cellular dyes at pH 6.4 and above; when they touch cells, they are taken up through the cell membrane and the pH drop across the membrane causes the polymersome capsules to open and release their contents in the cell. The key is down to the small pH difference inside and outside the cell. These polymersomes have been successfully used to transfect DNA, cellular dyes, and double stranded short hairpin RNA, but not been tested using single stranded mRNA (Giacomelli et al. 2006; Lomas 2007; Lomas et al. 2008). Therefore, polymersomes were tested using in vitro produced mRNA with the help of Dr. Irene Canton and Dr. Marzia Massignani, colleagues from Dr Battaglia's lab. See Figure 5.25 for an overview of polymersome encapsulation and transfection and refer to section 2.14 for the polymersome encapsulation protocol used.

Using GFP mRNA encapsulated in polymersomes, the efficiency of transfection at 24 and 48 hrs was very low as compared to all previous transfection methods, regardless of the concentration of mRNA used. In the best condition tested, 50 µg of encapsulated GFP mRNA was added to 2 wells of a 6-well plate in equal amounts containing 500,000 cells per well (5x higher than the mRNA concentration normally used for electroporation). Only ~20 cells/well in 2 wells of a 6-well plate could be found to express GFP at detectable levels by eye using UV microscopy. Normally 10 µg is enough to illuminate 1 million fibroblast cells using electroporation. While all conditions

resulted in very low, or undetectable levels of GFP, unlike lipofection reagents, almost no cells died, regardless of the amount/concentration of polymersomes used (see Figure 5.25 for photos of polymersome transfected cells).

In an effort to determine whether or not mRNA had been properly encapsulated in the polymersomes, polymersomes complexed with mRNA were run on a gel after lowering the pH to open up and de-polarise the polymersome capsules. A large mRNA band was detected, but it was found that the mRNA was so tightly bound to the polymer that it did not move down the gel and separate into a separate band appropriate to the mRNA's size, as is typical with double-stranded DNA (according to Dr Canton). Further experiments using a human dermal fibroblast (HDF) cell line that had consistently been successfully transduced using polymersomes previously (Lomas 2007; Lomas et al. 2008) also showed equally low mRNA transfection rates. It seems that the mRNA and the PMPC-PDPA polymer bind very tightly and only a fraction of the mRNA actually gets released into the cell for translation into protein. Unfortunately, the binding was not a variable that our colleagues in the chemistry department were able to adjust and we were forced to abandon this method of transfection despite showing the lowest levels of cell toxicity of any chemical transfection reagent tried.

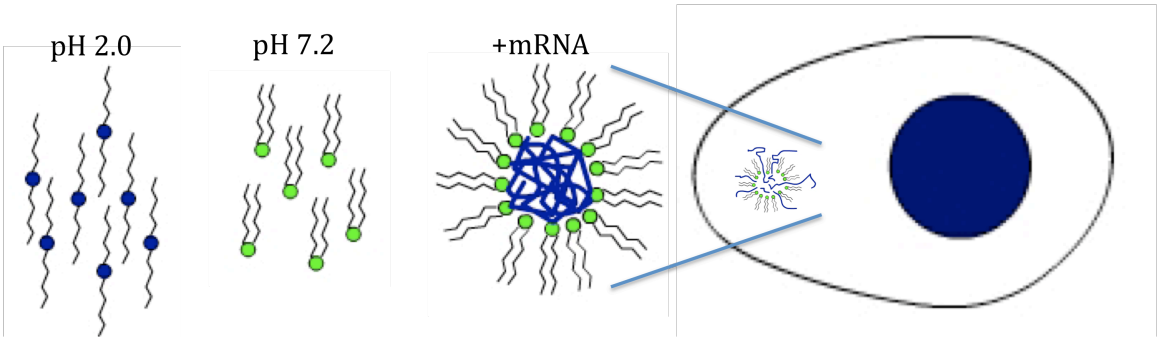

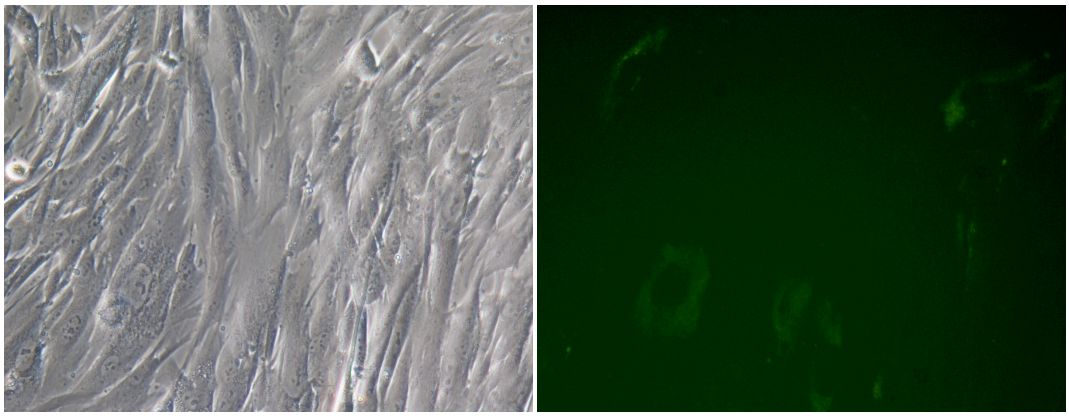

Phase Contrast **GFP**

Figure 5.25: Overview of polymersome transfection process
This experimental polymer is uniform and unorganised below pH 6.4, but then becomes polar at pH 6.4 and above, forming small capsules. By mixing materials for transfection with the polymer at pH 6.0 or lower, then gradually increasing the pH to 7 or above, the transfection material gets encapsulated. Dyes and DNA have been successfully encapsulated and transfected as the capsules are absorbed through the cell membrane, then open once inside the cell due to a minor pH drop. As shown, GFP from GFP mRNA was barely detectable 24 hours after polymersome transfection.

5.2.13.4 Microporation

Microporation is an improved method of electroporation boasting exceptional transfection efficiency and high cell viability, even when using difficult to transfect cells. We used the MP-100 system (Invitrogen, UK), which uses gold plated pipette tips instead of the traditional cuvettes used by most electroporation systems. The pipette system allows for cells to receive a more uniform shock with less generation of heat, H_2, O_2, harmful metal oxides, or abrupt changes in pH (see Figure 5.26). The system was first described by Kim et al., but has since been used in over 40 publications (Kim et al. 2008).

Following the manufacturer's instructions, a variety of conditions were tested in an effort to find the optimal conditions for MRC5 microporation, results were compared to electroporation (see Figure 5.27). Comparing the best conditions found for electroporation and microporation, microporation showed up to 20x higher transfection efficiency with comparable levels of cell death. Photos taken 24 hours after electroporation and microporation confirm that microporation is also less detrimental on cell health and morphology compared to electroporation (see Figure 5.28). Microporation gave the best results of all alternative methods tested in terms of transfection efficiency and cell survival post treatment, therefore we chose to move forward with microporation instead of electroporation.

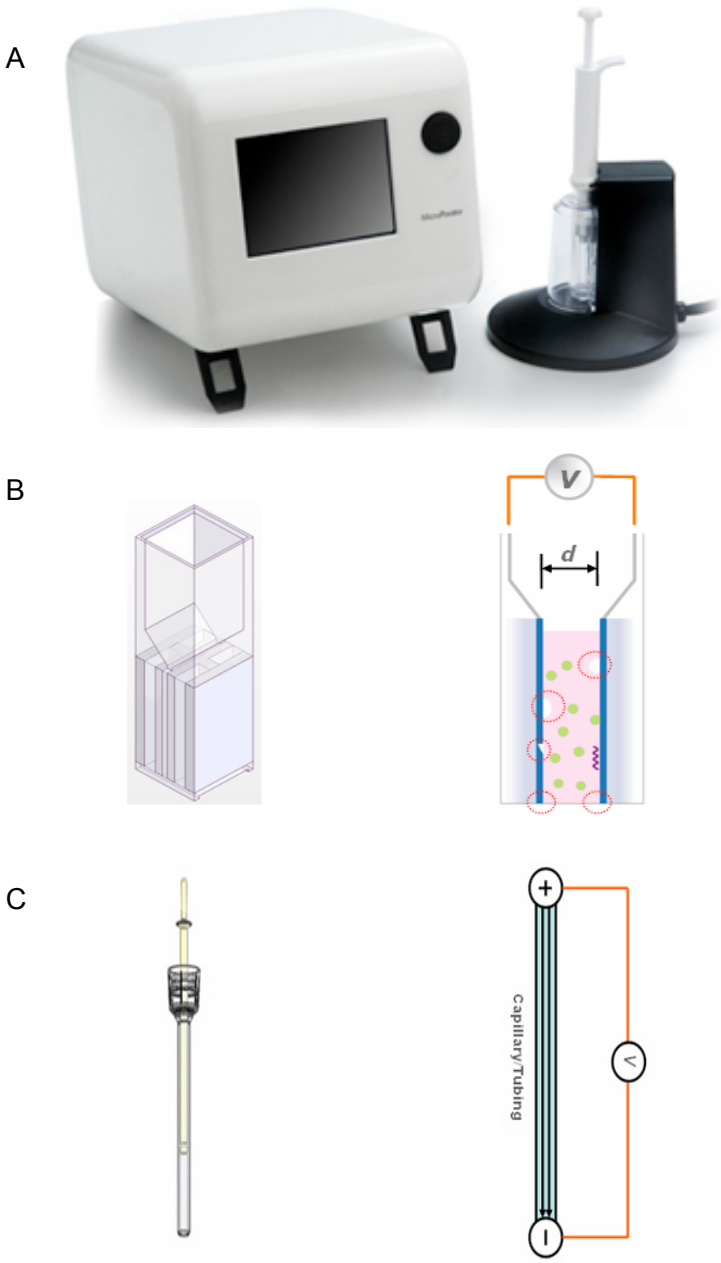

Figure 5.26: Microporation versus Traditional Electroporation
A) MP-100 Microporation system [Invitrogen] B) Traditional electroporation cuvette. This design with electroporation buffer flanked by metal plates has been shown to create uneven electrical fields, generation of heat, unwanted O_2 & H_2, rapid changes in pH, and harmful metal oxides. C) A diagram of the microporation tip. Due to its gold plating and capillary configuration, this tip generates relatively low levels of heat and harmful by products as compared to cuvette electroporation systems.

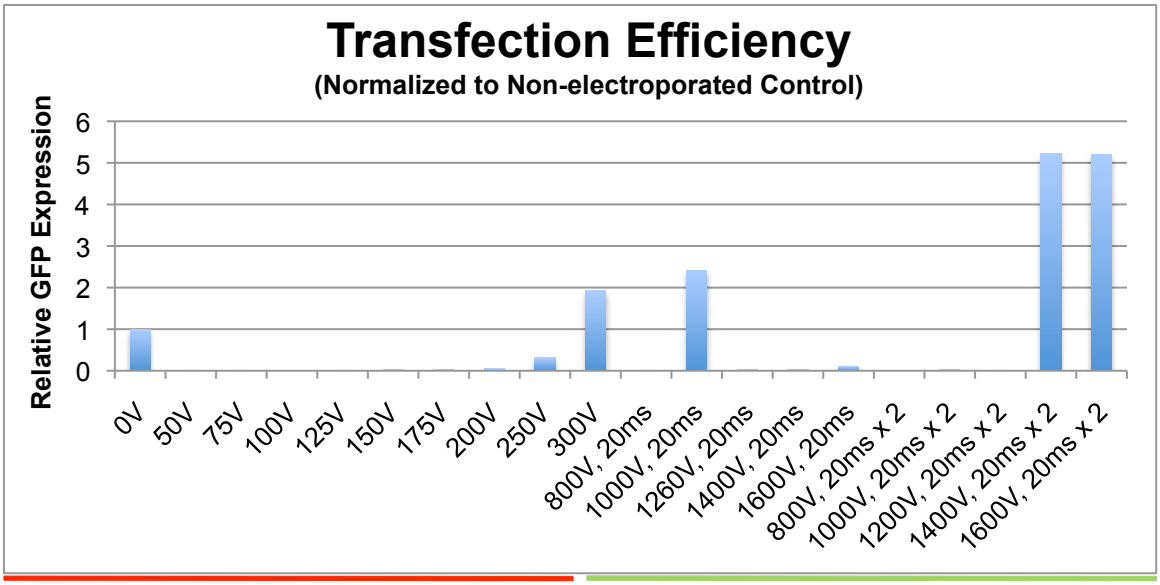

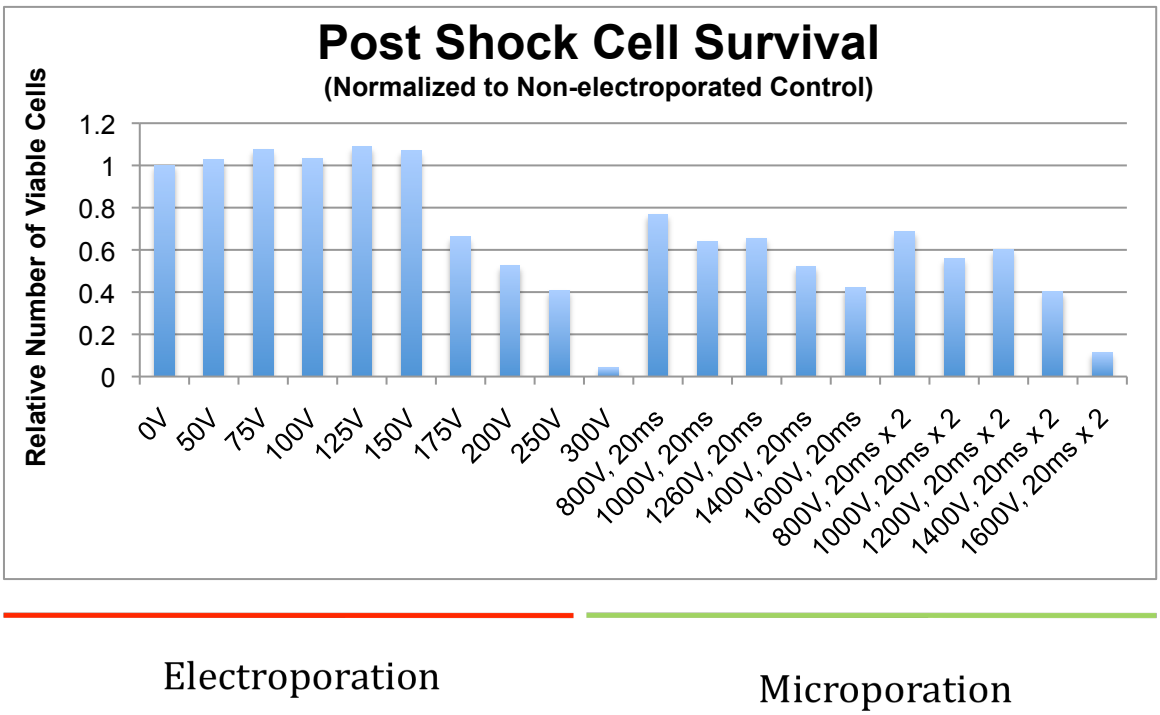

Figure 5.27: Microporation versus Electroporation Optimisation
MRC5 cells were electroporated and microporated across a range of conditions and compared using an InCell analyser (GE Healthcare). It was found that 1400V 2x20ms was the best condition for microporation of MRC5 cells, compared to 300V 3x 5ms using electroporation. Under optimum conditions for electroporation and microporation, microporation gave approximately 2.5x higher transfection efficiency with approximately 10x more cells surviving, making microporation much more effective than electroporation for transfection of MRC5 fibroblasts.

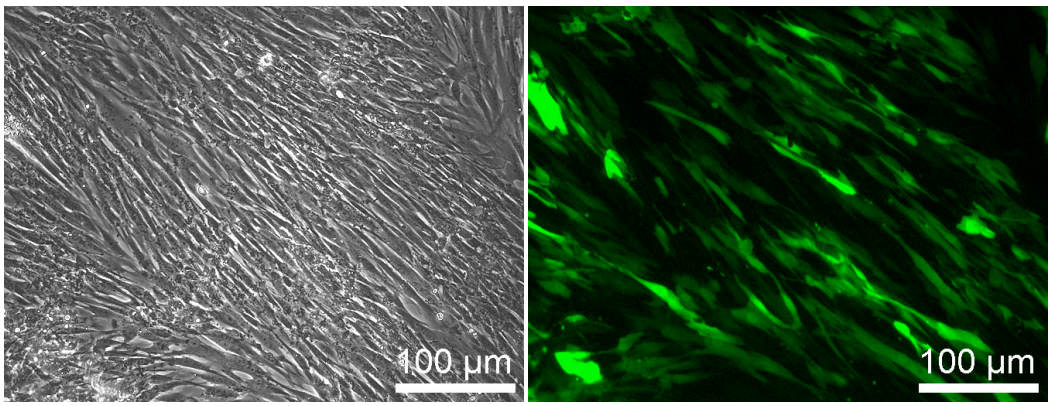

MRC5 cells 24 hours after *microporation* with GFP mRNA

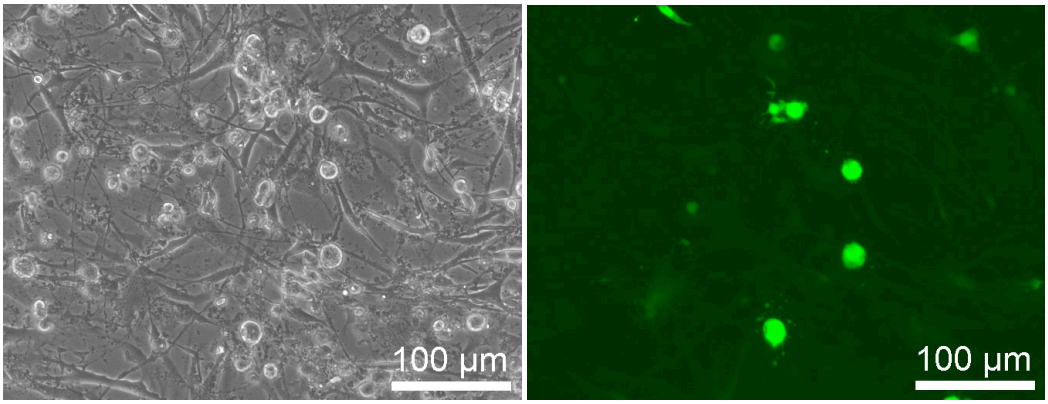

MRC5 cells 24 hours after *electroporation* with GFP mRNA

Figure 5.28: MRC5 Transfection Efficiency - Microporation vs. Electroporation
MRC5 cells were transfected with GFP mRNA using electroporation (300V 3x5ms) and microporation (1400V 2x 20ms). 24 hours later, the above photos were taken. It is clear that the microporator not only gives better transfection efficiency, but is also less detrimental on cell health and morphology.

5.2.14 MRC5 Microporation Optimisation

Through many experiments, it was noticed that GFP intensity and protein output was directly related to the dosage or amount of mRNA used and this dosage effect could be better controlled than when using DNA constructs. In an effort to prove what had been noticed anecdotally, MRC5 cells were microporated with GFP plasmid and GFP mRNA at three different dosages; then the percentage of GFP positive cells and the median GFP intensity was calculated by FACS (Dako) (see Figure 5.29). Results showed that, unlike plasmid GFP, all dosages of GFP mRNA were readily taken up at nearly 100% transfection efficiency and intensity increased with mRNA dosage. This gives evidence that we can relatively tightly dose cells and get a response proportional to mRNA dosage.

Also, it was noticed that fluorescence from transfected mRNA, whether from GFP, Cherry, or fluorescently labelled OCT4, would tend to fade away by 3-4 days post transfection. While it was assumed that since all our in vitro transcribed mRNA shared the same cap and tail sequence, they should all degrade at the same rate; a western blot was run following microporation of MRC5 cells with each of the Yamanaka factors with cells taken at 1, 2, 3, and 6 days after transfection to gauge protein levels and degradation (see Figure 5.30).

A

MRC5 + pDNA

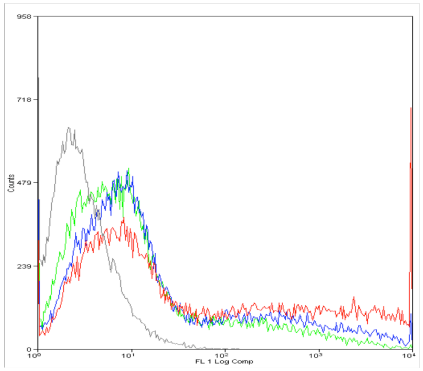

ug GFP DNA	% GFP +ve	Median Intensity
0	2.02	21.54
0.5	30.27	85.00
1	38.75	151.49
2	53.25	335.34

MRC5 + mRNA

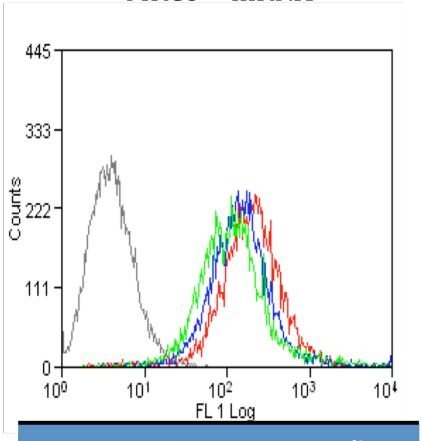

ug GFP mRNA	% GFP +ve	Median Intensity
0	2.64	16.73
5	99	113.48
10	99	146.12
20	98.5	202.25

B

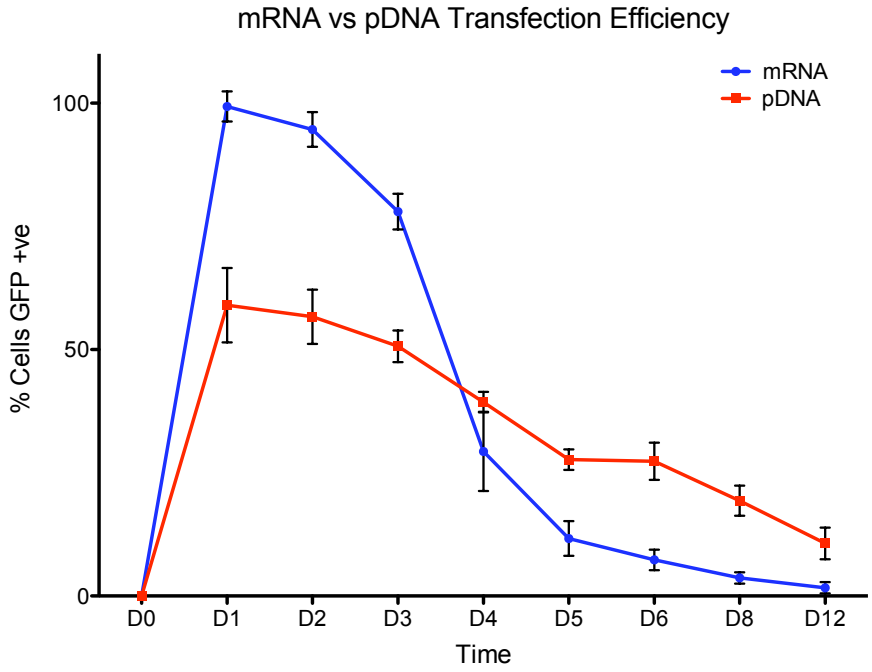

Figure 5.29: mRNA expression is dependent upon dosage
A) MRC5 cells were electroporated with GFP plasmid and GFP mRNA at three different doses; the % GFP positive and the median intensity were calculated by FACS. It was found that plasmid expression and intensity was difficult to control. However, mRNA was expressed at nearly 100% efficiency with dosage increasing the intensity in a controlled manner. B) While mRNA was taken up as higher efficiency, its expression dropped off very quickly by day 5, compared to plasmid DNA which showed a slow decrease in expression for over 10 days. NOTE: n = 3 and error bars represent standard deviation.

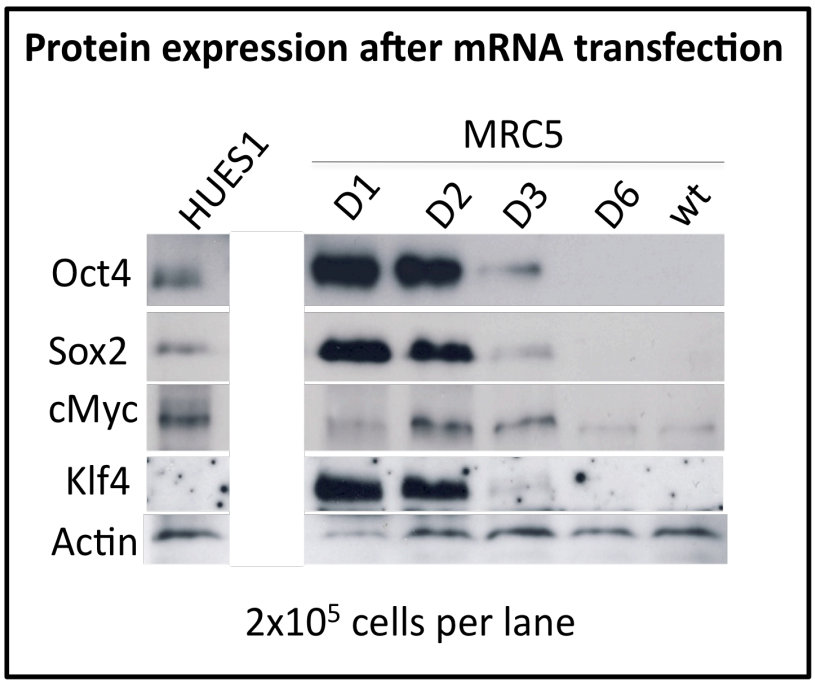

Figure 5.30: Western blot time course of MRC5s transfected with mRNA factors
MRC5 cells were transfected with the optimised set of Yamanaka factors and samples were taken for analysis by Western Blot at 1, 2, 3, and 6 days post-transfection. HUES1 human ES cells were used as a control. As anticipated, it was found that protein levels drop by day 3 and all but disappear completely shortly after.

5.2.15 Optimised mRNA Treatment using MRC5

In an effort to replicate the work done with HuF1 fibroblasts using MRC5 cells, MRC5 cells were treated with mRNA, BIX & VPA, and mRNA + BIX & VPA. Also, Rho-associated kinase inhibitor γ-27632 (ROCKi) was added to the culture medium 24 hours prior to microporation as it was shown to significantly increase human ES cell cloning efficiency (Watanabe et al. 2007) and, in our hands, increased the number of fibroblasts that attached and survived post shock (data not shown).

Two sets of four groups (3 replicates per group) of 1 million MRC5 cells were microporated as per the manufacturer's instructions in a total of 100 µL microporation buffer and mRNA as follows:

	Day 0	Day 2 & 3
Control	10 µg GFP	N/A
Small Molecules only	10 µg GFP	200nM BIX + 400 µM VPA
mRNA only	20 µg OCT4, 10 µg SOX2, 1 µg cMYC, and 10 µg KLF4	N/A
mRNA + Small Molecules	20 µg OCT4, 10 µg SOX2, 1 µg cMYC, and 10 µg KLF4	200nM BIX + 400 µM VPA

At 7 days post-microporation, one set of cells was taken for Q-PCR analysis to test for endogenous OCT4 and SOX2 levels (see Figure 5.31). Primer sets used were designed to specifically identify our ectopic mRNA versus endogenous mRNA transcripts by binding across the end of the coding region (cds) and the tail sequence, since the tail sequence of our in vitro transcribed mRNA differs from the endogenous sequence (see Material and Methods, Table 2.4 for primer sequences used). As seen previously with HuF1 cells, MRC5 cells similarly expressed increased levels of pluripotency genes when treated with mRNA and small molecules together (see Figure 5.31 and 5.32).

In the second set of cells, by 18 days post-microporation, small aggregates were detected in the group treated with small molecules only. At ~24 days post-microporation, small aggregates also appeared in the mRNA + small molecules group

and the mRNA only group. Using a fast-red alkaline phosphatase kit [Sigma], cells were tested at 28 days post-microporation for alkaline phosphatase activity (see section 2.7.4 for staining protocol). The small molecules only group did not appear to have any alkaline phosphatase activity. While mRNA alone showed evidence of alkaline phosphatase activity, the mRNA + small molecules group showed the highest level of alkaline phosphatase activity (see Figure 5.33). This was in agreement with our Q-PCR findings that combination treatment results in the highest expression of endogenous pluripotency genes.

Due to the increased efficiency of microporation, a few attempts were made to derive and expand aggregates from cells treated with one shock of the Yamanaka factors followed 24 hours later by 48 hours exposure to 200 nM BIX & 400 µM VPA. Treated cells were then grown in MEF conditioned human ES medium and aggregates were counted at 28 days post-microporation and larger aggregates that still appeared proliferative were manually dissected with pulled Pasteur pipettes and transferred to MEFs or gelatin (see Figure 5.35). As previously experienced with HuF1 cells, attempts at growing out these aggregates, either in pieces or as a whole aggregate clump, were typically unsuccessful. Some larger aggregates were trypsinised in an attempt to free potentially buried proliferative cells from the aggregate, but this only lead to outgrowths of fibroblasts of typical MRC5 morphology. On many occasions, trypsinisation was not enough to break apart the aggregate. On rare occasions, some aggregates that were dissected into multiple pieces, replated onto MEFs, and treated with MEF conditioned medium, appeared to attach and grow for up to 4 weeks, albeit very slowly. Although these surviving aggregates did not display typical ES morphology, to test whether these aggregates were partially reprogrammed, they were stained with OCT4 antibody. No aggregates beyond the 4 week time point treated with mRNA or small molecules alone showed signs of OCT4 expression, however, a few, but not all, aggregates treated with OSKM mRNA and VPA + BIX stained positive for OCT4 expression at 6 weeks post-microporation, inferring that endogenous OCT4 was

activated in a limited number of cells and confirmed reports that OCT4 is slow to be activated (see Figure 5.36). While the mRNA and initial boost in reprogramming factor proteins dissipates within 4-5 days of transfection, the changes that it catalyses appear to manifest a more permanent, lasting change in a small proportion of the cells treated. Under extended optimal growth conditions, these results show that reactivation of endogenous pluripotency factors using mRNA and small molecules is possible. However, not all the necessary factors, or perhaps factors in the right proportions, were activated, leaving aggregates that are only partially reprogrammed which eventually suffer apoptosis, senescence, or what appears to be reversion to a fibroblast phenotype.

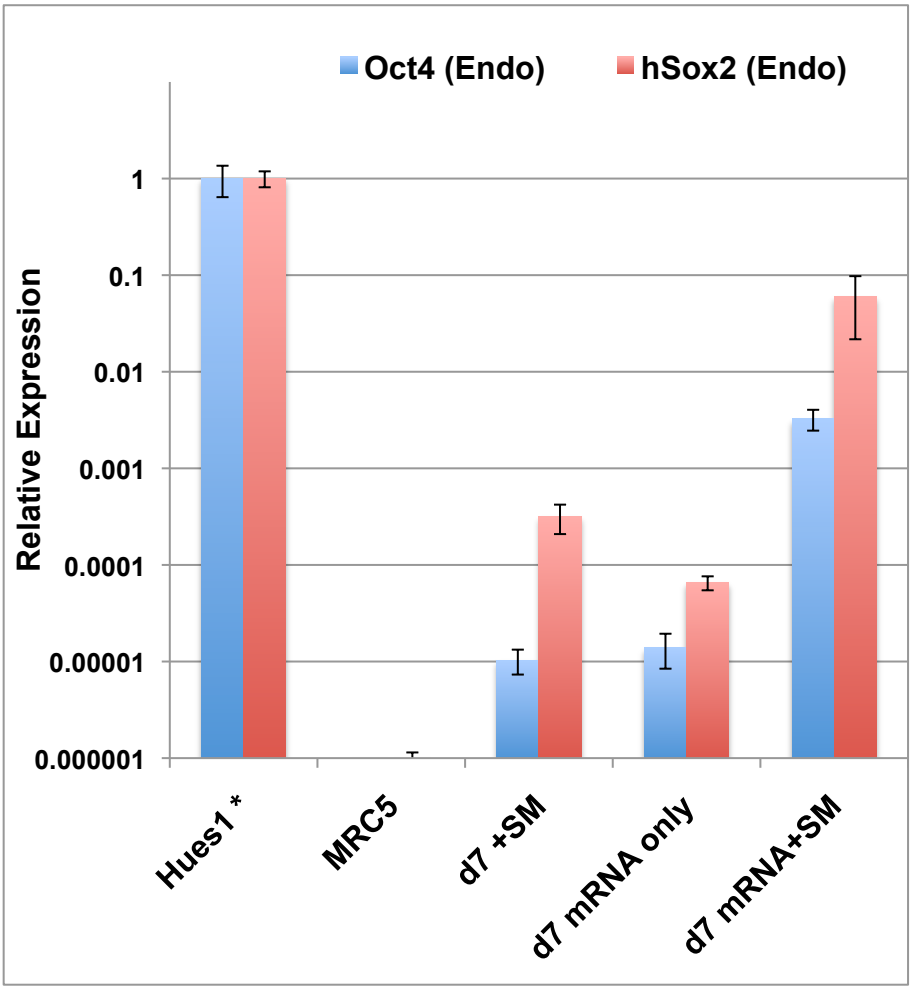

Figure 5.31: Activation and Increased Endogenous Expression of OCT4 & SOX2 at 7 days post-transfection with mRNA and small molecules
mRNA combined with SM treatment showed more than 10-fold higher endogenous OCT4 and SOX2 expression than mRNA or BIX & VPA alone. This is significant since mRNA dissipates by 3 days post-transfection. Both OCT4 and SOX2 were detected by Q-PCR using specific endogenous primers at 7 days post treatment with 200nM BIX + 400 µM VPA (SM), mRNA only (20 µg OCT4, 10 µg SOX2, 1 µg cMYC, and 10 µg KLF4), and mRNA + SM. Expression levels shown are normalised against a HUES1 human ES cell control and genes were normalised to GAPDH expression (logarithmic scale). NOTE: No OCT4 and only trace levels of SOX2 were detected in the MRC5 control. Also, n = 3 and error bars represent standard deviation.

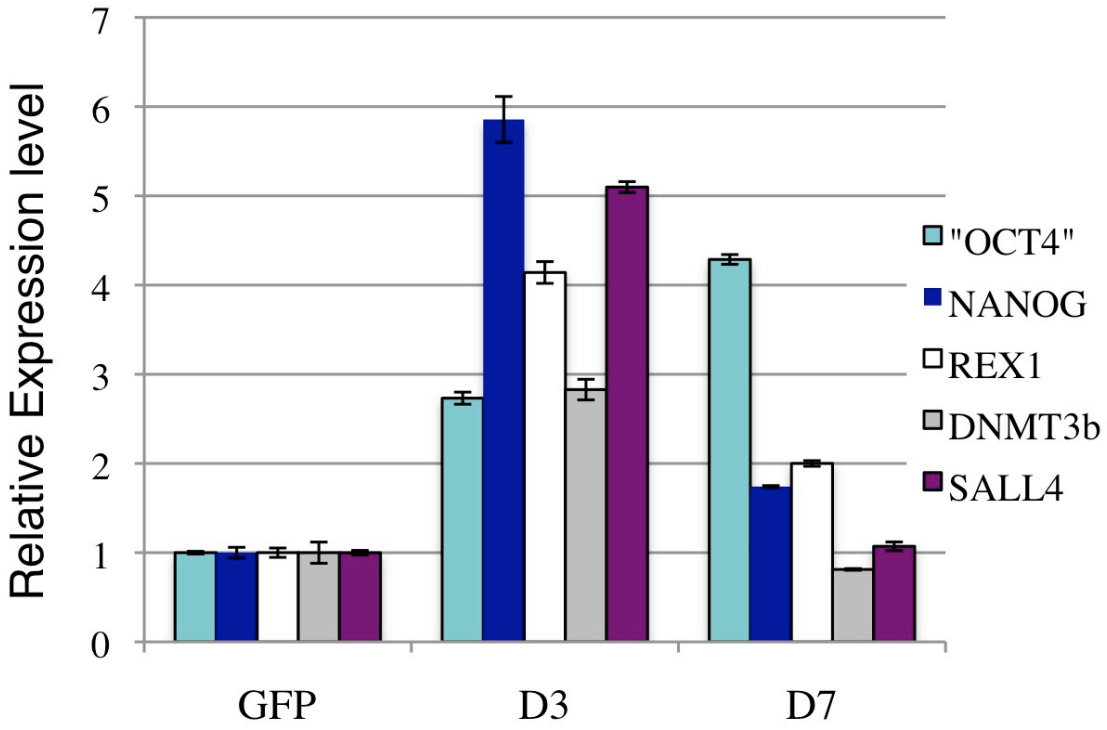

Figure 5.32: Activation of embryonic stem cell specific genes by mRNA transfection and small molecule treatment
Another Q-PCR showing a wider set of genes upregulated by 20 µg OCT4, 10 µg SOX2, 5 µg cMYC, 10 µg KLF4 and 10 µg SV40 Large T mRNA followed by 48 hours treatment with 200 nM BIX and 400 µM VPA. This set of mRNAs was developed after further optimisation (see section 5.2.16.3). Relative expression level of ES cell specific genes (as noted) is shown 3 and 7 days post mRNA transfection. The expression levels of these genes were normalised against an MRC5 fibroblast cell control transfected with 10 µg GFP mRNA. All the genes were normalised against GAPDH expression.

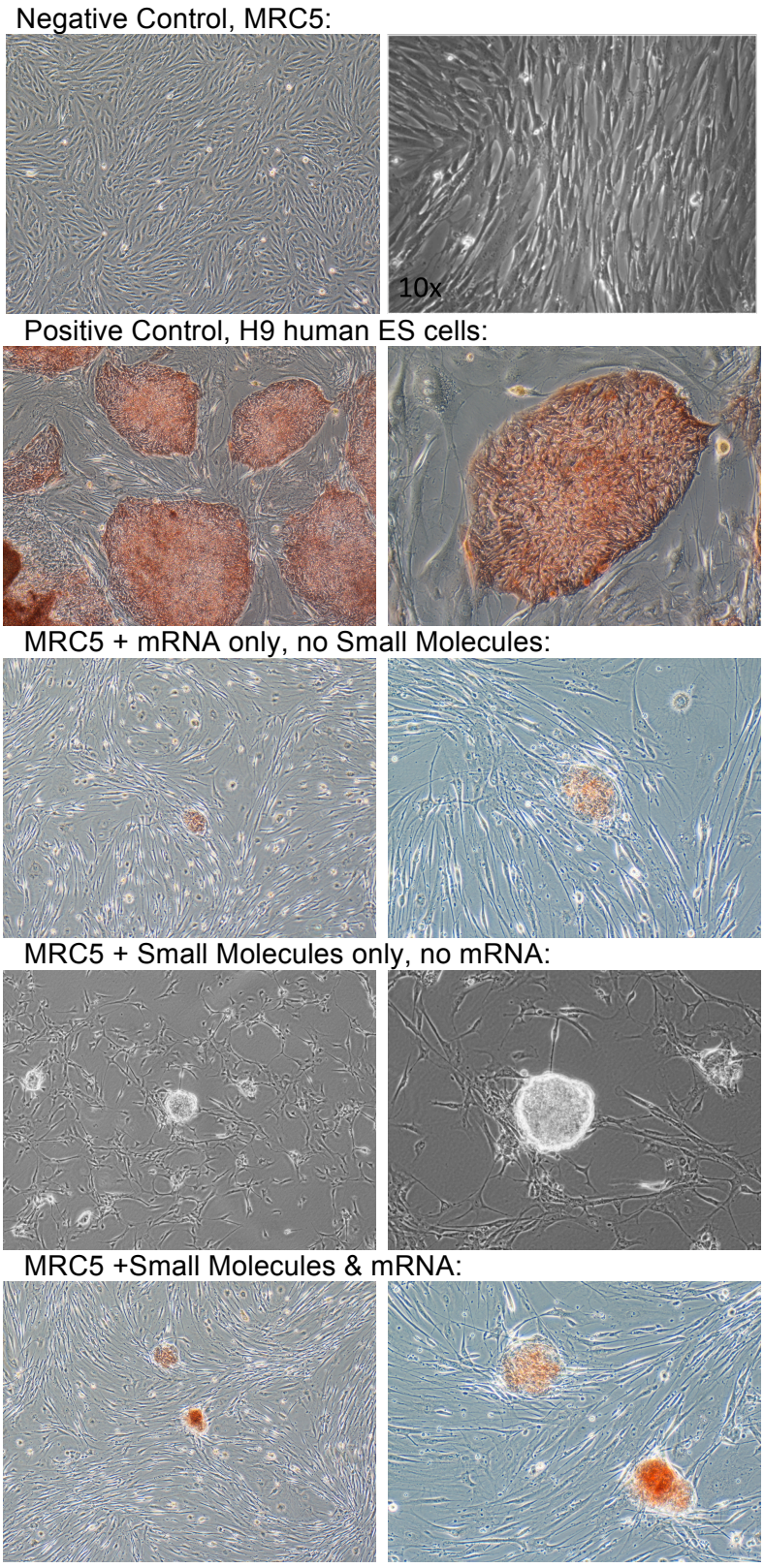

Figure 5.33: Alkaline Phosphatase staining, 28 days post-microporation
Only four factor mRNA with 200 nM BIX & 400 µM VPA treatment resulted in red aggregates of equal intensity as compared to the human ES control group.

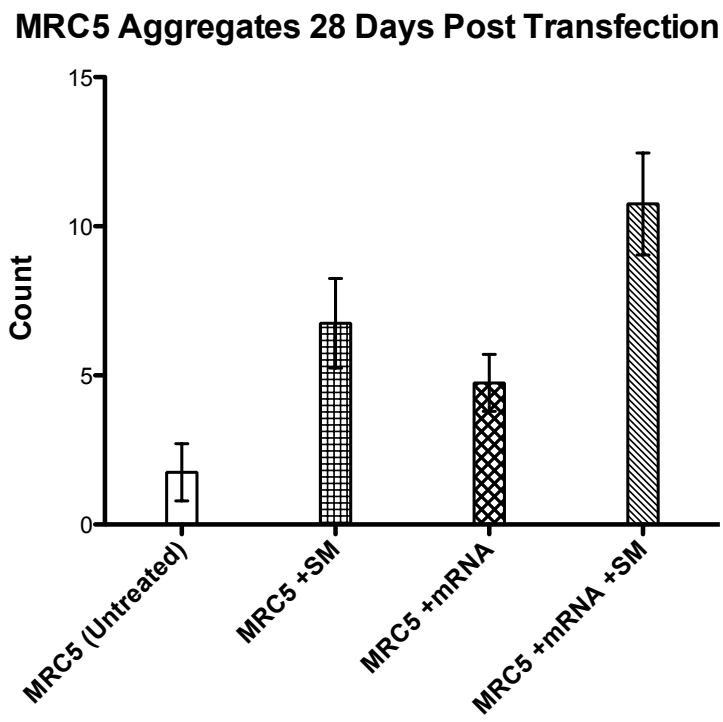

Figure 5.34: MRC5 aggregate count at 28 days post-microporation
The columns shown are representative of the mean with error bars showing standard deviation (n = 4). MRC5 treated with a combination of mRNA and small molecules repeatedly shows higher incidence of cell aggregates, also, as seen in HuF1 cells, the size (diameter) of detected aggregates is consistently larger than MRC5 cells treated with mRNA or small molecules alone. Compared to HuF1 cells, the incidence of aggregate formation was noticeably less.

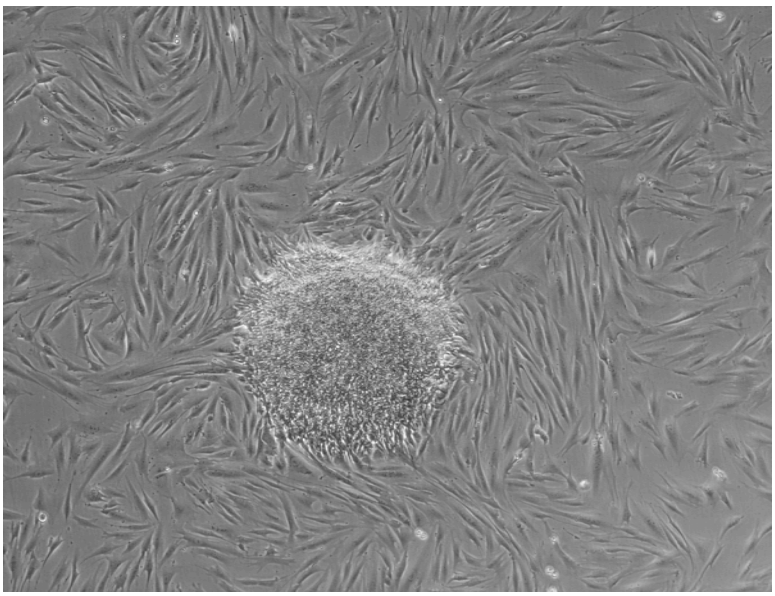

Figure 5.35: MRC5 Aggregate from mRNA + BIX & VPA treatment
This is an example of an aggregate that was manually dissected and transferred onto MEFs for further expansion. However, neither growth in human ES conditions nor fibroblast condtions fostered expansion. Although the cells attached and continued to display compact morphology, they became stagnant and would not expand.

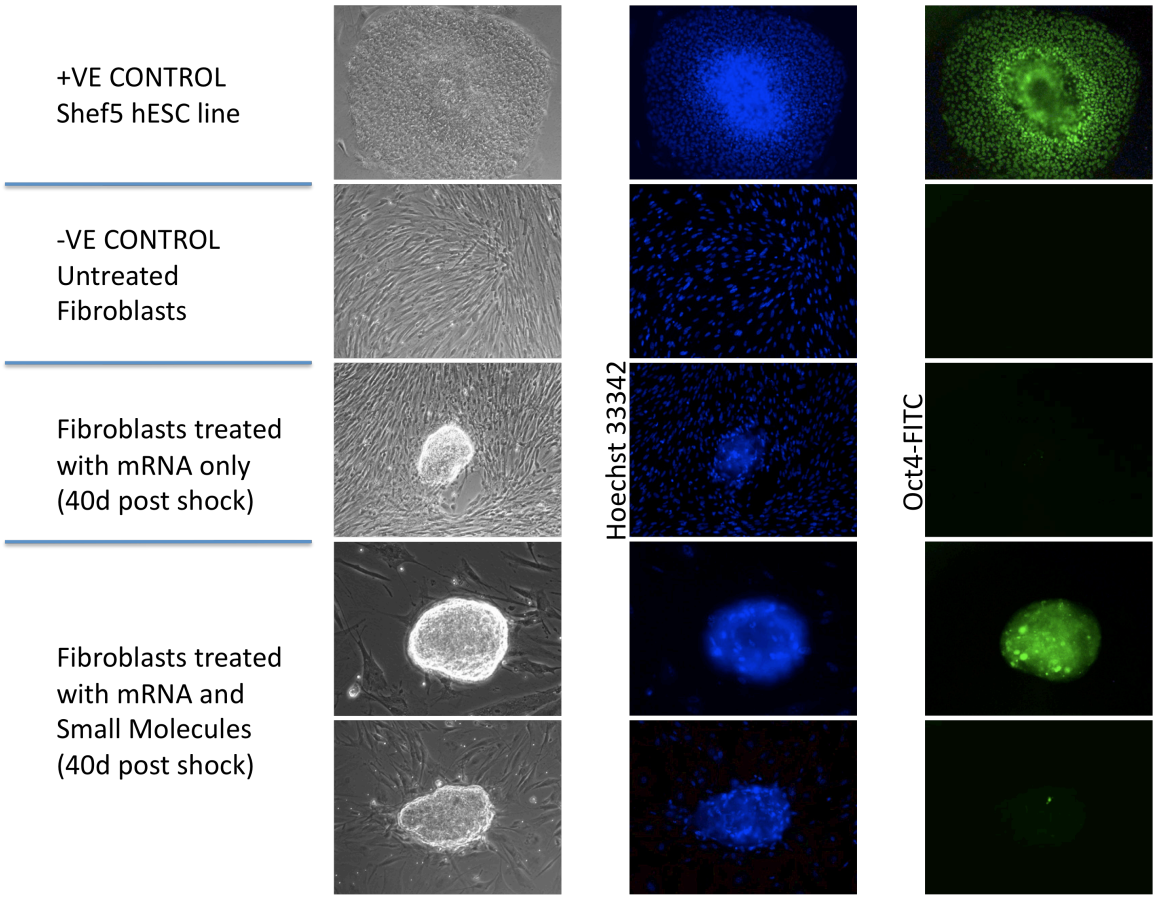

Figure 5.36: MRC5 Fibroblasts show endogenous OCT4 expression 6 weeks after single mRNA transfection and small molecule treatment

5.2.16 MRC5 Multi-Transfection of mRNA Factors

It was decided that MRC5 fibroblasts needed to experience prolonged expression of the reprogramming factors in order to completely shift into a pluripotent phenotype. To accomplish this, MRC5 cells were microporated with mRNA factors multiple times.

5.2.16.1 Repeat of previous multishock conditions with MRC5

First, 20 µg OCT4, 10 µg SOX2, 1 µg cMYC, and 10 µg KLF4 were microporated into MRC5 fibroblasts followed 24 hours later by 48 hours treatment with 200nM BIX and 400 µM VPA in MEF conditioned ES medium. From 24 hours after microporation onwards, the cells were fed MEF conditioned medium. At 4 days after the initial microporation, a second round of microporation with the same mRNA cocktail was used. However, similarly to HuF1 cells, the cells suffered high levels of cell death and apoptosis. On day 8, when cells were going to be microporated a third time, there were not enough cells to microporated; cells did not appear to grow between day 4 and day 8.

5.2.16.2 Human ES medium linked to poor recovery post-microporation

After a few replicates, it was clear that the abrupt change from DMEM +10% FBS to human ES or MEF conditioned human ES medium made it difficult for MRC5 cells to recover from microporation. Following 3 days growth in human ES medium, cells did not recover from the day 4 microporation. A new round of microporation optimisation was done on MRC5 cells that were grown out in human ES medium, however, across the whole range from 900V up to 1400V, less than 30% transfection efficiency was achieved and all groups suffered high levels of cell death. Following this, DMEM +10% FBS was used until all microporations were complete, then the medium was switched to human ES medium; this allowed for cells to be shocked multiple times without unusually high levels of cell death. Although viral publications inferred that switching the medium to human ES medium earlier increases reprogramming efficiency (Maherali et al. 2008a; Maherali et al. 2008b), it was found that the cells would not

recover properly and remain viable after multiple shocks without FBS. Therefore, DMEM +10% FBS was used for all subsequent multishock experiments.

5.2.16.3 Addition of SV40 LT mRNA boosts cell survival

As discussed previously, Daley's group, who also used MRC5 for reprogramming, showed that the addition of SV40 LT to their viral cocktail of OCT4, SOX2, cMYC, and KLF4 led to reduced levels of apoptosis and higher reprogramming efficiency (Park et al. 2008b). Parallel to other ongoing experiments, SV40 Large T (LT) mRNA was eventually made in a similar manner as the other factors. Following the Western blot timecourse and further experiments testing individual mRNA factors along with LT mRNA our mRNA cocktail was slightly altered. KLF4 was reduced to 5 µg instead of 10 µg as it was significantly higher in the Western Blot than our ES control. Since it was found that with the addition of 10 µg LT mRNA resulted in better cell health and survival following microporation, this allowed for an increase in cMYC to 5 µg instead of 1 µg. This new mRNA cocktail showed similar results to the previous one, but with increased cell survival and proliferation following microporation and was used from this point onwards. Since it is thought that reprogramming occurs primarily during cell division, we felt that increasing proliferation would increase our chances of success.

5.2.16.4 Multishock with improved mRNA cocktail

MRC5 fibroblasts were treated every 5 days with OCT4, SOX2, cMYC, KLF4, and LT mRNA with BIX and VPA added for 48 hours 1 day after the first round of microporation. Cells were kept in DMEM +10% FBS throughout. Previous attempts were shocked every 4 days, however, cells recovered so slowly, they were given an extra day recovery to maintain cell numbers. Following 3 rounds of transfection, similar aggregates were detected using the updated mRNA cocktail (see Figure 5.37). Cell growth slowed significantly after the third transfection and some samples suffered complete cell death.

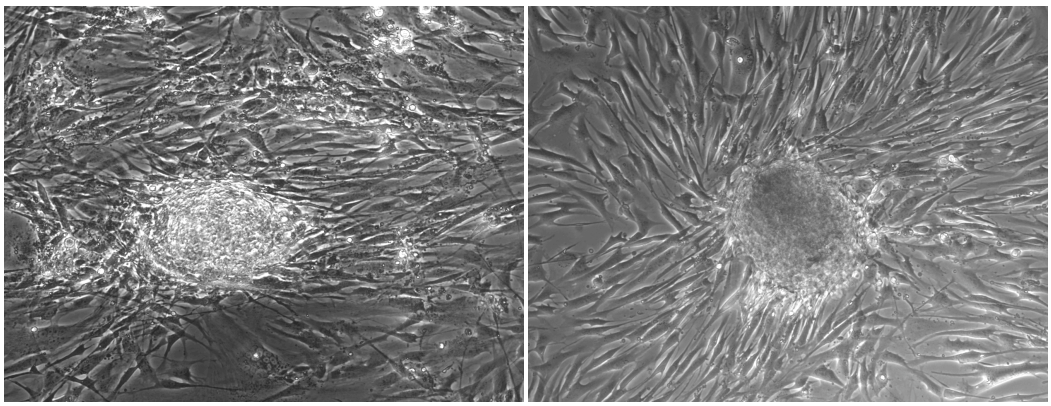

Figure 5.37: MRC5 Aggregates from 3 rounds of mRNA transfection with SMs
Similar aggregates previously seen after 1 round of mRNA transfection appeared up to a week sooner following 3 rounds of mRNA transfection.

5.2.16.5 Multishock Leads to More Aggregates and Morphology Changes

The previous multishock experiment (5.2.16.4) was repeated using more cells, enabling four rounds of microporation. Resulting aggregates showed the same morphology, however, additional shocks resulted in the formation of significantly more aggregates by day 21 (Figure 5.38) than previously seen at day 28 (Figure 5.34).

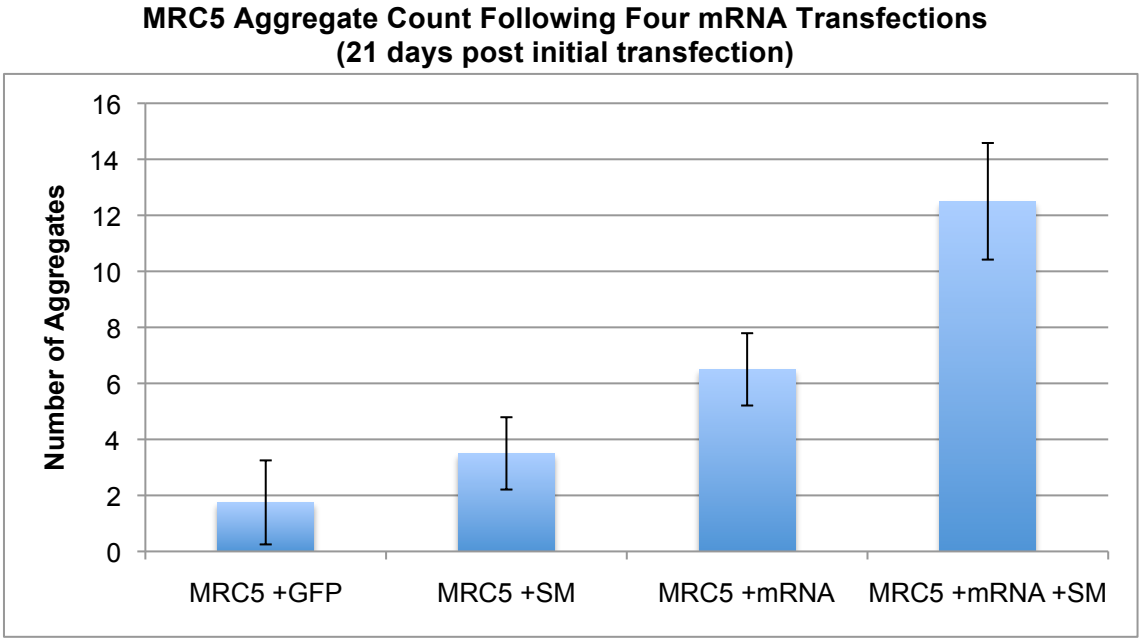

Figure 5.38: MRC5 aggregates following treatment at 21 days post-microporation
MRC5 cells treated with small molecules and four rounds with OSKMT mRNA reprogramming factors cocktail (20 µg OCT4, 10 µg SOX2, 5 µg cMYC, 10 µg KLF4, 10 µg SV40 LT) showed significantly more aggregates by 21 days post initial microporation than previously seen at 28 days following a single mRNA transfection. NOTE: this data only represents one replicate group. NOTE: n = 4 and error bars represent 1 standard deviation.

MRC5 fibroblasts were successfully microporated on day 0, 5, 10, and 15. Additional transfections were not attempted as the cells were too sparse and appeared unhealthy following four microporations. Following aggregate counts on day 21, cells were transferred onto MEFs and fed human ES medium in an effort to foster potentially reprogrammed cells. Although surviving cells were fed and monitored up to 8 weeks, no proliferative iPS-like cells were isolated. However, unusual morphologies developed following transfer into ES conditions. Some cells showed signs of what appeared to be blood production, based on the fact that they were visibly red down the microscope, but this was not confirmed by further testing. Others took on a more spindly, neuronal-like phenotype (see Figure 5.39).

It was reasoned that the spindly phenotype may represent a transdifferentiation or may potentially originate from cells that were briefly pluripotent, but then differentiated towards a neuronal lineage before they could be maintained in their pluripotent state. Using neural progenitor cells (NPCs) derived from human ES cells obtained from lab colleague Dr. Jie Na, some of the cells with altered morphology were fixed and stained for neuronal markers while others were taken for QPCR analyses to check for neuronal gene expression. Multishock and small molecule treated MRC5 cells did not show any signs of OCT4 or TuJ1 expression (see Figure 5.40). Also, QPCR analysis confirmed that there was no detectable expression of OCT4, SOX2, or typical neuronal genes Sox1, Pax6, or NeuroD1 (see Figure 5.41). While it is possible that the cells were not harvested quickly enough for testing and had already reached senescence prior to testing, it seems that the cell changes witnessed were not indicative of a neuronal phenotype.

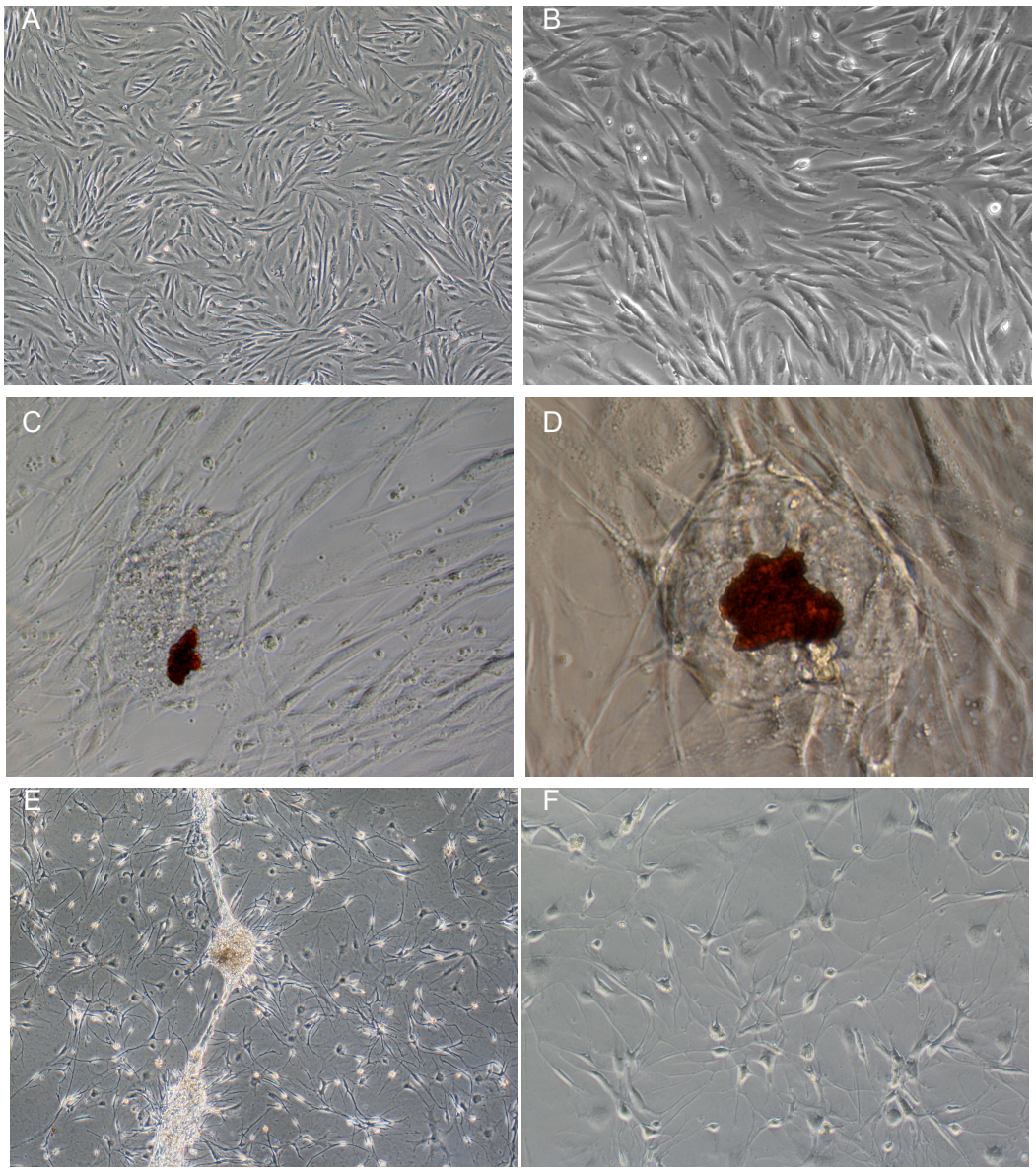

Figure 5.39: Blood-like and Neuronal-like cells appear after multishock treatment
A & B are typical, healthy MRC5 cells. C & D depict clumps of cells that appear to be producing red blood cells and were found in the samples that were treated with BIX and VPA only and mRNA + BIX and VPA. E & F show MRC5 cells on MEFs with spindly morphology that somewhat resemble cells of a neuronal lineage. Cells with the morphology depicted in E & F were only seen in the sample treated 4x with mRNA and 48 hours with small molecules.

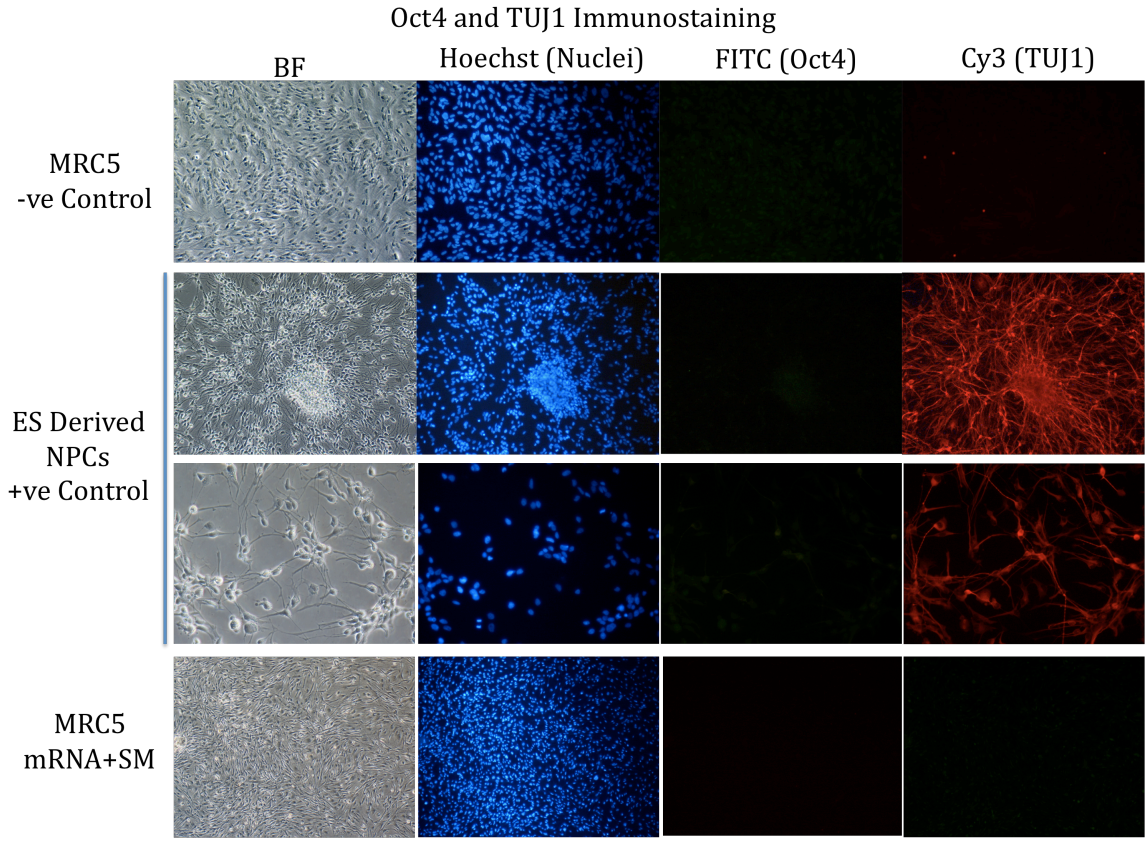

Figure 5.40: MRC5 multishock cells stained for neuronal markers
Despite their altered morphology, MRC5 cells treated with BIX and VPA for 48 hours and 4x with OSKMT mRNA did not show OCT4 or TuJ1 expression.

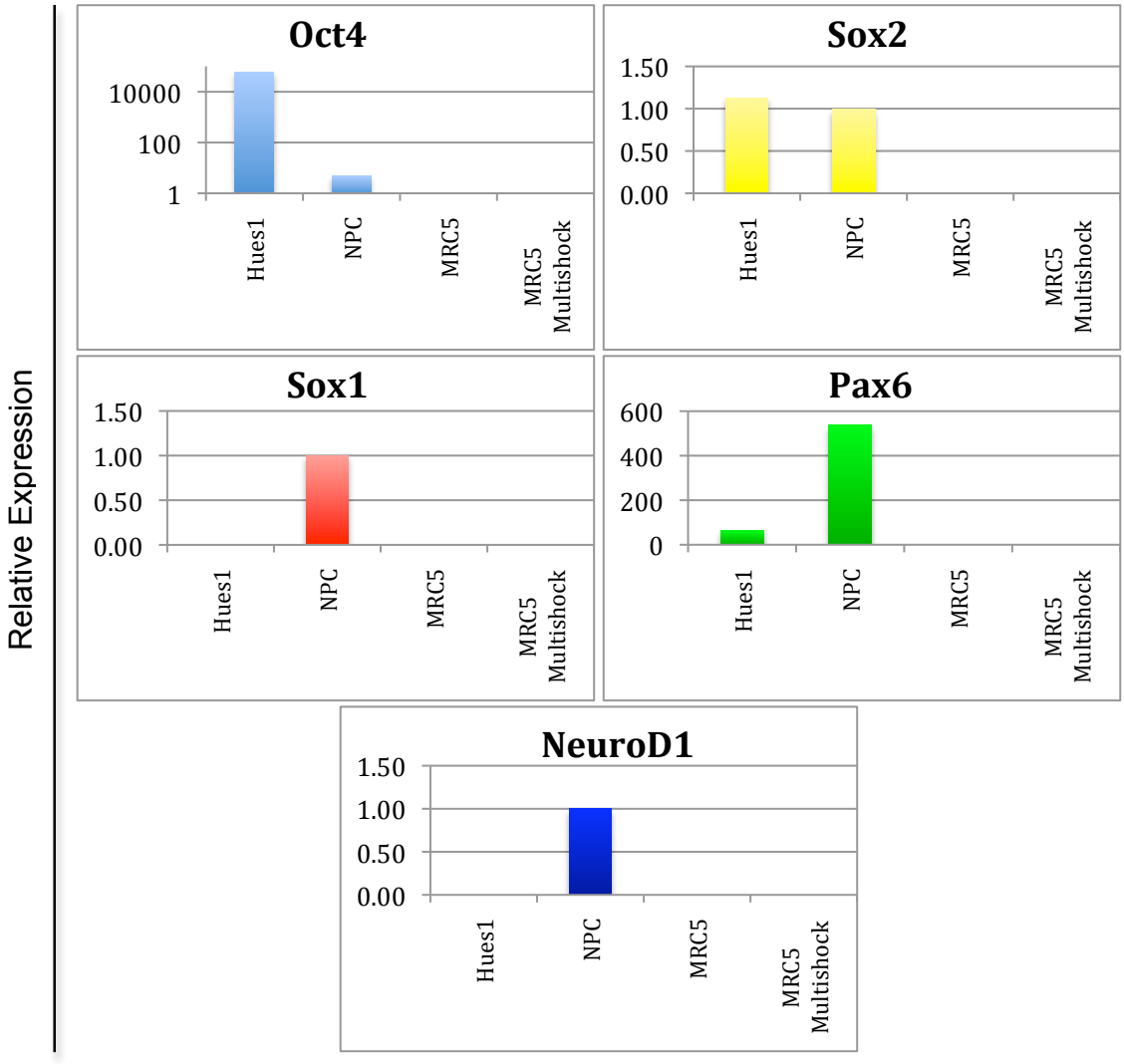

Figure 5.41: QPCR analysis comparing HUES1 ES cells, NPCs, untreated MRC5s, and MRC5s treated with small molecules and 4 rounds of mRNA transfection
Despite the unusual morphologies witnessed, Q-PCR did not indicate any upregulation of neuronal gene expression in MRC5 cells treated with 20 µg OCT4, 10 µg SOX2, 5 µg cMYC, 10 µg KLF4, 10 µg SV40 LT and 48 hours exposure to 200 nM BIX and 400 µM VPA.

Due to the fact that the aggregates seem to almost always senesce, it was hypothesised that the factors or treatment protocol may be activating the p53 apoptosis pathway. In an effort to detect whether or not this was the case, p21 levels were analysed in aggregates versus untreated fibroblasts and HUES1 human ES cells, along with MDM2 and CD1, genes related to cell cycle and checkpoint control. As shown in Figure 5.42, aggregates display relatively high levels of p21. This increased expression is likely tied directly to aggregate senescence and may be the critical barrier as to why the partially reprogrammed aggregates never fully develop into an ES-like phenotype.

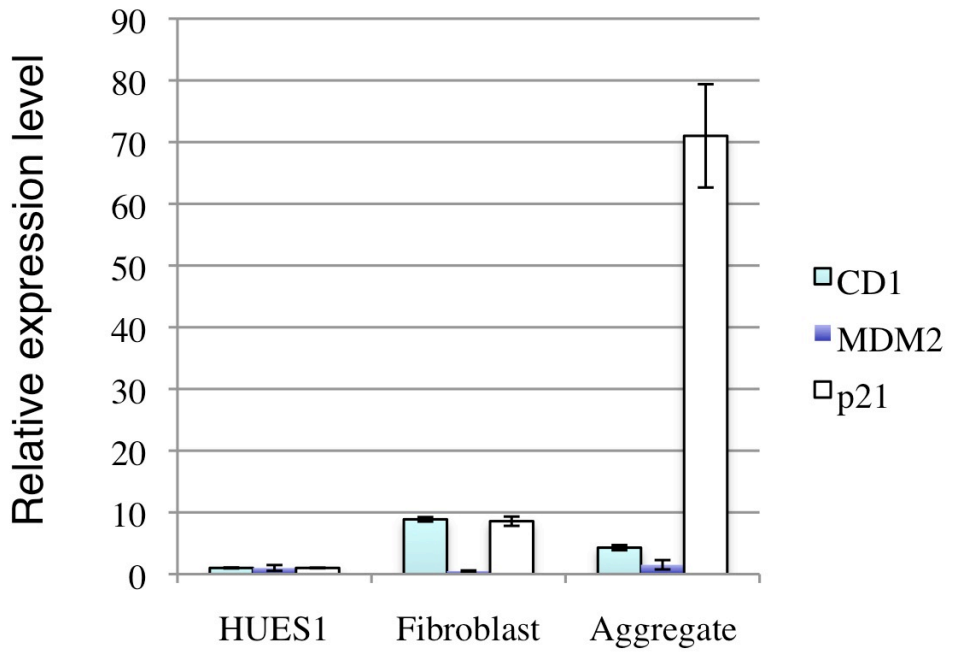

Figure 5.42: Aggregates show increased p21 expression
A variety papers were published after the completion of this project showing that p53 plays a key role in reprogramming. Cell lines that are very sensitive to p53 activation are more likely to go into apoptosis as opposed to progress through the reprogramming process. As shown here by Q-PCR, aggregates isolated following mRNA and small molecule treatment have high levels of p21 expression, a known activator of the p53 pathway leading to apoptosis. This infers that our partially reprogrammed aggregates are more prone to apoptosis and this may be playing a role in why aggregates reach senescence before full reprogramming.

5.2.16.6 Conclusions

Following repeated attempts and formulation changes, the fundamental flaw in our process continues to be related to efficient transfection and continuous expression of the mRNA factors. While there is evidence to show that a single transfection can in rare cases be enough to activate endogenous pluripotency genes when coupled with small molecules, in order to reach a process comparable to the viral reprogramming procedure, a better method of transfection needs to be found. While microporation has proven to be better than other transfection technologies available, it still involves the removal of the cells from their culture flask during a delicate time when they should be undergoing an epigenetic transition. Any disturbances could potentially affect the status of reprogramming negatively. Also, due to the detriment caused by microporation itself, transfection has been limited to once every 4-5 days. Whether or not the high levels of p21 are related directly to the transfection method used or simply the factors themselves, the aggregates are definitely more temperamental than the surrounding fibroblast population and unless this negative pressure can be checked, it seems that isolation of fully reprogrammed cells from mRNA and small molecules may not be possible. In order to push enough mRNA into the cells to keep levels of the factors adequate for the required length of time, mRNA and subsequent protein levels are ‘spiked’ to an abnormally high level, then gradually drop off as the cells make use of the factors. In an ideal situation, we would be able to transfect smaller doses on a daily basis, keeping the levels relatively constant and giving us a better idea of what levels are actually required to catalyse reprogramming.

Upon presenting some of this work at a conference in Rome in 2009, it was found that there was a consensus amongst other groups working on reprogramming that MRC5 is a particularly difficult cell line to reprogram and that, even with viral factors, the efficiency of this line is typically much lower than other fibroblast lines.

5.3 Chapter Discussion

Following exhaustive trials with various cell lines, mRNA factors, and small molecules, the correct balance of factors and a suitable method for transfection of somatic cells that results in iPS cells remains elusive. On each attempt, cells would begin to show signs of reprogramming, but then would eventually senesce or trigger apoptosis. However, cells that morphologically resemble iPS cells, express pluripotency genes and/or markers, including OCT4, were detected. While improved protocols gradually led to partially reprogrammed cells that were increasingly ES-like, further research is required before mRNA can be used as an effective tool for iPS cell derivation. A superior transfection technique that does not require the cells to be removed from the culture flask, that does not require FBS after each transfection, and a method that would allow smaller, more frequent doses of mRNA would likely result in a significant improvement by allowing more continuous and more stable expression of reprogramming factors.

From firsthand reports from researchers in other groups, and experience in our own lab using lentiviral vectors, MRC5 has been found to be one of the most difficult fibroblast lines to reprogram; therefore, it would be interesting to try other somatic cell types. For instance, keratinocytes have been shown to reprogram up to twice as fast along with a 100-fold increase in reprogramming efficiency over fibroblasts (Aasen et al. 2008). Also, in terms of deriving patient specific iPS cells, if they could be reproducibly derived from a single hair follicle, this would surely be preferred over a biopsy of other cells for the creation of a patient specific line. Also, due to the increased speed in which keratinocytes are reported to reprogram, mRNA, with its limited time period of expression, might be better suited for keratinocyte reprogramming.

While keratinocyte and neuronal cell reprogramming has been shown to be faster than fibroblasts, mouse cell reprogramming has also been shown to occur much faster as

well (Brambrink et al. 2008; Maherali et al. 2008b; Nakagawa et al. 2008). Having had difficulty isolating fully reprogrammed cells from human fibroblasts, mouse cells might be able to be reprogrammed with mRNA, showing an initial proof of principle before attempting further improvements or modifications to the existing process.

Although tests using the individual factors on HuF1 and MRC5 fibroblasts were performed, further examination of the individual effects and roles of the factors needs to be carried out. As briefly touched upon in this chapter, the individual reprogramming factors elicit a short-term, dose dependent response. While a small selection of genes related to reprogramming has been presented here, the technology could have wide spread applications for cell therapy as any gene could be transcribed into mRNA in vitro and used to help proliferation, differentiation, anti-apoptosis, transdifferentiation, cell cycle control, etc. Due to mRNA's transient nature, genome manipulation is avoided and expression takes place faster than when using plasmid DNA constructs or any construct that must first integrate into the genome. Also, constructs that integrate tend to have variable levels of expression, which is partially dependent on where in the genome they integrate, this leads to random, relatively uncontrollable levels of expression. Conversely, we have shown that transfection levels up to 99% can be reached using mRNA, even across a range of dosages, leading to more predictable, controllable expression of specific genes using mRNA.

While four factors have been shown to eventually catalyse reprogramming, the contents of an oocyte can remodel and reprogram a somatic cell's chromatin within 48 hours. This is surely due in part to additional, currently unknown factors. With a thorough analysis of oocyte and human ES cell cytoplasm, a selection of additional factors that would increase reprogramming speed and allow for successful mRNA transfection based reprogramming would surely be revealed. mRNA mediated gene expression is more controllable, and less toxic than DNA and remains an under used tool for manipulation of cell fate while avoiding genetic alteration.

Chapter 6 – General Discussion

6.1 Summary of Results

6.1.1 Review of Chapter 3 Results

Prior to the discoveries made by Yamanaka's group, many thought that differentiation was a unidirectional process. Only oocytes and pluripotent cells had shown potential to cause nuclear reprogramming and reversion to an embryonic state. Based on this, we used cytoplasts in an attempt to achieve the same thing, while trying to avoid alteration of the genomic DNA. A centrifugal enucleation protocol was developed, making the successfully isolation of cytoplasts possible. Also, an OCT4-GFP human fibroblast reporter line was derived to serve as a gauge of reprogramming efficiency, since OCT4 expression is a key marker of pluripotency. Pluripotent cytoplast fusion resulted in partial, temporary activation of the OCT4-GFP reporter line, but not full reprogramming. This work inspired the switch to total RNA and total mRNA.

6.1.2 Review of Chapter 4 Results

Following on from isolation of pluripotent cytoplasts, total RNA and total mRNA were hypothesised to contain all the factors necessary to catalyse reprogramming. To this end, an electroporation procedure was developed that lead to an effective method of RNA transfection for mammalian attachment and suspension cell types. Through transfection of total RNA and total mRNA, it was found that RNA transcripts from different cell types can be effectively transfected and translated resulting in temporary shifts in gene expression patterns. Through the use of NTERA2 total RNA and total mRNA, short-term expression of OCT4 and NANOG was detected, but no reprogrammed cells resulted. Interestingly, NTERA2 RNA also appeared to boost the expression of co-transfected GFP mRNA. While we did not confirm whether or not this effect occurred using other mRNAs, the effect is interesting in its own right and prompts further study. It may be that the addition of extra tRNAs, rRNAs, and microRNAs, or

other components of total RNA, provide cells with additional 'helper' translation machinery, thereby boosting gene expression. Total RNA and total mRNA work inspired the use of specific mRNAs coding for the transcription factors discovered by Yamanaka's group to catalyse somatic cell reprogramming.

6.1.3 Review of Chapter 5 Results

With the discovery that four factors (OCT4, SOX2, cMYC, and KLF4 or OCT4, SOX2, LIN28, and NANOG) alone were capable of catalysing human somatic cell reprogramming, total RNA work was shifted towards the development of an mRNA catalysed method of reprogramming. A method that would not cause genetic alteration and could potentially result in safer iPS cells than other available methods.

It was found that reprogramming is by no means achieved easily. It requires more than simple addition of the four factors in a 1:1:1:1 ratio, which initially caused widespread cell death using mRNA. The dosage of each individual reprogramming factor expression plays a key role. In our hands, mRNA coding for cMYC, which has been implicated in bolstering cell health and proliferation (Biro et al. 1993; Boxer et al. 2001), lead to increased levels of apoptosis in the somatic human cell lines transfected. Conversely, OCT4 conferred all somatic cell types tested with a temporary increase in proliferation rate. Treatment with SOX2 showed evidence of cell cycle alteration, holding treated cells in S-phase and also leading to cell aggregates with projections in all directions that resembled neurosphere formation. NANOG, in doses over 10ug per million cells, seemed to slow cell proliferation and may also affect the cell cycle. KLF4, and LIN28 did not appear to cause any noticeable effects. While further study is required to fully understand the effects of individual factors, our results allowed us to partially optimise the dosages of mRNA used. Moreover, it was found that mRNA had distinct advantages over DNA. Levels of protein expression tightly correlate with the amount of mRNA transfected and mRNA exhibited much higher transfection efficiency

and less cytotoxicity than DNA. Also, less cell death was observed in fibroblast cells transfected with 40 mg of mRNA than 3 mg of plasmid DNA (data not shown).

In an effort to improve the chances of reprogramming and potentially speed up the transformation, small molecules that alter cells' epigenetics, potentially opening up silenced pluripotency genes in the process, were introduced. Trichostatin A (TSA), 5-aza-2'-deoxycytidine (5Aza), BIX01294 (BIX), and valproic acid (VPA) were all tested individually and in concert, both as an alternative and supplement to mRNA in an effort to activate endogenous expression of pluripotency genes. It was found that these molecules were, like mRNA, capable of temporary upregulation of pluripotency gene expression in human fibroblasts, however, they were also detrimental to cell health and could not be used continuously. Combinations of 5Aza and TSA, BIX and VPA, and BIX, VPA, & 5Aza all lead to the formation of what we have termed 'proliferative aggregates' as well as detectable increases (by Q-PCR) in endogenous OCT4, SOX2, cMYC, and KLF4 as well as other pluripotency genes such as REX1 and NANOG. The increased levels in pluripotency gene expression detected by Q-PCR appeared minimal in comparison to standard human ES cell levels, so it was hypothesised that the 'normal', non-aggregated fibroblasts might be diluting the signal of the partially reprogrammed cell aggregates. Using the OCT4-GFP promoter line, it was shown that aggregates derived from small molecules had GFP expression, while surrounding cells did not; indicating endogenous OCT4 expression occurred primarily in aggregates, as hypothesised, albeit only temporarily and at relatively low levels.

After optimisation of the levels of mRNA factors used, proliferative aggregates were also derived from human fibroblasts treated with mRNA factors alone. Analysis by Q-PCR showed that mRNA treated cells did express the factors that we transfected them with and that mRNA is also capable of triggering expression of other pluripotency related genes temporarily. Since mRNA treatment alone did not result in reprogramming, small molecules were added along with mRNA to increase the effects.

Small molecules and mRNA together were found to have a synergistic effect, leading to larger proliferative aggregates and cell morphologies that more closely resembled ES cells, such as, in some instances, displaying prominent nucleoli. Using specific primers, Q-PCR confirmed that small molecules and mRNA together resulted in higher endogenous expression of reprogramming genes as well as related pluripotency genes, such as REX1, NANOG, and SALL4, as compared to mRNA or small molecules alone. Also, only after combination treatment with mRNA and small molecules were alkaline phosphatase positive colonies detected.

We came to find that timing and length of exposure to reprogramming factors is very important in terms of reprogramming efficiency (Mikkelsen et al. 2008). From running a Western blotting time course and daily FACS analysis of GFP mRNA treated fibroblasts, we found that protein expression from ectopic mRNA typically dissipates by 4 days post transfection. In an effort to prolong and intensify the effects of mRNA treatment, multiple rounds of transfection were attempted at intervals of 4-5 days. However, experiments involving multiple transfections typically induced widespread apoptosis, as most cells could not endure the stress of multiple electroporations.

After testing a variety of transfection technologies, an improved form of electroporation, called microporation, replaced electroporation as our primary method of transfection. Microporation increased the efficiency of mRNA transfection while being less detrimental on cell health. Although interesting cell morphologies were detected after multiple rounds of transfection, such as cells that resembled blood and neuronal phenotypes, no pluripotent or transdifferentiated cell lines could be passaged.

Under most conditions tested, aggregates derived from mRNA and/or small molecule treatment would rarely survive beyond 4-5 weeks post transfection before reaching senescence. However, improved transfection techniques and optimised mRNA dosage allowed for aggregates to grow, albeit very slowly, beyond 6 weeks post transfection. While most reports stated that reprogramming of human fibroblast cells should occur within 4 weeks following transfection, we found that it took over 7 weeks of culture before aggregates which express OCT4 could be detected by immunostaining.

Overall, mRNA and small molecule combination treatment resulted in phenotypes most closely resembling iPS cells, however, all cells selected either senesced or reached apoptosis. Results from a Q-PCR of pooled proliferative aggregates revealed 70-fold higher levels of p21 as compared to HUES1 human ES cells and over 7-fold higher than fibroblast controls; p21 is a direct target of p53 and is linked to cell cycle arrest (Benchimol 2001; Kawamura et al. 2009). While mRNA transfection serves as a useful tool, transfection and apoptosis related obstacles need to be solved before it can be successfully used for the production of genetic modification free iPS cells.

6.2 Implications of Research Findings

Although the overarching theme of this project was somatic cell reprogramming, along the way many tools were developed that have potential as uses in other areas of molecular biology. Centrifugal enucleation remains a useful tool for studying the individual roles of cytoplasmic and nuclear components of mammalian cells. Cytoplasts are interesting in their own right and may provide a useful, non-DNA approach to differentiation and transdifferentiation, as well as the study of cells in response to stimuli without nuclear instructions. Also, cytoplasts could answer questions pertaining to cell attachment, membrane repair, and cell motility. While transdifferentiation experiments have been previously attempted using cytoplast fusion, (Veomett et al. 1974), with modern FACS technology, the purity and specificity that can

be achieved may make cytoplasts more amenable than other options considering that a cytoplast could potentially contain hundreds of proteins and RNAs relating to the cell type it was derived from. This fact could make it better for differentiation and transdifferentiation experiments than using only a small number of genes in an attempt to catalyse phenotypic change.

Through development of a Total RNA transfection protocol, an electroporation protocol was developed which has since been successfully adapted for many other transfection uses, including successful transfection of human ES cells with greater efficiency than lipofection (data not shown). Total RNA and total mRNA transfection did not result in complete reprogramming, but did cause changes in gene expression and may be enough to catalyse transdifferentiation, which have been shown to occur in as little as three days using viral constructs (Zhou et al. 2008; Vierbuchen et al. 2010). Unlike viral factors, which integrate into the genome, total RNA and total mRNA have the advantage of being transient, while providing a large array of factors in a single transfection. By giving a cell the complete gene expression transcript for a particular cell type, it might provide a stronger or faster push towards the desired phenotype than a small group of specific factors.

Electroporation proved to be an effective transfection technique, however, microporation allowed for much more precise and efficient transfection. Using microporation, it was found that mRNA could be dosed in a specific manner at high efficiency, higher than with plasmid DNA. This technique could enable many quantitative expression studies, particularly in fields such as development, where the 3 day mRNA expression window may not be an issue for certain applications. Similarly, the use of the RN3P backbone to relatively conveniently produce mRNAs corresponding to any desired coding sequence could be used for a variety of purposes and benefits from its transient nature. Additionally, mRNA is arguably easier to

produce in vitro than protein and allows the transfected cell to provide the appropriate folding, something that is relatively difficult to accomplish in vitro. Also, since the cap and tail sequence is borrowed from Xenopus, specific primers can be used to easily identify ectopic transcripts from endogenous ones, allowing quantification of the influence of specific mRNA dosages on endogenous gene expression.

When the choice was made to pursue mRNA as the transient vehicle for reprogramming human somatic cells, protein was the other obvious choice. To date, there have been no successful reports using mRNA to reprogram human cells, however, the use of soluble protein reprogramming factors has been shown to result in iPS cells (Kim et al. 2009a; Zhou et al. 2009a). While mRNA still has its advantages in terms of production, there is currently no effective method for the transport of mRNA into cells through soluble means that is comparable to the system used for protein delivery. While lipofection and polymersomes (Lomas et al. 2008) were tested as methods to transport mRNA through the medium across the cell membrane, cell death and low efficiency prevented their use over microporation. However, a high efficiency system for transduction of siRNA using a double-stranded RNA binding protein fused with a cell membrane permeable domain has been developed (Eguchi et al. 2009). If this system were adapted to carry single-stranded mRNAs by replacing the double-stranded RNA binding protein with Nup153, the single-stranded equivalent (Ball et al. 2007), it could potentially solve the problem, allowing mRNA factors to be added to the medium, as needed, like the protein system.

Other methods of reprogramming with the goal of creating iPS cells without integrated reprogramming factors have also been published during the progress of this study. Piggybac transposons were used to selectively integrate and reprogram somatic cells, and were then excised from the genome using transposases (Woltjen et al. 2009). Similarly, Cre recombinase was used to excise reprogramming factors following reprogramming (Kaji et al. 2009). In an effort to combine the efficiency of viral

reprogramming while preventing integration, adenoviral vectors have also been reported to successfully reprogram somatic cells (Stadtfeld et al. 2008; Zhou et al. 2009b). However, these methods, while enabling reprogramming without permanent integration of reprogramming factors, all involve constructs that require DNA, in some form, to enter cells. Although the systems are designed to prevent integration or remove integrated reprogramming genes, there is still a chance that random integration can occur. Without thorough testing of resulting iPS clones, any number of mutations could occur, making these methods less desirable in terms of clinical application.

It was found that transfection of mRNAs encoding reprogramming factors can activate normally silenced embryonic genes within a few days. This result is in agreement with several recently published studies. In cell fusion experiments, somatic cells showed pluripotency gene expression within 1-2 days following fusion with ES cells (Yu et al. 2006; Ma et al. 2008; Pereira et al. 2008; Wong et al. 2008). Also, OCT4 and NANOG demethylation occurred just one day after fusion (Bhutani et al. 2009). When a somatic nucleus was place into a mouse zygote, the OCT4 gene was activated after only two cell cycles (Egli et al. 2007). These reports together with the work shown here suggest that, given sufficient amount of reprogramming factors, the de-differentiation process can be initiated rather rapidly. This therefore raises the question of why can iPS cells only be obtained after stable expression of defined factors for 3-4 weeks, while an enucleated oocyte can reprogram a somatic nucleus within a few days (Hochedlinger et al. 2002a)? In addition to OCT4, SOX2, cMYC, and KLF4, enucleated oocytes contain many regulators of chromatin modification, cell cycle and DNA damage response (Kocabas et al. 2006), which may be responsible for their robust reprogramming ability. Indeed, oocyte factors such as activation-induced cytidine deaminase and histone demethylase Jhdm2a can demethylate DNA and histones respectively and are required for reprogramming through the ES cell fusion method (Ma et al. 2008; Bhutani et al. 2009). It is conceivable that by adding the proper amount of additional “helper” factors to the Yamanaka 4-factor (OCT4, SOX2, cMYC,

KLF4) or Thomson 4-factor (OCT4, SOX2, LIN28, NANOG) set (Takahashi et al. 2007; Yu et al. 2007), the reprogramming process can be significantly accelerated, which may be achievable by an mRNA based method.

Transfection of mRNA reprogramming factors with small molecule treatment lead to changes in cell behaviour and phenotype; affecting proliferation, the cell cycle and cell orientation. Although cells often reached what could be described as a partially reprogrammed state, ultimately, reprogramming attempts were typically linked by the same issue, apoptosis and/or senescence. Only after review of the results as a whole, along with current published findings, have the reasons behind cell senescence become clear. Pooling together aggregates and testing by Q-PCR showed increased levels of p21 (also known as Cdkn1a). It has been shown that p21 is a direct target of p53 (also known as Trp53 in mice, TP53 in humans), leading to cell cycle arrest in G1, and inducing apoptosis (Benchimol 2001; Kawamura et al. 2009). However, only recently has the link between reprogramming factors (OCT4, SOX2, cMYC, and KLF4) and p53 activation been solidified (Zhao et al. 2008; Kawamura et al. 2009).

While it has been shown that p53 hinders the frequency and efficiency of somatic cell reprogramming (Zhao et al. 2008). It has also been shown that KLF4 plays a role in suppressing p53 activity by binding directly to its promoter, which should help to prevent p53 related apoptosis during the reprogramming process (Rowland et al. 2005). It may be that more KLF4 could have prevented or ameliorated aggregate senescence. However, it should be noted that blocking p53 also increases KLF4's propensity towards oncogenic transformation (Rowland et al. 2005); providing further evidence that the dosage of reprogramming factors must be kept in a very precise balance in order to result in successful somatic cell reprogramming. Factors such as this surely contribute to the low incidence of reprogramming and may explain why some cell types are more amenable to reprogramming than others, as different cell

types have different thresholds in terms of sensitivity to p21 and oncogenic transformation.

Further study is needed to assess the boundaries of reprogramming, for instance, at what point do reprogramming factors become dangerous by promoting oncogenesis and preventing repair of DNA damage? In addition to its ability to speed up reprogramming, cMYC is also known to cause DNA damaging reactive oxygen species, which can result in double-stranded DNA breaks, point mutations, and oncogenesis (Vafa et al. 2002). Although cMYC is a well known oncogene with links to oncogenesis through the reprogramming process (Okita et al. 2007), other factors such as KLF4, which is often considered integral to the reprogramming process, and SV40 Large T, which has been used to speed up the process of reprogramming (Mali et al. 2008), have also shown propensity to catalyse oncogenesis as well (Matker et al. 1998; Wang et al. 1998; Butel et al. 2003; Vilchez et al. 2003; Evans et al. 2008). With the correct balance (or dosage) of factors, preventing apoptosis and oncogenesis should be possible, allowing for proper dedifferentiation into iPS cells. However, until the individual roles of reprogramming genes and their interactions are fully understood, safety will remain a primary issue in terms of clinical use of iPS cells, further justifying the need for transient means of somatic cell reprogramming which can be accurately dose controlled and more easily safety tested.

6.3 Looking Ahead – Future Experiments

In addition to the experiments discussed above, there are a number of other interesting lines of experimentation that could be pursued using the protocols developed. Although the ultimate goal is to replace viruses with mRNA completely, mRNA could first be used to answer some interesting reprogramming kinetics questions by using lentiviral constructs together with mRNA factors, replacing one virus at a time with mRNA. This

way genes which need to be constitutively expressed in order for reprogramming to be successful can be determine and the levels of mRNA needed to catalyse reprogramming could be used to discover, in a more quantitative fashion, how much of each factor is required to cause reprogramming.

During this project, a viral lab was established and lentiviral reprogramming of MRC5 using the Thomson set (OCT4, SOX2, LIN28, and NANOG) was attempted. Initial attempts failed and only after over 50 days viral exposure were cells isolated that were characteristically ES-like, inferring that, as mentioned by colleagues from other labs, that the MRC5 line itself is more difficult to reprogram than other published somatic cell lines which typically take 21-28 days of viral exposure before isolation of iPS cells is possible (these lines are currently being characterised). It is likely that we would have found more reprogramming success with other somatic cell lines.

It was found that mRNA expression was limited to 3 days post transfection, however, for some applications, this does not pose an issue. In terms of reprogramming, mouse versions of OCT4, SOX2, cMYC, and KLF4 mRNA were made for the purpose of transfecting mouse neuronal cells which have been shown to reprogram within 1 week of viral transfection (A. Smith, correspondence 2009). Similarly, it was recently published that human amniotic fluid-derived cells can be efficiently reprogrammed within 6 days using recombinant retroviruses coding for OCT4, SOX2, cMYC, and KLF4 (Li et al. 2009). Considering that it takes time for retroviruses to integrate before stable expression is reached, mRNA factors may be able to substitute for viruses in this instance.

Considering the relatively vast epigenetic and gene expression changes involved in taking a unipotent cell and converting it to an embryonic, pluripotent state, smaller shifts in phenotype may be easier to accomplish using mRNA transfection as opposed

to complete somatic cell reprogramming. With this in mind, transdifferentiation has been shown to occur after exposure to a small set of viral factors. Recently, it was shown that fibroblast cells can be reprogrammed to neurons by defined factors within 3-5 days (Vierbuchen et al. 2010). Similarly, adenovirus transduction of NGN3, PDX1 and MAFA in adult pancreas led to appearance of new insulin secreting cells after 3 days, indicating trans-differentiation from exocrine β-cells to endocrine is a relatively fast process (Zhou et al. 2008). Both of these transdifferentiations, and potentially many more, fall within the expression window of mRNA and could provide a safer, better controlled method of transdifferentiation, negating the need for viruses.

While the focus of this work has been dedifferentiation, cytoplasts, total RNA, and specific mRNAs could all be used as catalysts for directed differentiation. Human ES cells, being highly sensitive to their environment, have shown potential to differentiate following co-culture and fusion with somatic cell types (Mummery et al. 2003; Yu et al. 2006; Mummery et al. 2007), theoretically, cytoplast fusion could potentially result in the same effect as cell-cell fusion. Similarly, total RNA isolated from somatic cell types could be used to temporarily confer the gene expression signature of a desired somatic cell type to human ES cells, promoting change towards that phenotype. Just as a small number of factors have been successful at catalysing transdifferentiation, specific mRNA factors should be able to be used to catalyse differentiation, particularly in instances where necessary exposure is 3 days or less.

Inducible cell lines are a useful tool for controlling the gene expression of specific genes of interest, however, isolating clones that express at appreciable levels and do not suffer from gene silencing can be difficult. For studies that require short-term upregulation of specific genes, mRNA transfection could be used to accurately dose cells with the gene of interest in a predictable fashion that does not suffer from silencing. Also, multiple genes can be tested simultaneously with high efficiency, providing new insight into gene expression pathways. mRNA could also be used with

existing inducible systems to 'rescue' suppressed expression in a dose controlled manner.

6.4 Conclusion

At the inception of this project, very few researchers were working on reprogramming, however, now there are over 200 publications outlining various approaches and uses of reprogramming technology. This work has attempted to evolve with the literature and take into consideration the constant advances in reprogramming research that have occurred over the past four years. However, this work is really only a starting point, an exploration of a rapidly growing sub-field of ES cell research that is quickly emerging as an important part of the future of regenerative medicine.

In this study, new routes toward induced pluripotency have been evaluated. With further study, it should be possible to expand and better define the uses of cytoplast, total RNA and mRNA transfection technology and potentially develop a system for successful derivation of DNA modification free, patient specific iPS cells that can be used for clinical, regenerative medicine purposes. Although, in the short-term, since specific mRNA mediated gene expression is more controllable and less toxic than using DNA constructs, this technology can be readily exploited to manipulate cell fate, avoiding unnecessary genetic alteration, and have wide applications in cell therapy, controlled gene expression, and the study of molecular mechanisms.

Chapter 7 – Validation

7.1 Introduction

This chapter has been included to satisfy the requirements of the Validation II module of the EngD programme and will discuss potential validation hurdles pertaining to the research carried out, and how these issues might be dealt with in an industrial setting for clinical or good manufacturing practice (GMP) grade production. The ideas presented are based on what validation concerns should be addressed if optimisation of the mRNA reprogramming approach had resulted in genetically unmodified induced pluripotent stem (iPS) cells and this process been adapted to a commercial production setting.

The European Medicines Agency (EMEA) is the major regulation body in charge of sanctioning therapeutic products in the EU and, currently, there are few regulations pertaining to processes that include production and transplantation of iPS cells. The validation issues covered in this section are based largely on the suggestions outlined in the EMEA's "Reflection paper on stem cell-based medicinal products [EMA/CAT/571134/2009]" (EMEA 2010). This document is a work in progress and represents the most current views from the EMEA and Committee for Advanced Therapies (CAT) involving the use of embryonic stem (ES) and induced pluripotent stem (iPS) cells as biological, therapeutic products.

The fictional process that this assessment is based on would involve the following steps as part of the manufacturing process:

1. Procurement of tissue or cells from a given patient/donor.
2. Expansion and characterisation of somatic donor tissue.
3. Reprogramming of donor cells through a defined process resulting in patient-specific iPS cells.
4. Expansion of iPS cells under conditions supporting growth of undifferentiated

cells.

5. In vitro differentiation of the cells.
6. Purification of the intended biologically active cell population (*e.g.* removal of undifferentiated pluripotent cells).
7. Verification of safety and functionality of the product (Final quality control and product approval)
8. Transplantation of patient matched differentiated cells/tissue.

7.2 Validation Issues

7.2.1 Starting Material – Donor Tissue

For human donor cells, the history of the cell line derivation and banking procedures, including the raw material used during production needs to be documented. Karyotype and viral safety of the starting cells should be addressed.

7.2.2 Expansion of Donor Cells

Care needs to be taken to perform all culture aseptically and patient samples should be reasonably separated and well labelled so as to avoid cross contamination or mixing of patient cells. Efforts should be made to avoid animal derived products and cells for the support of human cells.

7.2.3 mRNA Production and Storage

mRNA itself should be prepared to GMP standard in an clean room environment and stored at -80^{o}C. With regular quality control (QC) checks, a large bank of mRNA could be made from a verified DNA construct, checked by spectrophotometer for purity (A_{260}/A_{280} reading) and cryopreserved for months. This mRNA master bank could then be aliquoted and used to potentially derive thousands of iPS lines, but would need to be tested for efficacy across a wide range of cell lines to be certain that its potency and dosage remain within a given optimal range for cells donated from different patients.

Due to the fragile nature of mRNA, analyses would need to be run to assess its shelf life under standard freezing and thawing conditions. Although, due to its transient nature, mRNA is not associated with any permanent, negative effects and should readily fit within existing EMEA guidelines regarding its production, cryopreservation and use.

7.2.4 Use of Oncogenes

Due to the transient nature of mRNA, it is inherently safer than DNA plasmid or viral vectors which integrate or have the potential to integrate into the genome. Using clinically approved small molecules, such as valproic acid (which is used to treat epilepsy), may negate the need for oncogene mRNA. If oncogenes such as CMYC and KLF4 were required, further testing on their potential long term effects on somatic cells would need to be assessed to be certain that the temporary treatment with mRNA did not activate or increase the risk of reprogrammed cells becoming oncogenic in vivo.

7.2.5 Identification and characterisation of iPS cells

Current methods of initial human iPS isolation are typically based on morphology. While morphology is a good indicator of reprogramming to the trained eye, a number of analyses need to be carried out in order to verify that the isolated cells are in fact pluripotent. These analyses might include, but are not limited to: QPCR for pluripotency genes with human ES cell controls, immunostaining for pluripotency markers, ability to form embryoid bodies (EBs), differentiation into cell types from the three germ layers with relevant PCR and staining for relevant markers, evidence that they form teratomas in SCID mice, and proof that the cells can proliferate stably for an extended length of time (i.e. more than 6 months). Due to ethical concerns, the most stringent test of pluripotency, tetraploid embryo complementation, cannot be used.

There are also fundamental issues with testing of pluripotency that have not yet been fully addressed. One such issue is epigenetic state. While one can assess gene

expression and differentiation potential, reprogramming success depends greatly on successfully changing the methylation state of key pluripotency genes such as OCT4 and NANOG (Hochedlinger et al. 2009). However, currently there is no standard accepted protocol for what methylation patterns denote pluripotency versus partial or incomplete reprogramming.

Due to the plasticity of iPS cells and their ability to form teratomas in vivo, we would expect that only differentiated cells would be used for transplantation. Therefore, a suitable protocol would need to be developed for every differentiation such that cells differentiated from iPS cells would need to be checked for relevant markers and gene expression to verify that the differentiation to the desired cell type was complete. Also, a method to eliminate any remaining undifferentiated iPS cells from a group of differentiated cells would need to be established prior to transplantation. While there have been projects aimed at solving this goal, currently there is no standard, clinically accepted procedure to the elimination of undifferentiated cells from a heterogeneous population being prepared for transplantation.

7.2.6 iPS Culture Conditions

Culture conditions can influence the genomic stability of pluripotent cells (Baker et al. 2007; Harrison et al. 2007). It is therefore essential that iPS cell lines that have undergone substantial in vitro manipulation be evaluated for their chromosomal stability before the first clinical use. Also, iPS cells should be checked regularly for karyotypic abnormalities and, where possible, epigenetic analysis should be carried out shortly after reprogramming and on lines grown for extended periods of time in vitro.

7.2.7 HAMA Response

There is a risk that the mouse cells used as feeder cells for pluripotent cells may transmit molecules that elicit a human anti-mouse antibody (HAMA) response if used

clinically. Currently, there have only been limited reports of 'feeder free' iPS cell derivations (Sun et al. 2009), yet they still involve Matrigel, which contains animal derived components. The degree to which animal derived components need to be removed or limited in order to show safety in humans has not yet been quantified clinically, but where possible, effort to remove animal cells and animal derived components from the process should be taken. Currently, human feeder cells with non-animal derived culture medium are the standard for GMP ES cell growth (Skottman et al. 2006; Unger et al. 2008).

7.2.8 Lineage commitment and Tumourigenicity

Cells for transplantation should be fully differentiated with expression of known genes and cell surface markers. Differentiation protocols need to be verified across a range of cell lines from different patients. If differentiation is a multi-step process, each step and any irregularities need to be documented to establish a tight range of conditions which result in appropriately differentiated cells for use as a biotherapeutic.

Transplantation of cells derived from an undifferentiated/pluripotent starting population, such as iPS cells, carry an inherently higher risk of tumourigenicity. The number of proliferative and/or undifferentiated cells in the final product should be limited and justified. In addition to stringent differentiation protocols, serial dilutions of iPS cells could be transplanted into SCID mice or other animal models to estimate the level of risk of teratoma formation from non-lineage committed cells being transplanted into a patient. Where non-lineage committed cells are to be administered to patients, a strategy to minimise the risk of tumourigenicity should be designed and tested. Tests might include, but would not be limited to: PCR to assess appropriate gene expression, western blot to show production of proteins associated with the lineage committed cell type of interest and lack of pluripotency gene translation, extended culture of differentiated cells derived from iPS cells to show that cells do not revert to a pluripotent state, and histological analysis to assess morphology.

7.2.9 Biodistribution and Niche

Assuming preliminary efficacy has been established and verified, methods for tracking transplanted cells should be instituted. Marker genes or labelling of cells could be used to provide information about the propensity of transplanted cells to home to distant, potentially undesired locations. Since differentiation and function of iPS cells are dependent on and affected by the microenvironment, it is important that the niche that transplanted cells settle in is well understood and defined. Also, risks of aberrant, ectopic tissue formation in undesired niches should be evaluated. Studies showing correlation between the number of systematic applications of live cells and efficacy should be carried out, along with the related increase in risk of aberrant cell growth. Local, non-physiological or toxic effects that might be mediated by transplanted cells, such as immune suppression, should also be studied.

7.3 Additional Process Issues

7.3.1 Scale up

As with any process governed under the regulations of the EMEA, robustness would need to be quantified and demonstrated at each stage of the scale up from lab scale to full, commercial scale (size depending on treatment) as well as proof of the equivalency between the lab scale data and results obtained from the commercial scale process. Since iPS cells grow in colonies that are very susceptible to environment cues, a system for their expansion would likely require horizontal expansion (similar to Organogenesis), rather than simple scale up. Whereas many cell types have been adapted to growth in large flasks or bioreactors, growth of pluripotent human ES and iPS cells in these large scale systems is very difficult and requires further study to prove equivalence to growth in incubated flasks.

7.3.2 Transport and tracking of patient cells

Due to the extensive changes catalysed by reprogramming, a stringent system of tracking linked to cell karyotype would need to be put in place. Donor tissue would need to be karyotyped before undergoing the reprogramming process and any iPS lines derived from that donor tissue would need to be karyotyped prior to cryopreservation and transplantation. During growth stages of primary material expansion and expansion of iPS clones, a form of tracking each flask and it's link back to a particular patient might benefit from the use of radio frequency identification (RFID) technology. Small RFID chips could be attached to every flask and flasks could be electronically associated with particular patients, preventing mixing.

7.4 Discussion

While human ES cells have been studied for over 10 years and have come with the promise of revolutionising the future of medicine and biotherapeutics, many safety and validation issues remain. Human ES cells, with all the benefits of pluripotency, still come with the caveat of being derived from human embryos and not being patient specific. However, while iPS cells have been touted as the solution to the ethical and immunological concerns raised by human ES cells, they come with their own set of unique issues. Epigenetics, pluripotency, and oncogenesis are all key issues that are difficult to define and manage when considering the clinical use of iPS cells.

Epigenetically, iPS cells are highly variable. Despite their ability to demonstrate pluripotency, when compared to human ES cells, iPS cell methylation patterns can take on many forms and studies have shown that the expression patterns of the original cell phenotype from which the iPS cell line was derived (i.e. dermal fibroblasts) can often carry over to some extent (Hochedlinger et al. 2009). However, without extensive comparative studies, the degree to which these patterns match and whether or not that

affects iPS cell fate are unclear. The concern is that there is a clear link between epigenetics, reprogramming, and oncogenesis.

Initially shown in offspring from germline competent mouse iPS cells (Okita et al. 2007), the reprogramming factors required to catalyse reprogramming have also been implicated in promoting oncogenesis (Boxer et al. 2001; Vafa et al. 2002; Rowland et al. 2005). Using mRNA, the risks associated with using oncogenes as factors to promote reprogramming should be lessened, but further study is needed to verify this. When using integrated viral reprogramming factors, one of the primary risks is incomplete silencing or reactivation of previously silenced (methylated) reprogramming genes leading to oncogenesis. While transient factors, such as the use of soluble proteins, have been shown to be effective as reprogramming agents, whether or not the short lived proteins result in permanent epigenetic changes capable of increasing the probability of oncogenesis in the long term needs to be studied.

Although the term pluripotency is widely used and has been defined by a number of characteristics and analytical tests, as a cell state, it is variable. Not all human ES cell lines respond to stimuli in the same way, not all iPS cells grow and differentiate under the same conditions, and cell lines such as NTERA2, which are polyploidy and grow in monolayer, are still considered pluripotent. In terms of clinical use and evaluation for GMP production, a more precise definition of pluripotency and its implications in terms of safety needs to be settled upon. While non-genetically modified, patient specific pluripotent iPS cells should inherently be safer than pluripotent embryonal carcinoma cells, current means of defining pluripotency and differentiation potential do not necessarily provide proof of long term safety or stability when it comes to pluripotent cell lines. Due to the rather random nature of the reprogramming process and our current lack of understanding in terms of the step by step gene changes and epigenetic changes that occur to result in iPS cells, safety will certainly remain a key issue in terms of their clinical use for the foreseeable future. Initially, calculated risks will have

to be taken and the differentiated progeny of pluripotent cells will have to be thoroughly tested and cultured long term to judge the frequency of oncogenesis, if any from reprogrammed cell lines. With further elucidation of the necessary changes involved in the reprogramming process, increased safety measures and a better understanding of cell states or phenotypes should reveal itself.

Chapter 8 – Business Management

8.1 Introduction

This chapter has been included to satisfy the requirements of the Management II module of the EngD programme and aims to cover potential business implications pertaining to the research carried out. The business idea presented is fictional, based on the successful optimisation of the mRNA reprogramming approach resulting in genetically unmodified iPS cells and how these cells could be marketed as a product for regenerative medicine applications. The idea is modelled after the UK/US human umbilical cord blood preservation market. The business plan presented here was submitted to the London Entrepreneur's Challenge 2008/09 and won 'Best Postgraduate Idea.'

8.2 Contents – Longevity Bio Business Plan v1.1

8.3 Executive Summary

We are Longevity Bio, a company based around the derivation and storage of patient specific pluripotent stem cells, stem cells that are capable of becoming any cell type found in the body.

Our technology is a novel process by which fully differentiated, adult human cells can be reprogrammed to an embryonic state, resulting in cells that are phenotypically, morphologically, and functionally identical to human embryonic stem cells. However, unlike embryo derived stem cells, our reprogrammed cells are derived from each specific patient, regardless of age, essentially allowing patients to be their own donor for a wide variety of cell therapy applications, while also avoiding the controversy surrounding the use of embryos.

Our product is a service. Longevity Bio would charge a fee for the initial reprogramming and storage of a patient's cells and an annual upkeep fee to keep the cells cryopreserved (frozen in liquid nitrogen, effectively maintaining cell viability until needed). The process involves patients going to the hospital where a small tissue sample would be taken by standard biopsy, those cells would then be couriered to our facility where they would be reprogrammed and cryopreserved. Also, patient's cells would be split into 2 or more aliquots and stored in separate locations for extra security. When needed, cells would be revived and sent on for patient use.

The list of potential applications under research spans nearly every known degenerative disease and published research related to pluripotent stem cells is increasing at an exponential rate. Some of the applications currently in clinical trials include previously untreatable afflictions such as: pancreatic beta-islet cells for type 1 (or juvenile) diabetes, nervous system cell progenitors for spinal cord injuries, and neural cell progenitors for Parkinson's and Alzheimer's. As a customer, you would be investing in a healthy future by storing your own (or your child's) stem cells through Longevity Bio as a kind of organic insurance policy.

Although, in the future we may apply our expertise to the differentiation and transplantation aspects of stem cell therapy, at this time, we plan to focus on our core competencies of reprogramming and cryopreservation, leaving the other aspects of the process (see Figure 1) to established differentiation labs, supplying them with patient specific stem cells in an ethical and timely manner. Upon entry into the market, we plan to mimic umbilical cord blood stem cell (UCBSC) cryopreservation companies, however, providing a product that is superior in biological functionality and a service that is available to all, not just newborns.

Currently, we have a patent lawyer working on the IP for the process itself and may end up filing multiple patents. We hope to secure enough initial funding at this early stage to protect our IP and set up a small scale 'proof of concept' process lab at UCL or in an incubator lab in Central London. At the same time, we also plan to get in touch with companies in the marketplace that might be interested in licensing this technology, such as UCBSC companies and pharmaceutical companies. We estimate that we will need approximately £200,000 to cover the next 12 months while we attempt to reach these goals. Further costs would depend on whether or not we choose to move forward with licensing, partnership, or independent processing. However, at the rate that the UCBSC market is growing, we estimate that by licensing this technology we could provide a return on investment and potentially become profitable within one year with profits of £900k+/yr from year 2 onwards.

We recognize that we are primarily a group of scientists and as such, licensing is likely in our best interests as umbilical cord blood companies already have the infrastructure to support most of our process requirements. However, given the right mix of expertise, we would consider partnering with a firm to try to scale up our initial process lab into a commercial scale process.

8.4 Team

The following team members represent the core of Longevity Bio:

Jordan Plews – President, BEng degree (1st class) in Biochemical Engineering (UCL), currently a final year doctorate student through a joint UCL (Dept. of Biochemical Engineering), Axordia, and University of Sheffield programme. Jordan has also worked for Pfizer as a member of the bioprocess development group (BDG), a group dedicated to scaling up lab scale bioprocesses to industrial scale for large scale production and distribution.

Christian Unger – Head of Research, PhD in Molecular Biology and Stem Cell Differentiation from Karolinska Institute (Sweden). Christian is currently a Post-Doc at University of Sheffield. Previously, Christian has experience with induced pluripotent stem (iPS) cell derivation as well as human embryonic stem cell culture, storage, and differentiation.

Jessica Small – PR & Marketing, BSc in Advertising and Public Relations (Northern Arizona University), MA International Communications (University of Leeds). Jessica previously worked with Wells Fargo on their Marketing team and for Atlantis Advertising as a Traffic Coordinator and Media Buyer.

Whitney Andrews – Bioethics Advisor & Administrator, MSc in Biotechnological Law and Ethics (University of Sheffield). Whitney worked previously with the University of Sheffield and Axordia, a stem cell start-up, helping to secure millions of pounds in funding through stem cell research grants from the European Union.

8.5 Product/Service Description

We have developed a novel method for reprogramming adult (somatic) cells into pluripotent stem cells, cells functionally equivalent to embryonic stem cells. Importantly, unlike current published methods, our method accomplishes this *without* the use of viruses or genetic constructs that have the potential to directly alter the DNA, which can lead to genetic abnormalities. After reprogramming, these cells can then be cryopreserved until they are needed, at which point they can be limitlessly expanded in vitro, then potentially differentiated into any cell type needed to treat the donor patient, and distributed to the patient's clinic of choice for transplantation. This means that patients can be their own donors, potentially eliminating the need for donor tissue and the dangers of immunorejection.

Our product is a patentable bioprocess/service involving the derivation, storage, and (when necessary) distribution of reprogrammed cells. The process involves treating donor cells (obtained through a standard biopsy) with unique factors that activate a cascade of reprogramming genes, eventually leading to the isolation of reprogrammed, pluripotent, patient-matched stem cells that can be differentiated into any cell type in the body. The DNA code itself (karyotype) is not altered, only the way that the cell reads and interprets it, this is important as it means that there is no chance of cell mutation using our process and the cells will match the patient perfectly, eliminating the issue of immunorejection that plagues current transplantation therapies.

The DNA necessary to code for any cell type in our body is contained in the nucleus of every cell we have. However, a skin cell is a skin cell and a brain cell is a brain cell because most of our genome is effectively 'turned off', leaving only the necessary genes activated for a specific cell type to carry out its specific function within the body. Our process catalyses a reversion, reprogramming the cellular gene transcription circuitry back to an embryonic state, a state in which its function has not yet been assigned and can therefore be reassigned.

Our proposed bioprocess/service would require patient biopsies to be sent to a laboratory where they would be systematically cultured, reprogrammed, and cryopreserved (See Figure 1). Premiums would be charged for reprogramming a patient's cells and cryopreserving them and for a nominal upkeep charge, these cells would be stored until needed for any number of regenerative medicine or cosmetic applications, whenever they need it, whether for convenience or emergency.

Some of the potential tissue types and applications:
Pancreas – For diabetes

Liver – For cirrhosis of the liver

Cardiac (heart) muscle – For heart attack & heart disease patients

Neuronal cells – For Alzheimer's, Parkinson's, and other degenerative CNS diseases

Oligodendricytes – For spinal cord injuries

Fat – For cosmetics, e.g. breast implants (no more synthetic compounds!)

Epidermis (skin) – For burns victims and cosmetic 'rejuvenation'

Hair – For autologous hair transplants

Inner Ear cells – For deafness

Retinal Cells – For age related degenerative ocular diseases

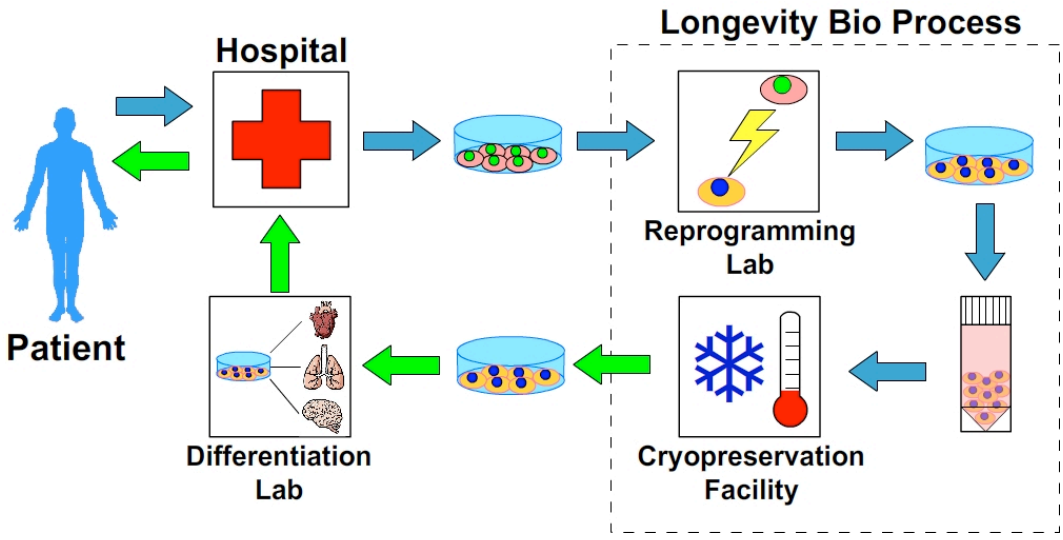

Figure 8.1: Process Diagram
The dotted line encompasses the process steps that Longevity Bio would be responsible for and is aiming to gain IP for.

7.4.1 Utilising Market Leaders Through Licensing

Our technology is unique. Although other research groups have attempted to make autologous stem cell lines (lines matching the genetic profile of the donor), none have approached the problem in the same way as we have. The methods used successfully by other groups to reprogram cells have involved the use of viruses or constructs that alter the genome such that they greatly increase the potential for causing genetic abnormalities (Okita et al. 2007). Our method does not involve the use of viruses, DNA altering constructs, or the destruction of embryos, allowing for the safe and ethical creation of patient-specific stem cell lines. Also, our patentable process utilises a combination of biochemical engineering and molecular biology techniques making it unlike anything else currently available.

Our biggest competitors at this stage are most likely umbilical cord blood stem cell (UCBSC) cryopreservation companies. These companies isolate UCBSCs from the umbilical cord of newborn babies with the intention of cryopreserving them for potential therapeutic use in the future. The process utilised by UCBSC companies is very similar to our process outlined above, however, instead of processing adult tissue, they process umbilical cord tissue and instead of a reprogramming step, they have a stem cell isolation step (in which they isolate the UCBSCs from the umbilical cord). Yet unlike UCBSC companies' services, we are not limited by patient age and our reprogrammed cells are technically more useful because they are capable of differentiating into any cell type needed, not simply a small subset.

Rather than try to compete with UCBSC companies, we feel that it would be in our best interest to utilise their existing infrastructure by offering to license our advanced technology to them, allowing them to offer a better product to a wider market and enabling our product to reach customers sooner. Due to the rate at which reprogramming and stem cell research is progressing, we feel that time-to-market is key to the success of Longevity Bio's service.

8.6 Business Model

Longevity Bio plans to mimic the successful business models of UCBSC cryopreservation companies such as Cord Blood America, ViaCord, Cells4Life, and Virgin Health Bank, and hopes to establish partnerships and/or licensing agreements with one or many such companies. Similar to Virgin Health Bank and other UCBSC companies, our primary focus will be obtaining, isolating (after reprogramming), and storing unique, autologous (patient-matched) cells that have the potential to be of great benefit, primarily to the patient, but also to others.

Companies such as Virgin Health Bank charge parents-to-be for a service that involves the collection and cryopreservation of their child's UCBSCs plus annual storage fees; total fees range from £1300 to £3000 ($1900 to $4300). Similarly, we would cryopreserve a small flask of the patient's reprogrammed cells, charging an initial fee plus upkeep fees for storing the cells and having them readily available when necessary. With patient consent, the cell bank could also be used to help others, or for a number of research applications. The important difference between our cells and those already bringing success to Virgin and others is that we can isolate our reprogrammed cells from ANY patient, regardless of age, not just at birth. Plus, our cells have the potential of becoming ANY cell type needed by a patient whereas UCBSCs can only differentiate into a limited number of cell types and are therefore not useful for many important applications (such as diabetes, neurodegenerative diseases, or paralysis).

Currently we are in the process of trying to acquire grants and investor funding in order to lease a pilot scale lab for reprogramming human cells as a proof of concept and, depending on licensing agreements, potentially for the eventual establishment of a commercial scale Good Manufacturing Practice (GMP) certified facility. After setting up our primary distribution chain, we plan to intensify our on-going research into stem cell epigenetics and regenerative medicine while expanding our IP portfolio to include other

uses for our reprogrammed cells, such as in vitro disease modeling, an area of research that many pharmaceutical companies have already shown interest in.

After evaluating our product and the market we recognise that the industry of stem cell cryopreservation has high barriers to entry due to extensive regulations and the high cost of facilities and marketing, but we feel that our advantage lies in our novel technology which we hope to market directly to existing companies that have already overcome most of these barriers. Currently we feel that there is little to no threat of substitutes, but we also recognize that the stem cell research is advancing at an exponential rate and that time-to-market is likely to be integral to the success of our product.

At this time, the supplier (in this case, the supplier of the laboratory equipment and consumables required for our reprogramming process) has little control over the market. The supplies needed are common, relatively inexpensive, and even with significant fluctuations in cost, the cost of supplies are unlikely to significantly decrease our profit margin. However, customer control of the market is likely to be one of the most important factors governing the success of our product in the market. However, since we hope to license our technology, we aim to pass this risk onto the licensee and given the operation costs estimated (See Financial Analysis section), we would only need to penetrate a small percentage of our target market in order for our product to be profitable.

8.7 Market and Customers

In general, we predict that our customer base will mainly consist of affluent individuals who wish to have their own genetically matched stem cells as a sort of organic insurance policy. We also predict that customers that would invest in UCBSC storage for their children would be interested in our technology for their children (instead) and possibly for themselves as well. Additionally, our technology will likely be of commercial value for biotech and pharmaceutical companies, particularly through the creation of genetic disease specific stem cells that would allow for the study of various diseases and drugs treatments on human cells prior to clinical trials.

7.4.2 Primary Target Audience Profile

Our customer will be male and female adults over the age of 40 living in the United States or United Kingdom. They will either be married or single, with or without kids. They are likely to own their own home and work in a professional or white-collar job with a household income of $200,000+ a year. They will be health conscience individuals who regularly partake in physical activity and are mindful of their nutrition/diet. They will have started thinking about the repercussions of getting older and will have life insurance policies taken out for themselves and want an insurance policy for their health as they age.

7.4.3 Secondary Target Audience Profile

Our customer will be expecting parents between the age of 25-44 living in the United States or United Kingdom. They are likely to be married and either be expecting their first child or a subsequent child. They will both be working and have a household income of $75,000+ a year. They could be renting or own their own home. These are parents who are particularly interested in taking precautionary steps for the well being of their child.

7.4.4 Tertiary Target Audience Profile

Since our reprogrammed cells can be derived from patients with genetic diseases and can divide infinitely (like human embryonic stem cells and unlike any other cells in the body), pharmaceutical and biotech companies might be interested in using our technology. Our customer will be biotech and pharmaceutical companies researching genetic disease targets. They would likely have the facilities to search for genetic disease drug targets via a high throughput analysis system, yet lack a human cell in vitro model to test. They would also likely be companies with abundant research budgets that would benefit from being able to test ex vivo human tissue prior to human clinical trials.

8.8 Financial Analysis

7.4.5 Costs for 'Proof of Concept' Pilot Scale Lab

Below is an estimated breakdown of costs to setup a non-GMP laboratory within UCL or Central London for approximately 12 months with the purpose of reprogramming adult (somatic) human cells from non-patient derived sources as a proof of concept for a full scale commercial process. Most costs are estimated or taken from past first-hand experience. Effort was made to make estimates as conservative as possible. See appendix for additional costing information.

Staff	#	cost/person/yr	Cost/yr
Lab Staff (researchers, cell culture)	3	£25000	£75000
Admin	1	£20000	£20000
Other	1	£15000	£15000
TOTAL			**£110000**

	Type	Facility Type	cost/yr
Facility	non-GMP	UCL	**£0**

Disposables	Cost/wk	Cost/mo	Cost/yr
Plasticware	25	£100	£1200
Consumables (Media, etc.)	10	£40	£480
Office Supplies			£500
TOTAL			**£2180**

Lab Equipment	#	Individual Cost	Total cost
Centrifuges	1	£3000	£3000
Incubators	1	£5000	£5000
TC Hoods	2	£15000	£30000
PCR Machines	1	£3000	£3000
Water Bath	2	£200	£400
Computers	2	£1000	£2000
Fridges	1	£500	£500
Freezers	1	£2000	£2000
Cryopreservation Dewers	1	£2000	£2000
Misc. QC Equipment	N/A	£5000	£5000
TOTAL			**£52900**

GRAND TOTAL (12 months)	**£165,080**

Assumptions not explicitly stated above:

Facility costs includes overheads	
One 500 mL bottle of cell nutrients (media + additives cost	£20
Tissue culture flask cost (each)	£2
# of flasks fed by a 500 mL bottle of cell nutrients (one process cycle)	£20
Flasks per incubator (4 shelf incubator) [4x3x3x3]	108
Flasks per patient	1
Customers/month	2046
Length of time (months) cells need to be in incubator	2
Number of incubators required (+1)	40
# of patient's cells that can be handled per technician per hour	8
Hours of operation per day	8
# of patient's cells processed per technician per day	64
per week (5 day work week)	320
Influx of customer cell samples per week	511
Cell Technicians needed to handle influx	2

7.4.6 Costs for Initial Commercial Scale Lab

Below is an estimated breakdown of costs to setup a GMP laboratory within Central London or the UK for the purpose of reprogramming adult (somatic) human cells from patient derived sources as a full scale commercial process. Most costs are estimated or taken from past first-hand experience. Effort was made to make estimates as conservative as possible.

Staff (on site)	#	cost/person/yr	Cost/yr
Lab Staff	6	£25000	£150,000
Admin	2	£20000	£40,000
Other	2	£15000	£30,000
TOTAL			**£220,000**

Staff (contracted)	Est. Biopsies in 1st year	Cost per biopsy	Cost/yr
Doctors/Clinicians (for biopsies)	**24552**	**£100**	**£2,500,000**

	Type	Location	cost/yr
Facility (inc. overheads)	GMP	Unknown	**£180,000**
Offsite Cryo-backup			**£61,000**

Disposables	Cost/wk	Cost/mo	Cost/yr
Plasticware	£5115	£20460	£250,000
Consumables (Media, etc.)	£1023	£4092	£50,000
Office Supplies			£5,000
TOTAL			**£300,000**

Lab Equipment	#	Individual Cost	Total cost
Centrifuges	2	£3000	£6,000
Incubators	40	£5000	£200,000
TC Hoods	6	£15000	£90,000
PCR Machines	2	£3000	£6,000
Water Bath	2	£200	£400
Computers	5	£1000	£5,000
Fridges	4	£500	£2,000
Freezers	4	£2000	£8,000
Cryopreservation Dewers	4	£2000	£8,000
Misc. QC Equipment	N/A	£20000	£20,000
TOTAL			**£345,400**

GRAND TOTAL	**£3,600,000**

Assumptions not explicitly stated above:

- A tissue culture flask costs £2
- One 500 mL bottle of cell nutrients (media + additives) costs £20 and can feed up to 5 flasks for one complete process cycle (cell expansion, reprogramming & isolation, and cryopreservation)
- Facility costs includes overheads

- A typical 9x9 cryovial box holds 81 patient samples and costs £200/year to store off-site (either in a rented facility or through a contracted cell bank)
- See Revenue calculations for assumptions behind estimated annual # of patient samples.

7.4.7 Estimated Initial Revenue Calculations

Below are calculations based on achieving 5% penetration of our target market. Our target market has been estimated to be a combination of the US and UK umbilical cord blood stem cell cryopreservation market and 5% of the affluent US and UK market (those with household incomes >$200,000/yr or equivalent).

US Population (2008)	**US Birth Rate (2008)**	**% of New Births that store UCBSC**	**Total US UCBSC Market**
303824640	4308233	5.00%	215412

UK Population (2008)	**UK Birth Rate (2008)**	**% of New Births that store UCBSC**	**Total UK UCBSC Market**
60943912	649053	5.00%	32453

US Households (2006)	**% of HH >$200k/yr**	**% of >$200k/yr HH interested in Personal Stem Cells**	**Total US 'Wealthy' Market**
116011000	3.46%	5.00%	200800

UK Households (2001)	**% of HH >$200k/yr**	**% of >$200k/yr HH interested in Personal Stem Cells**	**Total UK 'Wealthy' Market**
24479439	3.46%	5.00%	42371

TOTAL POTENTIAL MARKET	**491035**

Initial Target % of Market	5%
Total Target Market	24552
Fee for Processing+Storage	£1,500.00
Initial Revenue	£36,800,000

Sources:
US & UK Population and Birth rates: CIA World Factbook
US Household Info: Bureau of Labor Statistics and US Census Bureau
UK Household Info: National Statistics Website
UCBSC Market Estimates:
http://parentsguidecordblood.org/content/usa/banklists/index.shtml

Assumptions:
- 5% of those making >$200k/yr would be interested in stem cell cryopreservation
- % of UK Households with similar 'wealth' (approx. >$200k/yr) est. to be the same as US

7.4.8 Projected Profits

Based on our cost and revenue estimates, there is potentially a very lucrative market here. If we break down the assumptions into various scenarios, we can estimate how miscalculations and/or changes in the market might affect our figures. Please note, these scenarios are a sort of 'what if', if we chose to set up this process as an independent company and are included merely as a predicted assessment of the long term value of the technology. They do not take into consideration substitutes entering the market, but rather assume that the IP provides enough protection to prevent/deter them. Also, the full extent of depreciation and bottlenecks caused by lack of unskilled labour isn't taken into account. We hope that this data can be used to leverage the value of licensing or, if necessary, to sell the IP outright. For more in depth figures or explanation of calculations, please contact Jordan Plews (jordan.plews@ucl.ac.uk).

8.8.1.1 Scenario 1 – Base Case

Assumptions:

- 5% penetration of US and UK UCBSC cryopreservation and US and UK 'wealthy' markets (as outlined previously)
- 10% annual growth rate
- 10% annual increase in costs to reflect growth rate
- We can expand within our existing facility to cope with growth.
- Costs are as outlined previously
- Cost per patient is £1500 (including collection, reprogramming, and 20 years storage)

Scenario 1 Culmulative Cash Flow Graph (1st 10 years)

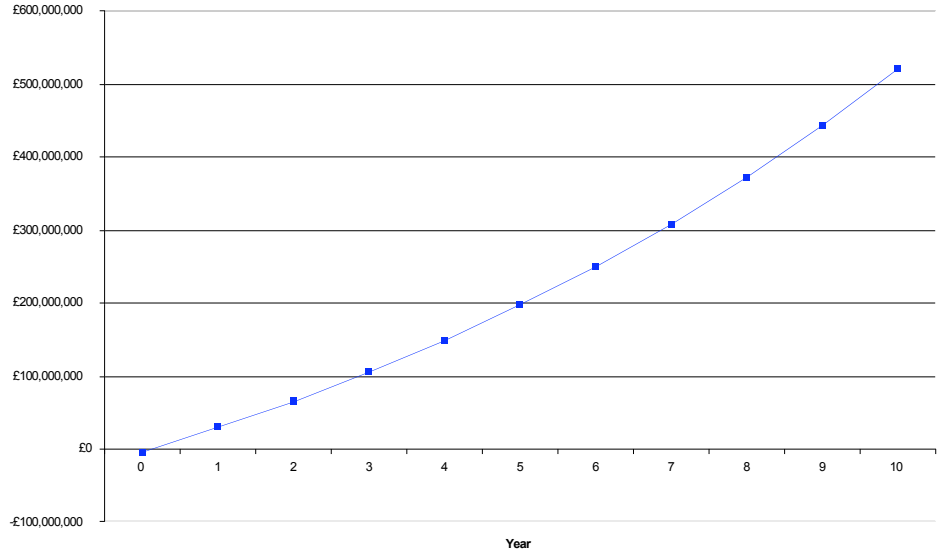

-£3.5 million initially with revenue of £36.8 million and greater after the 1st year.

8.8.1.2 Scenario 2 – 'Worst' case:

Assumptions:

- 1% penetration of US and UK UCBSC cryopreservation and US and UK 'wealthy' markets (as outlined previously)
- 5% annual growth rate
- Annual increase in costs mirrors growth rate
- Costs 50% greater than originally anticipated.
- We can expand within our existing facility to cope with growth.
- Costs are as outlined previously
- Cost per patient is £1000 (including collection, reprogramming, and 20 years storage)

Scenario 2 Culmulative Cash Flow Graph (1st 10 years)

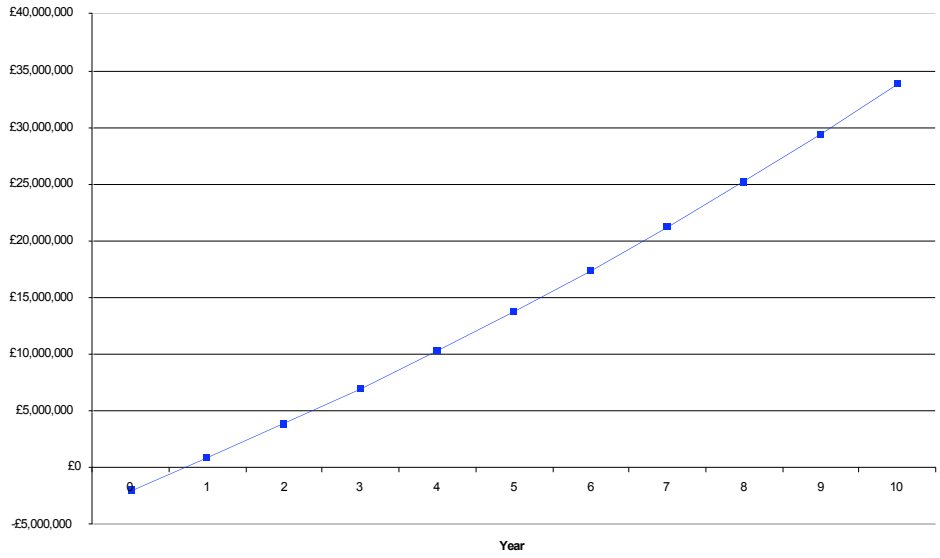

-£1.9 million initially with revenue of £0.9 million by the end of year 1.

8.8.1.3 Scenario 3 – 'Best' case:

Assumptions:

- 7.5% penetration of US and UK UCBSC cryopreservation and US and UK 'wealthy' markets (as outlined previously)
- 15% annual growth rate
- Annual increase in costs mirrors growth rate
- Costs 10% less than originally anticipated.
- We can expand within our existing facility to cope with growth.
- Costs are as outlined previously
- Cost per patient is £1750 (including collection, reprogramming, and 20 years storage)

Scenario 3 Culmulative Cash Flow Graph (1st 10 years)

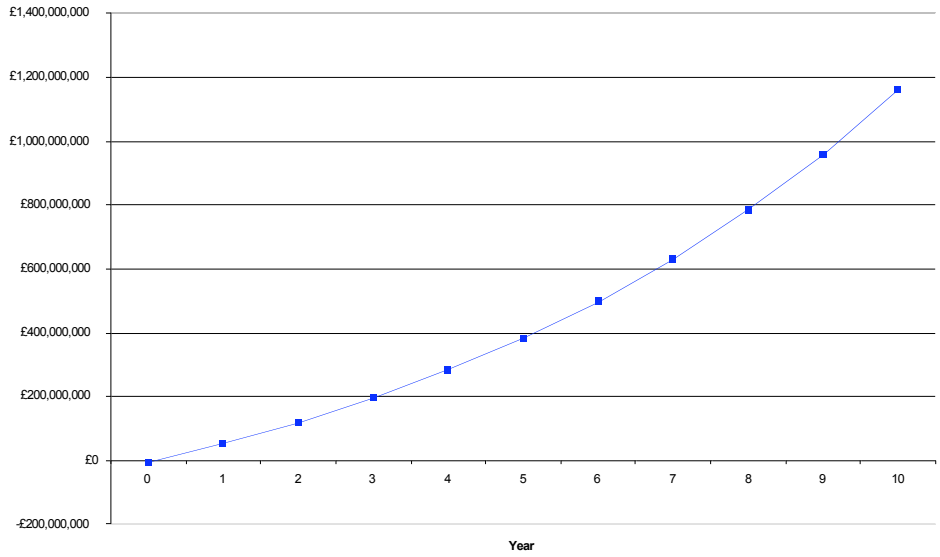

-£4.5 million initially with revenue of £53 million by the end of year 1.

*Please note, for this scenario, the costing/revenue is difficult to calculate as there would likely be a bottleneck in terms of the amount of skilled labour needed.

8.9 Appendix

7.4.9 UCBSC Cryopreservation Company Pricing

Initial fee will include: administrative costs & enrollment fees, collection kit, courier transport of baby's cord/cord blood and testing.

Total Cost includes 20 years of storage at the annual rate unless otherwise noted.

US Umbilical Cord Blood Stem Cell Cryopreservation Companies

Blood Cord Solutions
$1,795 Initial Fee
$125 Annual Storage Fees
$4,295 Total Cost
http://www.cordbloodsolutions.com/payment-options.aspx

Cord Blood Registry
$2,025 Initial Fee
$125 Annual Storage Fee
$3,875 Total Cost (reduced rate with prepaid 18 year storage)
http://www.cordblood.com/cord_blood_banking_with_cbr/pricing_domestic.asp

Cryobanks International
$1,749 Initial Fee
$120 Annual Storage Fees
$4,149 Total Cost
http://www.cryo-intl.com/why/pricing/

Cryo-Cell International
$1,720 Initial Fee
$125 Annual Storage Fee
$3,495 Total Cost (reduced rate with prepaid 21 year storage)
http://www.cryo-cell.com/services/pricing.asp

Family Cord Blood Services
$1,650 Initial Fee
$3,330 Total Cost
http://www.familycordbloodservices.com/fees.cfm

LifeBankUSA
$1,775 Initial Fee
$125 Annual Storage Fee
$3,325 Total Cost (reduced rate with prepaid 18 year storage)
http://www.lifebankusa.com/pricing_options.php

UK Umbilical Cord Blood Stem Cell Cryopreservation Companies

Cells4Life
£995 Initial Fee
£50 Annual Storage Fee
£1495 Total Cost (reduced rate with prepaid 25 year storage)
http://www.cells4life.co.uk/storage-plans.asp

Future Health
£995 Initial Fee
£30 Annual Storage Fee
£1295 Total Cost (reduced rate with prepaid 20 year storage)
http://www.futurehealth.co.uk/uploads/al/docs/UK/UK-Pricelist-en.pdf

Smart Cells
£995 Initial Fee
£1595 Total Cost (25 year storage)
http://www.smartcells.com/en/smart-cells-service-packages.htm

Virgin Health Bank
£1470 Total Cost
http://www.virginhealthbank.com/paying-for-it

Appendix

A.1 FACS Explanation of Fusion Events

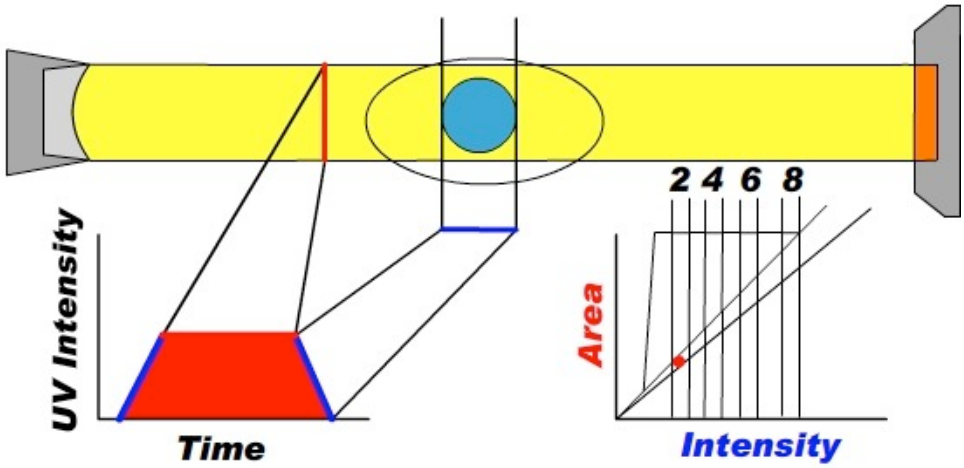

Figure A.1: Normal single cell 'event' read by FACS
Here the argon laser is represented by a wide yellow beam. The subsequent reading on the FACS plot is a combination of UV (Hoechst 33342) intensity (x-axis) and area (y-axis) (see Chapter 3 section 3.2.14 and Appendix Figures A.5 – A.11 for all plots relating to FACS of fused cells). Intensity increases with greater nuclear material, while area relates to the amount of time it takes for a positive UV (Hoechst) signal to traverse the beam. The mock graph in the bottom right shows how this normal cell event would be plotted, as a diploid (2n) cell.

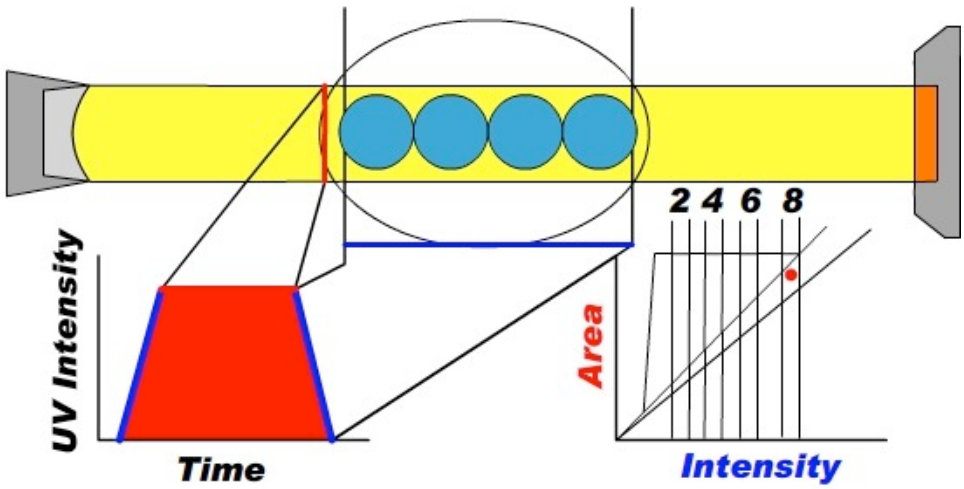

Figure A.2: Multinuclear 'event' read parallel to the UV laser
In this figure, a cell with four nuclei goes through the detection laser parallel to the beam direction. This causes a high intensity with a similar area readout, which should put it correctly into the 8n gate.

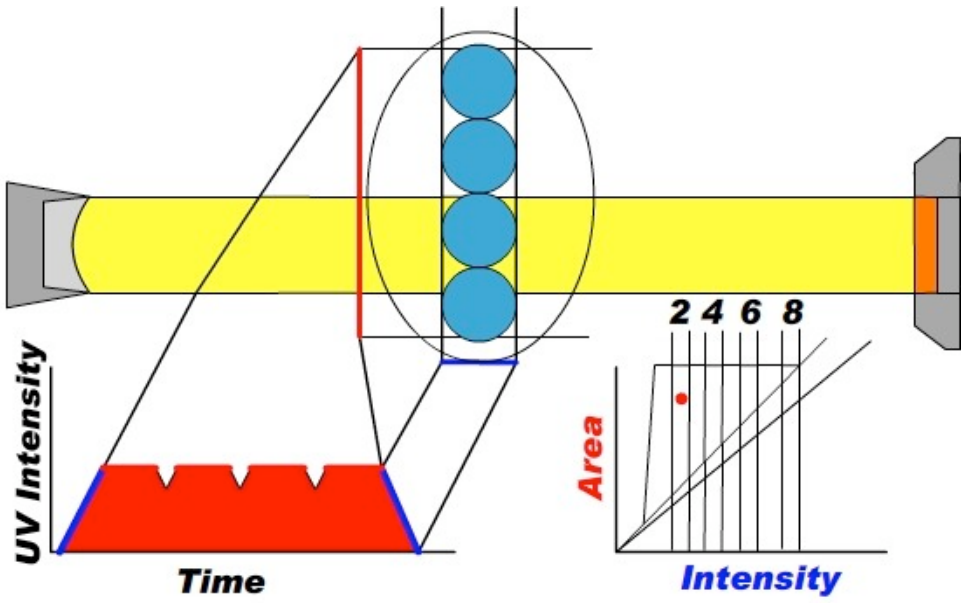

Figure A.3: Multinuclear 'event' read perpendicular to the UV laser
This cell, containing four nuclei crosses the detection laser perpendicularly. The FACS can not distinguish it as four separate events as the nuclei are too close together, leading to a high area, with an intensity no greater than a single cell. This leads to a misrepresentation of the actual number of nuclei as it is sorted into the 2n gate of the plot (bottom right).

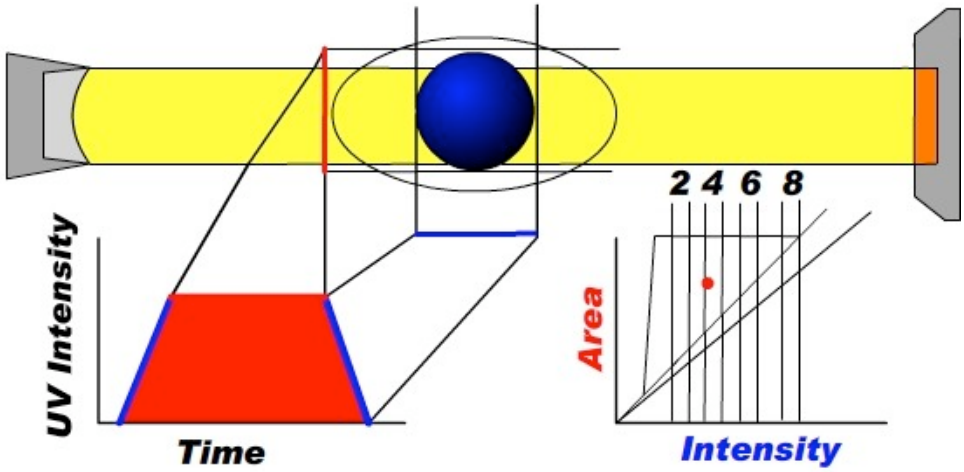

Figure A.4: Hybrid cell 'event' read parallel to the UV laser
Following cell fusion, often nuclei hybridise into a large nucleus with some or all of the nuclear DNA obtained from the individual cells fused. This leads to irregular intensity and area readings that make it difficult to design predictable gates in which to capture these types of events.

After multiple rounds of FACS following PEG_{6000} fusions, we could only reliably indicate which cells containing more than one nucleus using intensity and area. Therefore we had to analyse the samples more carefully using other parameters and visual observation to determine the beest conditions for fusion. Most hybrid cells did not survive for very long before going into apoptosis.

A.2 FACS Plots of Fusion Events

Below are the FACS plots described in section 3.2.14 used to make Figure 3.25. See Chapter 3, section 3.2.14 for more details.

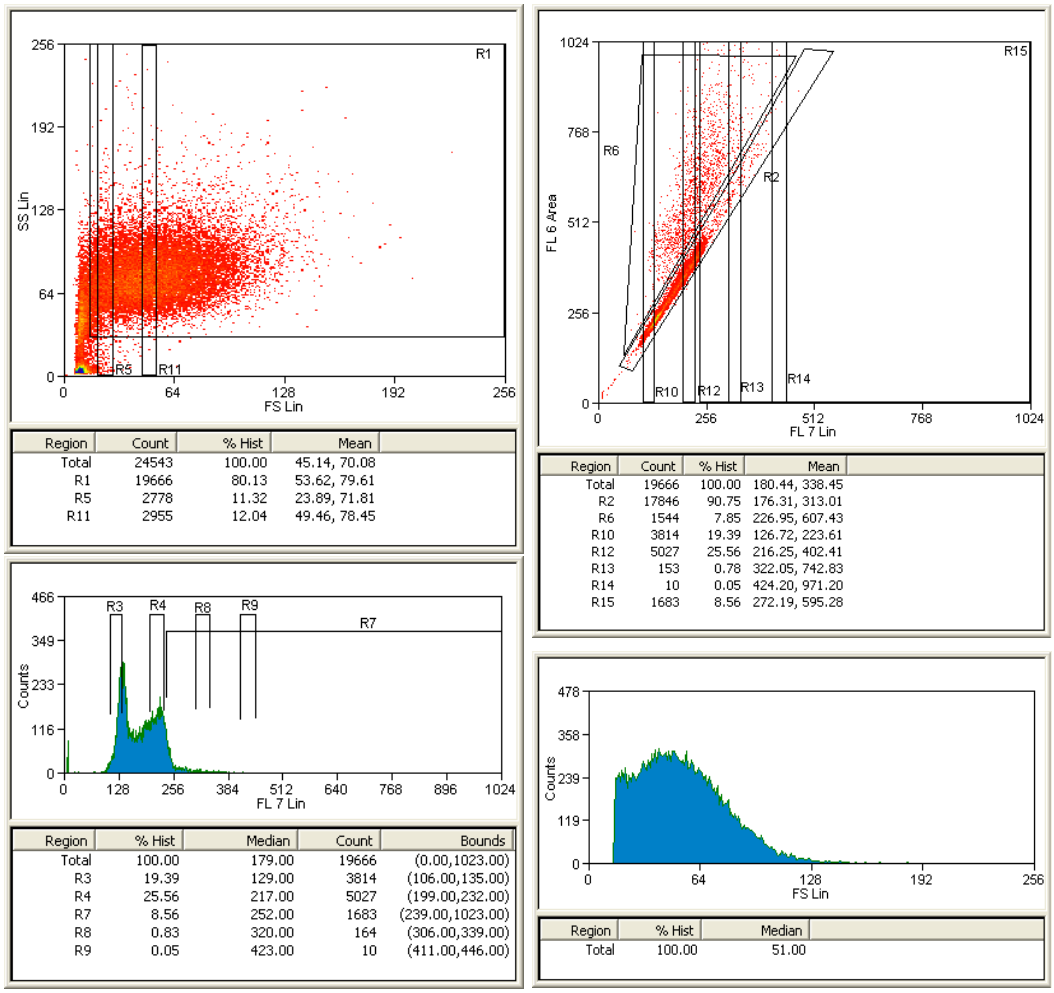

Figure A.5: 30 sec Suspension Fusion of NT2 cells

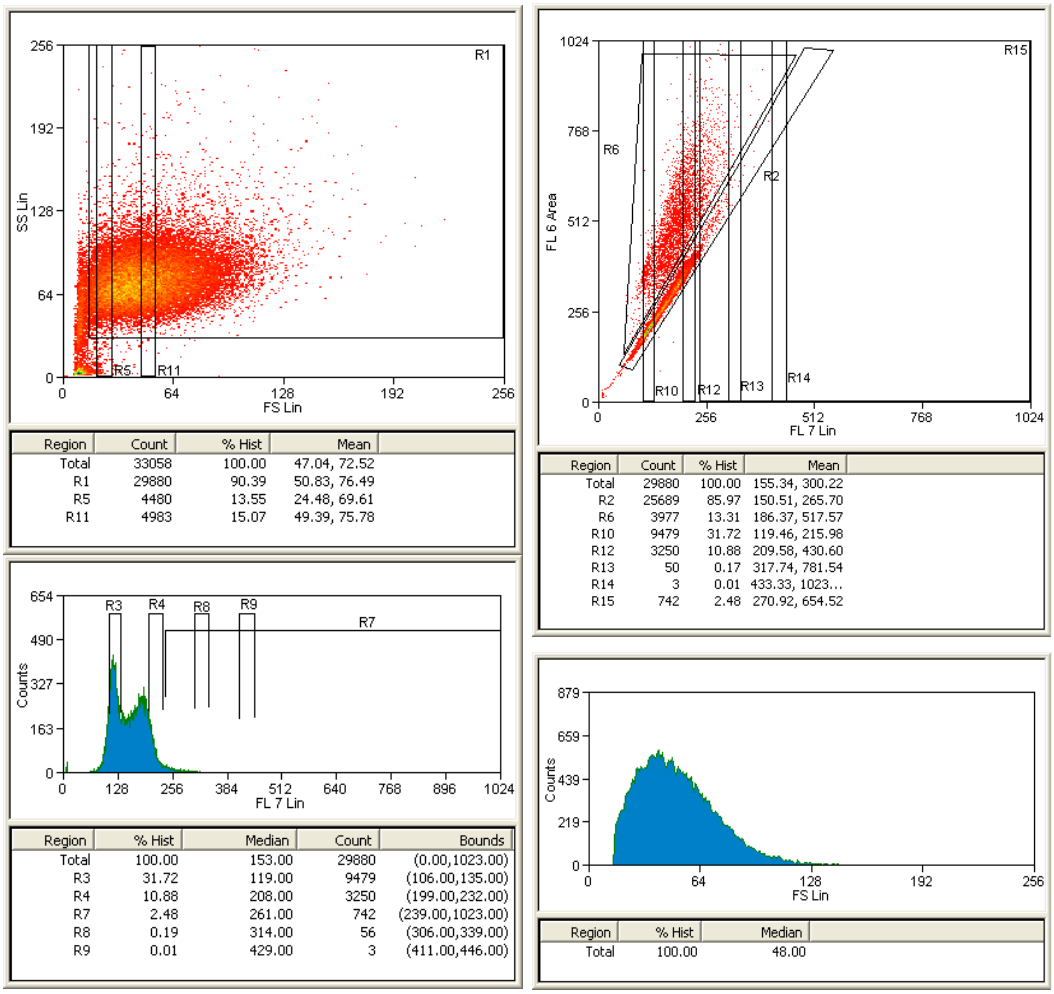

Region	Count	% Hist	Mean
Total	33058	100.00	47.04, 72.52
R1	29880	90.39	50.83, 76.49
R5	4480	13.55	24.48, 69.61
R11	4983	15.07	49.39, 75.78

Region	Count	% Hist	Mean
Total	29880	100.00	155.34, 300.22
R2	25689	85.97	150.51, 265.70
R6	3977	13.31	186.37, 517.57
R10	9479	31.72	119.46, 215.98
R12	3250	10.88	209.58, 430.60
R13	50	0.17	317.74, 781.54
R14	3	0.01	433.33, 1023...
R15	742	2.48	270.92, 654.52

Region	% Hist	Median	Count	Bounds
Total	100.00	153.00	29880	(0.00,1023.00)
R3	31.72	119.00	9479	(106.00,135.00)
R4	10.88	208.00	3250	(199.00,232.00)
R7	2.48	261.00	742	(239.00,1023.00)
R8	0.19	314.00	56	(306.00,339.00)
R9	0.01	429.00	3	(411.00,446.00)

Region	% Hist	Median
Total	100.00	48.00

Figure A.6: 1 minute Suspension Fusion of NT2 cells

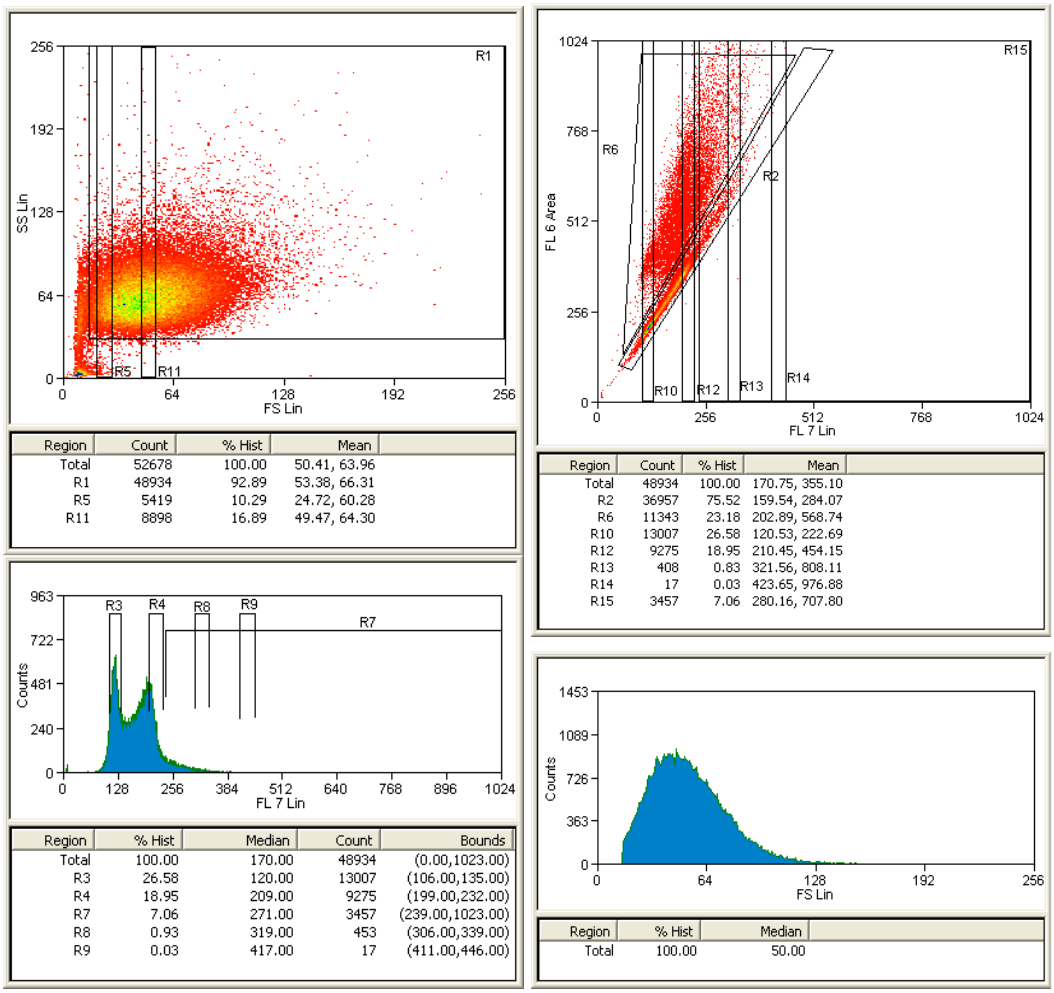

Region	Count	% Hist	Mean
Total	52678	100.00	50.41, 63.96
R1	48934	92.89	53.38, 66.31
R5	5419	10.29	24.72, 60.28
R11	8898	16.89	49.47, 64.30

Region	Count	% Hist	Mean
Total	48934	100.00	170.75, 355.10
R2	36957	75.52	159.54, 284.07
R6	11343	23.18	202.89, 568.74
R10	13007	26.58	120.53, 222.69
R12	9275	18.95	210.45, 454.15
R13	408	0.83	321.56, 808.11
R14	17	0.03	423.65, 976.88
R15	3457	7.06	280.16, 707.80

Region	% Hist	Median	Count	Bounds
Total	100.00	170.00	48934	(0.00,1023.00)
R3	26.58	120.00	13007	(106.00,135.00)
R4	18.95	209.00	9275	(199.00,232.00)
R7	7.06	271.00	3457	(239.00,1023.00)
R8	0.93	319.00	453	(306.00,339.00)
R9	0.03	417.00	17	(411.00,446.00)

Region	% Hist	Median
Total	100.00	50.00

Figure A.7: 2 minute Suspension Fusion of NT2 cells

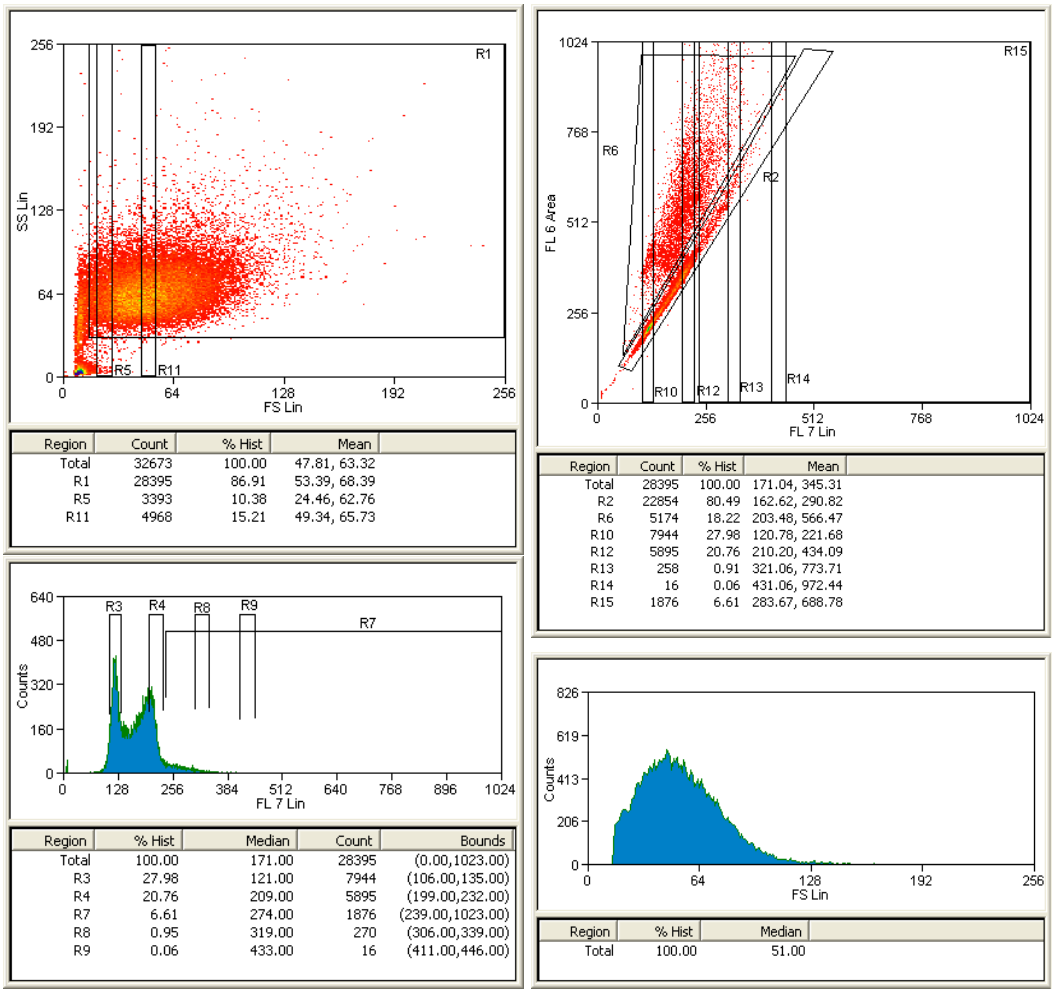

Region	Count	% Hist	Mean
Total	32673	100.00	47.81, 63.32
R1	28395	86.91	53.39, 68.39
R5	3393	10.38	24.46, 62.76
R11	4968	15.21	49.34, 65.73

Region	Count	% Hist	Mean
Total	28395	100.00	171.04, 345.31
R2	22854	80.49	162.62, 290.82
R6	5174	18.22	203.48, 566.47
R10	7944	27.98	120.78, 221.68
R12	5895	20.76	210.20, 434.09
R13	258	0.91	321.06, 773.71
R14	16	0.06	431.06, 972.44
R15	1876	6.61	283.67, 688.78

Region	% Hist	Median	Count	Bounds
Total	100.00	171.00	28395	(0.00,1023.00)
R3	27.98	121.00	7944	(106.00,135.00)
R4	20.76	209.00	5895	(199.00,232.00)
R7	6.61	274.00	1876	(239.00,1023.00)
R8	0.95	319.00	270	(306.00,339.00)
R9	0.06	433.00	16	(411.00,446.00)

Region	% Hist	Median
Total	100.00	51.00

Figure A.8: 5 minute Suspension Fusion of NT2 cells

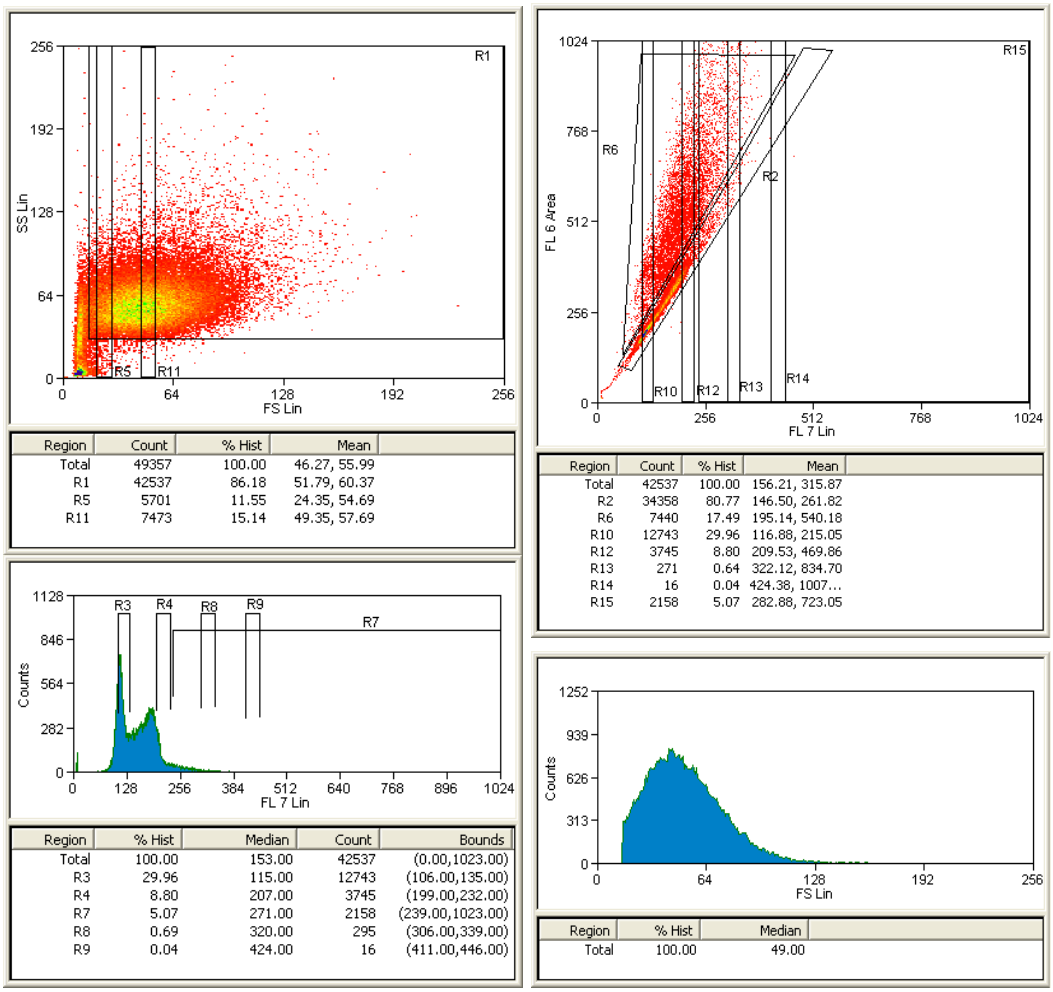

Region	Count	% Hist	Mean
Total	49357	100.00	46.27, 55.99
R1	42537	86.18	51.79, 60.37
R5	5701	11.55	24.35, 54.69
R11	7473	15.14	49.35, 57.69

Region	Count	% Hist	Mean
Total	42537	100.00	156.21, 315.87
R2	34358	80.77	146.50, 261.82
R6	7440	17.49	195.14, 540.18
R10	12743	29.96	116.88, 215.05
R12	3745	8.80	209.53, 469.86
R13	271	0.64	322.12, 834.70
R14	16	0.04	424.38, 1007...
R15	2158	5.07	282.88, 723.05

Region	% Hist	Median	Count	Bounds
Total	100.00	153.00	42537	(0.00,1023.00)
R3	29.96	115.00	12743	(106.00,135.00)
R4	8.80	207.00	3745	(199.00,232.00)
R7	5.07	271.00	2158	(239.00,1023.00)
R8	0.69	320.00	295	(306.00,339.00)
R9	0.04	424.00	16	(411.00,446.00)

Region	% Hist	Median
Total	100.00	49.00

Figure A.9: 1 min Monolayer Fusion of NT2 cells

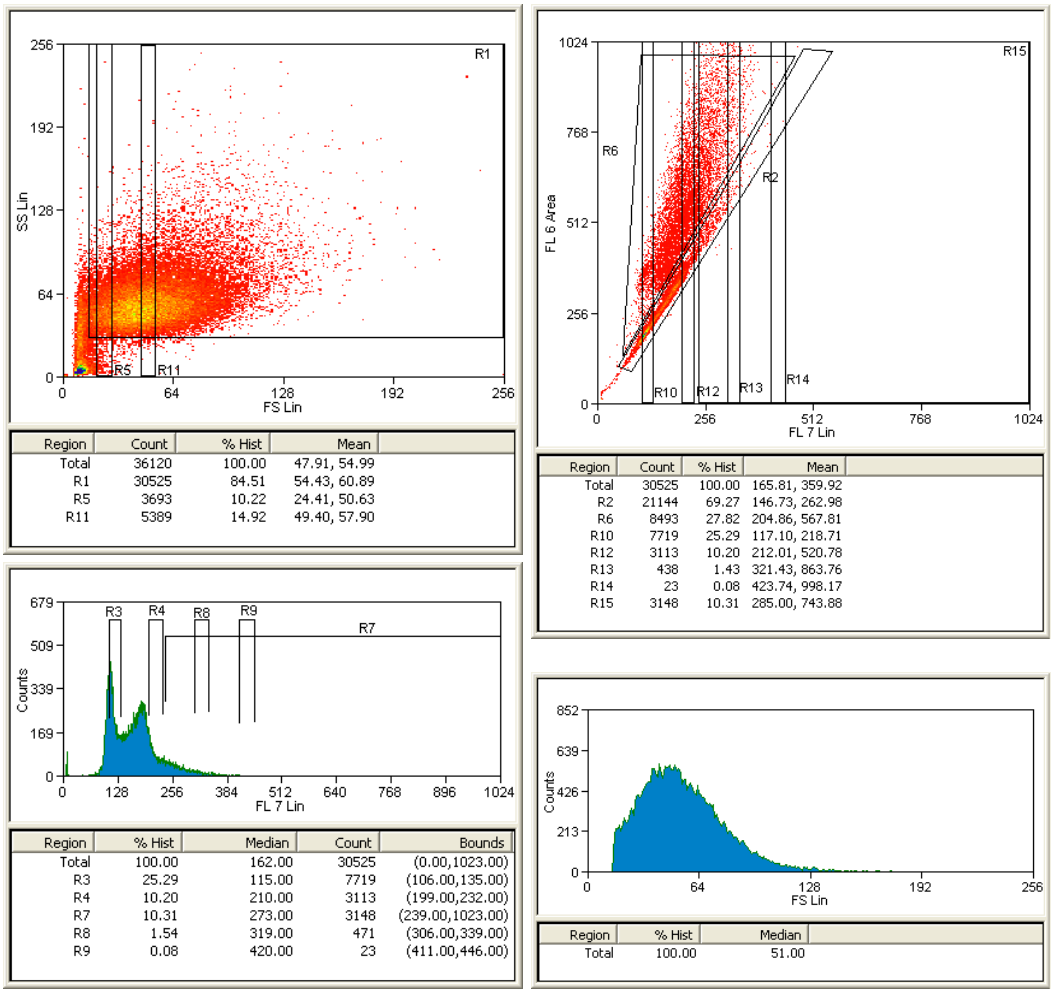

Region	Count	% Hist	Mean
Total	36120	100.00	47.91, 54.99
R1	30525	84.51	54.43, 60.89
R5	3693	10.22	24.41, 50.63
R11	5389	14.92	49.40, 57.90

Region	Count	% Hist	Mean
Total	30525	100.00	165.81, 359.92
R2	21144	69.27	146.73, 262.98
R6	8493	27.82	204.86, 567.81
R10	7719	25.29	117.10, 218.71
R12	3113	10.20	212.01, 520.78
R13	438	1.43	321.43, 863.76
R14	23	0.08	423.74, 998.17
R15	3148	10.31	285.00, 743.88

Region	% Hist	Median	Count	Bounds
Total	100.00	162.00	30525	(0.00,1023.00)
R3	25.29	115.00	7719	(106.00,135.00)
R4	10.20	210.00	3113	(199.00,232.00)
R7	10.31	273.00	3148	(239.00,1023.00)
R8	1.54	319.00	471	(306.00,339.00)
R9	0.08	420.00	23	(411.00,446.00)

Region	% Hist	Median
Total	100.00	51.00

Figure A.10: 5 min Monolayer Fusion of NT2 cells

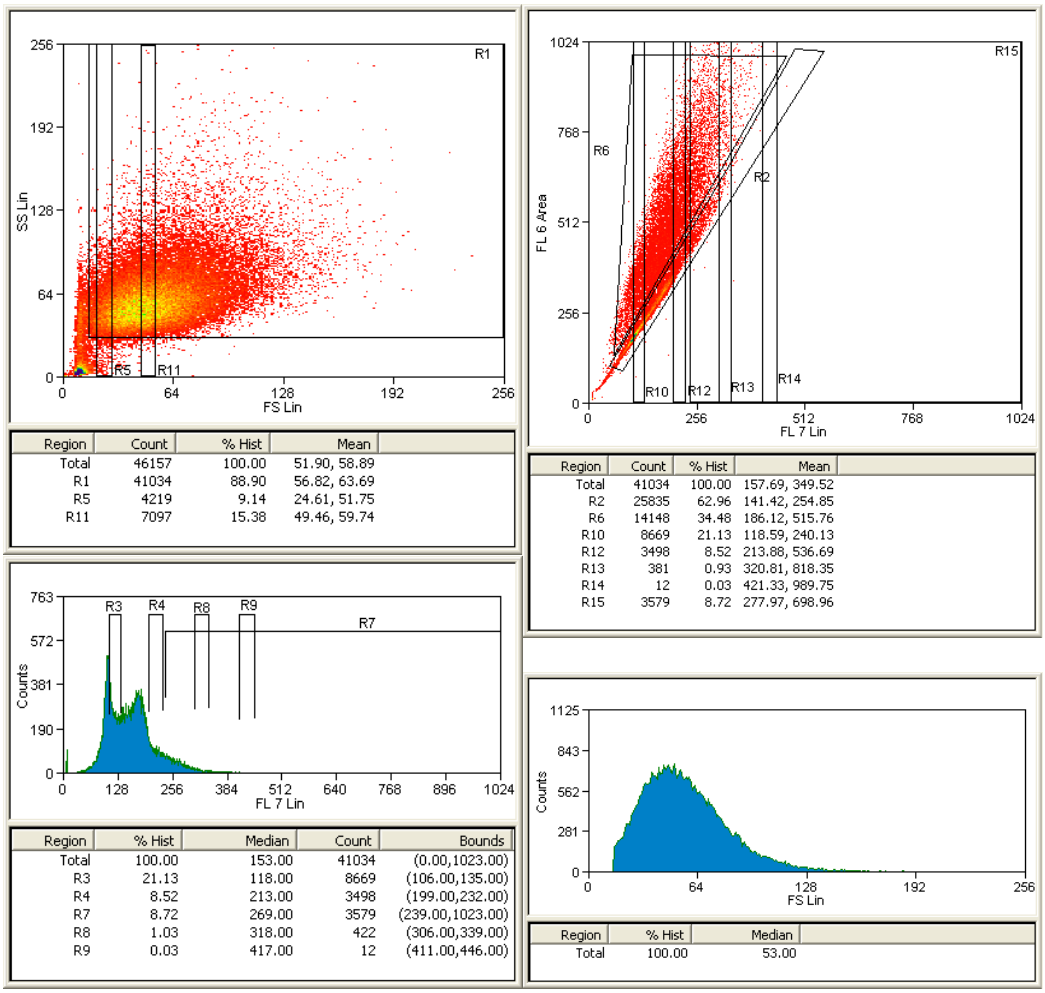

Region	Count	% Hist	Mean
Total	46157	100.00	51.90, 58.89
R1	41034	88.90	56.82, 63.69
R5	4219	9.14	24.61, 51.75
R11	7097	15.38	49.46, 59.74

Region	Count	% Hist	Mean
Total	41034	100.00	157.69, 349.52
R2	25835	62.96	141.42, 254.85
R6	14148	34.48	186.12, 515.76
R10	8669	21.13	118.59, 240.13
R12	3498	8.52	213.88, 536.69
R13	381	0.93	320.81, 818.35
R14	12	0.03	421.33, 989.75
R15	3579	8.72	277.97, 698.96

Region	% Hist	Median	Count	Bounds
Total	100.00	153.00	41034	(0.00,1023.00)
R3	21.13	118.00	8669	(106.00,135.00)
R4	8.52	213.00	3498	(199.00,232.00)
R7	8.72	269.00	3579	(239.00,1023.00)
R8	1.03	318.00	422	(306.00,339.00)
R9	0.03	417.00	12	(411.00,446.00)

Region	% Hist	Median
Total	100.00	53.00

Figure A.11: 10 min Monolayer Fusion of NT2 cells

A.3 Q-PCR Results from Individual SM Treatment

The following Q-PCR results are related to Chapter 5 section 5.2.9 and show the detection of OCT4, SOX2, cMYC, and KLF4 following 48 hour treatment with each individual small molecule shown. Results are given as relative expression, with genes normalised to GAPDH and ΔC_t values normalised to HUES1 human ES cells as a control. Notice that in all groups below, no individual small molecules resulted in the upregulation of OCT4 or SOX2.

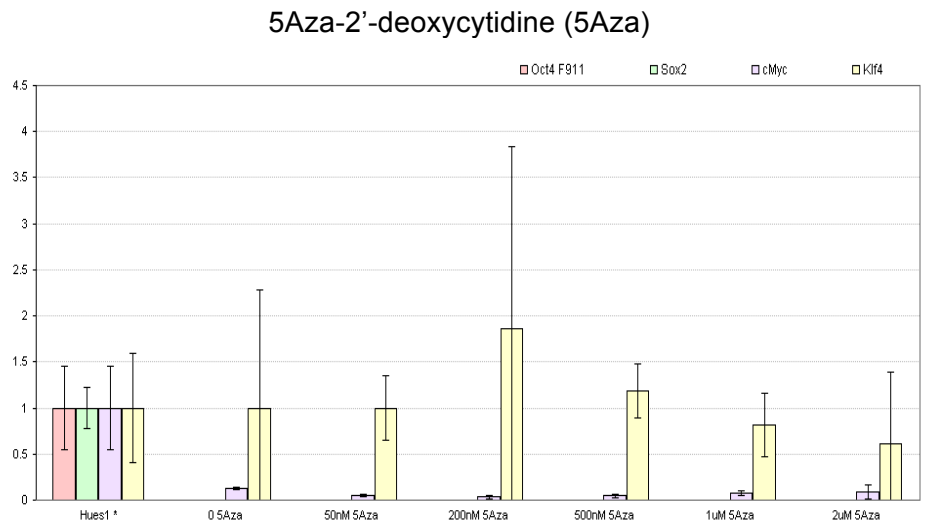

Figure A.12: Q-PCR Following 48 hours 5Aza-2'-deoxycytidine treatment

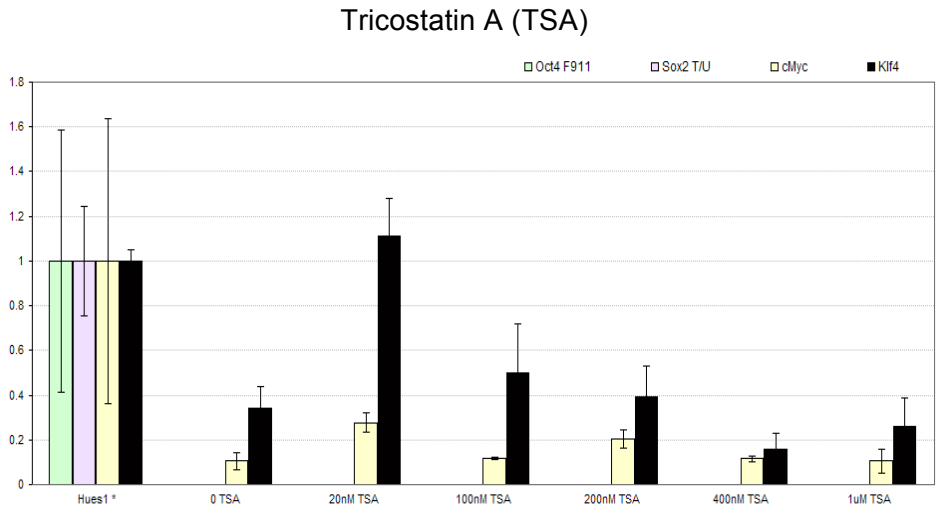

Figure A.13: Q-PCR Following 48 hours TSA treatment

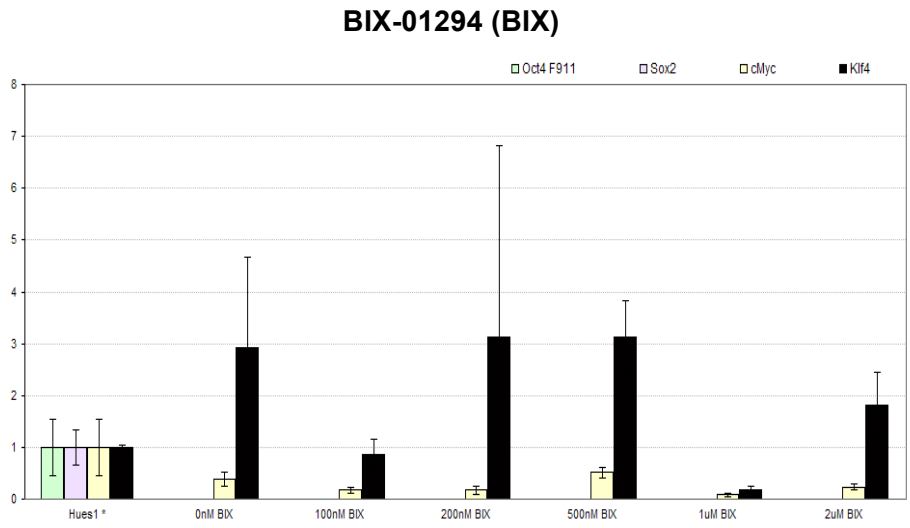

Figure A.14: Q-PCR Following 48 hours BIX treatment

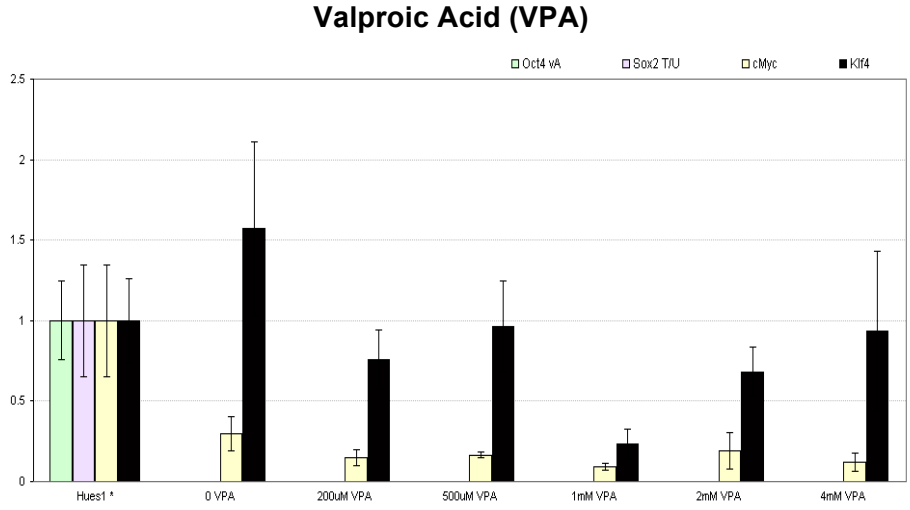

Figure A.15: Q-PCR Following 48 hours VPA treatment

References

Aasen, T., A. Raya, et al. (2008). "Efficient and rapid generation of induced pluripotent stem cells from human keratinocytes." Nat Biotechnol **26**(11): 1276-84.

Abken, H., H. Jungfer, et al. (1986). "Immortalization of human lymphocytes by fusion with cytoplasts of transformed mouse L cells." J Cell Biol **103**(3): 795-805.

Alvarez-Dolado, M., R. Pardal, et al. (2003). "Fusion of bone-marrow-derived cells with Purkinje neurons, cardiomyocytes and hepatocytes." Nature **425**(6961): 968-73.

Amatruda, J. M. and E. D. Finch (1979). "Modulation of hexose uptake and insulin action by cell membrane fluidity. The effects of temperature on membrane fluidity, insulin action, and insulin binding." J Biol Chem **254**(8): 2619-25.

Amit, M., M. K. Carpenter, et al. (2000). "Clonally derived human embryonic stem cell lines maintain pluripotency and proliferative potential for prolonged periods of culture." Dev Biol **227**(2): 271-8.

Andrews, P. W. (1984). "Retinoic acid induces neuronal differentiation of a cloned human embryonal carcinoma cell line in vitro." Dev Biol **103**(2): 285-93.

Andrews, P. W. (1988). "Human teratocarcinomas." Biochim Biophys Acta **948**(1): 17-36.

Andrews, P. W. (1998). "Teratocarcinomas and human embryology: pluripotent human EC cell lines. Review article." Apmis **106**(1): 158-67; discussion 167-8.

Andrews, P. W. (2002). "From teratocarcinomas to embryonic stem cells." Philos Trans R Soc Lond B Biol Sci **357**(1420): 405-17.

Andrews, P. W., G. Banting, et al. (1984a). "Three monoclonal antibodies defining distinct differentiation antigens associated with different high molecular weight polypeptides on the surface of human embryonal carcinoma cells." Hybridoma **3**(4): 347-61.

Andrews, P. W., N. Benvenisty, et al. (2005a). "The International Stem Cell Initiative: toward benchmarks for human embryonic stem cell research." Nat Biotechnol **23**(7): 795-7.

Andrews, P. W., D. L. Bronson, et al. (1980a). "A comparative study of eight cell lines derived from human testicular teratocarcinoma." Int J Cancer **26**(3): 269-80.

Andrews, P. W., J. Casper, et al. (1996). "Comparative analysis of cell surface antigens expressed by cell lines derived from human germ cell tumours." Int J Cancer **66**(6): 806-16.

Andrews, P. W., I. Damjanov, et al. (1994). "Inhibition of proliferation and induction of differentiation of pluripotent human embryonal carcinoma cells by osteogenic protein-1 (or bone morphogenetic protein-7)." Lab Invest **71**(2): 243-51.

Andrews, P. W., I. Damjanov, et al. (1984b). "Pluripotent embryonal carcinoma clones derived from the human teratocarcinoma cell line Tera-2. Differentiation in vivo and in vitro." Lab Invest **50**(2): 147-62.

Andrews, P. W., I. Damjanov, et al. (1985). "A pluripotent human stem-cell clone isolated from the TERA-2 teratocarcinoma line lacks antigens SSEA-3 and SSEA-4 in vitro, but expresses these antigens when grown as a xenograft tumor." Differentiation **29**(2): 127-35.

Andrews, P. W. and P. N. Goodfellow (1980b). "Antigen expression by somatic cell hybrids of a murine embryonal carcinoma cell with thymocytes and L cells." Somatic Cell Genet **6**(2): 271-84.

Andrews, P. W., P. N. Goodfellow, et al. (1982). "Cell-surface antigens of a clonal human embryonal carcinoma cell line: morphological and antigenic differentiation in culture." Int J Cancer **29**(5): 523-31.

Andrews, P. W., M. M. Matin, et al. (2005b). "Embryonic stem (ES) cells and embryonal carcinoma (EC) cells: opposite sides of the same coin." Biochem Soc Trans **33**(Pt 6): 1526-30.

Andrews, P. W., L. J. Meyer, et al. (1984c). "Two monoclonal antibodies recognizing determinants on human embryonal carcinoma cells react specifically with the liver isozyme of human alkaline phosphatase." Hybridoma **3**(1): 33-9.

Aoi, T., K. Yae, et al. (2008). "Generation of Pluripotent Stem Cells from Adult Mouse Liver and Stomach Cells." Science.

Assady, S., G. Maor, et al. (2001). "Insulin production by human embryonic stem cells." Diabetes **50**(8): 1691-7.

Babaie, Y., R. Herwig, et al. (2007). "Analysis of Oct4-dependent transcriptional networks regulating self-renewal and pluripotency in human embryonic stem cells." Stem Cells **25**(2): 500-10.

Bahrami, A. R., M. M. Matin, et al. (2005). "The CDK inhibitor p27 enhances neural differentiation in pluripotent NTERA2 human EC cells, but does not permit differentiation of 2102Ep nullipotent human EC cells." Mech Dev **122**(9): 1034-42.

Baker, D. E., N. J. Harrison, et al. (2007). "Adaptation to culture of human embryonic stem cells and oncogenesis in vivo." Nat Biotechnol **25**(2): 207-15.

Baker, M. (2009). "Stem cells: Fast and furious." Nature **458**(7241): 962-5.

Ball, J. R., C. Dimaano, et al. (2007). "Sequence preference in RNA recognition by the nucleoporin Nup153." J Biol Chem **282**(12): 8734-40.

Baron, M. H. and T. Maniatis (1986). "Rapid reprogramming of globin gene expression in transient heterokaryons." Cell **46**(4): 591-602.

Barski, G. and F. Cornefert (1962). "Characteristics of "hybrid"-type clonal cell lines obtained from mixed cultures in vitro." J Natl Cancer Inst **28**: 801-21.

Barski, G., S. Sorieul, et al. (1960). "[Production of cells of a "hybrid" nature in culturs in vitro of 2 cellular strains in combination.]." C R Hebd Seances Acad Sci **251**: 1825-7.

Bayne, S. and J. P. Liu (2005). "Hormones and growth factors regulate telomerase activity in ageing and cancer." Mol Cell Endocrinol **240**(1-2): 11-22.

Benchimol, S. (2001). "p53-dependent pathways of apoptosis." Cell Death Differ **8**(11): 1049-51.

Ber, R. and F. Wiener (1978). "Phenotypic trait transferred by cybridization." Cytogenet Cell Genet **21**(5): 304-8.

Berstine, E. G., M. L. Hooper, et al. (1973). "Alkaline phosphatase activity in mouse teratoma." Proc Natl Acad Sci U S A **70**(12): 3899-903.

Bestilny, L. J., C. B. Brown, et al. (1996). "Selective inhibition of telomerase activity during terminal differentiation of immortal cell lines." Cancer Res **56**(16): 3796-802.

Bhutani, N., J. J. Brady, et al. (2009). "Reprogramming towards pluripotency requires AID-dependent DNA demethylation." Nature.

Biro, S., Y. M. Fu, et al. (1993). "Inhibitory effects of antisense oligodeoxynucleotides targeting c-myc mRNA on smooth muscle cell proliferation and migration." Proc Natl Acad Sci U S A **90**(2): 654-8.

Borghi, R., R. Vene, et al. (2003). "Transient modulation of cytoplasmic and nuclear retinoid receptors expression in differentiating human teratocarcinoma NT2 cells." J Neurochem **84**(1): 94-104.

Boxer, L. M. and C. V. Dang (2001). "Translocations involving c-myc and c-myc function." Oncogene **20**(40): 5595-610.

Bradley, A., M. Evans, et al. (1984). "Formation of germ-line chimaeras from embryo-derived teratocarcinoma cell lines." Nature **309**(5965): 255-6.

Brambrink, T., R. Foreman, et al. (2008). "Sequential expression of pluripotency markers during direct reprogramming of mouse somatic cells." Cell Stem Cell **2**(2): 151-9.

Briggs, R. and T. J. King (1952). "Transplantation of Living Nuclei From Blastula Cells into Enucleated Frogs' Eggs." Proc Natl Acad Sci U S A **38**(5): 455-63.

Brinster, R. L. (1974). "The effect of cells transferred into the mouse blastocyst on subsequent development." J Exp Med **140**(4): 1049-56.

Bronson, D. L., P. W. Andrews, et al. (1980). "Cell line derived from a metastasis of a human testicular germ cell tumor." Cancer Res **40**(7): 2500-6.

Bunn, C. L. and J. M. Eisenstadt (1977). "Cybrid formation in mouse L cells: the influence of cytoplast-to-cell ratio." Somatic Cell Genet **3**(3): 335-41.

Butel, J. S., R. A. Vilchez, et al. (2003). "Association between SV40 and non-Hodgkin's lymphoma." Leuk Lymphoma **44 Suppl 3**: S33-9.
Byrne, J. A., D. A. Pedersen, et al. (2007). "Producing primate embryonic stem cells by somatic cell nuclear transfer." Nature **450**(7169): 497-502.
Carpenter, M. K., M. S. Inokuma, et al. (2001). "Enrichment of neurons and neural precursors from human embryonic stem cells." Exp Neurol **172**(2): 383-97.
Chang, D. C., B. M. Chassy, et al. (1992). Guide to Electroporation and Electrofusion, Academic Press.
Charras, G. T., C. K. Hu, et al. (2006). "Reassembly of contractile actin cortex in cell blebs." J Cell Biol **175**(3): 477-90.
Chen, S., Q. Zhang, et al. (2004). "Dedifferentiation of lineage-committed cells by a small molecule." J Am Chem Soc **126**(2): 410-1.
Chen, Y., Z. X. He, et al. (2003). "Embryonic stem cells generated by nuclear transfer of human somatic nuclei into rabbit oocytes." Cell Res **13**(4): 251-63.
Christman, J. K. (2002). "5-Azacytidine and 5-aza-2'-deoxycytidine as inhibitors of DNA methylation: mechanistic studies and their implications for cancer therapy." Oncogene **21**(35): 5483-95.
Collas, P. and R. Gammelsaeter (2007). "Novel approaches to epigenetic reprogramming of somatic cells." Cloning Stem Cells **9**(1): 26-32.
Cooper, J. A. (1987). "Effects of cytochalasin and phalloidin on actin." J Cell Biol **105**(4): 1473-8.
Cowan, C. A., J. Atienza, et al. (2005). "Nuclear reprogramming of somatic cells after fusion with human embryonic stem cells." Science **309**(5739): 1369-73.
Damjanov, I. and P. W. Andrews (1983). "Ultrastructural differentiation of a clonal human embryonal carcinoma cell line in vitro." Cancer Res **43**(5): 2190-8.
Dancker, P. and I. Low (1979). "Complex influence of cytochalasin B on actin polymerization." Z Naturforsch C **34**(7-8): 555-7.
Darlington, G. J., H. P. Bernhard, et al. (1974). "Proceedings: The expression of hepatic functions in mouse hepatoma x human leukocyte hybrids." Cytogenet Cell Genet **13**(1): 86-8.
Darlington, G. J., J. K. Rankin, et al. (1982). "Expression of human hepatic genes in somatic cell hybrids." Somatic Cell Genet **8**(3): 403-12.
deJong, G., A. H. Telenius, et al. (1999). "Mammalian artificial chromosome pilot production facility: large-scale isolation of functional satellite DNA-based artificial chromosomes." Cytometry **35**(2): 129-33.
Draper, J. S., H. D. Moore, et al. (2004a). "Culture and characterization of human embryonic stem cells." Stem Cells Dev **13**(4): 325-36.
Draper, J. S., C. Pigott, et al. (2002). "Surface antigens of human embryonic stem cells: changes upon differentiation in culture." J Anat **200**(Pt 3): 249-58.
Draper, J. S., K. Smith, et al. (2004b). "Recurrent gain of chromosomes 17q and 12 in cultured human embryonic stem cells." Nat Biotechnol **22**(1): 53-4.
Duinsbergen, D., M. Eriksson, et al. (2008). "Induced pluripotency with endogenous and inducible genes." Exp Cell Res **314**(17): 3255-63.
Duran, C., P. J. Talley, et al. (2001). "Hybrids of pluripotent and nullipotent human embryonal carcinoma cells: partial retention of a pluripotent phenotype." Int J Cancer **93**(3): 324-32.
Eggan, K., K. Baldwin, et al. (2004). "Mice cloned from olfactory sensory neurons." Nature **428**(6978): 44-9.
Egli, D., J. Rosains, et al. (2007). "Developmental reprogramming after chromosome transfer into mitotic mouse zygotes." Nature **447**(7145): 679-85.
Eguchi, A., B. R. Meade, et al. (2009). "Efficient siRNA delivery into primary cells by a peptide transduction domain-dsRNA binding domain fusion protein." Nat Biotechnol **27**(6): 567-71.
EMEA. (2010). "Reflection paper on stem cell-based medicinal products." Retrieved 16 March, 2010, from www.ema.europa.eu/pdfs/human/cat/57113409en.pdf.

Epsztejn-Litman, S., N. Feldman, et al. (2008). "De novo DNA methylation promoted by G9a prevents reprogramming of embryonically silenced genes." Nat Struct Mol Biol **15**(11): 1176-83.

Evans, M. J. and M. H. Kaufman (1981). "Establishment in culture of pluripotential cells from mouse embryos." Nature **292**(5819): 154-6.

Evans, P. M. and C. Liu (2008). "Roles of Krupel-like factor 4 in normal homeostasis, cancer and stem cells." Acta Biochim Biophys Sin (Shanghai) **40**(7): 554-64.

Feng, B., J. H. Ng, et al. (2009). "Molecules that promote or enhance reprogramming of somatic cells to induced pluripotent stem cells." Cell Stem Cell **4**(4): 301-12.

Finch, B. W. and B. Ephrussi (1967). "RETENTION OF MULTIPLE DEVELOPMENTAL POTENTIALITIES BY CELLS OF A MOUSE TESTICULAR TERATOCARCINOMA DURING PROLONGED CULTURE in vitro AND THEIR EXTINCTION UPON HYBRIDIZATION WITH CELLS OF PERMANENT LINES." Proc Natl Acad Sci U S A **57**(3): 615-621.

Flasza, M., A. F. Shering, et al. (2003). "Reprogramming in inter-species embryonal carcinoma-somatic cell hybrids induces expression of pluripotency and differentiation markers." Cloning Stem Cells **5**(4): 339-54.

Forsyth, N. R., A. Musio, et al. (2006). "Physiologic oxygen enhances human embryonic stem cell clonal recovery and reduces chromosomal abnormalities." Cloning Stem Cells **8**(1): 16-23.

Friedrich, G. and P. Soriano (1991). "Promoter traps in embryonic stem cells: a genetic screen to identify and mutate developmental genes in mice." Genes Dev **5**(9): 1513-23.

Furumai, R., Y. Komatsu, et al. (2001). "Potent histone deacetylase inhibitors built from trichostatin A and cyclic tetrapeptide antibiotics including trapoxin." Proc Natl Acad Sci U S A **98**(1): 87-92.

Garbuzova-Davis, S., A. E. Willing, et al. (2002). "Positive effect of transplantation of hNT neurons (NTera 2/D1 cell-line) in a model of familial amyotrophic lateral sclerosis." Exp Neurol **174**(2): 169-80.

Gardner, D. K., M. Lane, et al. (2004). A laboratory guide to the mammalian embryo. Oxford, Oxford University Press.

Gaustad, K. G., A. C. Boquest, et al. (2004). "Differentiation of human adipose tissue stem cells using extracts of rat cardiomyocytes." Biochem Biophys Res Commun **314**(2): 420-7.

Gearhart, J. (1998). "New potential for human embryonic stem cells." Science **282**(5391): 1061-2.

Gerrard, L., D. Zhao, et al. (2005). "Stably transfected human embryonic stem cell clones express OCT4-specific green fluorescent protein and maintain self-renewal and pluripotency." Stem Cells **23**(1): 124-33.

Giacomelli, C., L. Le Men, et al. (2006). "Phosphorylcholine-based pH-responsive diblock copolymer micelles as drug delivery vehicles: light scattering, electron microscopy, and fluorescence experiments." Biomacromolecules **7**(3): 817-28.

Gokhale, P. J., A. M. Giesberts, et al. (2000). "Brachyury is expressed by human teratocarcinoma cells in the absence of mesodermal differentiation." Cell Growth Differ **11**(3): 157-62.

Gottlicher, M., S. Minucci, et al. (2001). "Valproic acid defines a novel class of HDAC inhibitors inducing differentiation of transformed cells." EMBO J **20**(24): 6969-78.

Graves, K. H. and R. W. Moreadith (1993). "Derivation and characterization of putative pluripotential embryonic stem cells from preimplantation rabbit embryos." Mol Reprod Dev **36**(4): 424-33.

Grove, J. E., E. Bruscia, et al. (2004). "Plasticity of bone marrow-derived stem cells." Stem Cells **22**(4): 487-500.

Guan, K., K. Nayernia, et al. (2006). "Pluripotency of spermatogonial stem cells from adult mouse testis." Nature **440**(7088): 1199-203.

Guan, K., F. Wolf, et al. (2009). "Isolation and cultivation of stem cells from adult mouse testes." Nat Protoc **4**(2): 143-54.

Gurdon, J. B. (1962a). "Adult frogs derived from the nuclei of single somatic cells." Dev Biol **4**: 256-73.
Gurdon, J. B. (1962b). "Multiple genetically identical frogs." J Hered **53**: 5-9.
Gurdon, J. B. (1962c). "The developmental capacity of nuclei taken from intestinal epithelium cells of feeding tadpoles." J Embryol Exp Morphol **10**: 622-40.
Gurdon, J. B. (1962d). "The transplantation of nuclei between two species of Xenopus." Dev Biol **5**: 68-83.
Hakelien, A. M. and P. Collas (2002). "Novel approaches to transdifferentiation." Cloning Stem Cells **4**(4): 379-87.
Hakelien, A. M., K. G. Gaustad, et al. (2005). "Long-term in vitro, cell-type-specific genome-wide reprogramming of gene expression." Exp Cell Res **309**(1): 32-47.
Hansis, C., G. Barreto, et al. (2004). "Nuclear reprogramming of human somatic cells by xenopus egg extract requires BRG1." Curr Biol **14**(16): 1475-80.
Hanson, C. and G. Caisander (2005). "Human embryonic stem cells and chromosome stability." Apmis **113**(11-12): 751-5.
Harris, H. and J. F. Watkins (1965). "Hybrid Cells Derived from Mouse and Man: Artificial Heterokaryons of Mammalian Cells from Different Species." Nature **205**: 640-6.
Harrison, N. J., D. Baker, et al. (2007). "Culture adaptation of embryonic stem cells echoes germ cell malignancy." Int J Androl **30**(4): 275-81; discussion 281.
Hayashi, K. and M. A. Surani (2009). "Resetting the epigenome beyond pluripotency in the germline." Cell Stem Cell **4**(6): 493-8.
Hochedlinger, K. and R. Jaenisch (2002a). "Monoclonal mice generated by nuclear transfer from mature B and T donor cells." Nature **415**(6875): 1035-8.
Hochedlinger, K. and R. Jaenisch (2002b). "Nuclear transplantation: lessons from frogs and mice." Curr Opin Cell Biol **14**(6): 741-8.
Hochedlinger, K. and K. Plath (2009). "Epigenetic reprogramming and induced pluripotency." Development **136**(4): 509-23.
Hockemeyer, D., F. Soldner, et al. (2008). "A drug-inducible system for direct reprogramming of human somatic cells to pluripotency." Cell Stem Cell **3**(3): 346-53.
Horb, M. E., C. N. Shen, et al. (2003). "Experimental conversion of liver to pancreas." Curr Biol **13**(2): 105-15.
Huangfu, D., R. Maehr, et al. (2008a). "Induction of pluripotent stem cells by defined factors is greatly improved by small-molecule compounds." Nat Biotechnol **26**(7): 795-7.
Huangfu, D., K. Osafune, et al. (2008b). "Induction of pluripotent stem cells from primary human fibroblasts with only Oct4 and Sox2." Nat Biotechnol **26**(11): 1269-75.
Hui, S. W., T. Isac, et al. (1985). "Action of polyethylene glycol on the fusion of human erythrocyte membranes." J Membr Biol **84**(2): 137-46.
Huppertz, B., H. G. Frank, et al. (1998). "Villous cytotrophoblast regulation of the syncytial apoptotic cascade in the human placenta." Histochem Cell Biol **110**(5): 495-508.
Huppertz, B., D. S. Tews, et al. (2001). "Apoptosis and syncytial fusion in human placental trophoblast and skeletal muscle." Int Rev Cytol **205**: 215-53.
Inoue, K., H. Wakao, et al. (2005). "Generation of cloned mice by direct nuclear transfer from natural killer T cells." Curr Biol **15**(12): 1114-8.
Iwakura, Y., M. Nozaki, et al. (1985). "Pleiotropic phenotypic expression in cybrids derived from mouse teratocarcinoma cells fused with rat myoblast cytoplasts." Cell **43**(3 Pt 2): 777-91.
Jaenisch, R. and R. Young (2008). "Stem cells, the molecular circuitry of pluripotency and nuclear reprogramming." Cell **132**(4): 567-82.
Jang, Y. Y., M. I. Collector, et al. (2004). "Hematopoietic stem cells convert into liver cells within days without fusion." Nat Cell Biol **6**(6): 532-9.
Jenuwein, T. and C. D. Allis (2001). "Translating the histone code." Science **293**(5532): 1074-80.

Jewett, M. A. (1978). "Testis carcinoma: transplantation into nude mice." Natl Cancer Inst Monogr(49): 65-6.
Kahan, B. W. and B. Ephrussi (1970). "Developmental potentialities of clonal in vitro cultures of mouse testicular teratoma." J Natl Cancer Inst **44**(5): 1015-36.
Kaji, K., K. Norrby, et al. (2009). "Virus-free induction of pluripotency and subsequent excision of reprogramming factors." Nature **458**(7239): 771-5.
Kanatsu-Shinohara, M., K. Inoue, et al. (2004). "Generation of pluripotent stem cells from neonatal mouse testis." Cell **119**(7): 1001-12.
Kawamura, T., J. Suzuki, et al. (2009). "Linking the p53 tumour suppressor pathway to somatic cell reprogramming." Nature **460**(7259): 1140-4.
Kim, D., C. H. Kim, et al. (2009a). "Generation of human induced pluripotent stem cells by direct delivery of reprogramming proteins." Cell Stem Cell **4**(6): 472-6.
Kim, J. A., K. Cho, et al. (2008). "A novel electroporation method using a capillary and wire-type electrode." Biosens Bioelectron **23**(9): 1353-60.
Kim, J. B., V. Sebastiano, et al. (2009b). "Oct4-induced pluripotency in adult neural stem cells." Cell **136**(3): 411-9.
Kimura, H., M. Tada, et al. (2004). "Histone code modifications on pluripotential nuclei of reprogrammed somatic cells." Mol Cell Biol **24**(13): 5710-20.
Kleinsmith, L. J. and G. B. Pierce, Jr. (1964). "Multipotentiality of Single Embryonal Carcinoma Cells." Cancer Res **24**: 1544-51.
Kocabas, A. M., J. Crosby, et al. (2006). "The transcriptome of human oocytes." Proc Natl Acad Sci U S A **103**(38): 14027-32.
Krtolica, A. (2005). "Stem cell: balancing aging and cancer." Int J Biochem Cell Biol **37**(5): 935-41.
Kubicek, S., R. J. O'Sullivan, et al. (2007). "Reversal of H3K9me2 by a small-molecule inhibitor for the G9a histone methyltransferase." Mol Cell **25**(3): 473-81.
Kyte, J. A., L. Mu, et al. (2006). "Phase I/II trial of melanoma therapy with dendritic cells transfected with autologous tumor-mRNA." Cancer Gene Ther **13**(10): 905-18.
Labosky, P. A., D. P. Barlow, et al. (1994). "Mouse embryonic germ (EG) cell lines: transmission through the germline and differences in the methylation imprint of insulin-like growth factor 2 receptor (Igf2r) gene compared with embryonic stem (ES) cell lines." Development **120**(11): 3197-204.
Lemaire, P., N. Garrett, et al. (1995). "Expression cloning of Siamois, a Xenopus homeobox gene expressed in dorsal-vegetal cells of blastulae and able to induce a complete secondary axis." Cell **81**(1): 85-94.
Li, C., J. Zhou, et al. (2009). "Pluripotency can be rapidly and efficiently induced in human amniotic fluid-derived cells." Hum Mol Genet **18**(22): 4340-9.
Li, W. and S. Ding "Small molecules that modulate embryonic stem cell fate and somatic cell reprogramming." Trends Pharmacol Sci **31**(1): 36-45.
Liu, H., S. L. Ye, et al. (2003). "The microcell mediated transfer of human chromosome 8 into highly metastatic rat liver cancer cell line C5F." World J Gastroenterol **9**(3): 449-53.
Liu, Y., S. Shin, et al. (2006). "Genome wide profiling of human embryonic stem cells (hESCs), their derivatives and embryonal carcinoma cells to develop base profiles of U.S. Federal government approved hESC lines." BMC Dev Biol **6**: 20.
Lomas, H., Canton, I., MacNeil, S., Jianzhong Du, Steven P. Armes, Anthony J. Ryan, Andrew L. Lewis, and Giuseppe Battaglia (2007). "Biomimetic pH Sensitive Polymersomes for Efficient DNA
Encapsulation and Delivery." Adv. Mater.(19): 4238–4243.
Lomas, H., M. Massignani, et al. (2008). "Non-cytotoxic polymer vesicles for rapid and efficient intracellular delivery." Faraday Discuss **139**: 143-59; discussion 213-28, 419-20.
Loutit, J. F. and N. W. Nisbet (1982). "The origin of osteoclasts." Immunobiology **161**(3-4): 193-203.
Low, I. and P. Dancker (1976). "Effect of cytochalasin B on formation and properties of muscle F-actin." Biochim Biophys Acta **430**(2): 366-74.

Low, I., P. Dancker, et al. (1975). "Stabilization of F-actin by phalloidin. Reversal of the destabilizing effect of cytochalasin B." FEBS Lett **54**(2): 263-5.
Lugo, T. G., B. Handelin, et al. (1987). "Isolation of microcell hybrid clones containing retroviral vector insertions into specific human chromosomes." Mol Cell Biol **7**(8): 2814-20.
Ma, D. K., C. H. Chiang, et al. (2008). "G9a and Jhdm2a Regulate Embryonic Stem Cell Fusion-Induced Reprogramming of Adult Neural Stem Cells." Stem Cells.
Maherali, N., T. Ahfeldt, et al. (2008a). "A high-efficiency system for the generation and study of human induced pluripotent stem cells." Cell Stem Cell **3**(3): 340-5.
Maherali, N. and K. Hochedlinger (2008b). "Induced Pluripotency of Mouse and Human Somatic Cells." Cold Spring Harb Symp Quant Biol.
Maitra, A., D. E. Arking, et al. (2005). "Genomic alterations in cultured human embryonic stem cells." Nat Genet **37**(10): 1099-103.
Mali, P., Z. Ye, et al. (2008). "Improved efficiency and pace of generating induced pluripotent stem cells from human adult and fetal fibroblasts." Stem Cells **26**(8): 1998-2005.
Markovic, S. N., A. B. Dietz, et al. (2006). "Preparing clinical-grade myeloid dendritic cells by electroporation-mediated transfection of in vitro amplified tumor-derived mRNA and safety testing in stage IV malignant melanoma." J Transl Med **4**: 35.
Martin, G. R. (1981). "Isolation of a pluripotent cell line from early mouse embryos cultured in medium conditioned by teratocarcinoma stem cells." Proc Natl Acad Sci U S A **78**(12): 7634-8.
Matker, C. M., P. Rizzo, et al. (1998). "The biological activities of simian virus 40 large-T antigen and its possible oncogenic effects in humans." Monaldi Arch Chest Dis **53**(2): 193-7.
Matsui, Y., K. Zsebo, et al. (1992). "Derivation of pluripotential embryonic stem cells from murine primordial germ cells in culture." Cell **70**(5): 841-7.
Matsumura, H., M. Tada, et al. (2007). "Targeted chromosome elimination from ES-somatic hybrid cells." Nat Methods **4**(1): 23-5.
McBurney, M. W. (1977a). "Chimeric mice derived from normal embryos injected with teratocarcinoma cells." Am J Pathol **89**(3): 685-6.
McBurney, M. W. (1977b). "Hemoglobin synthesis in cell hybrids formed between teratocarcinoma and Friend erythroleukemia cells." Cell **12**(3): 653-62.
McBurney, M. W., M. S. Featherstone, et al. (1978). "Activation of teratocarcinoma-derived hemoglobin genes in teratocarcinoma-Friend cell hybrids." Cell **15**(4): 1323-30.
McBurney, M. W. and B. Strutt (1979). "Fusion of embryonal carcinoma cells to fibroblast cells, cytoplasts, and karyoplasts. Developmental properties of viable fusion products." Exp Cell Res **124**(1): 171-80.
Merrill, B. J. (2008). "Develop-WNTs in somatic cell reprogramming." Cell Stem Cell **3**(5): 465-6.
Mikkelsen, T. S., J. Hanna, et al. (2008). "Dissecting direct reprogramming through integrative genomic analysis." Nature **454**(7200): 49-55.
Miller, R. A. and F. H. Ruddle (1976). "Pluripotent teratocarcinoma-thymus somatic cell hybrids." Cell **9**(1): 45-55.
Miller, R. A. and F. H. Ruddle (1977a). "Properties of teratocarcinoma-thymus somatic cell hybrids." Somatic Cell Genet **3**(3): 247-61.
Miller, R. A. and F. H. Ruddle (1977b). "Teratocarcinoma X friend erythroleukemia cell hybrids resemble their pluripotent embryonal carcinoma parent." Dev Biol **56**(1): 157-73.
Minami, K., Y. Yamaguchi, et al. (2005). "Generation of antigen-presenting cells using cultured dendritic cells and amplified autologous tumor mRNA." Oncology **69**(5): 399-407.
Mintz, B. and K. Illmensee (1975). "Normal genetically mosaic mice produced from malignant teratocarcinoma cells." Proc Natl Acad Sci U S A **72**(9): 3585-9.

Moasser, M. M., V. E. Reuter, et al. (1995). "Overexpression of the retinoic acid receptor gamma directly induces terminal differentiation of human embryonal carcinoma cells." Oncogene **10**(8): 1537-43.
Moreadith, R. W. and K. H. Graves (1992). "Derivation of pluripotential embryonic stem cells from the rabbit." Trans Assoc Am Physicians **105**: 197-203.
Mu, L. J., G. Gaudernack, et al. (2003). "A protocol for generation of clinical grade mRNA-transfected monocyte-derived dendritic cells for cancer vaccines." Scand J Immunol **58**(5): 578-86.
Mummery, C., D. Ward-van Oostwaard, et al. (2003). "Differentiation of human embryonic stem cells to cardiomyocytes: role of coculture with visceral endoderm-like cells." Circulation **107**(21): 2733-40.
Mummery, C. L., D. Ward, et al. (2007). "Differentiation of human embryonic stem cells to cardiomyocytes by coculture with endoderm in serum-free medium." Curr Protoc Stem Cell Biol **Chapter 1**: Unit 1F 2.
Nakagawa, M., M. Koyanagi, et al. (2008). "Generation of induced pluripotent stem cells without Myc from mouse and human fibroblasts." Nat Biotechnol **26**(1): 101-6.
Norwood, T. H., C. J. Zeigler, et al. (1976). "Dimethyl sulfoxide enhances polyethylene glycol-mediated somatic cell fusion." Somatic Cell Genet **2**(3): 263-70.
Odorico, J. S., D. S. Kaufman, et al. (2001). "Multilineage differentiation from human embryonic stem cell lines." Stem Cells **19**(3): 193-204.
Okita, K., T. Ichisaka, et al. (2007). "Generation of germline-competent induced pluripotent stem cells." Nature **448**(7151): 313-7.
Page, R. L., S. Ambady, et al. (2009). "Induction of Stem Cell Gene Expression in Adult Human Fibroblasts without Transgenes." Cloning Stem Cells.
Papaioannou, V. E., E. P. Evans, et al. (1979). "Growth and differentiation of an embryonal carcinoma cell line (C145b)." J Embryol Exp Morphol **54**: 277-95.
Papaioannou, V. E., R. L. Gardner, et al. (1978). "Participation of cultured teratocarcinoma cells in mouse embryogenesis." J Embryol Exp Morphol **44**: 93-104.
Papaioannou, V. E., M. W. McBurney, et al. (1975). "Fate of teratocarcinoma cells injected into early mouse embryos." Nature **258**(5530): 70-73.
Park, H., A. Varadi, et al. (2007a). "mGluR5 is involved in dendrite differentiation and excitatory synaptic transmission in NTERA2 human embryonic carcinoma cell-derived neurons." Neuropharmacology.
Park, H., A. Varadi, et al. (2007b). "mGluR5 is involved in dendrite differentiation and excitatory synaptic transmission in NTERA2 human embryonic carcinoma cell-derived neurons." Neuropharmacology **52**(6): 1403-14.
Park, I. H., P. H. Lerou, et al. (2008a). "Generation of human-induced pluripotent stem cells." Nat Protoc **3**(7): 1180-6.
Park, I. H., R. Zhao, et al. (2008b). "Reprogramming of human somatic cells to pluripotency with defined factors." Nature **451**(7175): 141-6.
Pereira, C. F., R. Terranova, et al. (2008). "Heterokaryon-based reprogramming of human B lymphocytes for pluripotency requires Oct4 but not Sox2." PLoS Genet **4**(9): e1000170.
Phan, V., F. Errington, et al. (2003). "A new genetic method to generate and isolate small, short-lived but highly potent dendritic cell-tumor cell hybrid vaccines." Nat Med **9**(9): 1215-9.
Ponsaerts, P., G. Van den Bosch, et al. (2002a). "Messenger RNA electroporation of human monocytes, followed by rapid in vitro differentiation, leads to highly stimulatory antigen-loaded mature dendritic cells." J Immunol **169**(4): 1669-75.
Ponsaerts, P., V. F. Van Tendeloo, et al. (2002b). "mRNA-electroporated mature dendritic cells retain transgene expression, phenotypical properties and stimulatory capacity after cryopreservation." Leukemia **16**(7): 1324-30.
Poste, G. and P. Reeve (1971). "Formation of hybrid cells and heterokaryons by fusion of enucleated and nucleated cells." Nat New Biol **229**(4): 123-5.

Poulsom, R., M. R. Alison, et al. (2002). "Adult stem cell plasticity." J Pathol **197**(4): 441-56.
Pralong, D., K. Mrozik, et al. (2005). "A novel method for somatic cell nuclear transfer to mouse embryonic stem cells." Cloning Stem Cells **7**(4): 265-71.
Prescott, D. M. and J. B. Kirkpatrick (1973). "Mass enucleation of cultured animal cells." Methods Cell Biol **7**: 189-202.
Qin, M., G. Tai, et al. (2005). "Cell extract-derived differentiation of embryonic stem cells." Stem Cells **23**(6): 712-8.
Resnick, J. L., L. S. Bixler, et al. (1992). "Long-term proliferation of mouse primordial germ cells in culture." Nature **359**(6395): 550-1.
Reubinoff, B. E., P. Itsykson, et al. (2001). "Neural progenitors from human embryonic stem cells." Nat Biotechnol **19**(12): 1134-40.
Reubinoff, B. E., M. F. Pera, et al. (2000). "Embryonic stem cell lines from human blastocysts: somatic differentiation in vitro." Nat Biotechnol **18**(4): 399-404.
Rowland, B. D., R. Bernards, et al. (2005). "The KLF4 tumour suppressor is a transcriptional repressor of p53 that acts as a context-dependent oncogene." Nat Cell Biol **7**(11): 1074-82.
Ruau, D., R. Ensenat-Waser, et al. (2008). "Pluripotency associated genes are reactivated by chromatin-modifying agents in neurosphere cells." Stem Cells **26**(4): 920-6.
Ruggero, D. (2009). "The role of Myc-induced protein synthesis in cancer." Cancer Res **69**(23): 8839-43.
Saeboe-Larssen, S., E. Fossberg, et al. (2002). "mRNA-based electrotransfection of human dendritic cells and induction of cytotoxic T lymphocyte responses against the telomerase catalytic subunit (hTERT)." J Immunol Methods **259**(1-2): 191-203.
Schimrosczyk, K., Y. H. Song, et al. (2008). "Liposome-mediated transfection with extract from neonatal rat cardiomyocytes induces transdifferentiation of human adipose-derived stem cells into cardiomyocytes." Scand J Clin Lab Invest **68**(6): 464-72.
Scholer, H. R., R. Balling, et al. (1989). "Octamer binding proteins confer transcriptional activity in early mouse embryogenesis." Embo J **8**(9): 2551-7.
Schuldiner, M., R. Eiges, et al. (2001). "Induced neuronal differentiation of human embryonic stem cells." Brain Res **913**(2): 201-5.
Schultz, R. A., P. J. Saxon, et al. (1987). "Microcell-mediated transfer of a single human chromosome complements xeroderma pigmentosum group A fibroblasts." Proc Natl Acad Sci U S A **84**(12): 4176-9.
Schwartz, C. M., C. E. Spivak, et al. (2005). "NTERA2: a model system to study dopaminergic differentiation of human embryonic stem cells." Stem Cells Dev **14**(5): 517-34.
Shay, J. W. (1987). "Cell enucleation, cybrids, reconstituted cells, and nuclear hybrids." Methods Enzymol **151**: 221-37.
Shi, L. H., Y. L. Miao, et al. (2008a). "Trichostatin A (TSA) improves the development of rabbit-rabbit intraspecies cloned embryos, but not rabbit-human interspecies cloned embryos." Dev Dyn **237**(3): 640-8.
Shi, Y., C. Desponts, et al. (2008b). "Induction of pluripotent stem cells from mouse embryonic fibroblasts by Oct4 and Klf4 with small-molecule compounds." Cell Stem Cell **3**(5): 568-74.
Shi, Y., J. T. Do, et al. (2008c). "A combined chemical and genetic approach for the generation of induced pluripotent stem cells." Cell Stem Cell **2**(6): 525-8.
Skotheim, R. I., G. E. Lind, et al. (2005). "Differentiation of human embryonal carcinomas in vitro and in vivo reveals expression profiles relevant to normal development." Cancer Res **65**(13): 5588-98.
Skottman, H., M. S. Dilber, et al. (2006). "The derivation of clinical-grade human embryonic stem cell lines." FEBS Lett **580**(12): 2875-8.

Skowronski, J. and M. F. Singer (1985). "Expression of a cytoplasmic LINE-1 transcript is regulated in a human teratocarcinoma cell line." Proc Natl Acad Sci U S A **82**(18): 6050-4.
Song, L. and R. S. Tuan (2004). "Transdifferentiation potential of human mesenchymal stem cells derived from bone marrow." Faseb J **18**(9): 980-2.
Stadtfeld, M., M. Nagaya, et al. (2008). "Induced pluripotent stem cells generated without viral integration." Science **322**(5903): 945-9.
Sukoyan, M. A., S. Y. Vatolin, et al. (1993). "Embryonic stem cells derived from morulae, inner cell mass, and blastocysts of mink: comparisons of their pluripotencies." Mol Reprod Dev **36**(2): 148-58.
Sun, N., N. J. Panetta, et al. (2009). "Feeder-free derivation of induced pluripotent stem cells from adult human adipose stem cells." Proc Natl Acad Sci U S A **106**(37): 15720-5.
Surani, M. A., K. Hayashi, et al. (2007). "Genetic and epigenetic regulators of pluripotency." Cell **128**(4): 747-62.
Szutorisz, H. and N. Dillon (2005). "The epigenetic basis for embryonic stem cell pluripotency." Bioessays **27**(12): 1286-93.
Tada, M., T. Tada, et al. (1997). "Embryonic germ cells induce epigenetic reprogramming of somatic nucleus in hybrid cells." Embo J **16**(21): 6510-20.
Tada, M., Y. Takahama, et al. (2001). "Nuclear reprogramming of somatic cells by in vitro hybridization with ES cells." Curr Biol **11**(19): 1553-8.
Takahashi, K., K. Tanabe, et al. (2007). "Induction of pluripotent stem cells from adult human fibroblasts by defined factors." Cell **131**(5): 861-72.
Takahashi, K. and S. Yamanaka (2006). "Induction of pluripotent stem cells from mouse embryonic and adult fibroblast cultures by defined factors." Cell **126**(4): 663-76.
Taranger, C. K., A. Noer, et al. (2005). "Induction of dedifferentiation, genomewide transcriptional programming, and epigenetic reprogramming by extracts of carcinoma and embryonic stem cells." Mol Biol Cell **16**(12): 5719-35.
Taylor, M. V. (2000). "Muscle development: molecules of myoblast fusion." Curr Biol **10**(17): R646-8.
Terada, N., T. Hamazaki, et al. (2002). "Bone marrow cells adopt the phenotype of other cells by spontaneous cell fusion." Nature **416**(6880): 542-5.
Thomson, J. A., J. Itskovitz-Eldor, et al. (1998). "Embryonic stem cell lines derived from human blastocysts." Science **282**(5391): 1145-7.
Thomson, J. A., J. Kalishman, et al. (1995). "Isolation of a primate embryonic stem cell line." Proc Natl Acad Sci US A **92**(17): 7844-7848.
Till, J. E. and C. E. Mc (1963). "Early repair processes in marrow cells irradiated and proliferating in vivo." Radiat Res **18**: 96-105.
Till, J. E. and E. A. McCulloch (1964). "Repair Processes in Irradiated Mouse Hematopoietic Tissue." Ann N Y Acad Sci **114**: 115-25.
Till, J. E., L. Siminovitch, et al. (1967). "The effect of plethora on growth and differentiation of normal hemopoietic colony-forming cells transplanted in mice of genotype W/Wv." Blood **29**(1): 102-13.
Unger, C., H. Skottman, et al. (2008). "Good manufacturing practice and clinical-grade human embryonic stem cell lines." Hum Mol Genet **17**(R1): R48-53.
Vafa, O., M. Wade, et al. (2002). "c-Myc can induce DNA damage, increase reactive oxygen species, and mitigate p53 function: a mechanism for oncogene-induced genetic instability." Mol Cell **9**(5): 1031-44.
Vassilopoulos, G., P. R. Wang, et al. (2003). "Transplanted bone marrow regenerates liver by cell fusion." Nature **422**(6934): 901-4.
Veomett, G., D. M. Prescott, et al. (1974). "Reconstruction of mammalian cells from nuclear and cytoplasmic components separated by treatment with cytochalasin B." Proc Natl Acad Sci U S A **71**(5): 1999-2002.
Vierbuchen, T., A. Ostermeier, et al. (2010). "Direct conversion of fibroblasts to functional neurons by defined factors." Nature **463**(7284): 1035-41.

Vignery, A. (2000). "Osteoclasts and giant cells: macrophage-macrophage fusion mechanism." Int J Exp Pathol **81**(5): 291-304.
Vilchez, R. A. and J. S. Butel (2003). "SV40 in human brain cancers and non-Hodgkin's lymphoma." Oncogene **22**(33): 5164-72.
Wakayama, T., A. C. Perry, et al. (1998a). "Full-term development of mice from enucleated oocytes injected with cumulus cell nuclei." Nature **394**(6691): 369-74.
Wakayama, T., V. Tabar, et al. (2001). "Differentiation of embryonic stem cell lines generated from adult somatic cells by nuclear transfer." Science **292**(5517): 740-3.
Wakayama, T. and R. Yanagimachi (1998b). "Fertilisability and developmental ability of mouse oocytes with reduced amounts of cytoplasm." Zygote **6**(4): 341-6.
Wallace, D. C., C. L. Bunn, et al. (1975). "Cytoplasmic transfer of chloramphenicol resistance in human tissue culture cells." J Cell Biol **67**(1): 174-88.
Wang, J. and R. L. Garcea (1998). "Simian virus 40 DNA sequences in human brain and bone tumours." Dev Biol Stand **94**: 13-21.
Wang, X., H. Willenbring, et al. (2003). "Cell fusion is the principal source of bone-marrow-derived hepatocytes." Nature **422**(6934): 897-901.
Watanabe, K., M. Ueno, et al. (2007). "A ROCK inhibitor permits survival of dissociated human embryonic stem cells." Nat Biotechnol **25**(6): 681-6.
Wernig, M., A. Meissner, et al. (2007). "In vitro reprogramming of fibroblasts into a pluripotent ES-cell-like state." Nature **448**(7151): 318-24.
Wertkin, A. M., R. S. Turner, et al. (1993). "Human neurons derived from a teratocarcinoma cell line express solely the 695-amino acid amyloid precursor protein and produce intracellular beta-amyloid or A4 peptides." Proc Natl Acad Sci U S A **90**(20): 9513-7.
Wigler, M. H. and I. B. Weinstein (1975). "A preparative method for obtaining enucleated mammalian cells." Biochem Biophys Res Commun **63**(3): 669-74.
Wilmut, I., A. E. Schnieke, et al. (1997). "Viable offspring derived from fetal and adult mammalian cells." Nature **385**(6619): 810-3.
Woltjen, K., I. P. Michael, et al. (2009). "piggyBac transposition reprograms fibroblasts to induced pluripotent stem cells." Nature **458**(7239): 766-70.
Wong, C. C., A. Gaspar-Maia, et al. (2008). "High-efficiency stem cell fusion-mediated assay reveals Sall4 as an enhancer of reprogramming." PLoS One **3**(4): e1955.
Wu, X., S. Ding, et al. (2004). "Small molecules that induce cardiomyogenesis in embryonic stem cells." J Am Chem Soc **126**(6): 1590-1.
Xu, C., J. Jiang, et al. (2004). "Immortalized fibroblast-like cells derived from human embryonic stem cells support undifferentiated cell growth." Stem Cells **22**(6): 972-80.
Yu, J., M. A. Vodyanik, et al. (2006). "Human embryonic stem cells reprogram myeloid precursors following cell-cell fusion." Stem Cells **24**(1): 168-76.
Yu, J., M. A. Vodyanik, et al. (2007). "Induced pluripotent stem cell lines derived from human somatic cells." Science **318**(5858): 1917-20.
Zhao, Y., X. Yin, et al. (2008). "Two supporting factors greatly improve the efficiency of human iPSC generation." Cell Stem Cell **3**(5): 475-9.
Zhou, H., S. Wu, et al. (2009a). "Generation of induced pluripotent stem cells using recombinant proteins." Cell Stem Cell **4**(5): 381-4.
Zhou, Q., J. Brown, et al. (2008). "In vivo reprogramming of adult pancreatic exocrine cells to beta-cells." Nature **455**(7213): 627-32.
Zhou, W. and C. R. Freed (2009b). "Adenoviral gene delivery can reprogram human fibroblasts to induced pluripotent stem cells." Stem Cells **27**(11): 2667-74.

Presentations

1. Poster: Relative Quantification of Transcription Factors During Reprogramming of Pluripotent Stem Cells
   Unger C, Plews J, Na J, Feki A, Andrews PW
   ISSCR Annual Conference, Barcelona, Spain (2009)

2. Talk: Altering Cell Fate Using mRNA of Defined Factors
   International Networking for Young Scientists – Stem Cell Conference, Taiwan (2009)

3. Poster: A Study of ES Cell Gene Reactivation During Somatic Cell Reprogramming Using a Novel mRNA Based Approach
   Plews J, Na J, Mason C, Andrews PW
   ESTOOLS Annual Conference, Rome, Italy (2009)

4. Poster: Altering Cell Fate Using mRNA Activated Transcription Factors
   Plews J, Na J, Mason C, Andrews PW
   UCL Industrial Open Day, London, UK (2009)

5. Poster: Reprogramming Cell Fate Using mRNA of Defined Factors
   Plews J, Na J, Mason C, Andrews PW
   ESTOOLS Annual Conference, Budapest, Hungary (2008)

Publications

1. **Review Article:** "Molecular mechanisms of pluripotency and reprogramming"
   Authors: Christian Unger, Jie Na, Jordan Plews, Jack Li, Timo Tuuri, Anis Feki, Peter W Andrews
   Journal: Stem Cell Research & Therapy

2. **Paper:** Activation of Pluripotency Genes in Human Fibroblast Cells by a Novel mRNA Based Approach
   Authors: Jordan Plews, JianLiang Li, Mark Jones, Chris Mason, Peter W. Andrews and Jie Na

Accolades

- Won "Best Postgraduate Business Idea" in the London Entrepreneur's Challenge 08/09
- Participated in the CSEL London Entrepreneur's Challenge 2006/07
- Won "Best Postgraduate Business Idea" in the CSEL London Entrepreneur's Challenge 2005/06
- Won "Best Intellectual Property Strategy" as part of the 2004/05 Biotechnology YES competition